

Westinghouse Non-Proprietary Class 3

*Rec'd w/WR  
11/18/98  
9811240248*



WCAP-14279

Revision 1

# Evaluation of Capsules from the Kewaunee and Capsule A-35 from the Maine Yankee Nuclear Plant Reactor Vessel Radiation Surveillance Programs

Westinghouse Energy Systems



9811240258 981118  
PDR ADOCK 05000305  
P PDR

WCAP-14279  
Revision 1


**EVALUATION OF CAPSULES FROM THE KEWAUNEE  
AND CAPSULE A-35 FROM THE MAINE YANKEE  
NUCLEAR PLANT REACTOR VESSEL RADIATION  
SURVEILLANCE PROGRAMS**

C. C. Kim

E. Terek

S. L. Anderson

September 1998

Approved:   
C. H. Boyd, Manager  
Engineering & Materials Technology

Work Performed Under Shop Order KFZP-106

Prepared by Westinghouse Electric Company  
for the Wisconsin Public Service Corporation

---

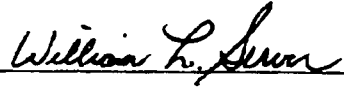
Westinghouse Electric Company  
Energy Systems  
PO Box 355  
Pittsburgh, PA 15230-0355

©1998 Westinghouse Electric Company  
All Rights Reserved

---

PREFACE

This report has been technically reviewed and verified by:

  
\_\_\_\_\_

W. L. Server

## FORWARD

This report along with four other companion documents have been prepared by Westinghouse Electric Corporation and ATI Consulting to assess and document the integrity of the Kewaunee Nuclear Power Plant (KNPP) reactor vessel relative to the requirements of 10 CFR 50.60, 10 CFR 50.61, Appendices G and H to 10 CFR Part 50, (which encompass pressurized thermal shock (PTS) and upper shelf energy (USE) evaluations), and any potential impact on low temperature overpressure (LTOP) limits or pressure-temperature limits. These reports: (1) summarize the KNPP weld metal (1P3571) surveillance capsule test results performed to date (WCAP-15074); (2) document supplemental surveillance capsule fracture toughness testing results for the KNPP weld metal both in the unirradiated and irradiated condition (WCAP-14279, Rev. 1); (3) introduce and apply a new methodology, based on the Master Curve Approach, for assessing the integrity of the KNPP reactor vessel (WCAP-15075); (4) include various PTS evaluations conducted in accordance with the methodology given in 10 CFR 50.61 and the Master Curve Approach for KNPP (WCAP-14280, Rev. 1); and (5) present heatup and cooldown curves corresponding to end of plant life fluence (WCAP-14278, Rev. 1). The heatup and cooldown limit curves presented in WCAP-14278, Rev. 1 are derived using ASME Code Case N-588. These five documents support a new proposed amendment to modify the KNPP Technical Specification limits for heatup, cooldown, and low temperature overpressure protection. The current Technical Specification heatup and cooldown limit curves will expire at 20 EFPY which is scheduled to occur in spring of 1999. The engineering evaluations incorporate all known data pertinent to the analysis of structural integrity of the KNPP reactor vessel and therefore meet and exceed the intent of NRC regulation and expectations.

Background for much of this work is linked to ongoing efforts by the NRC staff to generically resolve concerns raised during their review of reactor vessel integrity for the Yankee Rowe Nuclear Power Station. As part of this effort, the NRC staff issued Generic Letter 92-01, Revision 1 and Generic Letter 92-01, Revision 1, Supplement 1. These generic communiqué seek to obtain certain information that will permit the NRC staff to independently assess and ensure that licensees are in compliance with requirements regarding reactor pressure vessel integrity.

During review of the responses to Generic Letter 92-01, Revision 1 and Generic Letter 92-01, Revision 1, Supplement 1 the NRC discovered inconsistencies within the industry concerning the methodology used to assess reactor pressure vessel integrity including:

1. Large variability in the reported chemistries, i.e., copper and nickel contents, for welds fabricated from the same heat of weld wire.
2. Different initial properties ( $RT_{NDT}$ ) for welds fabricated from the same heat and weld wire.
3. Different transition temperature shifts for welds fabricated from the same heat and weld wire.
4. Operation with irradiation temperature less than 525°F.

5. Different approaches for determining fluence of the limiting material.

In response to this discovery, to provide assurance that all plants will maintain adequate protection against PTS events, the practice of the NRC staff has been to require that evaluations be performed using conservative inputs. This increase in conservatism seems to apply equally to all areas of assessment of reactor vessel integrity. When best estimate values have been used by utilities for the chemical composition of the reactor vessel, it appears that the NRC staff may require the use of increased margin terms to account for potential variability in chemistries. Furthermore, through the process of issuing RAIs, the NRC staff has requested that evaluations be performed using generic values for initial properties and a corresponding higher margin value from either 28°F to 56°F (if the initial  $RT_{NDT}$  is measured) or 44°F to 66°F (if the generic  $RT_{NDT}$  is used). Other recent changes include the mandatory use of the ratio procedure, if applicable; a 1°F penalty for each degree Fahrenheit when the irradiation temperature is less than 525°F; and other penalties on the projected fluence of the limiting reactor vessel beltline material at end of license. Collectively, this practice of requiring multiple conservative inputs in a layered fashion for assessment of reactor vessel integrity has the effect that a reactor vessel would be predicted to reach the PTS screening criteria at an earlier date than that given by the PTS assessment methodology given in 10 CFR 50.61. A situation of applying too much conservatism can create the illusion that a reactor vessel is unsafe to operate when in fact it may possess sufficient fracture toughness. If too much conservatism is applied the overall affect can be a decrease in safety because of unnecessary changes made to plant operations and design for the sole reason of addressing a conservative but erroneous PTS evaluation.

At about the same time Generic Letter 92-01, Revision 1, Supplement 1 was being issued, the NRC staff became aware of ABB-CE proprietary data that could affect the PTS assessment of the KNPP reactor vessel. Subsequently, ABB-CE provided KNPP a summary of the data for its evaluation in a letter dated April 6, 1995. The NRC staff met with the KNPP staff on April 13, 1995 to discuss the effect that the ABB-CE data and its plant specific surveillance data would have on their PTS assessment. Prior to this meeting, the NRC staff verbally expressed concern to KNPP management that the KNPP reactor vessel may reach the PTS screening criteria before the end of their license. The KNPP staff presented its plant specific surveillance program results and some new information related to the reactor vessel chemistry variability. Based upon using best estimate input parameters, the KNPP staff showed that the KNPP reactor vessel will not reach the PTS screening criteria before the end of their license. Recognizing that the NRC staff was still concerned about the possibility of the KNPP reactor vessel reaching the PTS screening criteria prior to end of license, the KNPP staff remained steadfast in their use of best estimate input parameters for assessment of reactor vessel integrity. At the same time KNPP committed resources to develop industry programs that would facilitate implementation of the applicable requirements specified in the 1992 Edition of Appendix G to 10 CFR 50 should it become necessary: supplemental fracture toughness tests of the beltline material after exposure to neutron irradiation; perform analysis that demonstrates the existence of equivalent margins of safety for continued operation, and thermal annealing. At the conclusion of the April 13, 1995 meeting, the KNPP staff described their future plans to ensure compliance with the requirements for reactor vessel integrity. These plans included participation with industry groups to create programs and a data base detailing the chemical composition of reactor vessel beltline materials; demonstration of the feasibility for annealing of

a PWR reactor vessel of US design; and direct measurement of fracture toughness from irradiated surveillance capsule specimens.

In a NRC internal memorandum (dated May 6, 1995 from Jack R. Strosnider, Chief - Materials and Chemical Engineering Branch, Division of Engineering to Ashok C. Thadani, Associate Director for Technical Assessment, Office of Nuclear Reactor Regulation) released following the April 13, 1995 meeting, the NRC staff wrote that they had not completed their review of the new information on the KNPP reactor vessel. The NRC staff noted that the new chemistry data could significantly change the KNPP PTS evaluation. However, based on conservative evaluations, the NRC staff concluded that the KNPP reactor vessel will not reach the PTS screening criteria in the near future. During this same time period, WPSC submitted a proposed amendment to the NRC to modify KNPP Technical Specification limits relating to heatup, cooldown, and low temperature overpressure protection (LTOP). The NRC issued two requests for additional information regarding this proposed amendment, dealing with surveillance capsule fluence and material properties, and then requested that WPSC withdraw it from the docket pending resolution of Generic Letter 92-01, Revision 1, Supplement 1 activities.

While the NRC was performing a detailed review of licensee responses to Generic Letter 92-01, Revision 1, each of the PWR NSSS Owners Groups developed and implemented programs dealing with measurement of fracture toughness for reactor vessel materials. WPSC has funded both the WOG and ABB-CE/RVWG to measure the fracture toughness of two 1P3571 archive weld metal (utilizing different coils of weld wire) using the Master Curve Approach. The WOG and ABB-CE/RVWG have obtained unirradiated  $T_0$  values for weld metal 1P3571 in accordance with ASTM E1921-97. The WOG has also obtained the fracture toughness for 1P3571 weld metal from unirradiated 1/2T-CT specimens. Furthermore, the WOG has generated irradiated  $T_0$  values for the two 1P3571 weldments reconstituted from surveillance capsule specimens from the KNPP and Maine Yankee reactor vessels that were irradiated to  $3.36 \times 10^{19}$  n/cm<sup>2</sup> and  $6.11 \times 10^{19}$  n/cm<sup>2</sup>, respectively. The ASME B&PVC is currently working under the direction of PVRC to develop recommendations and guidelines for the use of  $T_0$  values in lieu of  $RT_{NDT}$  values for assessment of reactor vessel integrity. The results of the supplemental fracture toughness testing for both the unirradiated and irradiated 1P3571 weld metal, along with application of the results, has been presented to the PVRC and ASME.

WPSC concluded that it is prudent to report the results of the recently completed fracture toughness testing of the EOL and beyond EOL irradiated 1P3571 weld metal along with the values derived for the various PTS evaluations given by the methodology described in 10 CFR 50.61. The results of the irradiated fracture toughness testing will serve as a means of assuring adequate conservatism is incorporated into the integrity assessment of the KNPP reactor vessel. Furthermore, since the fracture toughness transition shift is larger and more accurate than the Charpy transition shift, it is felt that continued use of the Charpy results could be inappropriate. The KNPP has volunteered to be a lead plant on behalf of the WOG for application of the Master Curve Approach. NRC feedback obtained on this application of the Master Curve Method will be considered, as appropriate, by the WOG. The fracture toughness results along with the methodology presented in WCAP-15075 indicate that the KNPP 1P3571

weld metal will continue to conservatively provide adequate fracture toughness up to and beyond extended end-of-life fluence.

## TABLE OF CONTENTS

1.0	SUMMARY OF RESULTS .....	1-1
1.1	FLUENCE EVALUATION .....	1-1
1.1.1	Kewaunee Capsule S .....	1-1
1.1.2	Maine Yankee Capsule A-35 .....	1-1
1.2	CHARPY V-NOTCH IMPACT TESTS .....	1-1
1.2.1	Kewaunee Capsule S .....	1-1
1.2.2	Maine Yankee Capsule A-35 .....	1-2
1.3	"MASTER CURVE" FRACTURE TOUGHNESS TESTS .....	1-2
1.3.1	Kewaunee Capsule S .....	1-2
1.3.2	Maine Yankee A-35 Capsule .....	1-2
1.4	ANALYSIS .....	1-3
1.4.1	Kewaunee Charpy V-notch Toughness .....	1-3
1.4.2	"Master Curve" Fracture Toughness .....	1-4
2.0	INTRODUCTION .....	2-1
3.0	BACKGROUND .....	3-1
4.0	DESCRIPTION OF TESTING PROGRAM .....	4-1
4.1	CHARPY V-NOTCH IMPACT AND TENSILE TESTS .....	4-2
4.1.1	Kewaunee .....	4-2
4.1.2	Maine Yankee .....	4-2
4.2	DOSIMETERS AND THERMAL MONITORS .....	4-2
4.2.1	Kewaunee .....	4-2
4.2.2	Maine Yankee .....	4-3
4.3	MASTER CURVE TESTS FOR KEWAUNEE AND MAINE YANKEE SURVEILLANCE WELDS .....	4-3
5.0	TESTING METHODS AND RESULTS .....	5-1
5.1	OVERVIEW OF TESTING METHODS .....	5-1
5.1.1	Charpy V-notch Impact Tests .....	5-1
5.1.2	Tensile Tests .....	5-2
5.1.3	Master Curve Fracture Toughness Tests .....	5-3
5.1.4	Qualification of Reconstituted Charpy Size Three-Point Bend Specimens .....	5-4
5.2	CHARPY V-NOTCH IMPACT TEST RESULTS .....	5-5
5.2.1	Forging Material .....	5-5
5.2.2	Weld Metal .....	5-6
5.2.3	Heat-Affected-Zone (HAZ) .....	5-6
5.2.4	Correlation Monitor Material .....	5-6
5.2.5	Analysis .....	5-7
5.3	TENSILE TEST RESULTS .....	5-8
5.4	"MASTER CURVE" FRACTURE TOUGHNESS TEST RESULTS .....	5-8
5.4.1	Results for 1/2T-CT Specimens for Kewaunee Surveillance Weld (Unirradiated) .....	5-9
5.4.2	Results for Whole and Reconstituted Precracked Charpy Specimens for Kewaunee Surveillance Weld (Unirradiated) .....	5-9
5.4.3	Results for Whole Precracked Charpy Specimens for Maine Yankee Surveillance Weld (Unirradiated) .....	5-9



5.4.4	Results for Reconstituted Precracked Charpy Specimens for Kewaunee Surveillance Weld (Irradiated at $3.36 \times 10^{19}$ n/cm <sup>2</sup> ) .....	5-9
5.4.5	Results for Reconstituted Precracked Charpy Specimens for Maine Yankee Surveillance Weld (Irradiated at $6.11 \times 10^{19}$ n/cm <sup>2</sup> ) .....	5-9
5.4.6	Summary of T <sub>0</sub> Values .....	5-9
6.0	RADIATION ANALYSIS AND NEUTRON DOSIMETRY .....	6-1
6.1	KEWAUNEE .....	6-1
6.1.1	Introduction .....	6-1
6.1.2	Discrete Ordinates Analysis .....	6-2
6.1.3	Neutron Dosimetry .....	6-5
6.2	MAINE YANKEE .....	6-9
7.0	SURVEILLANCE CAPSULE REMOVAL SCHEDULE .....	7-1
8.0	CONCLUSIONS .....	8-1
8.1	FLUENCE EVALUATION .....	8-1
8.1.1	Kewaunee Capsule S .....	8-1
8.1.2	Maine Yankee Capsule A-35 .....	8-2
8.2	CHARPY V-NOTCH IMPACT TESTS .....	8-2
8.2.1	Kewaunee Capsule S .....	8-2
8.2.2	Maine Yankee Capsule A-35 .....	8-3
8.3	"MASTER CURVE" FRACTURE TOUGHNESS TESTS .....	8-3
8.4	ANALYSIS .....	8-4
8.4.1	Charpy V-notch Toughness Based .....	8-4
8.4.2	Master Curve Fracture Toughness Based .....	8-5
9.0	REFERENCES .....	9-1
APPENDIX A	LOAD-TIME RECORDS FOR CHARPY SPECIMEN TESTS .....	A-1
APPENDIX B	DOCUMENTATION OF THE CREDIBILITY OF THE KEWAUNEE WELD METAL SURVEILLANCE PROGRAM TEST RESULTS .....	B-1
APPENDIX C	DETERMINATION OF GIRTH WELD INITIAL RT <sub>NDT</sub> .....	C-1

## LIST OF TABLES

Table 4-1	Chemical Composition (wt%) of the Kewaunee Reactor Vessel Beltline Region Surveillance Material <sup>[5]</sup> .....	4-4
Table 4-2	Heat Treatment of the Kewaunee Reactor Vessel Beltline Region Surveillance Material <sup>[5]</sup> .....	4-5
Table 4-3	Chemical Composition of the A533 Grade B, Class 1 ASTM Correlation Monitor Material (HSST Plate 02) in the Kewaunee Reactor Vessel Surveillance Program <sup>[5]</sup> .....	4-6
Table 4-4	Heat Treatment of the A533 Grade B, Class 1 ASTM Correlation Monitor Material (HSST Plate 02) in the Kewaunee Reactor Vessel Surveillance Program .....	4-6
Table 5-1	Materials, Conditions, Geometries, and Test Temperatures for the Transition Region Fracture Toughness Program .....	5-11
Table 5-2	$K_{Ic}$ Limits .....	5-12
Table 5-3	Charpy V-notch Data for the Kewaunee Intermediate Shell Forging 122X208VA1 Irradiated to a Fluence of $3.36 \times 10^{19}$ n/cm <sup>2</sup> (E > 1.0 MeV) (Tangential Orientation) .....	5-13
Table 5-4	Charpy V-notch Data for the Kewaunee Lower Shell Forging 123X167VA1 Irradiated to a Fluence of $3.36 \times 10^{19}$ n/cm <sup>2</sup> (E > 1.0 MeV) (Tangential Orientation) .....	5-14
Table 5-5	Charpy V-notch Data for the Kewaunee Surveillance Weld Metal Irradiated to a Fluence of $3.36 \times 10^{19}$ n/cm <sup>2</sup> (E > 1.0 MeV) .....	5-15
Table 5-6	Charpy V-notch Data for the Kewaunee Heat-Affected-Zone (HAZ) Metal Irradiated to a Fluence of $3.36 \times 10^{19}$ n/cm <sup>2</sup> (E > 1.0 MeV) .....	5-15
Table 5-7	Charpy V-notch Data for the A533 Grade B Class 1 ASTM Correlation Monitor Material (HSST Plate 02) to a Fluence of $3.36 \times 10^{19}$ n/cm <sup>2</sup> (E > 1.0 MeV) .....	5-16
Table 5-8	Instrumented Charpy Impact Test Results for the Kewaunee Intermediate Shell Forging 122X208VA1 Irradiated to a Fluence of $3.36 \times 10^{19}$ n/cm <sup>2</sup> (E > 1.0 MeV) (Tangential Orientation) .....	5-17
Table 5-9	Instrumented Charpy Impact Test Results for the Kewaunee Lower Shell Forging 123X167VA1 Irradiated to a Fluence of $3.36 \times 10^{19}$ n/cm <sup>2</sup> (E > 1.0 MeV) (Tangential Orientation) .....	5-18

## LIST OF TABLES (Continued)

Table 5-10	Instrumented Charpy Impact Test Results for the Kewaunee Surveillance Weld Metal Irradiated to a Fluence of $3.36 \times 10^{19}$ n/cm <sup>2</sup> (E > 1.0 MeV) .....	5-19
Table 5-11	Instrumented Charpy Impact Test Results for the Kewaunee Surveillance Heat-Affected-Zone (HAZ) Metal Irradiated to a Fluence of $3.36 \times 10^{19}$ n/cm <sup>2</sup> (E > 1.0 MeV) .....	5-20
Table 5-12	Instrumented Charpy Impact Test Results for the A533 Grade B Class 1 ASTM Correlation Monitor Material (HSST Plate 02) Irradiated to a Fluence of $3.36 \times 10^{19}$ n/cm <sup>2</sup> (E > 1.0 MeV) .....	5-21
Table 5-13	Effect of Irradiation to $3.36 \times 10^{19}$ n/cm <sup>2</sup> (E > 1.0 MeV) on the Notch Toughness Properties of the Kewaunee Reactor Vessel Surveillance Materials .....	5-22
Table 5-14	Comparison of the Kewaunee Surveillance Material 30 ft-lb Transition Temperature Shifts and Upper Shelf Energy Decreases with Regulatory Guide 1.99, Revision 2, Predictions .....	5-23
Table 5-15	Tensile Properties of the Kewaunee Reactor Vessel Surveillance Materials Irradiated to $3.36 \times 10^{19}$ n/cm <sup>2</sup> (E > 1.0 MeV) .....	5-24
Table 5-16	Unirradiated 1092 Weld Metal K <sub>Jc</sub> Results .....	5-25
Table 5-17	Irradiated Kewaunee Weld Metal K <sub>Jc</sub> Results Fluence = $3.36 \times 10^{19}$ n/cm <sup>2</sup> .....	5-26
Table 5-18	Irradiated MY IP3571 Weld Metal K <sub>Jc</sub> Results Fluence = $6.11 \times 10^{19}$ n/cm <sup>2</sup> .....	5-27
Table 5-19	T <sub>0</sub> Results .....	5-28
Table 6-1	Calculated Neutron Exposure Parameters at Surveillance Capsule Specimen Geometric Center .....	6-12
Table 6-2	Calculated Azimuthal Variation of Neutron Flux (E > 1.0 MeV) at the Pressure Vessel Clad/Base Metal Interface .....	6-13
Table 6-3	Calculated Azimuthal Variation of Neutron Flux (E > 0.1 MeV) at the Pressure Vessel Clad/Base Metal Interface .....	6-14

## LIST OF TABLES (Continued)

Table 6-4	Calculated Azimuthal Variation of Iron Displacement Rate (dpa) at the Pressure Vessel Clad/Base Metal Interface .....	6-15
Table 6-5	Relative Radial Distributions of Neutron Flux ( $E > 1.0$ MeV) within the Pressure Vessel Wall .....	6-16
Table 6-6	Relative Radial Distributions of Neutron Flux ( $E > 0.1$ MeV) within the Pressure Vessel Wall .....	6-17
Table 6-7	Relative Radial Distributions of Iron Displacement Rate (dpa) within the Pressure Vessel Wall .....	6-18
Table 6-8	Nuclear Parameters for Neutron Flux Monitors .....	6-19
Table 6-9	Monthly Thermal Generation during the First Nineteen Fuel Cycles of the Kewaunee Reactor .....	6-20
Table 6-10	Measured Sensor Activities and Reactor Rates Surveillance Capsule V .....	6-23
Table 6-11	Measured Sensor Activities and Reactor Rates Surveillance Capsule R .....	6-25
Table 6-12	Measured Sensor Activities and Reactor Rates Surveillance Capsule P .....	6-27
Table 6-13	Measured Sensor Activities and Reactor Rates Surveillance Capsule S .....	6-29
Table 6-14	Summary of Neutron Dosimetry Results at Surveillance Capsule V Specimen Geometric Center .....	6-31
Table 6-15	Summary of Neutron Dosimetry Results at Surveillance Capsule R Specimen Geometric Center .....	6-32
Table 6-16	Summary of Neutron Dosimetry Results at Surveillance Capsule P Specimen Geometric Center .....	6-33
Table 6-17	Summary of Neutron Dosimetry Results at Surveillance Capsule S Specimen Geometric Center .....	6-34
Table 6-18	Comparison of Measured and Ferret Calculated Reaction Rates at Surveillance Capsule V Specimen Geometric Center .....	6-35

### LIST OF TABLES (Continued)

Table 6-19	Comparison of Measured and Ferret Calculated Reaction Rates at Surveillance Capsule R Specimen Geometric Center .....	6-36
Table 6-20	Comparison of Measured and Ferret Calculated Reaction Rates at Surveillance Capsule P Specimen Geometric Center .....	6-37
Table 6-21	Comparison of Measured and Ferret Calculated Reaction Rates at Surveillance Capsule S Specimen Geometric Center .....	6-38
Table 6-22	Best Estimate Neutron Energy Spectrum at Surveillance Capsule V Specimen Geometric Center .....	6-39
Table 6-23	Best Estimate Neutron Energy Spectrum at Surveillance Capsule R Specimen Geometric Center .....	6-40
Table 6-24	Best Estimate Neutron Energy Spectrum at Surveillance Capsule P Specimen Geometric Center .....	6-41
Table 6-25	Best Estimate Neutron Energy Spectrum at Surveillance Capsule S Specimen Geometric Center .....	6-42
Table 6-26	Comparison of Calculated and Best Estimate Exposure Levels for Kewaunee Surveillance Capsules at Specimen Geometric Center .....	6-43
Table 6-27	Neutron Exposure Projections at Key Locations on the Pressure Vessel Clad / Base Metal Interface .....	6-44
Table 6-28	Kewaunee In-Core Fuel Management Forecast (Assumed for Calculation Purposes Only) .....	6-45
Table 6-29	Neutron Exposure Values for the Kewaunee Reactor Vessel .....	6-46
Table 6-30	Updated Lead Factors for Kewaunee Surveillance Capsules .....	6-47
Table 7-1	Kewaunee Reactor Vessel Surveillance Capsule Withdrawal Schedule .....	7-1

## LIST OF ILLUSTRATIONS

Figure 4-1	Arrangement of Surveillance Capsules in the Kewaunee Reactor Vessel .....	8
Figure 4-2	Capsule S Diagram Showing the Location of Specimens, Thermal Monitors, ..... and Dosimeters .....	9
Figure 5-1	Charpy Weld Reconstitution Schematic Showing Process from Start to Finish. Drawing is not to Scale. ....	29
Figure 5-2	Charpy V-Notch Impact Properties for Kewaunee Reactor Vessel Intermediate Shell Forging 122X208VA1 (Tangential Orientation) .....	30
Figure 5-3	Charpy V-Notch Impact Properties for Kewaunee Reactor Vessel Lower Shell Forging 123X167VA1 (Tangential Orientation) .....	31
Figure 5-4	Charpy V-Notch Impact Properties for Kewaunee Reactor Vessel Surveillance Weld Metal .....	32
Figure 5-5	Charpy V-Notch Impact Properties for Kewaunee Reactor Vessel Weld Heat-Affected-Zone Metal .....	33
Figure 5-6	Charpy V-Notch Impact Properties for A533 Grade B Class 1 ASTM Correlation Monitor Material (HSST Plate 02) (Tangential Orientation) .....	34
Figure 5-7	Charpy Impact Specimen Fracture Surfaces for Kewaunee Reactor Vessel Intermediate Shell Forging 122X208VA1 (Tangential Orientation) .....	35
Figure 5-8	Charpy Impact Specimen Fracture Surfaces for Kewaunee Reactor Vessel Lower Shell Forging 123X167VA1 (Tangential Orientation) .....	36
Figure 5-9	Charpy Impact Specimen Fracture Surfaces for Kewaunee Reactor Vessel Surveillance Weld Metal .....	37
Figure 5-10	Charpy Impact Specimen Fracture Surfaces for Kewaunee Reactor Vessel Heat-Affected-Zone Metal .....	38
Figure 5-11	Charpy Impact Specimen Fracture Surfaces for A533 Grade B Class 1 ASTM Correlation Monitor Material ( HSST Plate 02) .....	39
Figure 5-12	Tensile Properties for Kewaunee Reactor Vessel Intermediate Shell Forging 122X208VA1 (Tangential Orientation) .....	40
Figure 5-13	Tensile Properties for Kewaunee Reactor Vessel Lower Shell Forging 123X167VA1 (Tangential Orientation) .....	41

---

**LIST OF ILLUSTRATIONS (Continued)**

Figure 5-14	Tensile Properties for Kewaunee Reactor Vessel Surveillance Weld Metal .....	42
Figure 5-15	Fractured Tensile Specimens from Kewaunee Reactor Vessel Intermediate Shell Forging 122X208VA1 (Tangential Orientation) .....	43
Figure 5-16	Fractured Tensile Specimens from Kewaunee Reactor Vessel Lower Shell Forging 123X167VA1 (Tangential Orientation) .....	44
Figure 5-17	Fractured Tensile Specimens from Kewaunee Reactor Vessel Surveillance Weld Metal .....	45
Figure 5-18	Engineering Stress-Strain Curves for Intermediate Shell Forging 122X208VA1 Tensile Specimens P10 and P9 (Tangential Orientation) .....	46
Figure 5-19	Engineering Stress-Strain Curves for Intermediate Shell Forging 122X208VA1 Tensile Specimens P11 and P12 (Tangential Orientation) .....	47
Figure 5-20	Engineering Stress-Strain Curves for Lower Shell Forging 123X167VA1 Tensile Specimens S7 and S8 (Tangential Orientation) .....	48
Figure 5-21	Engineering Stress-Strain Curve for Lower Shell Forging 123X167VA1 Tensile Specimen S9 (Tangential Orientation) .....	49
Figure 5-22	Engineering Stress-Strain Curves for Weld Metal Tensile Specimens W5 and W6 .....	50
Figure 5-23	Unirradiated Kewaunee Surveillance Weld Master Curve Fit for ½T-CT Specimens .....	51
Figure 5-24	Unirradiated Kewaunee Surveillance Weld Master Curve Fit for Precracked Charpy Size 3PB Specimens .....	51
Figure 5-25	Unirradiated Kewaunee Surveillance Weld Master Curve Fit for Precracked and Reconstituted Charpy Size 3PB Specimens .....	52
Figure 5-26	Irradiated Kewaunee Surveillance Weld Master Curve Fit for Precracked and Reconstituted Charpy Size 3PB Specimens .....	52
Figure 5-27	Irradiated Maine Yankee Surveillance Weld Master Curve Fit for Precracked and Reconstituted Charpy Size 3PB Specimens .....	53
Figure 5-28	Unirradiated Maine Yankee Surveillance Weld Master Curve Fit for Precracked Charpy Size 3PB Specimens .....	53
Figure 6-1	Plan View of Reactor Vessel Surveillance Capsule .....	6-11

## 1.0 SUMMARY OF RESULTS

The evaluation of the reactor vessel materials primarily has focused on the weld metal contained in surveillance Capsule S, the fourth capsule removed from the Kewaunee reactor pressure vessel surveillance program. Additionally, the weld metal in capsule A-35, the second accelerated capsule removed from the Maine Yankee surveillance program, has been tested and evaluated. The following conclusions have been drawn:

### 1.1 FLUENCE EVALUATION

#### 1.1.1 Kewaunee Capsule S

- The capsule received an average fast neutron fluence ( $E > 1.0$  MeV) of  $3.36 \times 10^{19}$  n/cm<sup>2</sup> determined using the latest ENDF/B-VI dosimetry cross sections after 16.2 effective full power years (EFPY) of plant operation. This value is compared to a fluence ( $E > 1.0$  MeV) of  $3.45 \times 10^{19}$  n/cm<sup>2</sup> in 1995 calculated using the ENDF/B-V dosimetry cross sections.
- The calculated end-of-life (33 EFPY) and extended life (51 EFPY) maximum neutron fluences ( $E > 1.0$  MeV) using the latest ENDF/B-VI dosimetry cross sections for the Kewaunee reactor vessel are as follows:

	33 EFPY	51 EFPY
Vessel inner radius =	$3.34 \times 10^{19}$ n/cm <sup>2</sup>	$5.06 \times 10^{19}$ n/cm <sup>2</sup>
Vessel 1/4 thickness =	$2.15 \times 10^{19}$ n/cm <sup>2</sup>	$3.26 \times 10^{19}$ n/cm <sup>2</sup>
Vessel 3/4 thickness =	$6.74 \times 10^{18}$ n/cm <sup>2</sup>	$1.02 \times 10^{19}$ n/cm <sup>2</sup>

\* Clad/base metal interface

#### 1.1.2 Maine Yankee Capsule A-35

- The capsule received an average fast neutron fluence ( $E > 1.0$  MeV) of  $6.11 \times 10^{19}$  n/cm<sup>2</sup> determined using the latest ENDF/B-VI dosimetry cross sections after 4.5 effective full power years (EFPY) of plant operation.

## 1.2 CHARPY V-NOTCH IMPACT TESTS

#### 1.2.1 Kewaunee Capsule S

- Irradiation of the reactor vessel intermediate shell forging 122X208VA1 Charpy specimens, oriented with the longitudinal axis of the specimen parallel to the working direction of the forging (tangential orientation), to  $3.36 \times 10^{19}$  n/cm<sup>2</sup> ( $E > 1.0$  MeV) resulted in a 30 ft-lb transition temperature increase of 60°F and a 50 ft-lb transition temperature increase of 35°F. This results in an irradiated 30 ft-lb transition temperature of 35°F and an irradiated 50 ft-lb transition temperature of 50°F for the tangentially oriented specimens.



- The average upper shelf energy of the intermediate shell forging 122X208VA1 (tangential orientation) resulted in an average energy decrease of 12 ft-lb after irradiation to  $3.36 \times 10^{19}$  n/cm<sup>2</sup> (E > 1.0 MeV). This results in an irradiated average upper shelf energy of 148 ft-lb for the tangentially oriented specimens.
- Irradiation of the 1P3571 weld metal Charpy specimens to  $3.36 \times 10^{19}$  n/cm<sup>2</sup> (E > 1.0 MeV) resulted in a 30 ft-lb transition temperature increase of 250°F and a 50 ft-lb transition temperature increase of 268°F. This results in an irradiated 30 ft-lb transition temperature of 200°F and an irradiated 50 ft-lb transition temperature of 258°F.
- The average upper shelf energy of the weld metal Charpy specimens resulted in an average energy decrease of 62 ft-lb after irradiation to  $3.36 \times 10^{19}$  n/cm<sup>2</sup> (E > 1.0 MeV). This results in an irradiated average upper shelf energy of 64 ft-lb for the weld metal specimens.

### 1.2.2 Maine Yankee Capsule A-35

- No measurements of Charpy V-notch were performed under the program. Charpy V-notch test results are not used in this report. Since the Charpy V-notch specimens were reconstituted for Master Curve fracture toughness testing, the original Charpy results are of interest as reported in WCAP-9875 issued in 1981.

## 1.3 "MASTER CURVE" FRACTURE TOUGHNESS TESTS

### 1.3.1 Kewaunee Capsule S

- Irradiation of the Kewaunee weld metal precracked three point bend reconstituted Charpy specimens to  $3.36 \times 10^{19}$  n/cm<sup>2</sup> (E > 1.0 MeV) resulted in a Master Curve T<sub>0</sub> transition temperature increase of 284°F following ASTM E1921-97. This results in an irradiated T<sub>0</sub> transition temperature of 136°F, based upon an initial unirradiated T<sub>0</sub> value of -148°F determined from precracked Charpy specimens. Unirradiated tests using 1/2-T compact specimens (1/2T-CT) and reconstituted precracked Charpy specimens resulted in values of the initial unirradiated T<sub>0</sub> of -129°F and -154°F, respectively.

### 1.3.2 Maine Yankee A-35 Capsule

- Irradiation of the Maine Yankee weld metal precracked three point bend reconstituted Charpy specimens to  $6.11 \times 10^{19}$  n/cm<sup>2</sup> (E > 1.0 MeV) resulted in a Master Curve T<sub>0</sub> transition temperature increase of 390°F following ASTM E1921-97. This results in an irradiated T<sub>0</sub> transition temperature of 232°F, based upon an initial T<sub>0</sub> value of -158°F as determined from precracked Charpy specimens.

## 1.4 ANALYSIS

### 1.4.1 Kewaunee Charpy V-notch Toughness

- A comparison of the Kewaunee reactor vessel beltline material test results with the Regulatory Guide 1.99, Revision 2, predictions led to the following conclusions:
  - The intermediate shell forging 122X208VA1 material measured 30 ft-lb transition temperature increase for Capsule S is greater by 11°F than the Regulatory Guide 1.99, Revision 2, prediction. However, Regulatory Guide 1.99, Revision 2, requires a 2 sigma allowance of 34°F for base metal be added to the predicted reference transition temperature to obtain a conservative upper bound value.
  - The measured 30 ft-lb transition temperature increase for the weld metal is less than the Regulatory Guide 1.99, Revision 2, prediction for fluences greater than  $2.74 \times 10^{19}$  n/cm<sup>2</sup>, but less than the Regulatory Guide prediction for lower fluences. On average, the data for the weld metal are close to the Regulatory Guide predictions.
  - The surveillance Capsule S test results indicate that all of the surveillance material average upper shelf energy decreases are less than the Regulatory Guide 1.99, Revision 2, predictions.
- The Regulatory Guide 1.99, Revision 2, credibility evaluation of the Kewaunee surveillance program weld metal presented in Appendix B of this report indicates that the Kewaunee reactor vessel surveillance results are credible.
- The initial  $RT_{NDT}$  evaluation for the Kewaunee surveillance weld metal (weld wire heat 1P3571) presented in Appendix C of this report indicates that the initial  $RT_{NDT}$  is -50°F.
- The Capsule S surveillance results (if assumed to be adequate surrogates of the reactor vessel) indicate that the beltline region materials should have adequate toughness throughout the life of the vessel (33 EFPY) since the measured Capsule S fluence is approximately equal to the peak vessel inner surface fluence at 33 EFPY.
- All beltline surveillance materials exhibit a more than adequate upper shelf energy level for continued safe plant operation and are expected to maintain an upper shelf energy greater than 50 ft-lb throughout the life of the vessel (33 EFPY) as required by 10CFR50, Appendix G.

### 1.4.2 "Master Curve" Fracture Toughness

- The Master Curve based transition temperature increase ( $\Delta T_0$ ) in accordance with ASTM E1921-97, using only precracked Charpy specimens, is higher than the 30 ft-lb Charpy V-notch based transition temperature increase (284°F vs. 250°F) for the Kewaunee surveillance weld metal.
- Based on all of the test data combined, using the multi-temperature maximum likelihood evaluation method, an increase of 292°F in the Master Curve  $T_0$  transition temperature for the Kewaunee surveillance weld is obtained. This was based on the maximum likelihood initial  $T_0$  of -144°F (from the combined results of 1/2 T compact specimens, precracked Charpy specimens, and reconstituted precracked Charpy specimens) and an irradiated condition  $T_0$  of 148°F (from the results of irradiated reconstituted precracked Charpy specimens and 1XWOL specimens). This result is 8°F higher than the result obtained using only precracked Charpy specimens.
- Master Curve transition temperature data for the Maine Yankee surveillance weld, when analyzed using the multi-temperature maximum likelihood method, yields the same results as those generated following ASTM E1921-97. As for the Kewaunee surveillance weld, the Master Curve transition temperature increase ( $\Delta T_0$ ) is higher than the 30 ft-lb Charpy V-notch transition temperature (390°F vs. 345°F) for the Maine Yankee surveillance weld.

## 2.0 INTRODUCTION

This report presents the results of the supplemental tests and evaluation of Capsule S, the fourth capsule removed from the reactor in the continuing surveillance program which monitors the effects of neutron irradiation on the Wisconsin Public Service Corporation (WPSC) Kewaunee Nuclear Power Plant reactor pressure vessel materials under actual operating conditions. The results of the evaluation of the Capsule S were originally reported in Revision 0 of this report in 1995<sup>[1]</sup>. This report, Revision 1, is issued to add the following supplemental tests and evaluation:

- 1) the results of the Master Curve fracture toughness testing of the Kewaunee archive weld material and Capsule S reconstituted precracked Charpy specimens
- 2) the results of the Master Curve fracture toughness testing of the Maine Yankee Capsule A-35 reconstituted precracked Charpy specimens
- 3) fluence evaluation of all of the Kewaunee surveillance capsules and the Maine Yankee Capsule A-35 using the latest ENDF/B-VI<sup>[2]</sup> dosimetry cross sections.

The Master Curve fracture toughness approach, a new methodology, was initiated as an industry program involving the three pressurized water reactor owners groups: Westinghouse Owners Group (WOG), B&W Reactor Vessel Owners Group (B&W/RVOG), and Combustion Engineering Reactor Vessel Working Group (CE/RVWG). Each owners group selected reactor vessel steels including welds, that are applicable to the reactor vessels covered under each of the owners group. WOG selected SA533 B-1 plate, Linde 1092 weld metal, and Linde 0091 weld metal. The selected vessel materials were represented by the archive and surveillance capsule materials available. For the Linde 1092 weld metal, the Kewaunee surveillance weld was selected as agreed to by WPSC. The Kewaunee surveillance weld metal corresponds to the circumferential weld in the Kewaunee reactor vessel and is the limiting material for reactor vessel integrity evaluation.

WPSC took the WOG program as an opportunity to further develop a supplemental testing program. The WOG program was designed to test both the unirradiated and irradiated fracture toughness of this Linde 1092 weld using archive and surveillance Capsule S material. As a part of the supplemental test program, WPSC decided to add another surveillance capsule material of Linde 1092 weld from the Maine Yankee (MY) surveillance program. The additional Linde 1092 weld from the MY surveillance weld was a coordinated effort by American Electric Power Service Corporation (AEP), WPSC and MY. Both Kewaunee and Maine Yankee reactor vessels and surveillance welds were fabricated from the same weld wire heat, 1P3571, using a Linde 1092 flux, flux lot 3958. The reactor vessel of the D.C. Cook 1 power plant operated by AEP also includes the same Linde 1092 weld.

The irradiated fracture toughness testing of the Maine Yankee surveillance weld was included as a part of the WPSC supplement to the WOG test program. The unirradiated testing of the

Maine Yankee surveillance weld was reported as part of the CE/RVWG program. The results of the unirradiated condition are utilized in the supplemental program.

In 1995 when surveillance Capsule S was removed and tested, the ENDF/B-V dosimetry cross sections was used to evaluate the applicable fluence. Since 1995, the Kewaunee plant has operated two additional fuel cycles and the ENDF/B-VI dosimetry cross sections have become available. Therefore, a fluence re-evaluation was performed using the latest ENDF/B-VI dosimetry cross sections. Also, the fluence for Maine Yankee Capsule A-35 was re-evaluated using the ENDF/B-VI cross sections to make the fluence evaluation method consistent. Note that the other Main Yankee capsules were not re-evaluated using the ENDF/B-VI dosimetry cross sections.

The broken Capsule S weld and HAZ Charpy specimens tested in 1995 were reconstituted into three point bend fracture toughness test specimens, fatigue precracked, and tested in slow bending. The process of reconstitution was qualified using unirradiated Charpy specimens, and the process met the requirements of ASTM E1253<sup>[3]</sup>. Maine Yankee surveillance weld Charpy specimens from Capsule A-35<sup>[4]</sup> were also reconstituted, precracked and tested in slow bending. Maine Yankee capsule A-35 was the second accelerated capsule, which was removed after 4.5 EFPY and exposed to a higher fluence than Kewaunee capsule S. The Maine Yankee surveillance weld was fabricated as mentioned earlier, using the same B-4 weld wire heat, 1P3571, and Linde 1092 flux, lot 3958, as the Kewaunee surveillance weld. The testing and results for the Maine Yankee reconstituted irradiated specimens are included in this report, as well as the results obtained elsewhere for the Maine Yankee unirradiated weld metal.

The surveillance program for the WPSC Kewaunee reactor pressure vessel materials was designed and recommended by the Westinghouse Electric Corporation. A description of the surveillance program and the preirradiation mechanical properties of the reactor vessel materials is presented in WCAP-8107, "Wisconsin Public Service Corp. Kewaunee Nuclear Power Plant Reactor Vessel Radiation Surveillance Program"<sup>[5]</sup>. The surveillance program was planned to cover the 40-year design life of the reactor pressure vessel and was based on ASTM E185-70, "Recommended Practice for Surveillance Tests on Nuclear Reactor Vessels".<sup>[6]</sup> Capsule S was removed from the reactor after 16.2 EFPY of exposure and shipped to the Westinghouse Science and Technology Center Hot Cell Facility, where the postirradiation mechanical testing of the Charpy V-notch impact and tensile surveillance specimens was performed. The fracture toughness testing of both the Kewaunee and Maine Yankee surveillance welds was also conducted at the Westinghouse Science and Technology Center Hot Cell facility.

### 3.0 BACKGROUND

The ability of the large steel pressure vessel containing the reactor core and its primary coolant to resist fracture constitutes an important factor in ensuring safety in the nuclear industry. The beltline region of the reactor pressure vessel is the most critical region of the vessel because it is subjected to significant fast neutron bombardment. The overall effects of fast neutron irradiation on the mechanical properties of low alloy, ferritic pressure vessel steels such as SA 508 Class 2 (base material of the Kewaunee reactor pressure vessel beltline) and associated welds are well documented in the literature. Generally, low alloy ferritic materials show an increase in hardness and tensile properties and a decrease in ductility and toughness during high-energy neutron irradiation.

A method for ensuring the integrity of reactor pressure vessels has been presented in "Protection Against Nonductile Failure," Appendix G to Section III of the ASME Boiler and Pressure Vessel Code<sup>[7]</sup>. The method uses fracture mechanics concepts and is based on the reference nil-ductility transition temperature ( $RT_{NDT}$ ).

$RT_{NDT}$  is defined as the greater of either the drop weight nil-ductility transition temperature (NDTT per ASTM E-208<sup>[8]</sup>) or the temperature 60°F less than the minimum 50 ft-lb (and 35-mil lateral expansion) temperature as determined from Charpy specimens oriented normal (transverse) to the major working direction of the plate or forging. The  $RT_{NDT}$  of a given material is used to index that material to a reference stress intensity factor curve ( $K_{IR}$  curve) which appears in Appendix G to the ASME Code. The  $K_{IR}$  curve is a lower bound of dynamic, crack arrest, and static fracture toughness results obtained from several heats of pressure vessel steel. When a given material is indexed to the  $K_{IR}$  curve, allowable stress intensity factors can be obtained for this material as a function of temperature. Allowable operating limits can then be determined using these allowable stress intensity factors.

$RT_{NDT}$  and, in turn, the operating limits of nuclear power plants can be adjusted to account for the effects of radiation on the reactor vessel material properties. The changes in mechanical properties of a given reactor pressure vessel steel, due to irradiation, can be monitored by a reactor surveillance program, such as the Kewaunee reactor vessel radiation surveillance program, in which a surveillance capsule is periodically removed from the operating nuclear reactor and the encapsulated specimens tested. The increase in the average Charpy V-notch 30 ft-lb temperature ( $\Delta RT_{NDT}$ ) due to irradiation is added to the initial  $RT_{NDT}$  to adjust the  $RT_{NDT}$  for radiation embrittlement. This adjusted reference temperature (ART) ( $RT_{NDT}$  initial +  $\Delta RT_{NDT}$  + margin), is used to index the material to the  $K_{IR}$  curve and, in turn, to set operating limits for the nuclear power plant that take into account the effects of irradiation on the reactor vessel materials.

The Code of Federal Regulations, 10 CFR Part 50<sup>[9]</sup>, deals with reactor pressure vessel integrity, primarily through Appendix G and the PTS Rule (10 CFR 50.61).<sup>[10]</sup> Prior to about 1992, the requirements included an alternative method of meeting the intent of the requirements when screening criteria concerning upper shelf or PTS could not be met before end of operating life. One of the alternatives was to generate irradiated fracture toughness data to show that

adequate safety margin exists for the material(s) of concern. This alternative requirement for producing fracture toughness data for irradiated surveillance capsule weld metal (1P3571) has been taken for the Kewaunee vessel. In addition to the standard surveillance capsule testing performed using Charpy V-notch and tensile specimens, reconstituted precracked Charpy specimens have been tested to demonstrate the fracture toughness behavior of the Kewaunee and Maine Yankee irradiated weld metals.

Reconstituted precracked Charpy specimens in the irradiated condition and 1/2T-CT, precracked whole Charpy, and reconstituted precracked Charpy specimens in the unirradiated condition have been tested in accordance with ASTM E1921-97.<sup>[11]</sup> The ASTM Standard Test Method was finalized and published in late 1997. The Master Curve fracture toughness testing for this program was initiated when the ASTM Standard was still in draft form. When the ASTM Standard was approved in 1997, all the test data generated to the draft were re-evaluated to fully satisfy ASTM E1921-97.

The Master Curve fracture toughness transition temperature,  $T_o$ , has been generated and applied in the same manner as the traditional Charpy V-notch toughness based approach to evaluate the integrity of the Kewaunee reactor vessel (see WCAP-15075).<sup>[12]</sup>

$T_o$  values were determined in accordance with ASTM E-1921-97 in this report, and the multi-temperature, maximum likelihood method of determining  $T_o$  was also used. The application methodology and appropriate descriptions are contained in WCAP-15074<sup>[13]</sup> and WCAP-15075.<sup>[12]</sup>

## 4.0 DESCRIPTION OF TESTING PROGRAM

As explained in the Section 2.0 INTRODUCTION, this report presents the results of two main programs: 1) the Kewaunee Capsule S test program performed in 1995 and 2) the WOG /WPSC/AEP supplemental test program. The supplemental test program primarily consists of performing the Master Curve fracture toughness testing of both the Kewaunee and Maine Yankee surveillance welds (Linde 1092 weldments of heat number 1P3571). The supplemental test program includes fluence evaluation using the latest ENDF/B-VI dosimetry cross sections on the Kewaunee capsules and the Maine Yankee A-35 capsule. Results of the fluence evaluation are reported in Section 6.0 of this report.

Six surveillance capsules for monitoring the effects of neutron exposure on the Kewaunee reactor pressure vessel core region (beltline) materials were inserted in the reactor vessel prior to initial plant start-up. The six capsules were positioned in the reactor vessel between the thermal shield and the vessel wall as shown in Figure 4-1. The vertical center of the capsules is opposite the vertical center of the core. The capsules contain specimens made from intermediate shell forging 122X208VA1, lower shell forging 123X167VA1 and weld metal fabricated with 3/16-inch Mil B-4 weld filler wire, heat number 1P3571 and Linde 1092 flux, lot number 3958. This is the identical weld wire heat and flux as that used in the actual fabrication of the Kewaunee vessel intermediate to lower shell girth weld seam, which has been the limiting beltline material in the Kewaunee reactor pressure vessel. To date, four surveillance capsules have been removed and evaluated: Capsules V, R, P, and S.

Capsule S, the most recent surveillance capsule, was removed after 16.2 effective full power years (EFPY) of plant operation. This capsule contained Charpy V-notch, tensile, and 1X Wedge Opening Loading (WOL) fracture mechanics specimens made from intermediate shell forging 122X208VA1, lower shell forging 123X167VA1 and submerged arc weld metal identical to the closing girth weld seam. In addition, this capsule contained Charpy V-notch specimens from the weld Heat-Affected-Zone (HAZ) of forging 122X208VA1 and from the 12-inch thick ASTM correlation monitor material (HSST plate 02).

All test specimens were machined from the 1/4 thickness location of the forgings after performing a simulated postweld, stress-relieving treatment on the test material. The test specimens represent material taken at least one forging thickness from the quenched ends of the forging. Specimens were machined from weld and HAZ metal from a stress-relieved weldment joining intermediate shell forging 122X208VA1 and lower shell forging 123X167VA1. All heat-affected-zone specimens were obtained from the weld heat-affected-zone of intermediate shell forging 122X208VA1.

Maine Yankee Capsule A-35 was the second accelerated surveillance capsule removed and tested in early 1980s. The surveillance Capsule A-35 was selected because it had been exposed to a fluence of equivalent to the extended end-of-life for the Kewaunee vessel. Results of the tests were reported in WCAP-9875. The Charpy V-notch and tensile results were not duplicated in this report since the data were not required. Broken Charpy specimens were used to reconstitute three-point bend fracture toughness specimens for the Master Curve testing.



## 4.1 CHARPY V-NOTCH IMPACT AND TENSILE TESTS

### 4.1.1 Kewaunee

All base metal Charpy V-notch impact and tensile specimens were machined with the longitudinal axis of the specimen parallel to the principal working direction of the forgings. The notch of the forging Charpy specimens was machined such that the direction of crack propagation in the specimen was in transverse to the working direction. This orientation is termed as "tangential". Charpy V-notch and tensile specimens from the weld metal were oriented such that the longitudinal axis of the specimen was normal to the welding direction. The notch of the weld metal Charpy specimens was machined such that the direction of crack propagation in the specimen was in the welding direction.

The chemical composition and heat treatment of the surveillance material is presented in Tables 4-1 through 4-4. The data in Tables 4-1 through 4-4 were obtained from the unirradiated surveillance program, WCAP-8107 Appendices A and B, and WCAP-15074.

### 4.1.2 Maine Yankee

No Charpy V-notch impact and tensile tests were performed as part of this program for Maine Yankee Capsule A-35. The Charpy V-notch weld metal specimens used for reconstitution were oriented in the same orientation as those for the Kewaunee surveillance weld.

## 4.2 DOSIMETERS AND THERMAL MONITORS

### 4.2.1 Kewaunee

Capsule S contained dosimeter wires of pure copper, iron, nickel, and aluminum-0.15 weight percent cobalt (cadmium-shielded and unshielded). In addition, cadmium shielded dosimeters of neptunium ( $\text{Np}^{237}$ ) and uranium ( $\text{U}^{238}$ ) were placed in the capsule to measure the integrated flux at specific neutron energy levels.

The capsule contained thermal monitors made from two low-melting-point eutectic alloys and sealed in Pyrex tubes. These thermal monitors were used to define the maximum temperature attained by the test specimens during irradiation. The composition of the two eutectic alloys and their melting points are as follows:

2.5% Ag, 97.5% Pb

Melting Point: 579°F (304°C)

1.75% Ag, 0.75% Sn, 97.5% Pb

Melting Point: 590°F (310°C)

The arrangement of the various mechanical specimens, dosimeters and thermal monitors contained in capsule S is shown in Figure 4-2.

## 4.2.2 Maine Yankee

Capsule A-35 contents and their evaluation in March 1981 are described in WCAP-9875. Note that the dosimetry analysis has been re-evaluated here using the ENDF/B-VI dosimetry reaction cross-section library.

## 4.3 MASTER CURVE TESTS FOR KEWAUNEE AND MAINE YANKEE SURVEILLANCE WELDS

Testing of Kewaunee surveillance weld archive material and reconstituted Charpy specimens to directly measure the fracture toughness properties was a part of the Westinghouse Owners Group (WOG) sponsored "Master Curve" testing program. The Kewaunee surveillance weld was selected for the WOG program to represent typical Linde 1092 weld material.

Reconstituted irradiated Charpy size specimens of the Maine Yankee surveillance weld from Capsule A-35 were added to the program (as a sister Linde 1092 weld material) with a higher fluence than the Kewaunee surveillance weld from Capsule S. The testing program for the two Linde 1092 weld materials (heat 1P3571) tested under the WOG program is shown below.

Surveillance Weld	Neutron Fluence (n/cm <sup>2</sup> ; E>1 MeV)	Specimen Type	Reconstituted or Whole
Kewaunee	0	1/2T-CT PCVN PCVN	Whole Whole Reconstituted
Kewaunee	3.36 x 10 <sup>19</sup>	PCVN 1XWOL <sup>a</sup>	Reconstituted Whole
Maine Yankee	0	PCVN <sup>b</sup>	Whole
Maine Yankee	6.11 x 10 <sup>19</sup>	PCVN	Reconstituted

a. Limited to only two specimens

b. Not tested by Westinghouse as a part of this program -- results provided by WPSC.

The archive weld material available at Westinghouse was used to machine 1/2T-CT and Charpy size three point bend specimens to measure the fracture toughness properties in the unirradiated condition. Broken Charpy impact specimens were reconstituted and machined to Charpy size three point bend specimen for the fracture toughness in both the unirradiated and irradiated conditions. All "Master Curve" fracture toughness testing was performed in accordance with the draft version of ASTM E1921. When the ASTM E1921 Standard Test Method was published in November 1997, all of the results of the "Master Curve" fracture toughness tests were re-evaluated in accordance with the finalized ASTM E1921-97. These results were found to satisfy the requirements of ASTM E1921-97 in its entirety. Additionally, all of the fracture toughness data for each material/condition were pooled together, and a multi-temperature evaluation process was employed to evaluate the Master Curve transition temperature (T<sub>0</sub>). See WCAP-15075.

All the 1XWOL test specimens were machined with the simulated crack in the specimen perpendicular to the hoop direction and the major surfaces of the shell ring forging. This orientation is known as "tangential" The 1XWOL test specimens were fatigue precracked consistent with the requirements of ASTM E1921-97.

**Table 4-1 Chemical Composition (wt%) of the Kewaunee Reactor Vessel Beltline Region Surveillance Material<sup>[5]</sup>**

Element	Intermediate Shell Forging 122X208VA1	Lower Shell Forging 123X167VA1	Weld Metal
C	0.21	0.20	0.12
Si	0.25	0.28	0.20
Mo	0.58	0.58	0.48
Cu	0.06	0.06	0.219 <sup>(a)</sup>
Ni	0.71	0.75	0.724 <sup>(a)</sup>
Mn	0.69	0.79	1.37
Cr	0.40	0.35	0.090
V	<0.02	<0.02	0.002
Co	0.011	0.012	<0.001
Sn	0.01	0.01	0.004
Ti	<0.001	<0.001	<0.001
Zr	0.001	0.001	<0.001
As	0.001	0.004	0.004
Sb	<0.001	0.001	0.001
S	0.011	0.009	0.011
P	0.01	0.01	0.016
Al	0.004	0.006	0.010
B	<0.003	<0.003	<0.003
N <sub>2</sub>	0.006	0.010	0.012
Zn	--	--	<0.001

(a) Based upon averaged results as described in report WCAP-15074.<sup>[13]</sup>

**Table 4-2 Heat Treatment of the Kewaunee Reactor Vessel Beltline Region Surveillance Material<sup>[5]</sup>**

Material	Temperature (°F)	Time (hr)	Coolant
Intermediate Shell Forging 122X208VA1	Austenitized @ 1550	8	Water quenched
	Tempered @ 1230	14	Air cooled
	Stress Relieved @ 1150	21	Furnace cooled
Lower Shell Forging 123X167VA1	Austenitized @ 1550	8	Water quenched
	Tempered @ 1220	14	Air cooled
	Stress Relieved @ 1150	21	Furnace cooled
Weldment	Stress Relieved @ 1150	19-1/4	Furnace cooled

**Table 4-3 Chemical Composition of the A533 Grade B, Class 1 ASTM Correlation Monitor Material (HSST Plate 02) in the Kewaunee Reactor Vessel Surveillance Program<sup>[5]</sup>**

Element	Chemical Analysis (wt. %)
C	0.22
Mn	1.48
P	0.012
S	0.018
Si	0.25
Ni	0.68
Mo	0.52
Cu	0.14

**Table 4-4 Heat Treatment of the A533 Grade B, Class 1 ASTM Correlation Monitor Material (HSST Plate 02) in the Kewaunee Reactor Vessel Surveillance Program**

Temperature (°F)	Time (hr)	Coolant
1675 ± 25	4	Air cooled
1600 ± 25	4	Water quenched
Tempered @ 1225 ± 25	4	Furnace cooled
Stress Relieved @ 1150 ± 25	40	Furnace cooled to 600°F

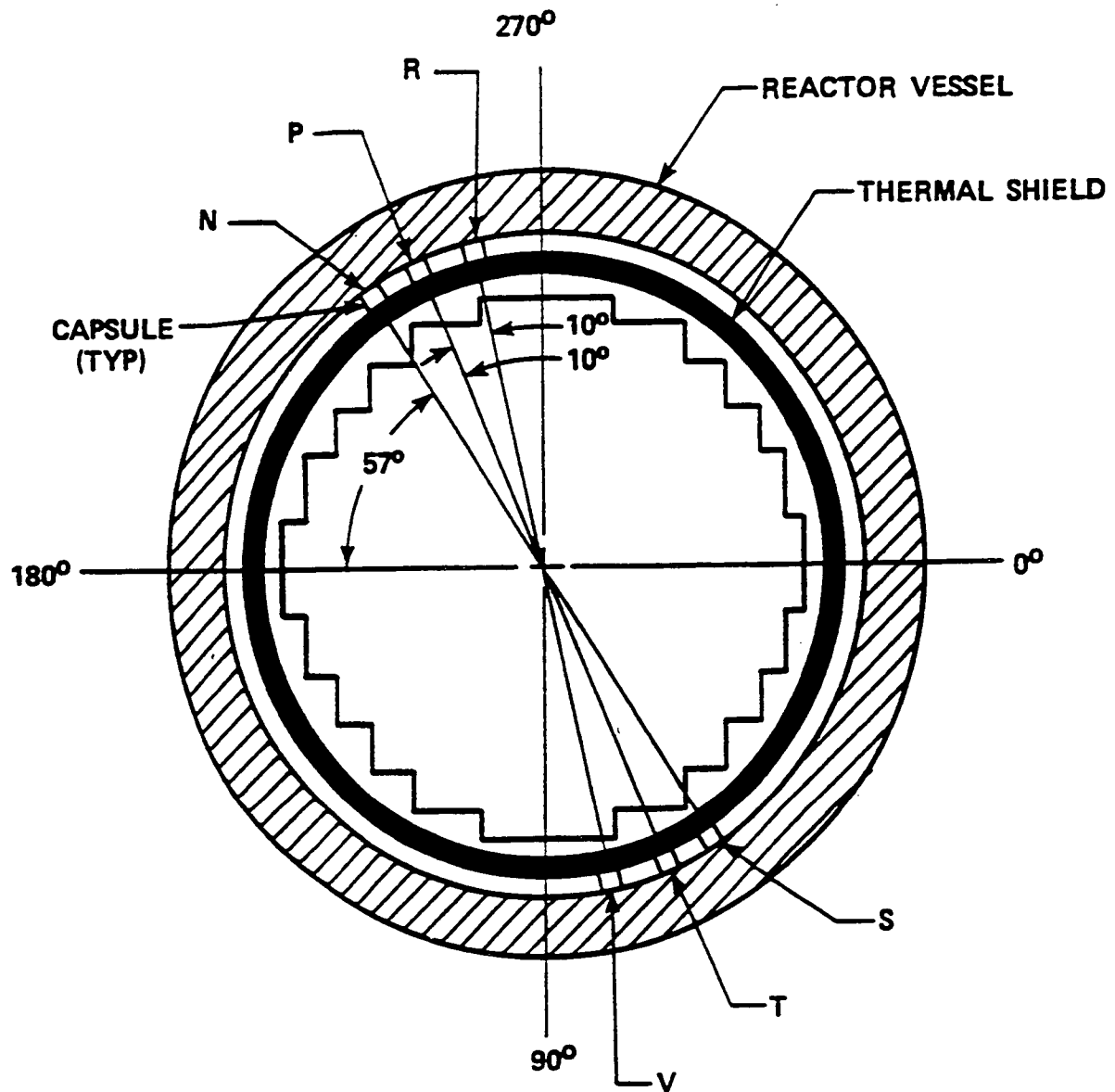
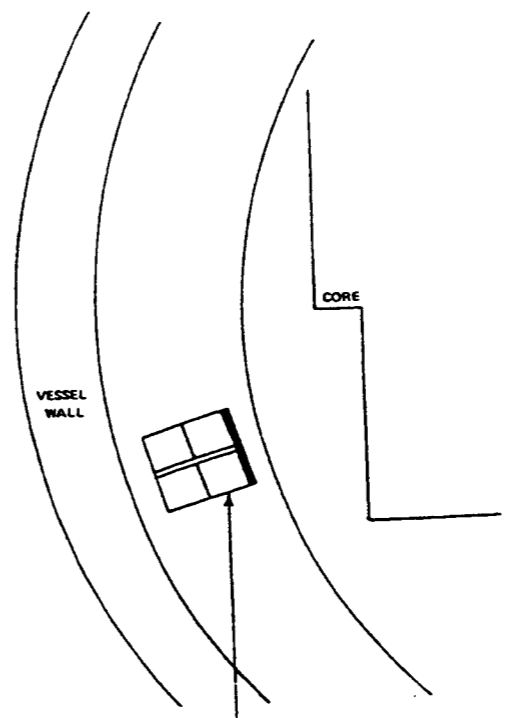
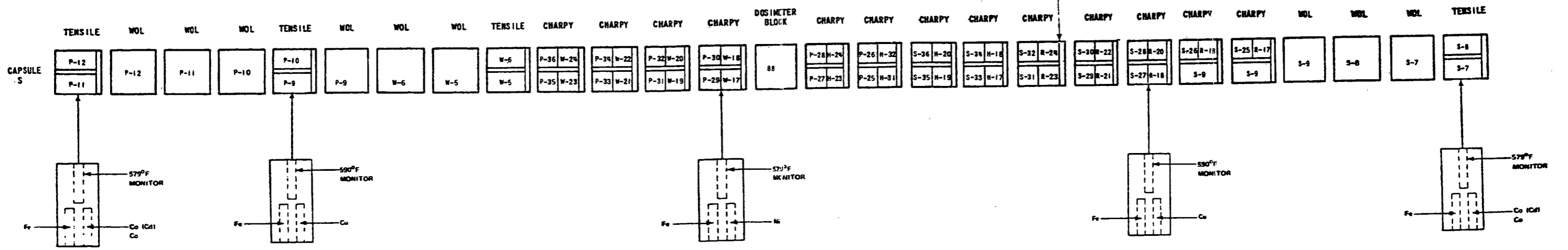


Figure 4-1 Arrangement of Surveillance Capsules in the Kewaunee Reactor Vessel

SPECIMEN NUMBERING CODE  
 P - FORGING 122X208VA1  
 S - FORGING 123X167VA1  
 W - WELD METAL  
 H - HEAT AFFECTED ZONE  
 R - ASTM CORRELATION MONITOR



*APR 1978*  
*CHS*



9811240258-01

Figure 4-2. Capsule S Diagram Showing the Location of Specimens, Thermal Monitors, and Dosimeters



## 5.0 TESTING METHODS AND RESULTS

### 5.1 OVERVIEW OF TESTING METHODS

The post-irradiation mechanical testing of the Charpy V-notch impact specimens, tensile specimens, and Master Curve fracture toughness test specimens was performed in the Remote Metallographic Facility at the Westinghouse Science and Technology Center. Testing was performed in accordance with 10CFR50, Appendices G and H, ASTM Specification E185-82, ASTM E1921-97, ASTM E1253, and Westinghouse Procedure MHL 8402, Revision 2 as modified by Westinghouse RMF Procedures 8102, Revision 1, and 8103, Revision 1. The Westinghouse procedures have been audited to the Westinghouse ESBU Quality Assurance program.

Upon receipt of the capsule at the hot cell laboratory, the specimens and spacer blocks were carefully removed, inspected for identification number, and checked against the master list in WCAP-8107. No discrepancies were found.

Examination of the two low-melting point 579°F (304°C) and 590°F (310°C) eutectic alloys indicated no melting of either type of thermal monitor. Based on this examination, the maximum temperature to which the test specimens were exposed was less than 579°F (304°C).

#### 5.1.1 Charpy V-notch Impact Tests

The Charpy impact tests were performed per ASTM Specification E23-93a<sup>(14)</sup> and RMF Procedure 8103, Revision 1, on a Tinius-Olsen Model 74, 358J machine. The tup (striker) of the Charpy impact test machine is instrumented with a GRC 830-I instrumentation system, feeding information into an IBM compatible 486 computer. With this system, load-time and energy-time signals can be recorded in addition to the standard measurement of Charpy energy ( $E_D$ ). From the load-time curve (Appendix A), the load of general yielding ( $P_{GY}$ ), the time to general yielding ( $t_{GY}$ ), the maximum load ( $P_M$ ), and the time to maximum load ( $t_M$ ) can be determined. Under some test conditions, a sharp drop in load indicative of fast fracture was observed. The load at which fast fracture was initiated is identified as the fast fracture load ( $P_F$ ), and the load at which fast fracture terminated is identified as the arrest load ( $P_A$ ). The energy at maximum load ( $E_M$ ) was determined by comparing the energy-time record and the load-time record. The energy at maximum load is approximately equivalent to the energy required to initiate a crack in the specimen. Therefore, the propagation energy for the crack ( $E_p$ ) is the difference between the total energy to fracture ( $E_D$ ) and the energy at maximum load ( $E_M$ ).

The yield stress ( $\sigma_Y$ ) was calculated from the three-point bend formula having the following expression:

$$\sigma_Y = (P_{GY} * L) / [B * (W - a)^2 * C] \quad (1)$$

where:

L = distance between the specimen supports in the impact machine

- B = the width of the specimen measured parallel to the notch  
 W = height of the specimen, measured perpendicularly to the notch  
 a = notch depth

The constant C is dependent on the notch flank angle ( $\phi$ ), notch root radius ( $\rho$ ) and the type of loading (i.e., pure bending or three-point bending). In three-point bending, for a Charpy specimen in which  $\phi = 45^\circ$  and  $\rho = 0.010$  inch, Equation 1 is valid with  $C = 1.21$ . Therefore, (for  $L = 4W$ ),

$$\sigma_Y = (P_{GY} * L) / [B * (W - a)^2 * 1.21] = (3.33 * P_{GY} * W) / [B * (W - a)^2] \quad (2)$$

For the Charpy specimen,  $B = 0.394$  inch,  $W = 0.394$  inch and  $a = 0.079$  inch. Equation 2 then reduces to:

$$\sigma_Y = 33.3 * P_{GY} \quad (3)$$

where  $\sigma_Y$  is in units of psi and  $P_{GY}$  is in units of lbs. The flow stress was calculated from the average of the yield and maximum loads, also using the three-point bend formula in Equation 3.

The symbol A in columns 4, 5, and 6 of Tables 5-6 through 5-10 is the cross-section area under the notch of the Charpy specimens:

$$A = B * (W - a) = 0.1241 \text{ sq. in.} \quad (4)$$

Percent shear was determined from post-fracture photographs using the ratio-of-areas method in compliance with ASTM Specification A370-92<sup>[15]</sup>. The lateral expansion was measured using a dial gage rig similar to that shown in the same specification.

### 5.1.2 Tensile Tests

Tensile tests were performed on a 20,000-pound Instron, split-console test machine (Model 1115) per ASTM Specification E8-93<sup>[16]</sup> and E21-92<sup>[17]</sup>, and RMF Procedure 8102, Revision 1. All pull rods, grips, and pins were made of Inconel 718. The upper pull rod was connected through a universal joint to improve axiality of loading. The tests were conducted at a constant crosshead speed of 0.05 inches per minute throughout the test.

Extension measurements were made with a linear variable displacement transducer extensometer. The extensometer knife edges were spring-loaded to the specimen and operated through specimen failure. The extensometer gage length was 1.00 inch. The extensometer is rated as Class B-2 per ASTM E83-93<sup>[18]</sup>.

Elevated test temperatures were obtained with a three-zone electric resistance split-tube furnace with a 9-inch hot zone. All tests were conducted in air. Because of the difficulty in remotely

attaching a thermocouple directly to the specimen, the following procedure was used to monitor specimen temperatures. Chromel-alumel thermocouples were positioned at the center and at each end of the gage section of a dummy specimen and in each tensile machine gripper. In the test configuration, with a slight load on the specimen, a plot of specimen temperature versus upper and lower tensile machine gripper and controller temperatures was developed over the range from room temperature to 550°F. During the actual testing, the grip temperatures were used to obtain desired specimen temperatures. Experiments have indicated that this method is accurate to  $\pm 2^\circ\text{F}$ .

The yield load, ultimate load, fracture load, total elongation, and uniform elongation were determined directly from the load-extension curve. The yield strength, ultimate strength, and fracture strength were calculated using the original cross-sectional area. The final diameter and final gage length were determined from post-fracture photographs. The fracture area used to calculate the fracture stress (true stress at fracture) and percent reduction in area was computed using the final diameter measurement.

### 5.1.3 Master Curve Fracture Toughness Tests

Specimens were secured in an insulating chamber and cooled with liquid nitrogen for below room temperature tests and were heated in a three zone furnace which surrounded the test fixture for above room temperature tests. A Fluke 2166A Digital Thermometer and J-type thermocouple monitored the temperature in the chamber. Table 5-1 lists the primary test temperatures for all of the specimen groups in this program. The test temperatures were selected based on the recommendations in ASTM E1921-97 as shown below.

$$T = T_{28J} + C \quad (5)$$

where:

$T$  = calculated test temperature ( $^\circ\text{C}$ )

$T_{28J}$  = Charpy V-notch energy of 28 J ( $^\circ\text{C}$ )

$C$  = constant ( $^\circ\text{C}$ ) which is a function of specimen size as shown next.

Specimen Size (nT)	Constant, C ( $^\circ\text{C}$ )
0.4T <sup>a</sup>	-32
0.5T	-28
1T	-18
2T	-8
3T	-1
4T	2

Note: For precracked Charpy specimens, use  $C=50^\circ\text{C}$ .

For CT and 1XWOL tests, a clip gage measured the displacement. Two razor blades attached to the specimen were used to mount the clip gage. For three-point-bend tests, an LVDT was utilized to measure the displacement. This technique offered the significant advantage of directly measuring the load-line displacement, as opposed to the clip gage, which has to be corrected to obtain the load-line displacement. A necessary precaution was keeping the LVDT warm and preventing freezing of its components so that the unloading compliances were correct.

For all unirradiated tests, 150,000 pound Instron Reversible Load Cell measured the force applied to the specimens and a 20,000 pound load cell was used for the irradiated tests. A 2,000 lb load range was used for testing all Charpy-sized three point bend specimens. A 5,000 lb range was used for the 1/2T-CT specimens and the 1XWOL tests used a range of 20,000 lb. Loading was incremental; in other words, loading took place to a certain value, followed by an unloading, then loading to a higher value. Unloadings were used to obtain compliance measurements which are used to estimate stable crack extension from the fatigue pre-crack.

Load and displacement readings, converted to a calibrated voltage signal by Fluke 8842A and Keithly 178 multimeters, went through a Fluke Hydra Data Acquisition Unit, which logged values into a Microsoft Excel data file, and also to Hewlett-Packard 7046A and 7004B XY Recorders, which served as backup to the digital logger.

After material failure, each specimen was warmed to room temperature. The fracture faces were then measured to determine the fatigue pre-crack length. Nine measurements, two of which were edge readings, were taken. The mean edge fatigue pre-crack measurement was calculated, and this value was averaged with the remaining seven values to obtain the overall mean fatigue pre-crack value.

The entire program was performed according to ASTM E1921-97 for determining the fracture toughness transition temperature,  $T_o$ . Table 5-2 shows the maximum  $K_{Ic}$  limits for the 1P3571 welds tested in accordance with the ASTM E1921-97 Test Method using a constraint factor,  $M$ , of 30 as allowed.

#### **5.1.4 Qualification of Reconstituted Charpy Size Three-Point Bend Specimens**

Typically, broken Charpy halves contain a large portion of untested material. This untested material can be machined from a broken half of a sample to obtain an "insert." "End tabs" of similar material can then be welded to the "insert." The welded sample (insert with two end tabs) is machined to obtain a smooth Charpy-sized three-point bend specimen. Note that orientation of the insert is carefully maintained to match the original test orientation.

In order to verify that reconstituted Charpy specimens yielded the same results as the conventional sized Charpy specimen, unirradiated ASTM A533B-1 plate material and unirradiated Kewaunee weld material were tested in both the conventional and reconstituted Charpy-sized three point bend configurations. These results showed that reconstituted samples

produced essentially the same results as conventional samples. These data are shown and summarized in Table 5-19.

Weld reconstitution is used to obtain additional toughness data from previously tested material, specifically previously tested Charpy specimens. ASTM has developed a recommended guide for reconstituted Charpy specimens, "Reconstitution of Irradiated Charpy Specimens," E1253. This guide provides recommendations for Charpy insert size, heat input, reconstitution technique qualification, and dimensional requirements. E1253 was used where it was applicable in this reconstitution program since Charpy sized three-point bend specimens can be precracked and used to determine the fracture toughness properties and the  $T_0$  transition temperature. Figure 5-1 shows the process for obtaining additional specimens from a previously tested Charpy specimen. Note that this figure is for Charpy specimen geometry, and a three point bend fracture toughness specimen could have the notch area configured differently to facilitate fatigue precracking.

## 5.2 CHARPY V-NOTCH IMPACT TEST RESULTS

The results of the Charpy V-notch impact tests performed on the various materials contained in capsule S, which was irradiated to  $3.36 \times 10^{19}$  n/cm<sup>2</sup> ( $E > 1.0$  MeV), are presented in Tables 5-3 through 5-12 and are compared with unirradiated results as shown in Figures 5-2 through 5-6. The transition temperature increases and upper shelf energy decreases for the capsule S materials are summarized in Table 5-13.

The fracture surface appearance of each irradiated Charpy specimen from the various materials is shown in Figures 5-7 through 5-11 and show an increasingly ductile (tougher) fracture appearance with increasing test temperature.

The load-time records for individual instrumented Charpy specimen tests are shown in Appendix A.

### 5.2.1 Forging Material

Irradiation of the reactor vessel intermediate shell forging 122X208VA1 Charpy specimens oriented with the longitudinal axis of the specimen parallel to the working direction of the forging (tangential orientation) to  $3.36 \times 10^{19}$  n/cm<sup>2</sup> ( $E > 1.0$  MeV) (Figure 5-2) resulted in a 30 ft-lb transition temperature increase of 60°F and a 50 ft-lb transition temperature increase of 35°F. This resulted in an irradiated 30 ft-lb transition temperature of 35°F and an irradiated 50 ft-lb transition temperature of 50°F (tangential orientation).

The average upper shelf energy (USE) of the intermediate shell forging 122X208VA1 Charpy specimens (tangential orientation) resulted in an energy decrease of 12 ft-lb after irradiation to  $3.36 \times 10^{19}$  n/cm<sup>2</sup> ( $E > 1.0$  MeV). This results in an irradiated average USE of 148 ft-lb (Figure 5-2).

Irradiation of the reactor vessel lower shell forging 123X167VA1 Charpy specimens oriented with the longitudinal axis of the specimen parallel to the working direction of the plate (tangential orientation) to  $3.36 \times 10^{19}$  n/cm<sup>2</sup> (E > 1.0 MeV) (Figure 5-3) resulted in a 30 ft-lb transition temperature increase of 50°F and a 50 ft-lb transition temperature increase of 48°F. This resulted in an irradiated 30 ft-lb transition temperature of 0°F and an irradiated 50 ft-lb transition temperature of 23°F (tangential orientation).

The average upper shelf energy (USE) of the intermediate shell forging 123X167VA1 Charpy specimens (tangential orientation) resulted in an energy decrease of 5 ft-lb after irradiation to  $3.36 \times 10^{19}$  n/cm<sup>2</sup> (E > 1.0 MeV). This results in an irradiated average USE of 152 ft-lb (Figure 5-3).

### 5.2.2 Weld Metal

Irradiation of the surveillance weld metal Charpy specimens to  $3.36 \times 10^{19}$  n/cm<sup>2</sup> (E > 1.0 MeV) (Figure 5-4) resulted in a 30 ft-lb transition temperature shift of 250°F and a 50 ft-lb transition temperature increase of 268°F. This results in an irradiated 30 ft-lb transition temperature of 200°F and an irradiated 50 ft-lb transition temperature of 258°F.

The average USE of the surveillance weld metal resulted in an energy decrease of 62 ft-lb after irradiation to  $3.36 \times 10^{19}$  n/cm<sup>2</sup> (E > 1.0 MeV). This resulted in an irradiated average USE of 64 ft-lb (Figure 5-4).

### 5.2.3 Heat-Affected-Zone (HAZ)

Irradiation of the reactor vessel weld HAZ metal Charpy specimens to  $3.36 \times 10^{19}$  n/cm<sup>2</sup> (E > 1.0 MeV) (Figure 5-5) resulted in a 30 ft-lb transition temperature increase of 200°F and a 50 ft-lb transition temperature increase of 225°F. This resulted in an irradiated 30 ft-lb transition temperature of 85°F and an irradiated 50 ft-lb transition temperature of 155°F.

The average USE of the weld HAZ metal resulted in an energy decrease of 41 ft-lb after irradiation to  $3.36 \times 10^{19}$  n/cm<sup>2</sup> (E > 1.0 MeV). This resulted in an irradiated average USE of 139 ft-lb (Figure 5-5).

### 5.2.4 Correlation Monitor Material

Irradiation of the A533 Grade B Class 1 ASTM correlation monitor material (HSST Plate 02) Charpy specimens oriented with the longitudinal axis of the specimen parallel to the major rolling direction of the plate (longitudinal orientation) to  $3.36 \times 10^{19}$  n/cm<sup>2</sup> (E > 1.0 MeV) (Figure 5-6) resulted in a 30 ft-lb transition temperature increase of 158°F and a 50 ft-lb transition temperature increase of 160°F. This results in an irradiated 30 ft-lb transition temperature of 203°F and an irradiated 50 ft-lb transition temperature of 240°F (longitudinal orientation).

The average USE of the A533 Grade B Class 1 ASTM correlation monitor material (HSST Plate 02) Charpy specimens (longitudinal orientation) resulted in an energy decrease of 25 ft-lb after irradiation to  $3.36 \times 10^{19}$  n/cm<sup>2</sup> (E > 1.0 MeV). This results in an irradiated average USE of 98 ft-lb (Figure 5-6).

### 5.2.5 Analysis

Presented in Table 5-14 is a comparison of the Kewaunee surveillance material test results with the Regulatory Guide 1.99, Revision 2, predictions. The predicted values presented in Table 5-14 are based on the weight percent of copper and nickel listed in Table 4-1 and reported in the comparison report WCAP-15074 for the weld metal. This comparison led to the following conclusions:

- For Capsule S the intermediate shell forging 122X208VA1, lower shell forging 123X167VA1 and the ASTM correlation monitor surveillance material measured 30 ft-lb transition temperature increases are slightly greater than the Regulatory Guide 1.99, Revision 2, predictions. However, Regulatory Guide 1.99, Revision 2, requires a 2 sigma allowance of 34 °F for base metal be added to the predicted reference transition temperature to obtain a conservative upper bound value. The measured reference transition temperatures of these materials is bounded by the 2 sigma allowance for shift prediction (for all capsule results for base metal).
- The measured 30 ft-lb transition temperature increase for the weld metal is less than the Regulatory Guide 1.99, Revision 2, prediction for fluences greater than  $2.74 \times 10^{19}$  n/cm<sup>2</sup>, but less than the Regulatory Guide 1.99, Revision 2, predictions at the two lower fluences. On average, the data for the weld are close to the Regulatory Guide predictions.
- The surveillance capsule S test results indicate that all of the surveillance material average upper shelf energy decreases are less than the Regulatory Guide 1.99, Revision 2, predictions.

The Capsule S surveillance results (if assumed to be adequate surrogates of the reactor vessel) indicate that all core region materials should have adequate toughness throughout the life of the vessel (33 EFPY) since the measured capsule S fluence is approximately equal to the peak vessel inner surface fluence at 33 EFPY.

All beltline surveillance materials exhibit a more than adequate upper shelf energy level for continued safe plant operation and are expected to maintain an upper shelf energy of no less than 50 ft-lb throughout the life of the vessel (33 EFPY) as required by 10CFR50, Appendix G.

The Regulatory Guide 1.99, Revision 2, credibility evaluation of the Kewaunee surveillance program weld metal presented in Appendix B of this report indicates that the Kewaunee reactor vessel surveillance results are credible.

The initial  $RT_{NDT}$  evaluation for the surveillance weld metal presented in Appendix C of this report indicates that the initial  $RT_{NDT}$  is  $-50^{\circ}\text{F}$ .

### 5.3 TENSILE TEST RESULTS

The results of the tensile tests performed on the various materials contained in capsule S irradiated to  $3.36 \times 10^{19} \text{ n/cm}^2$  ( $E > 1.0 \text{ MeV}$ ) are presented in Table 5-15 and are compared with unirradiated results as shown in Figures 5-12 through 5-14.

The results of the tensile tests performed on the intermediate shell forging 122X208VA1 (tangential orientation) indicated that irradiation to  $3.36 \times 10^{19} \text{ n/cm}^2$  ( $E > 1.0 \text{ MeV}$ ) caused a 5 to 13 ksi increase in the 0.2 percent offset yield strength and a 2 to 10 ksi increase in the ultimate tensile strength when compared to unirradiated data (Figure 5-12).

The results of the tensile tests performed on the lower shell forging 123X167VA1 (tangential orientation) indicated that irradiation to  $3.36 \times 10^{19} \text{ n/cm}^2$  ( $E > 1.0 \text{ MeV}$ ) caused a 8 to 10 ksi increase in the 0.2 percent offset yield strength and a 7 to 8 ksi increase in the ultimate tensile strength when compared to unirradiated data (Figure 5-13).

The results of the tensile tests performed on the surveillance weld metal indicated that irradiation to  $3.36 \times 10^{19} \text{ n/cm}^2$  ( $E > 1.0 \text{ MeV}$ ) caused a 32 to 35 ksi increase in the 0.2 percent offset yield strength and a 26 to 33 ksi increase in the ultimate tensile strength when compared to unirradiated data (Figure 5-14).

The fractured tensile specimens for the intermediate shell forging 122X208VA1 and lower shell forging 123X167VA1 material are shown in Figures 5-15 and 5-16, while the fractured specimens for the surveillance weld metal are shown in Figure 5-17.

The engineering stress-strain curves for the tensile tests are shown in Figures 5-18 through 5-22.

### 5.4 "MASTER CURVE" FRACTURE TOUGHNESS TEST RESULTS

Results from all of the Master Curve fracture toughness tests are listed in Tables 5-16 through 5-18. The tables list the as-measured  $K_{Jc}$  values and the 1T size-adjusted  $K_{Jc}$  values ( $K_{Jc(1T)}$ ). A breakdown by the specimen type and material/condition are presented in this section. All the results reported in this section are based on evaluations in accordance with ASTM E1921-97.

ASTM E1921-97 requires a yield strength value to estimate a  $K_{Jc}$  limit as the fracture toughness test temperature (see Table 5-2). For this program, the yield strength was always chosen to be conservative for determining the  $K_{Jc}$  limit values. The test temperatures for the fracture toughness tests never matched with the temperatures for the measured values for yield strength, so values at a higher temperature were used to establish the  $K_{Jc}$  limits. Since yield strength decreases with increasing test temperature, using a higher temperature yield strength value will provide a lower (conservative) level of the  $K_{Jc}$  limit.



#### 5.4.1 Results for 1/2T-CT Specimens for Kewaunee Surveillance Weld (Unirradiated)

Results for 1/2T-CT specimens are shown in Table 5-16. It was necessary to run seven 1/2T-CT specimens to meet the requirements of the ASTM E1921-97 Test Method. A  $T_0$  value of  $-129^{\circ}\text{F}$  was determined from the seven specimens as shown in Table 5-19.

#### 5.4.2 Results for Whole and Reconstituted Precracked Charpy Specimens for Kewaunee Surveillance Weld (Unirradiated)

Individual results for both the whole precracked Charpy (PCVN) and reconstituted precracked Charpy (RPCVN) specimens are shown in Table 5-16.  $T_0$  values of  $-148^{\circ}\text{F}$  and  $-154^{\circ}\text{F}$  were determined from the results of the whole and reconstituted precracked Charpy-size three point bend specimens, respectively as shown in Table 5-19. The lower  $T_0$  results from the PCVN and RPCVN specimens as compared to the 1/2T-CT result (approximately  $20^{\circ}\text{F}$ ) are within the typical data scatter for this type of material and test method.

#### 5.4.3 Results for Whole Precracked Charpy Specimens for Maine Yankee Surveillance Weld (Unirradiated)

The individual test results for the precracked Charpy specimens for the Maine Yankee surveillance weld in the unirradiated condition were provided by Wisconsin Public Service Corporation (WPSC) as shown in Table 5-16. A  $T_0$  value of  $-158^{\circ}\text{F}$  was determined from the results as shown in Table 5-19. The  $T_0$  value for the Maine Yankee surveillance weld is  $10^{\circ}\text{F}$  lower than that for the Kewaunee surveillance weld, but this difference is within typical data.

#### 5.4.4 Results for Reconstituted Precracked Charpy Specimens for Kewaunee Surveillance Weld (Irradiated at $3.36 \times 10^{19} \text{ n/cm}^2$ )

Individual results are shown in Table 5-17, and the  $T_0$  value determined from the results is  $140^{\circ}\text{F}$  as shown in Table 5-19. Nine (9) valid test results were obtained, and the H20 specimen result exceeded the  $K_{Ic}$  limit (see Table 5-2). This result was included in the analysis to obtain  $T_0$  by using the censoring method in ASTM E-1921-97.

#### 5.4.5 Results for Reconstituted Precracked Charpy Specimens for Maine Yankee Surveillance Weld (Irradiated at $6.11 \times 10^{19} \text{ n/cm}^2$ )

Test results are shown in Table 5-18, and the  $T_0$  value determined from the results is  $232^{\circ}\text{F}$  as shown in Table 5-19. The result for specimen 371a, exceed the  $K_{Ic}$  limit, but was included in determining  $T_0$  using the ASTM E1921-97 censoring method.

#### 5.4.6 Summary of $T_0$ Values

Table 5-19 summarizes all of the  $T_0$  values determined by the ASTM E1921-97 Standard Test Method for the different types of specimens for the Kewaunee and Maine Yankee surveillance

welds. The test temperatures and the median values of  $K_{Ic}$  for the 1-T equivalent size are also listed in Table 5-19. Figures 5-23 through 5-27 show the median Master Curves with 5% lower tolerance and the 95% upper tolerance bounds based on the data; these figures only show the data at a single test temperature following ASTM E1921-97. Figure 5-28 shows the result for unirradiated Maine Yankee surveillance weld; the 5% lower tolerance, the median, and a projected conservative lower bound curve are shown in this case as furnished by WPSC.

Although this report presents the Master Curve data  $T_0$  generated in accordance with the ASTM E1921-97 Test Method, the companion report WCAP-15075, "Master Curve Assessment Strategy", evaluates all of the Master Curve fracture toughness data using the multi-temperature maximum likelihood method. Details for these different evaluations are described in WCAP-15075. The results are summarized in Table 5-19 in the last column. Note that all of the test results are combined and used in the determination of  $T_0$  using the multi-temperature maximum likelihood method of evaluation. Note that the results for the Maine Yankee surveillance weld do not change since the data being evaluated are at one test temperature for one specimen type/size.

The shift in  $T_0$  due to irradiation is 284°F for the Kewaunee surveillance weld using only precracked Charpy data. If the multi-temperature approach using all data is used, the transition temperature shift is slightly higher at 292°F. This  $\Delta T_0$  is higher than the corresponding Charpy 30 ft-lb temperature shift ( $\Delta T_{30}$ ) of 250°F. For the Maine Yankee surveillance weld, the  $\Delta T_0$  is 390°F which compares with a Charpy 30 ft-lb temperature shift of 345°F. Both cases exhibit a higher fracture toughness transition temperature shift than the corresponding Charpy energy transition temperature shift.

**Table 5-1 Materials, Conditions, Geometries, and Primary Test Temperatures for the Transition Region Fracture Toughness Program**

1P3571 Surveillance Weld	Neutron Fluence n/cm <sup>2</sup>	Specimen	Test Temperature (°F)	Test Temperature (°C)	Number of Specimens Tested	Number of Valid Test Specimens
KW	0	PCVN	-200	-129	10	8
		RPCVN	-200	-129	7	7
		0.5TCT	-187	-122	7	7
KW	3.36 x 10 <sup>19</sup>	RPCVN	136	58	13	9
		1XWOL	136	58	2	2
MY	0	PCVN	-200	-129	7	7
MY	6.11 x 10 <sup>19</sup>	RPCVN	210	98	10	7

KW - Kewaunee

MY - Maine Yankee

Table 5-2 $K_{Jc}$ Limits			
1P3571 Surveillance Plant	Fluence (n/cm <sup>2</sup> )	Specimen	$K_{Jc}$ limit M=30 ksi $\sqrt{in.}$ (MPa $\sqrt{m}$ )
KW	0	PCVN 0.5TCT	118.8 (130.5) 189.2 (207.9)
Irradiated KW	$3.36 \times 10^{19}$	RPCVN 1XWOL	140.1 (154.0) 192.0 (211.0)
MY	0	PCVN	120 (132)
Irradiated MY	$6.11 \times 10^{19}$	RPCVN	144.0 (158.3)

KW - Kewaunee  
MY - Maine Yankee

Table 5-3 Charpy V-notch Data for the Kewaunee Intermediate Shell Forging 122X208VA1 Irradiated to a Fluence of $3.36 \times 10^{19}$ n/cm <sup>2</sup> (E > 1.0 MeV) (Tangential Orientation)							
Sample Number	Temperature		Impact Energy		Lateral Expansion		Shear
	(°F)	(°C)	(ft-lb)	(J)	(mils)	(mm)	(%)
P28	-25	-32	14	19	8	0.20	0
P31	10	-12	17	23	12	0.30	5
P33	25	-4	26	35	22	0.56	10
P35	40	4	55	75	42	1.07	15
P25	50	10	39	53	28	0.71	15
P30	60	16	65	88	46	1.17	20
P34	75	24	78	106	52	1.32	30
P26	100	38	100	136	69	1.75	40
P27	150	66	123	167	81	2.06	60
P32	200	93	130	176	85	2.16	85
P29	200	93	142	193	81	2.06	100
P36	300	149	154	209	85	2.16	100

**Table 5-4 Charpy V-notch Data for the Kewaunee Lower Shell Forging  
123X167VA1 Irradiated to a Fluence of  $3.36 \times 10^{19}$  n/cm<sup>2</sup> (E > 1.0 MeV)  
(Tangential Orientation)**

Sample Number	Temperature		Impact Energy		Lateral Expansion		Shear (%)
	(°F)	(°C)	(ft-lb)	(J)	(mils)	(mm)	
S31	-50	-46	13	18	8	0.20	0
S33	-25	-32	36	49	24	0.61	10
S27	-10	-23	5	7	4	0.10	0
S35	-5	-21	69	94	51	1.30	20
S30	0	-18	48	65	35	0.89	10
S36	10	-12	37	50	26	0.66	10
S26	50	10	48	65	35	0.89	15
S28	75	24	87	118	60	1.52	25
S29	100	38	115	156	76	1.93	50
S34	150	66	154	209	91	2.31	100
S25	200	93	147	199	90	2.29	100
S32	300	149	156	212	77	1.96	100

Sample Number	Temperature		Impact Energy		Lateral Expansion		Shear (%)
	(°F)	(°C)	(ft-lb)	(J)	(mils)	(mm)	
W18	0	-18	3	4	4	0.10	0
W22	100	38	16	22	11	0.28	10
W17	150	66	23	31	17	0.43	20
W19	200	93	22	30	17	0.43	15
W20	225	107	51	69	41	1.04	65
W21	250	121	56	76	46	1.17	80
W23	325	163	62	84	49	1.24	100
W24	400	204	65	88	51	1.30	100

Sample Number	Temperature		Impact Energy		Lateral Expansion		Shear (%)
	(°F)	(°C)	(ft-lb)	(J)	(mils)	(mm)	
H18	-25	-32	28	38	25	0.64	25
H24	50	10	24	33	19	0.48	10
H17	100	38	30	41	21	0.53	25
H23	150	66	48	65	34	0.86	40
H21	225	107	146	198	90	2.29	100
H22	300	149	109	148	73	1.85	100
H19	375	191	155	210	89	2.26	100
H20	450	232	146	198	81	2.06	100

**Table 5-7 Charpy V-notch Data for the A533 Grade B Class 1 ASTM Correlation Monitor Material (HSST Plate 02) to a Fluence of  $3.36 \times 10^{19}$  n/cm<sup>2</sup> (E > 1.0 MeV)**

Sample Number	Temperature		Impact Energy		Lateral Expansion		Shear (%)
	(°F)	(°C)	(ft-lb)	(J)	(mils)	(mm)	
R17	100	38	8	11	5	0.13	10
R20	175	79	20	27	15	0.38	15
R24	200	93	29	39	24	0.61	20
R19	225	107	35	47	28	0.71	30
R18	265	129	85	115	63	1.60	65
R21	300	149	86	117	66	1.68	80
R22	375	191	102	138	81	2.06	100
R23	450	232	94	127	76	1.93	100



**Table 5-8 Instrumented Charpy Impact Test Results for the Kewaunee Intermediate Shell Forging 122X208VA1 Irradiated to a Fluence of  $3.36 \times 10^{19}$  n/cm<sup>2</sup> (E > 1.0 MeV) (Tangential Orientation)**

Sample No.	Test Temp. (°F)	Charpy Energy E <sub>0</sub> (ft-lb)	Normalized Energies (ft-lb/in <sup>3</sup> )			Yield Load P <sub>cy</sub> (lb)	Time to Yield t <sub>cy</sub> (μsec)	Max. Load P <sub>M</sub> (lb)	Time to Max. t <sub>M</sub> (μsec)	Fast Fract. Load P <sub>f</sub> (lb)	Arrest Load P <sub>A</sub> (lb)	Yield Stress σ <sub>v</sub> (ksi)	Flow Stress (ksi)
			Charpy E <sub>0</sub> /A	Max. E <sub>M</sub> /A	Prop. E <sub>f</sub> /A								
P28	-25	14	113	65	47	3961	0.21	4099	0.24	4099	223	132	134
P31	10	17	137	83	54	3718	0.16	4082	0.25	4082	364	123	130
P33	25	26	209	181	29	3590	0.15	4522	0.42	4522	144	119	135
P35	40	55	443	341	102	3545	0.14	4724	0.69	4697	120	118	137
P25	50	39	314	240	74	3770	0.16	4782	0.51	4782	420	125	142
P30	60	65	523	369	154	3460	0.19	4705	0.77	4609	144	115	136
P34	75	78	628	373	255	3561	0.18	4678	0.77	4419	446	118	137
P26	100	100	805	354	451	3318	0.18	4568	0.76	3349	1071	110	131
P27	150	123	990	401	589	3236	0.14	4529	0.83	2454	1186	107	129
P32	200	130	1047	334	713	2923	0.19	4330	0.77	2352	1427	97	120
P29	200	142	1143	381	763	3077	0.15	4335	0.83	**	**	102	123
P36	300	154	1240	297	943	2857	0.15	4172	0.7	**	**	95	117

**Table 5-9 Instrumented Charpy Impact Test Results for the Kewaunee Lower Shell Forging 123X167VA1 Irradiated to a Fluence of  $3.36 \times 10^{19}$  n/cm<sup>2</sup> (E > 1.0 MeV) (Tangential Orientation)**

Sample No.	Test Temp. (°F)	Charpy Energy E <sub>d</sub> (ft-lb)	Normalized Energies (ft-lb/in <sup>2</sup> )			Yield Load P <sub>cy</sub> (lbs)	Time to Yield t <sub>cy</sub> (μsec)	Max. Load P <sub>M</sub> (lbs)	Time to Max. t <sub>M</sub> (μsec)	Fast Fract. Load P <sub>f</sub> (lbs)	Arrest Load P <sub>A</sub> (lbs)	Yield Stress σ <sub>y</sub> (ksi)	Flow Stress (ksi)
			Charpy E <sub>p</sub> /A	Max. E <sub>M</sub> /A	Prop. E <sub>p</sub> /A								
S31	-50	13	105	61	44	3952	0.19	4234	0.22	4234	217	131	136
S33	-25	36	290	260	30	3919	0.16	4910	0.53	4909	120	130	147
S27	-10	5	40	18	22	2673	0.12	2673	0.12	2673	148	89	89
S35	-5	69	556	368	187	3651	0.18	4946	0.74	4946	209	121	143
S30	0	48	387	354	33	3878	0.16	4925	0.69	4914	76	129	146
S36	10	37	298	270	28	3670	0.19	4995	0.57	4995	179	122	144
S26	50	48	387	341	45	3524	0.15	4749	0.69	4738	148	117	137
S28	75	87	701	369	332	3551	0.18	4754	0.76	4308	323	118	138
S29	100	115	926	360	566	3372	0.18	4680	0.76	2946	736	112	134
S34	150	154	1240	394	846	3218	0.14	4537	0.82	**	**	107	129
S25	200	147	1184	309	874	3077	0.14	4364	0.69	**	**	102	124
S32	300	156	1256	299	957	2877	0.14	4279	0.69	**	**	96	119

**Table 5-10 Instrumented Charpy Impact Test Results for the Kewaunee Surveillance Weld Metal Irradiated to a Fluence of  $3.36 \times 10^{19}$  n/cm<sup>2</sup> (E > 1.0 MeV)**

Sample No.	Test Temp. (°F)	Charpy Energy E <sub>D</sub> (ft-lb)	Normalized Energies (ft-lb/in <sup>2</sup> )			Yield Load P <sub>CV</sub> (lbs)	Time to Yield t <sub>CV</sub> (μsec)	Max. Load P <sub>M</sub> (lbs)	Time to Max. t <sub>M</sub> (μsec)	Fast Fract. Load P <sub>F</sub> (lbs)	Arrest Load P <sub>A</sub> (lbs)	Yield Stress σ <sub>V</sub> (ksi)	Flow Stress (ksi)
			Charpy E <sub>D</sub> /A	Max. E <sub>M</sub> /A	Prop. E <sub>V</sub> /A								
W18	0	3	24	12	12	1471	0.11	1471	0.11	1471	86	49	49
W22	100	16	129	82	47	4020	0.21	4237	0.26	4237	107	134	137
W17	150	23	185	131	55	3823	0.16	4505	0.32	4505	814	127	138
W19	200	22	177	131	46	3551	0.15	4302	0.33	4302	503	118	130
W20	225	51	411	222	189	3797	0.21	4601	0.51	4594	3381	126	139
W21	250	56	451	216	235	3603	0.16	4591	0.47	4128	2952	120	136
W23	325	62	499	199	300	3654	0.15	4554	0.44	**	**	121	136
W24	400	65	523	195	329	3562	0.22	4365	0.5	**	**	118	132

\*\* Fully ductile fracture.

**Table 5-11 Instrumented Charpy Impact Test Results for the Kewaunee Surveillance Heat-Affected-Zone (HAZ) Metal Irradiated to a Fluence of  $3.36 \times 10^{19}$  n/cm<sup>2</sup> (E > 1.0 MeV)**

Sample No.	Test Temp. (°F)	Charpy Energy E <sub>D</sub> (ft-lb)	Normalized Energies (ft-lb/in <sup>2</sup> )			Yield Load P <sub>GY</sub> (lbs)	Time to Yield t <sub>GY</sub> (μsec)	Max. Load P <sub>M</sub> (lbs)	Time to Max. t <sub>M</sub> (μsec)	Fast Fract. Load P <sub>F</sub> (lbs)	Arrest Load P <sub>A</sub> (lbs)	Yield Stress σ <sub>y</sub> (ksi)	Flow Stress (ksi)
			Charpy E <sub>D</sub> /A	Max. E <sub>M</sub> /A	Prop. E <sub>P</sub> /A								
H18	-25	28	225	130	95	4200	0.16	4680	0.31	4680	1229	140	147
H24	50	24	193	134	59	4089	0.22	4545	0.36	4545	168	136	143
H17	100	30	242	203	39	3892	0.16	4647	0.44	4647	707	129	142
H23	150	48	387	278	109	3589	0.19	4677	0.61	4677	2145	119	137
H21	225	146	1176	367	809	3434	0.21	4716	0.78	**	**	114	135
H22	300	109	878	325	553	3353	0.14	4551	0.68	**	**	111	131
H19	375	155	1248	339	909	3076	0.21	4288	0.79	**	**	102	122
H20	450	146	1176	309	866	3070	0.14	4293	0.69	**	**	102	122

\*\* Fully ductile fracture

Sample No.	Test Temp. (°F)	Charpy Energy E <sub>D</sub> (ft-lb)	Normalized Energies (ft-lb/in <sup>2</sup> )			Yield Load P <sub>CV</sub> (lbs)	Time to Yield t <sub>GY</sub> (μsec)	Max. Load P <sub>M</sub> (lbs)	Time to Max. t <sub>M</sub> (μsec)	Fast Fract. Load P <sub>F</sub> (lbs)	Arrest Load P <sub>A</sub> (lbs)	Yield Stress σ <sub>v</sub> (ksi)	Flow Stress (ksi)
			Charpy E <sub>D</sub> /A	Max. E <sub>M</sub> /A	Prop. E <sub>P</sub> /A								
R17	100	8	64	30	35	2867	0.16	2867	0.16	2867	130	95	95
R20	175	20	161	109	53	3372	0.15	4065	0.31	4065	843	112	124
R24	200	29	234	176	58	3454	0.16	4410	0.42	4410	801	115	131
R19	225	35	282	169	113	3397	0.14	4590	0.4	4590	2242	113	133
R18	265	85	684	293	392	3370	0.2	4559	0.65	3832	2935	112	132
R21	300	86	692	281	412	3269	0.19	4565	0.63	3479	2849	109	130
R22	375	102	821	291	531	3228	0.18	4465	0.65	**	**	107	128
R23	450	94	757	225	532	3375	0.18	4437	0.52	**	**	112	130

\*\* Fully ductile fracture.

**Table 5-13 Effect of Irradiation to  $3.36 \times 10^{19}$  n/cm<sup>2</sup> (E > 1.0 MeV) on the Notch Toughness Properties of the Kewaunee Reactor Vessel Surveillance Materials**

Material	Average 30 (ft-lb) <sup>(a)</sup> Transition Temperature (°F)			Average 35 mil Lateral <sup>(a)</sup> Expansion Temperature (°F)			Average 50 ft-lb <sup>(a)</sup> Transition Temperature (°F)			Average Energy Absorption <sup>(a)</sup> at Full Shear (ft-lb)		
	Unirradiated	Irradiated	ΔT	Unirradiated	Irradiated	ΔT	Unirradiated	Irradiated	ΔT	Unirradiated	Irradiated	ΔT
Intermediate Shell Forging 122X208VA1 (tangential)	-25	35	60	-15	45	60	15	50	35	160	148	-12
Lower Shell Forging 123X167VA1 (tangential)	-50	0	50	-45	25	70	-25	23	48	157	152	-5
Weld Metal	-50	200	250	-35	238	273	-10	258	268	126	64	-62
HAZ Metal	-115	85	200	-100	165	265	-70	155	225	180	139	-41
Correlation Monitor	45	203	158	60	233	173	80	240	160	123	98	-25

(a) "Average" is defined as the value read from the curve fit through the data points of the Charpy tests (see Figures 5-2 through 5-6)

**Table 5-14 Comparison of the Kewaunee Surveillance Material 30 ft-lb Transition Temperature Shifts and Upper Shelf Energy Decreases with Regulatory Guide 1.99, Revision 2, Predictions**

Material	Capsule	Fluence (n/cm <sup>2</sup> , E > 1.0 MeV)	30 ft-lb Transition Temperature Shift		Upper Shelf Energy Decrease	
			Predicted <sup>(a)</sup> (°F)	Measured (°F)	Predicted <sup>(a)</sup> (%)	Measured (%)
Intermediate Shell Forging 122X208VA1 (tangential)	V	5.97 × 10 <sup>18</sup>	32	0	17	0
	R	1.81 × 10 <sup>19</sup>	44	15	22	0
	P	2.74 × 10 <sup>19</sup>	47	25	24	2
	S	3.36 × 10 <sup>19</sup>	49	60	26	8
Lower Shell Forging 123X167VA1 (tangential)	V	5.97 × 10 <sup>18</sup>	32	0	17	0
	R	1.81 × 10 <sup>19</sup>	44	20	22	3
	P	2.74 × 10 <sup>19</sup>	47	20	24	0
	S	3.36 × 10 <sup>19</sup>	49	50	26	3
Weld Metal	V	5.97 × 10 <sup>18</sup>	165	175	40	35
	R	1.81 × 10 <sup>19</sup>	224	235	47	38
	P	2.74 × 10 <sup>19</sup>	244	230	50	40
	S	3.36 × 10 <sup>19</sup>	253	250	51	49
HAZ Metal	V	5.97 × 10 <sup>18</sup>	-	80	-	19
	R	1.81 × 10 <sup>19</sup>	-	150	-	22
	P	2.74 × 10 <sup>19</sup>	-	220	-	24
	S	3.36 × 10 <sup>19</sup>	-	200	-	23
Correlation Monitor Materials	V	5.97 × 10 <sup>18</sup>	89	95	21	11
	R	1.81 × 10 <sup>19</sup>	120	140	27	23
	P	2.74 × 10 <sup>19</sup>	131	155	30	18
	S	3.36 × 10 <sup>19</sup>	135	158	31	20

(a) Based on Regulatory Guide 1.99, Revision 2, methodology using Mean weight percent values obtained from WCAP-15074 for the weld metal and the Kewaunee GL-92-01 response<sup>[19]</sup> and WCAP 8107<sup>[51]</sup> for base metals.

**Table 5-15 Tensile Properties of the Kewaunee Reactor Vessel Surveillance Materials Irradiated to  $3.36 \times 10^{19}$  n/cm<sup>2</sup> (E > 1.0 MeV)**

Material	Sample Number	Test Temp. (°F)	0.2% Yield Strength (ksi)	Ultimate Strength (ksi)	Fracture Load (kip)	Fracture Stress (ksi)	Fracture Strength (ksi)	Uniform Elongation (%)	Total Elongation (%)	Reduction in Area (%)
Intermediate	P9	72	73.3	92.7	2.85	178.7	58.1	11.3	25.2	68
Shell Forging	P10	115	72.1	91.7	2.70	181.8	55.0	10.5	22.4	70
122X208VA1	P11	250	69.3	87.6	2.65	166.2	54.0	9.8	22.5	68
	P12	550	70.8	92.7	2.85	151.0	58.1	9.0	22.1	62
Lower Shell (tangential)	S7	50	79.4	98.8	2.95	172.6	60.1	11.3	25.1	65
Forging	S8	135	74.4	92.7	2.75	155.6	56.0	9.3	23.5	64
123X167VA1	S9	550	67.7	98.6	2.90	195.3	59.1	9.0	21.6	70
(tangential)										
Weld Metal	W5	200	101.3	112.0	4.00	192.9	81.5	10.5	21.8	58
	W6	550	91.7	105.9	4.00	176.2	81.5	9.8	19.7	54



**Table 5-16 Unirradiated 1P3571 Weld Metal  $K_{Jc}$  Results**

Specimen	$K_{Jc}$ (ksi $\sqrt{in}$ )	$K_{Ic(1T)}$ (ksi $\sqrt{in}$ )
<b>KW Charpy Size 3PB tested at -200°F</b>		
WPS201	108.0	89.4
WPS202	61.8	52.8
WPS205	67.4	57.2
WPS206	61.3	52.3
WPS207	66.1	56.1
WPS208	79.5	66.8
WPS209	79.1	66.5
WPS210	81.1	68.0
<b>MY* Charpy Size 3PB tested at -200°F</b>		
CO4-4	62.0	52.9
CO4-5	67.2	57.0
CO4-2	88.0	73.5
CO4-7	88.4	73.7
CO4-8	90.4	75.4
CO4-3	94.5	78.7
CO4-6	95.5	79.4

<b>KW Reconstituted Charpy Size 3PB tested at -200°F</b>		
RKW1	91.0	75.9
RKW3	77.4	65.1
RKW6	59.1	50.5
RKW7	73.7	62.2
RKW8	91.0	75.9
RKW10	102.4	84.9
RKW11	61.7	52.7
<b>KW 1/2T-CT tested at -187°F</b>		
WPS101	86.2	75.4
WPS102	63.7	56.5
WPS103	85.5	74.8
WPS104	71.8	63.3
WPS105	72.3	63.7
WPS106	48.6	43.8
WPS107	67.4	59.6

\*Provided by WPSC<sup>[20]</sup>

<b>Table 5-17 Irradiated Kewaunee Weld Metal <math>K_{Jc}</math> Results; Fluence = <math>3.36 \times 10^{19}</math> n/cm<sup>2</sup></b>		
<b>Specimen</b>	<b><math>K_{Jc}</math> (ksi√in)</b>	<b><math>K_{Jc(1T)}</math> (ksi√in)</b>
<b>Charpy Size 3PB Reconstituted tested at 136°F</b>		
W24	97.9	81.3
W19	68.1	57.7
H17	131.7	108.1
H18	119.3	98.3
W23	124.4	102.3
H20	144.4*	114.8
H19	78.0	65.6
W17	100.6	83.5
H21	103.8	86.1
<b>Reconstituted Charpy Size - Data Tested at 59°F</b>		
W21	53.3	46.4
W20	59.2	51.0
W22	64.5	55.2
<b>1XWOL Tested at 136°F</b>		
W5	70.4	70.4
W6	55.9	55.9

\* - Exceeds  $K_{Jc}$  limit.

Table 5-18 Irradiated MY 1P3571 Weld Metal $K_{Ic}$ Results; Fluence = $6.11 \times 10^{19}$ n/cm <sup>2</sup>		
Specimen	$K_{Ic}$ (ksi√in)	$K_{Jc(CTT)}$ (ksi√in)
Charpy Size 3PB Reconstituted tested at 210°F		
322	72.6	61.3
36a	54.7	47.1
313	95.3	79.3
371a	152.0*	124.2
33u	65.6	55.8
375	78.4	65.9
371b	76.0	64.0
37ua	100.8	83.6

\* - Exceeds  $K_{Jc}$  limit.

Table 5-19 T <sub>0</sub> Results				
Test Class	K <sub>Ic(1med 1T)</sub> (ksi√in)	Test Temp (°F)	ASTM E1921-97 T <sub>0</sub> (°F)	WCAP-15075 T <sub>0</sub> (°F)
<b>Unirradiated KW</b>				
1/2T-CT Charpy (M=30)	62.6	-187	-129	-144
-Whole- Charpy (M=30)	64.2	-200	-148	
-Reconstituted-	66.6	-200	-154	
<b>Unirradiated MY</b>				
Charpy (M=30) -Whole-	68.3	-200	-158	-158
<b>Irradiated KW</b>				
Charpy (M=30) -Reconstituted-	100.2	136	136	148*
<b>Irradiated MY</b>				
Charpy (M=30) - Reconstituted -	77.2	210	232	232

KW - Kewaunee

MY - Maine Yankee

\*Including the two 1X WOL test results

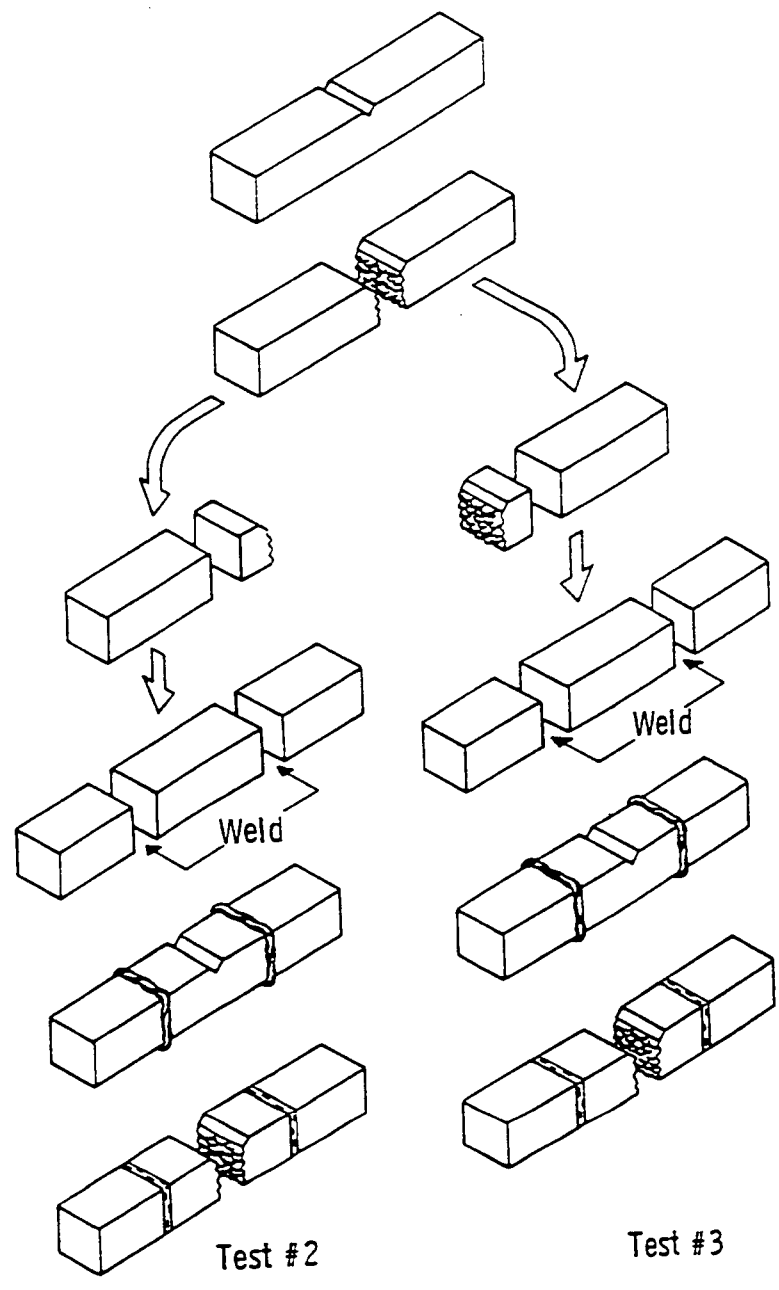


Figure 5-1 Charpy Weld Reconstitution Schematic Showing Process from Start to Finish. Drawing is not to Scale.

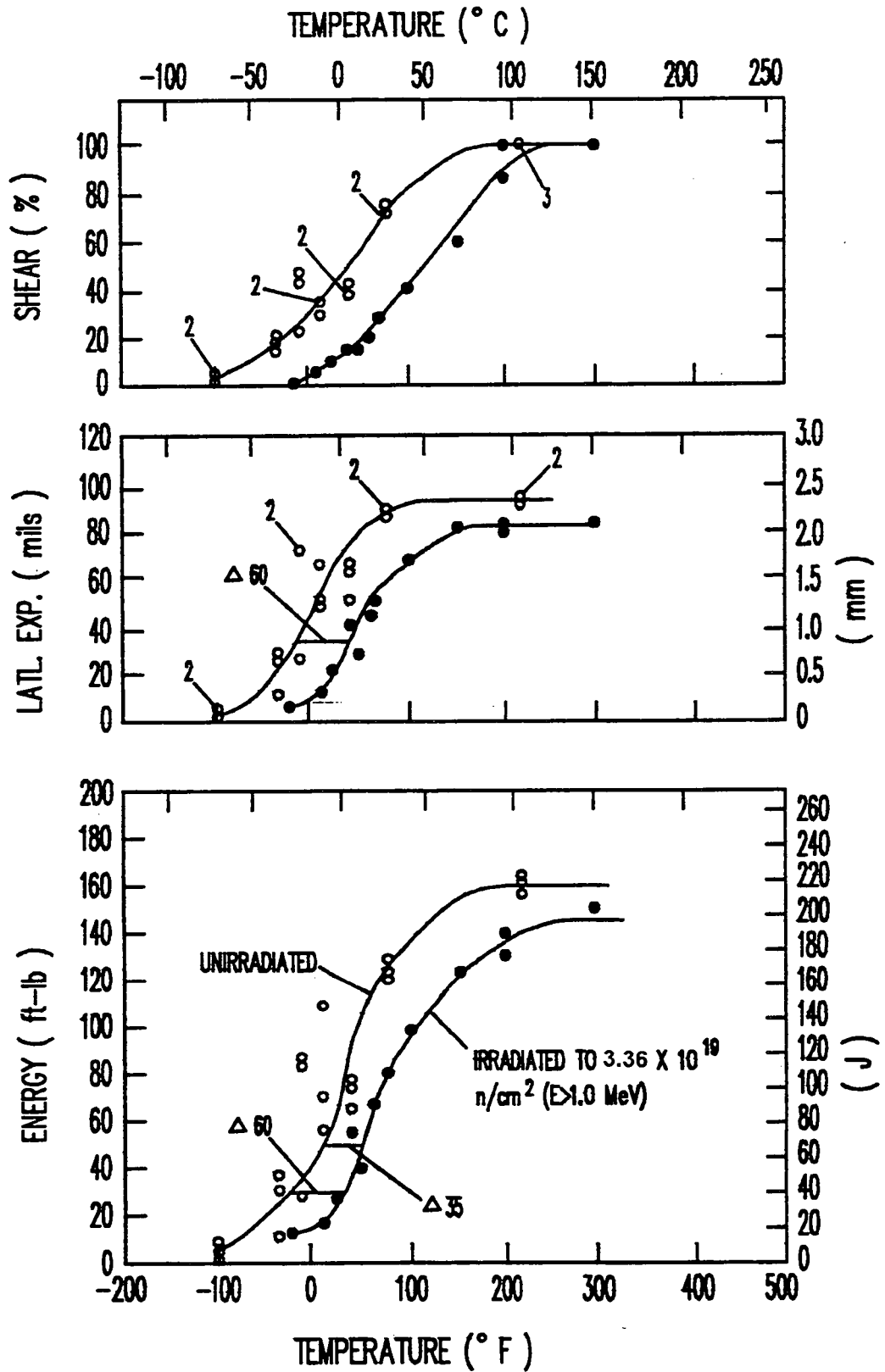


Figure 5-2 Charpy V-Notch Impact Properties for Kewaunee Reactor Vessel Intermediate Shell Forging 122X208VA1 (Tangential Orientation)

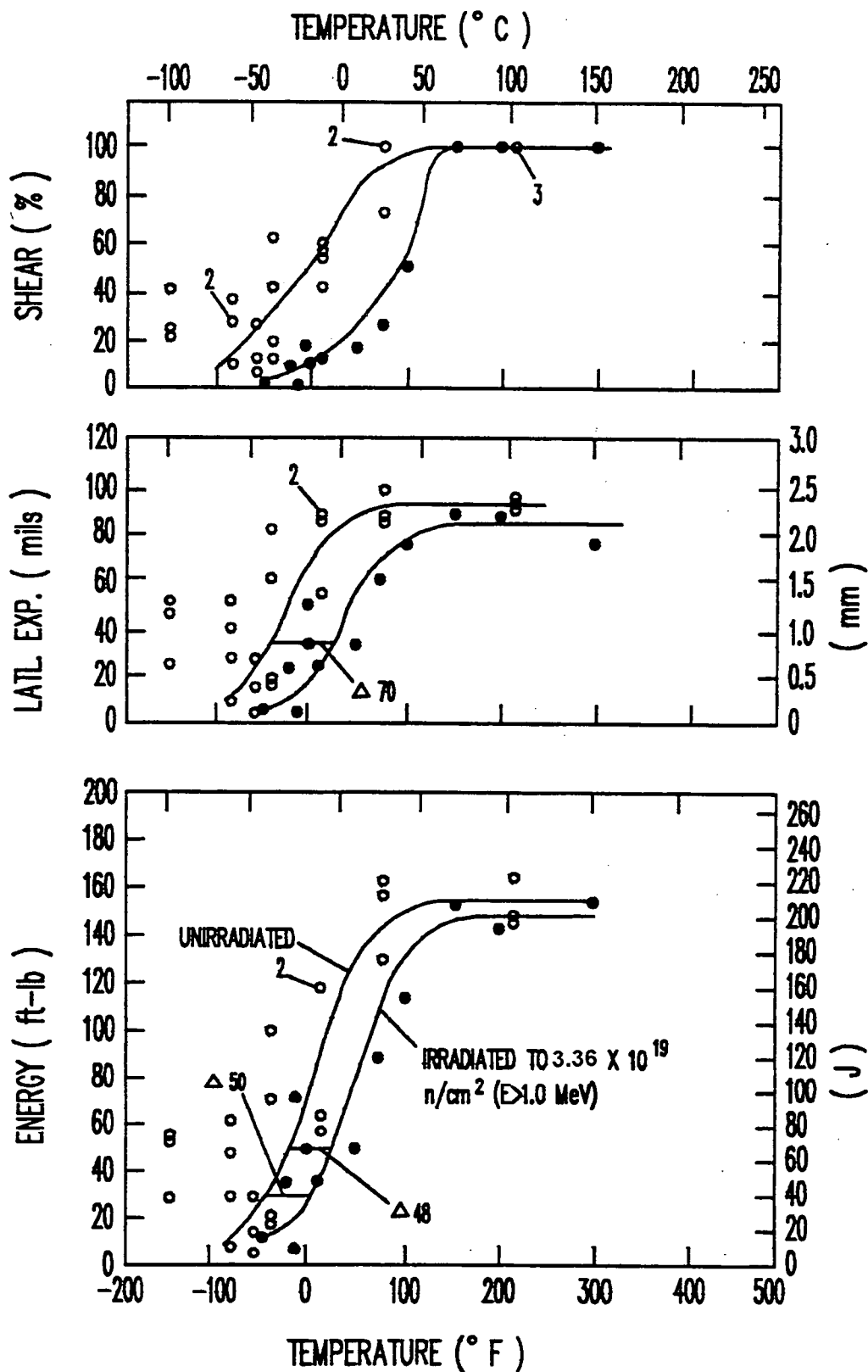


Figure 5-3 Charpy V-Notch Impact Properties for Kewaunee Reactor Vessel Lower Shell Forging 123X167VA1 (Tangential Orientation)

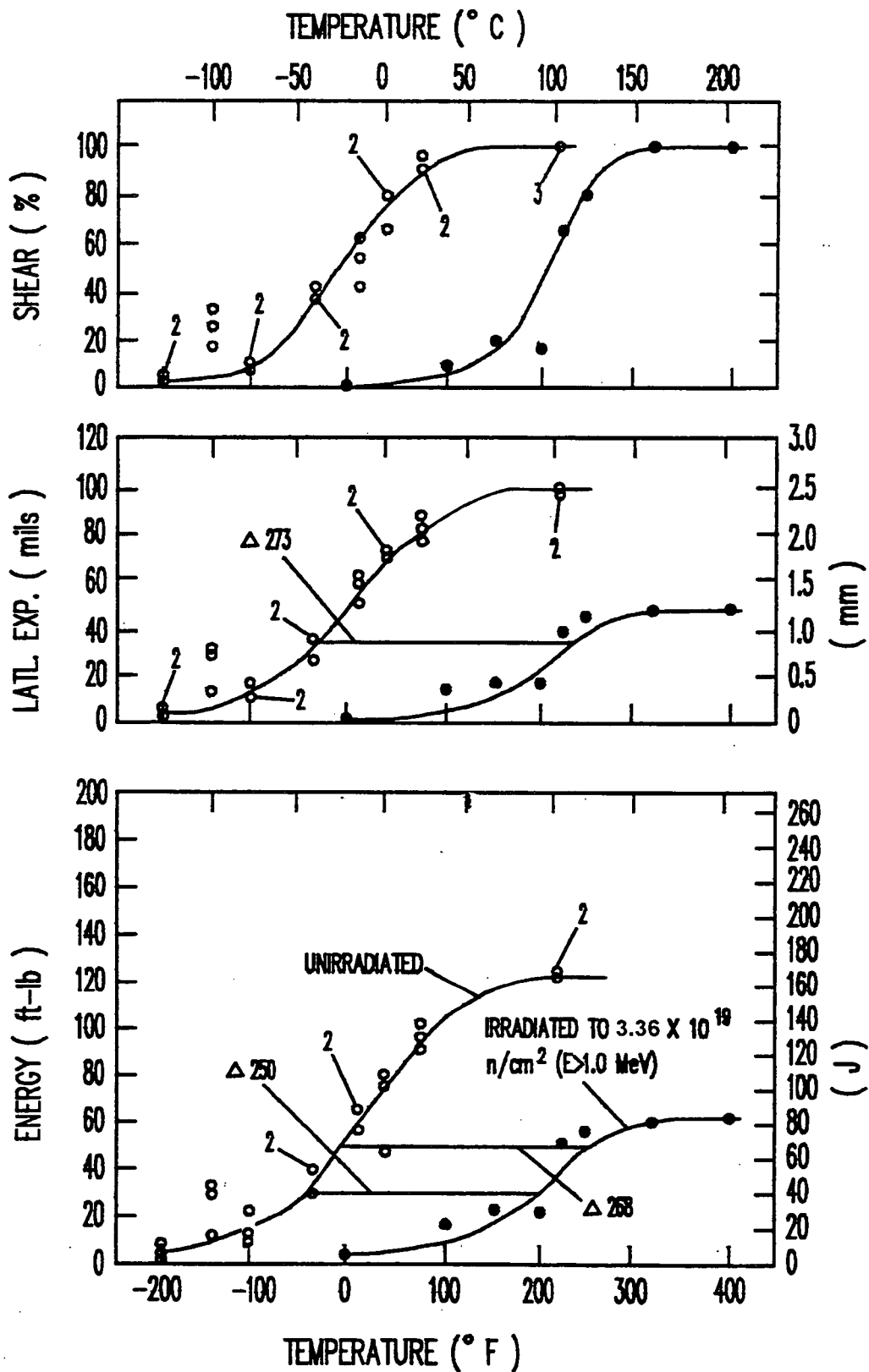


Figure 5-4 Charpy V-Notch Impact Properties for Kewaunee Reactor Vessel Surveillance Weld Metal



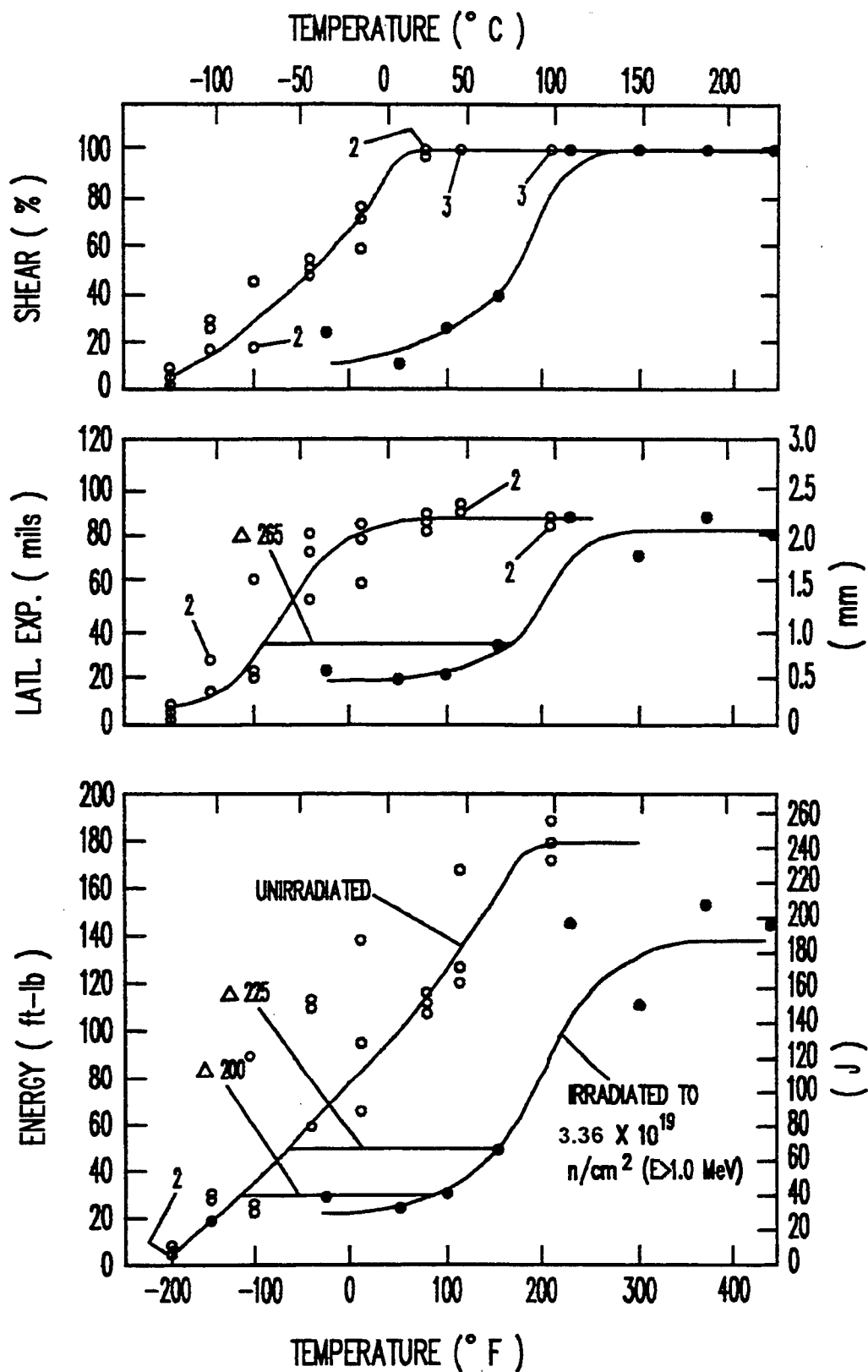


Figure 5-5 Charpy V-Notch Impact Properties for Kewaunee Reactor Vessel Weld Heat-Affected-Zone Metal

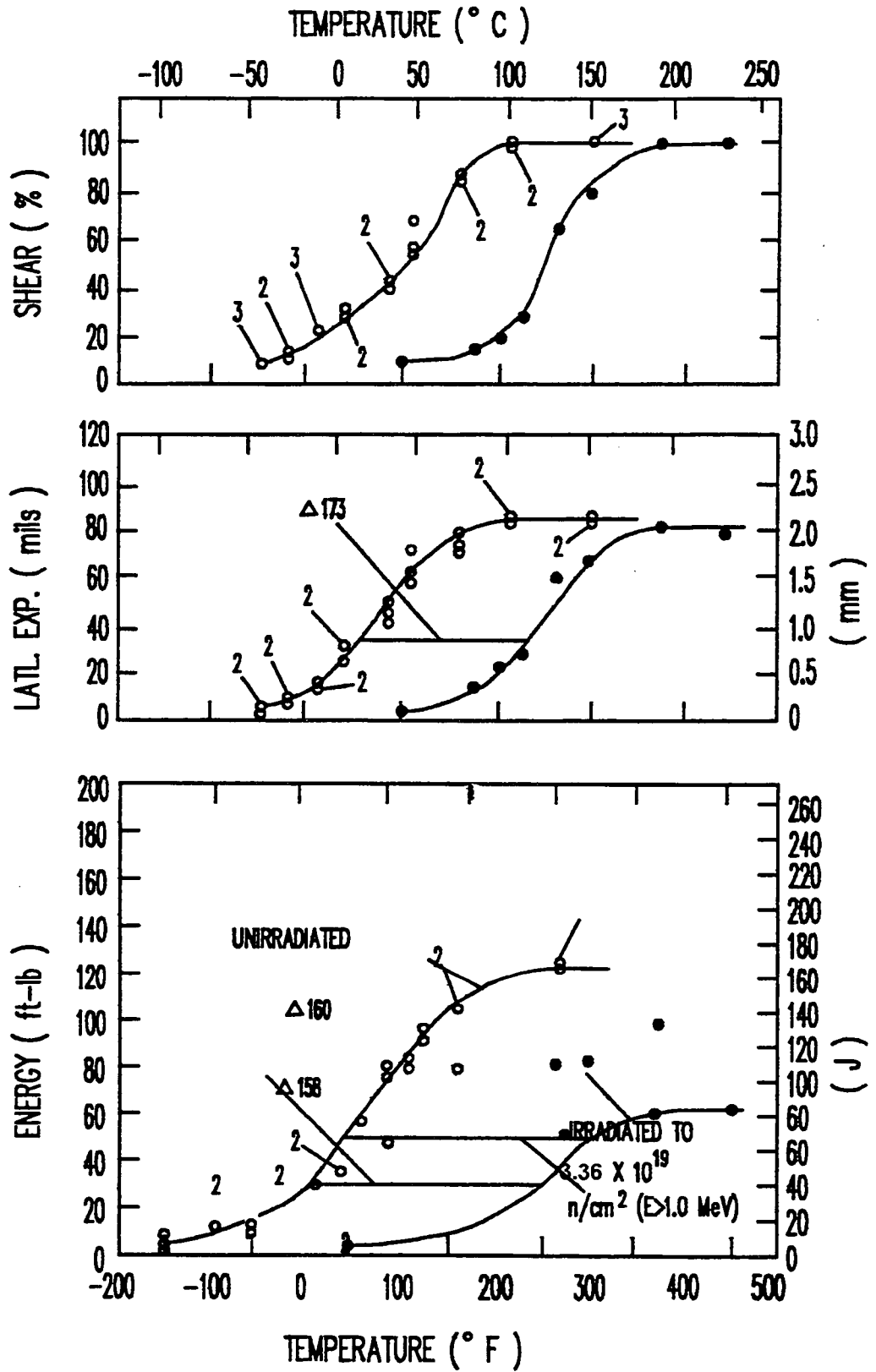


Figure 5-6 Charpy V-Notch Impact Properties for A533 Grade B Class 1 ASTM Correlation Monitor Material (HSST Plate 02) (Tangential Orientation)

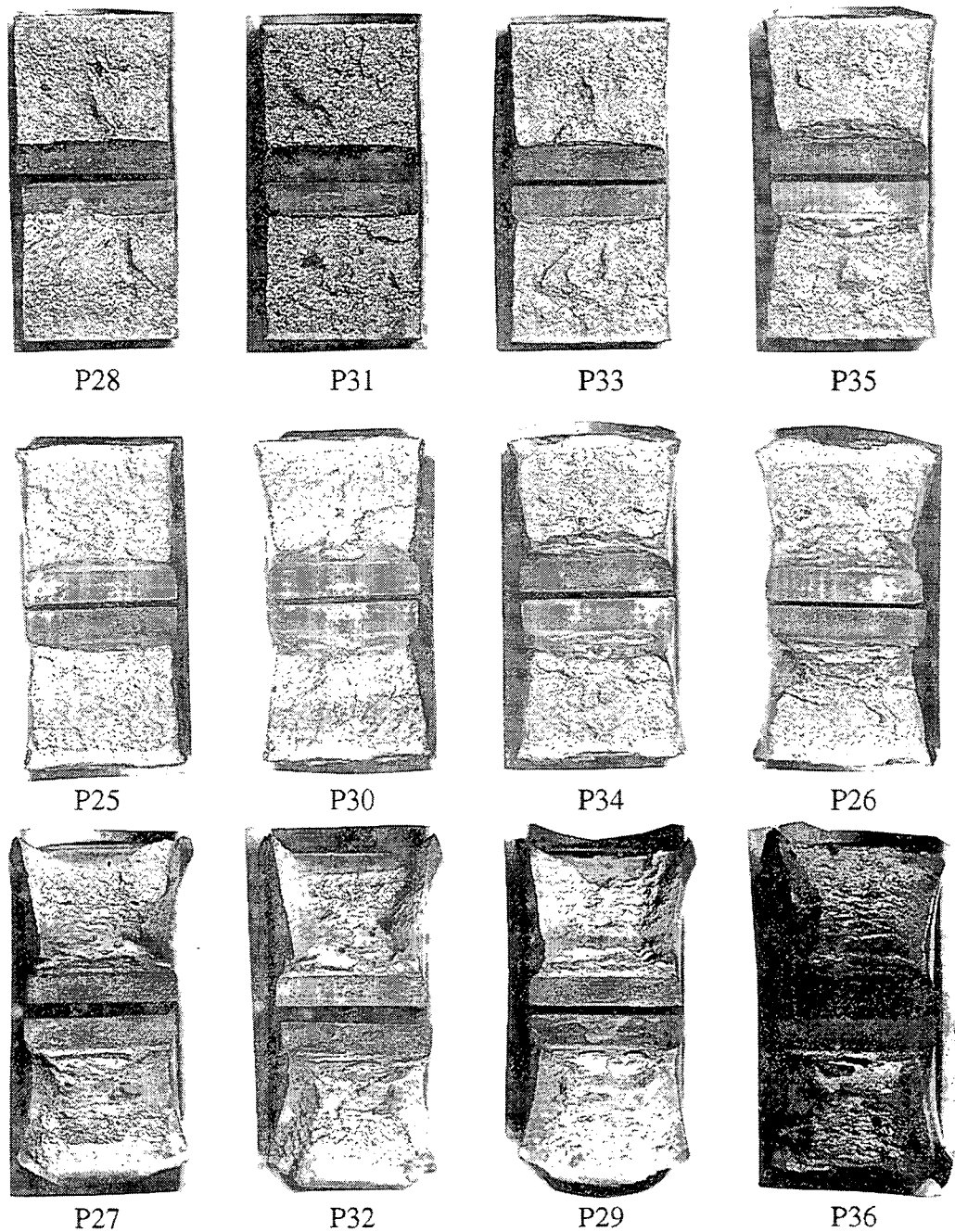


Figure 5-7 Charpy Impact Specimen Fracture Surfaces for Kewaunee Reactor Vessel Intermediate Shell Forging 122X208VA1 (Tangential Orientation)

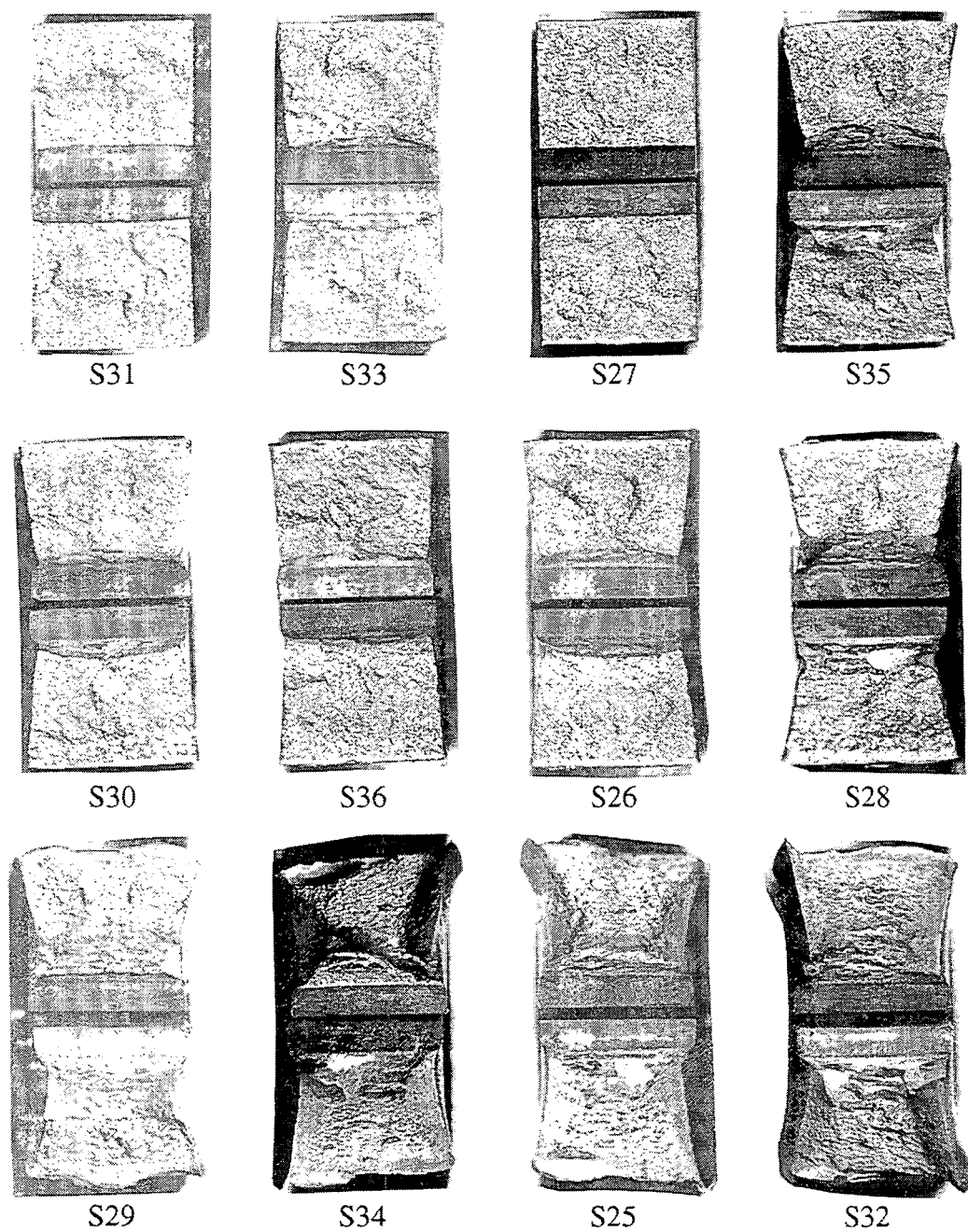


Figure 5-8 Charpy Impact Specimen Fracture Surfaces for Kewaunee Reactor Vessel Lower Shell Forging 123X167VA1 (Tangential Orientation)

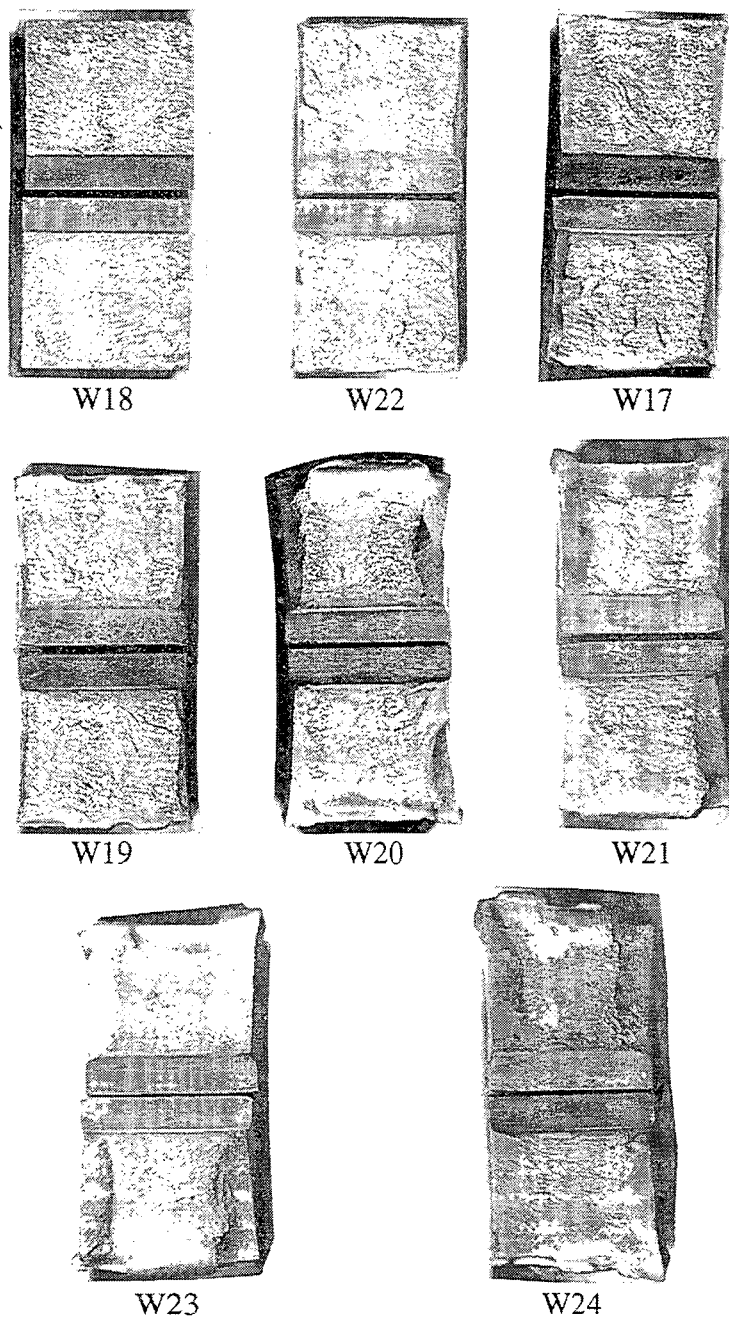


Figure 5-9 Charpy Impact Specimen Fracture Surfaces for Kewaunee Reactor Vessel Surveillance Weld Metal

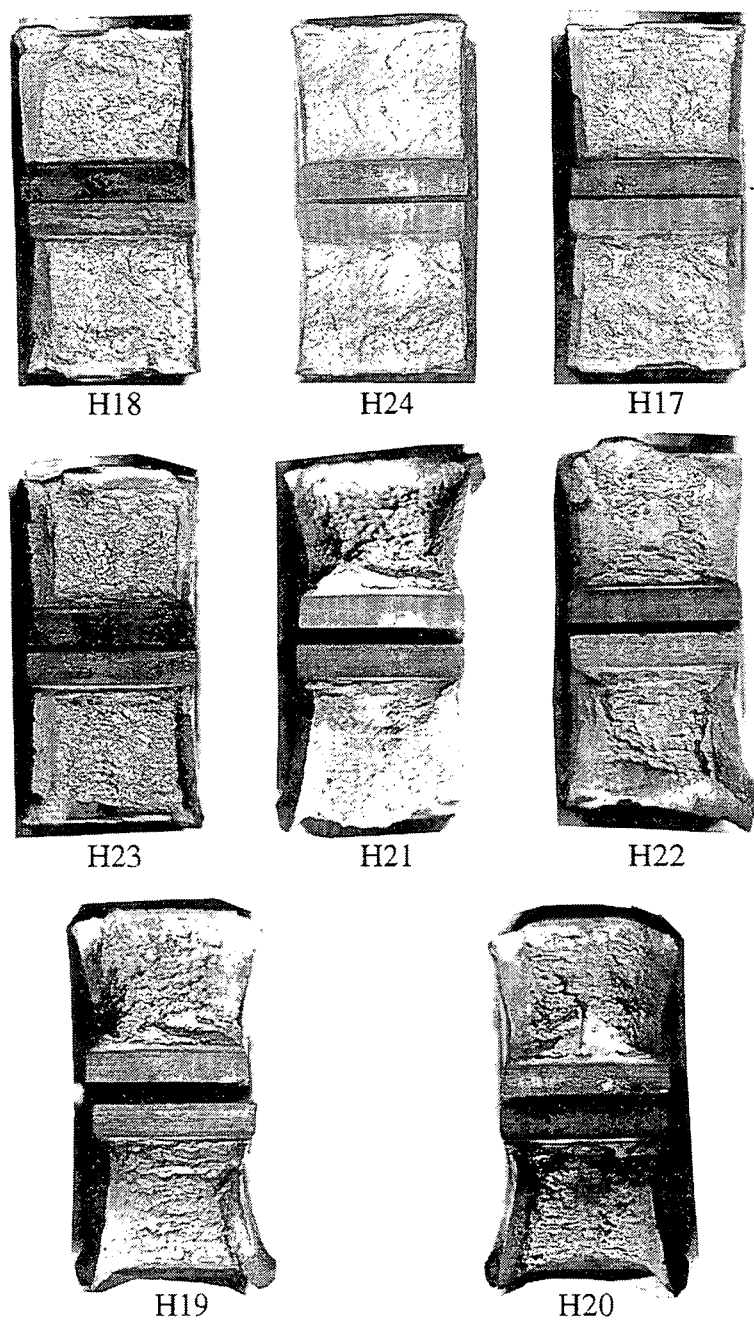


Figure 5-10 Charpy Impact Specimen Fracture Surfaces for Kewaunee Reactor Vessel Heat-Affected-Zone Metal

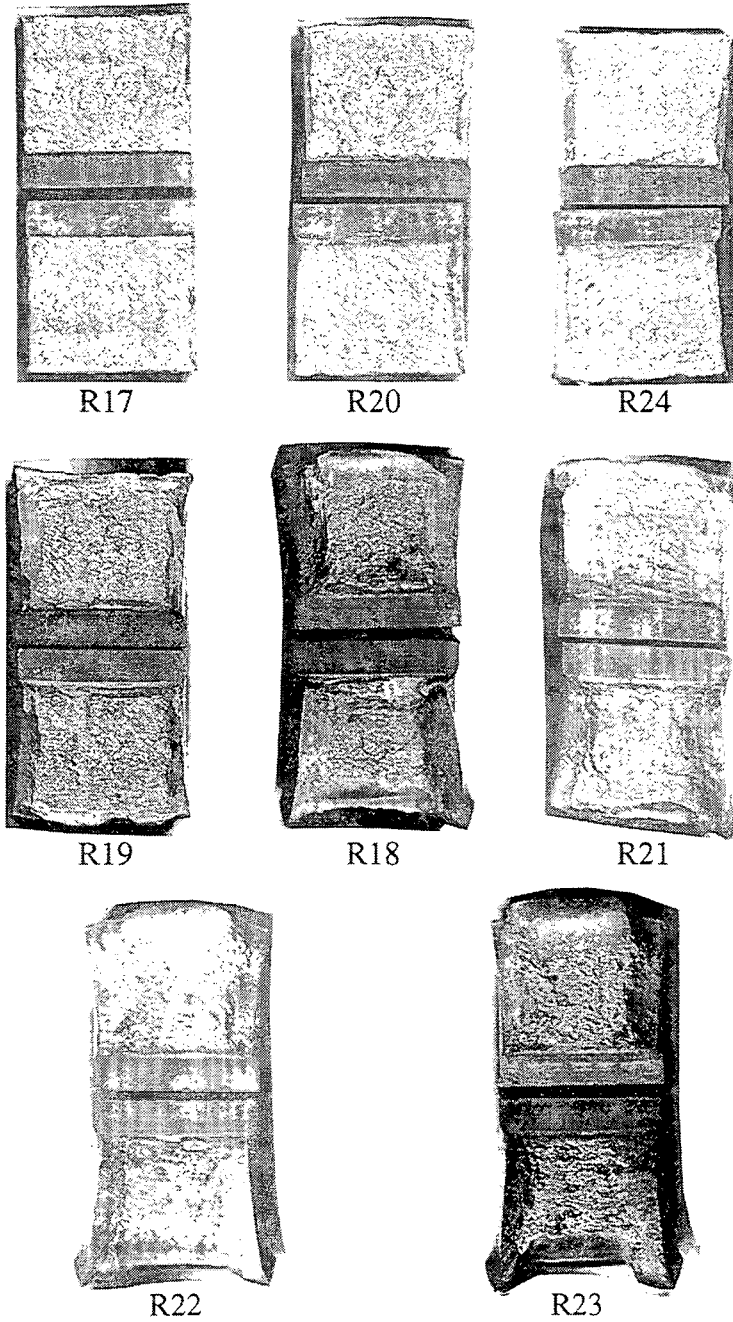
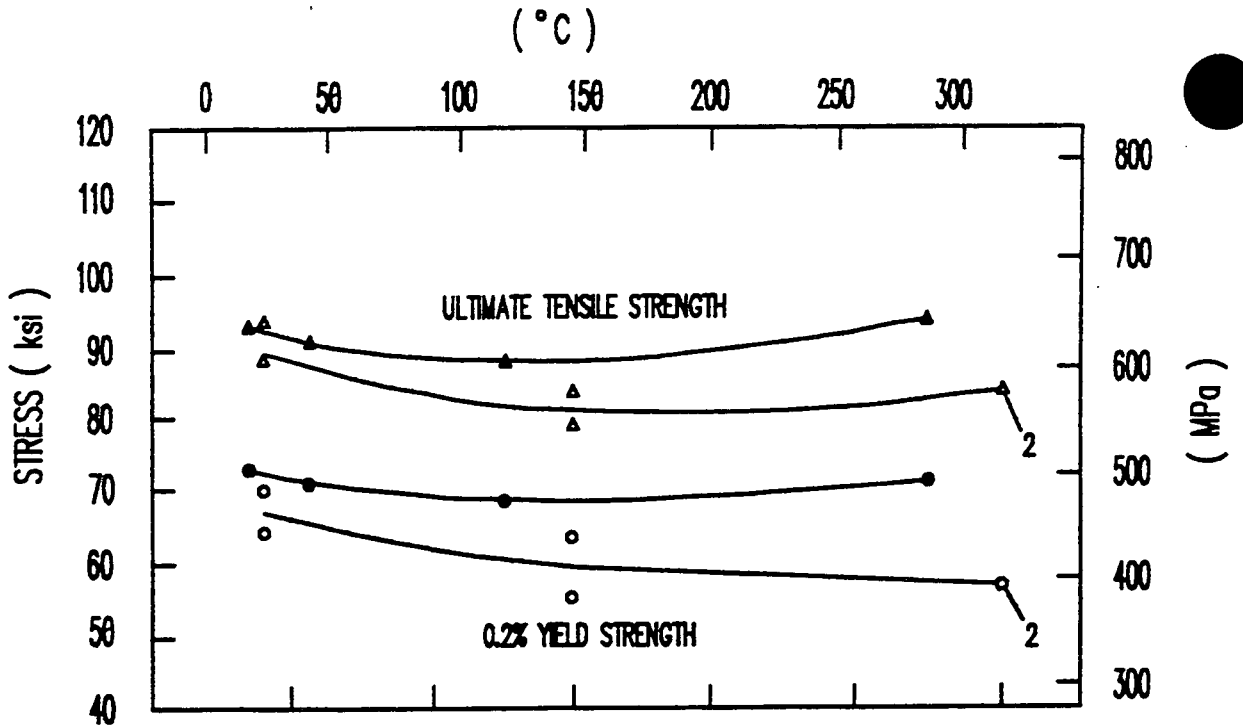


Figure 5-11 Charpy Impact Specimen Fracture Surfaces for A533 Grade B Class 1 ASTM Correlation Monitor Material ( HSST Plate 02)



CODE:  
 OPEN POINTS - UNIRRADIATED  
 CLOSED POINTS - IRRADIATED TO  $3.36 \times 10^{21} \text{ n/cm}^2$  ( $E > 1.0 \text{ MeV}$ )

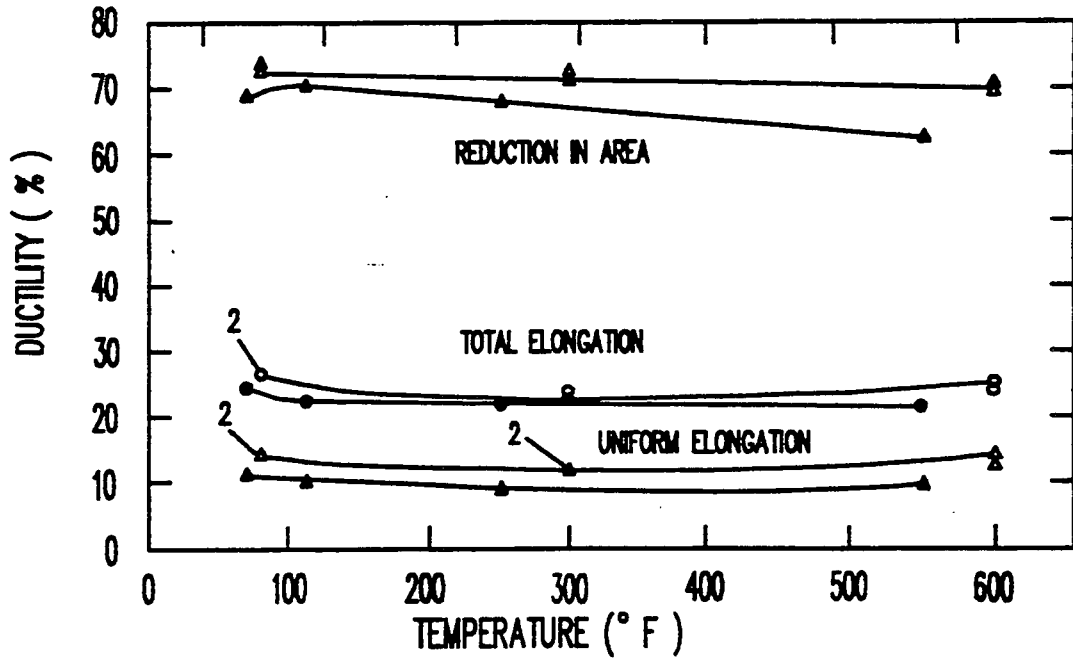
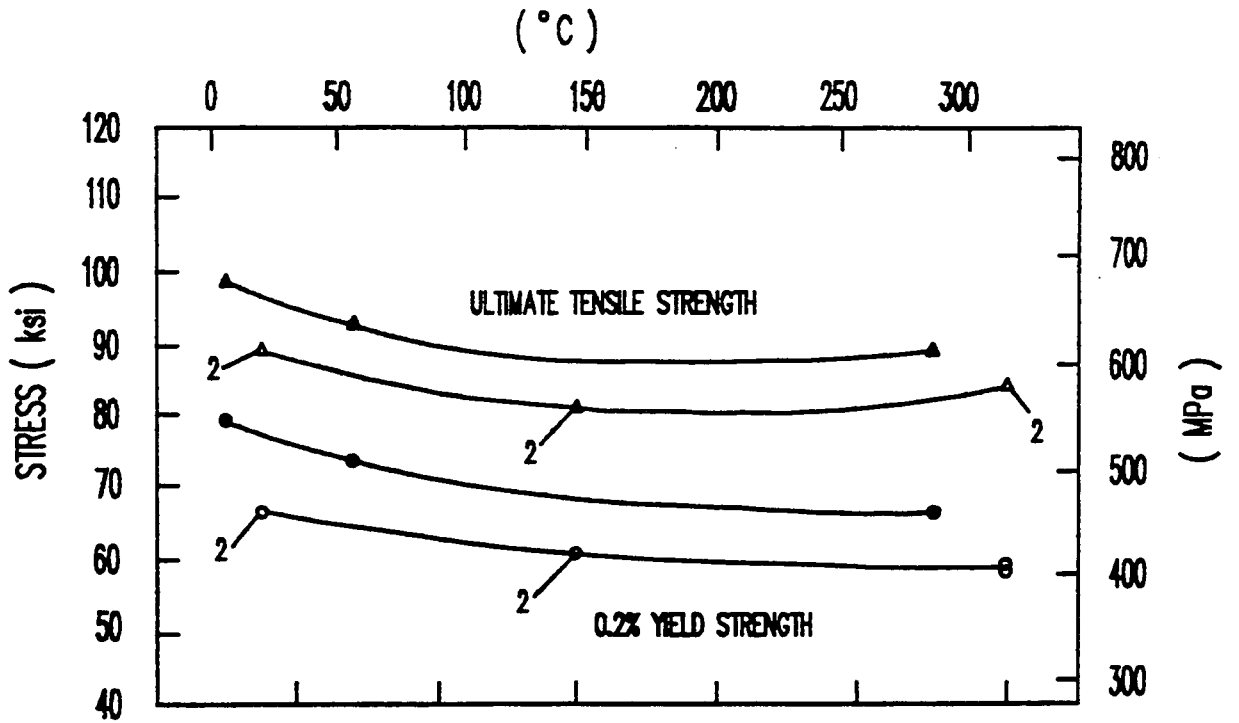


Figure 5-12 Tensile Properties for Kewaunee Reactor Vessel Intermediate Shell Forging 122X208VA1 (Tangential Orientation)





CODE:  
 OPEN POINTS - UNIRRADIATED  
 CLOSED POINTS - IRRADIATED TO  $3.36 \times 10^{19} \text{ n/cm}^2$  ( $E > 1.0 \text{ MeV}$ )

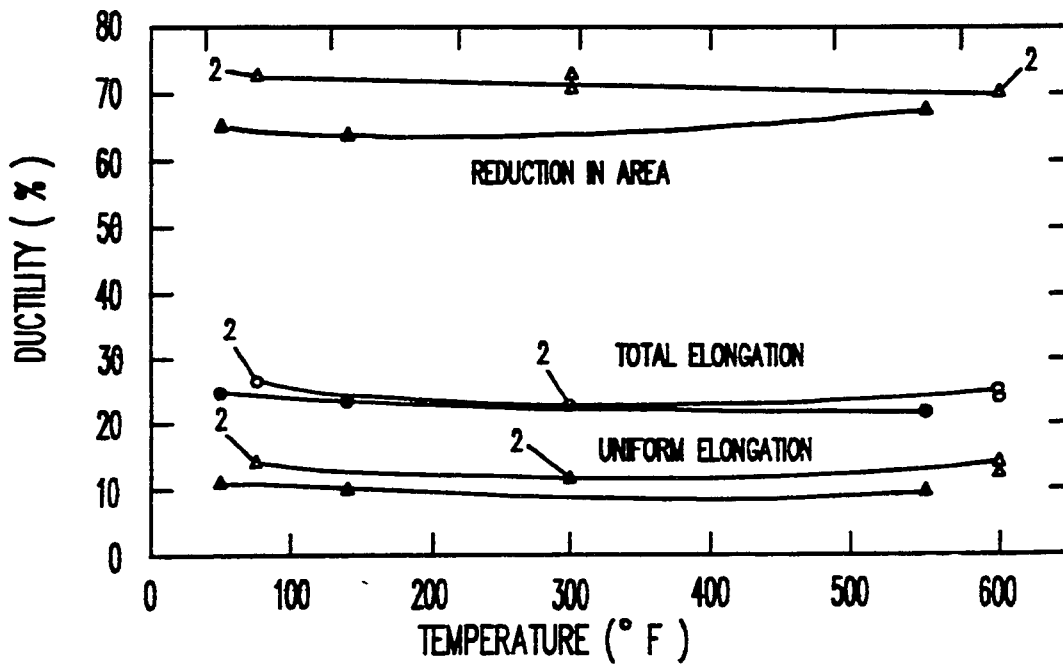
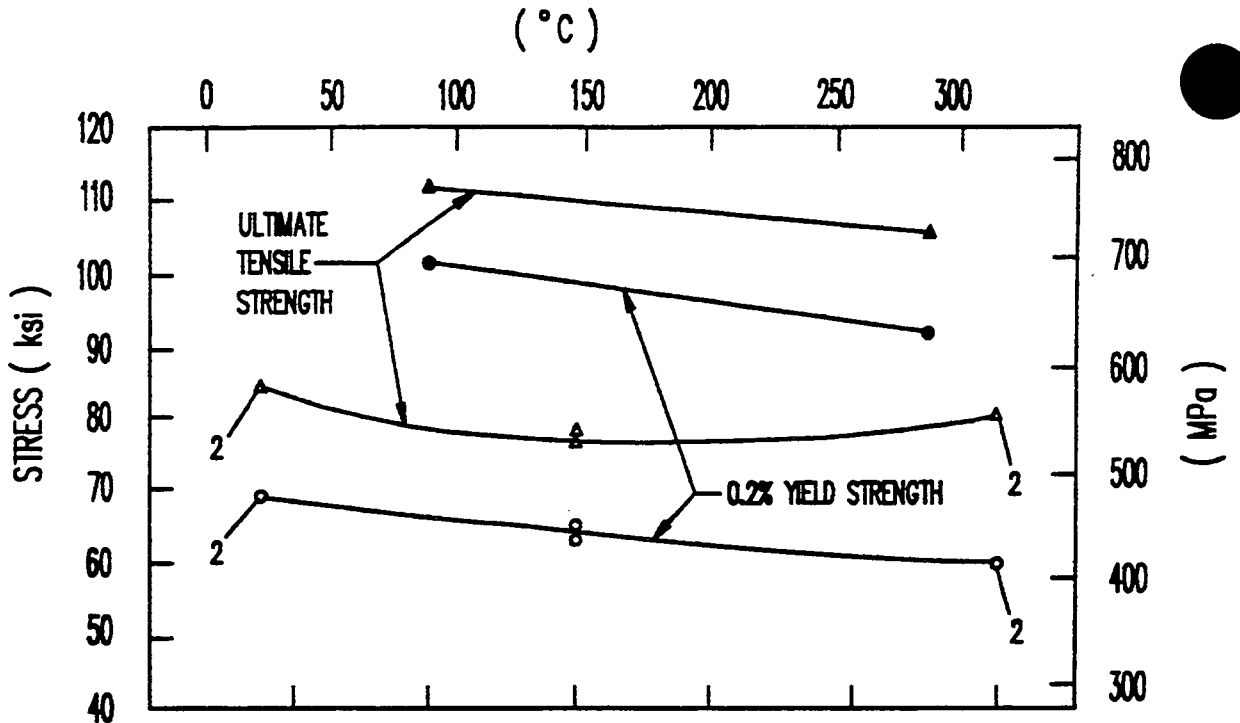


Figure 5-13 Tensile Properties for Kewaunee Reactor Vessel Lower Shell Forging 123X167VA1 (Tangential Orientation)



CODE:  
 OPEN POINTS - UNIRRADIATED  
 CLOSED POINTS - IRRADIATED TO  $3.36 \times 10^{22} \text{ n/cm}^2$  (  $E > 1.0 \text{ MeV}$  )

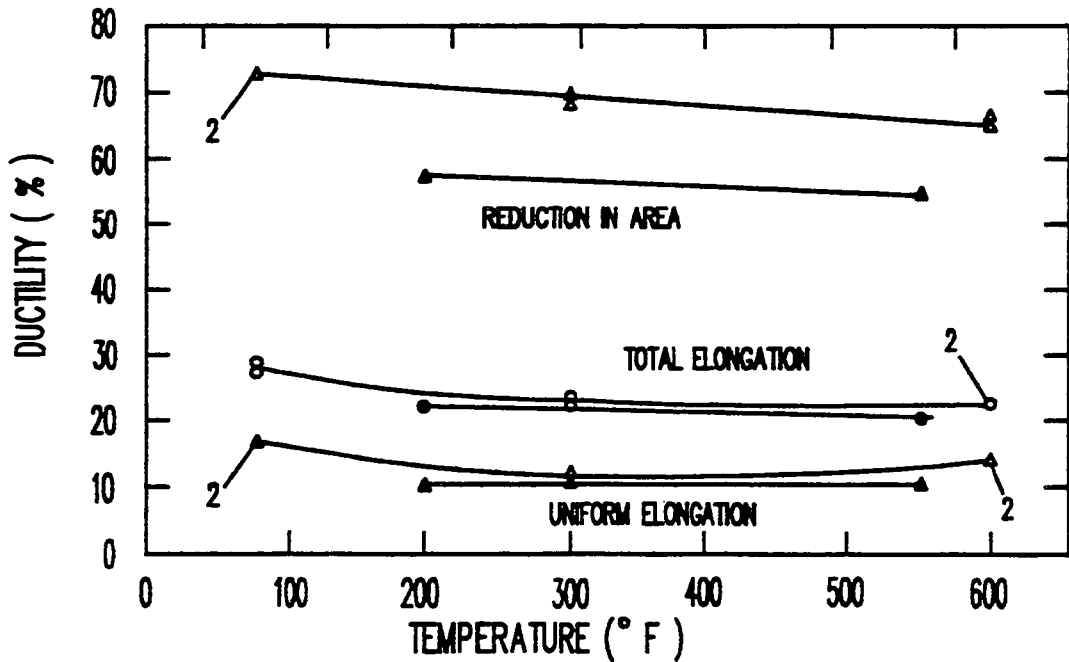
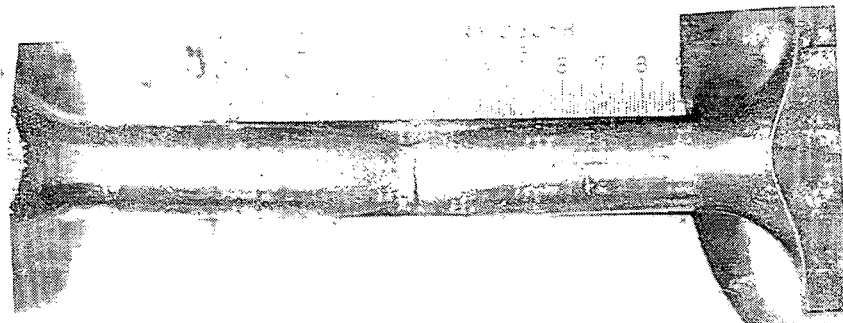
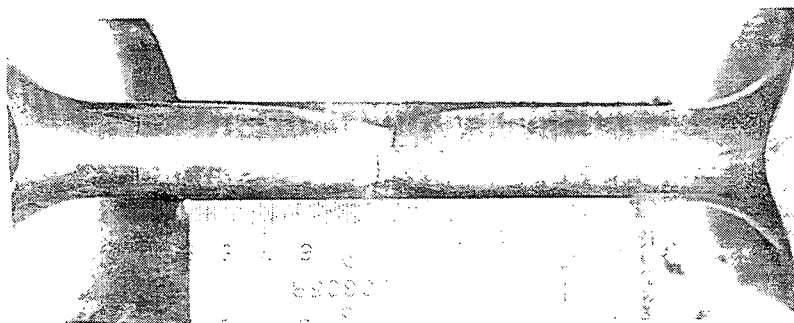


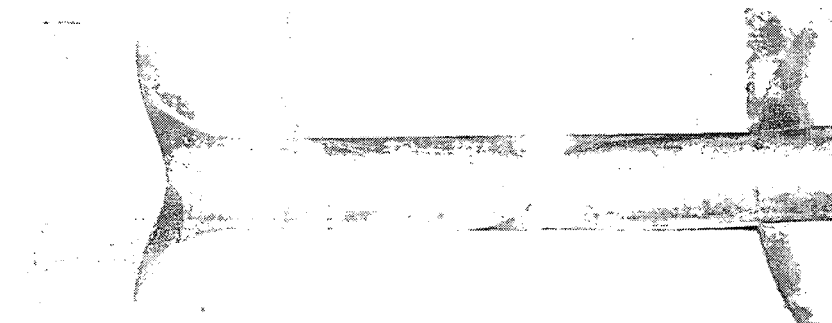
Figure 5-14 Tensile Properties for Kewaunee Reactor Vessel Surveillance Weld Metal



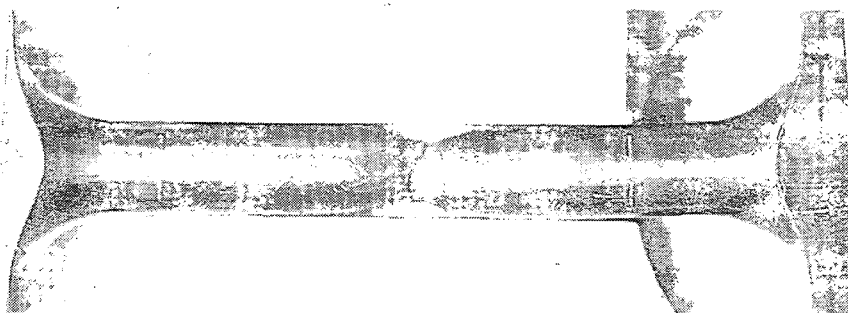
Specimen P9 Tested at 72°F



Specimen P10 Tested at 115°F

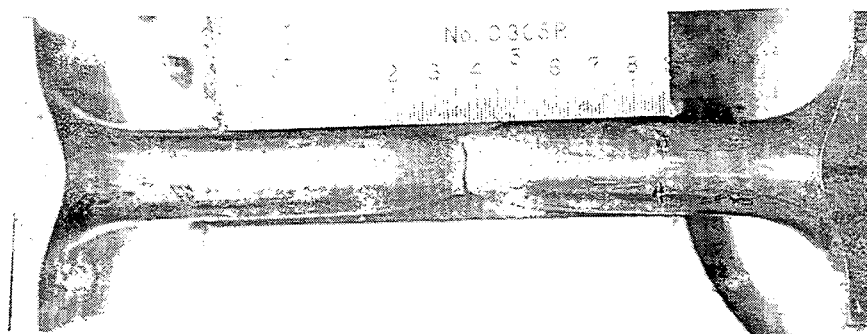


Specimen P11 Tested at 250°F



Specimen P12 Tested at 550°F

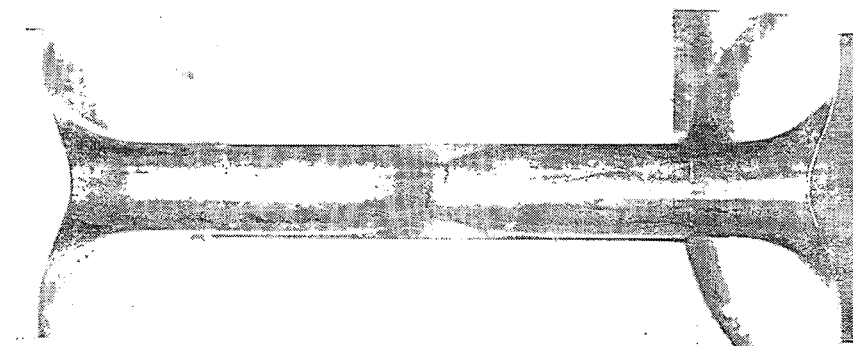
Figure 5-15 Fractured Tensile Specimens from Kewaunee Reactor Vessel Intermediate Shell Forging 122X208VA1 (Tangential Orientation)



Specimen S7 Tested at 50°F

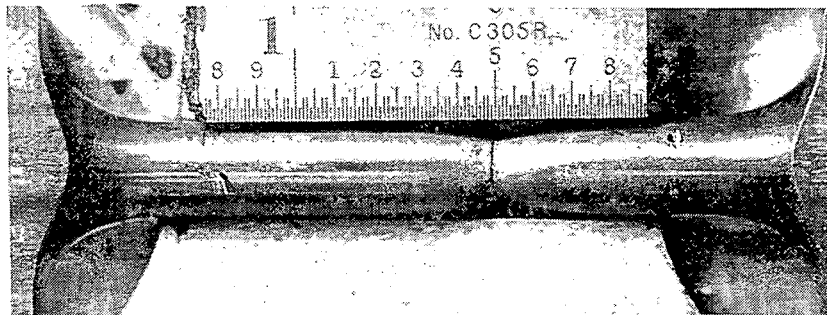


Specimen S8 Tested at 135°F

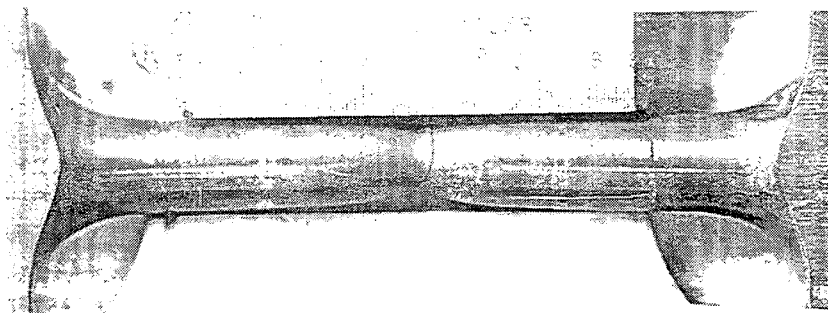


Specimen S9 Tested at 550°F

Figure 5-16 Fractured Tensile Specimens from Kewaunee Reactor Vessel Lower Shell Forging 123X167VA1 (Tangential Orientation)



Specimen W5 Tested at 200°F



Specimen W6 Tested at 550°F

Figure 5-17 Fractured Tensile Specimens from Kewaunee Reactor Vessel Surveillance Weld Metal

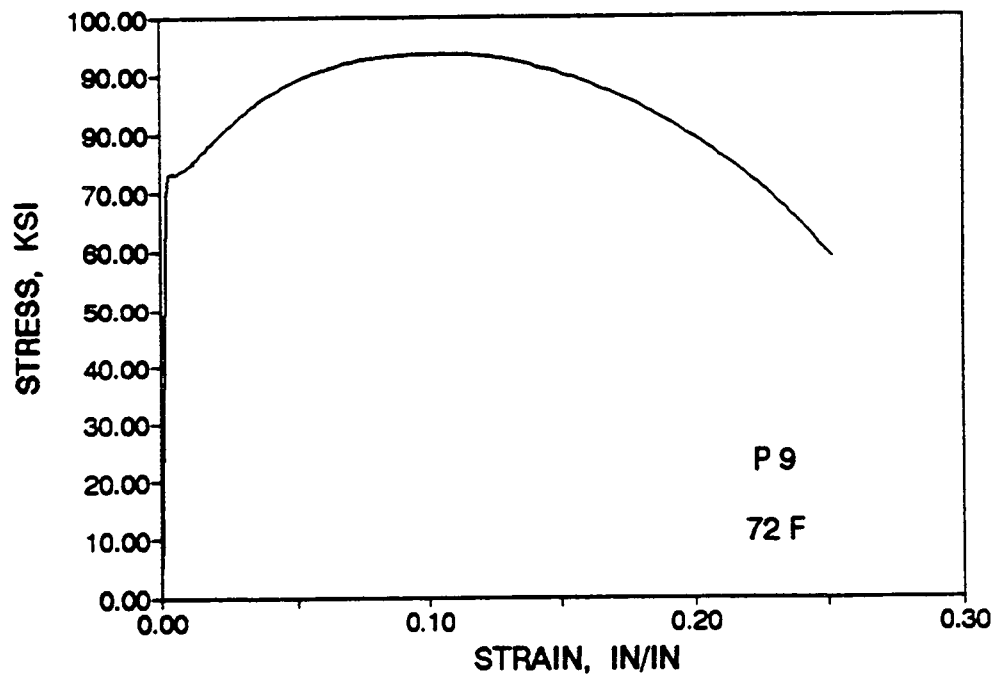
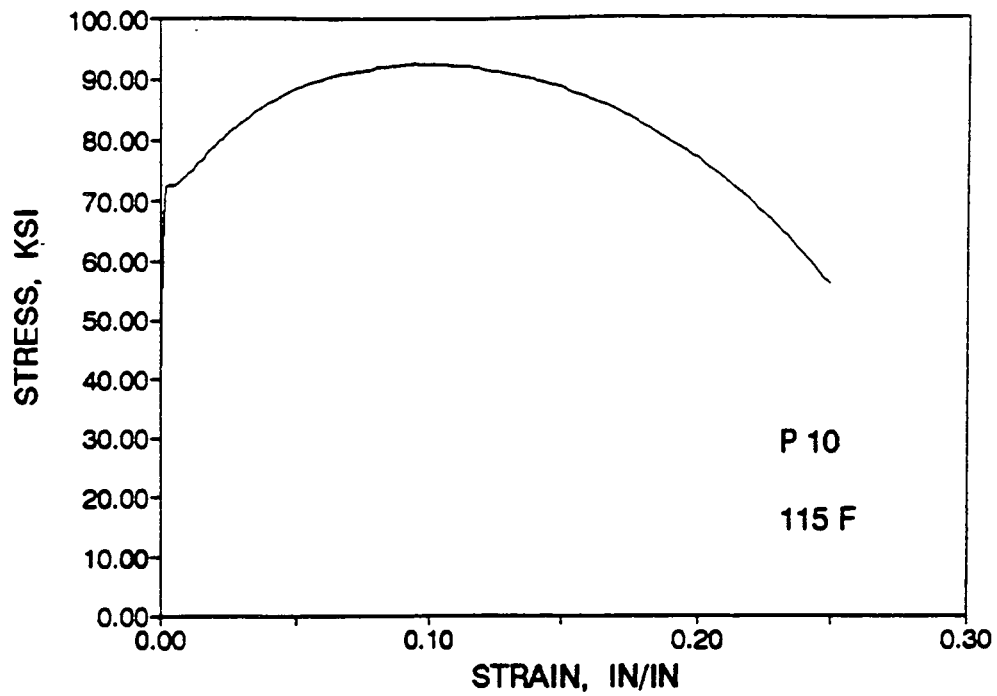


Figure 5-18 Engineering Stress-Strain Curves for Intermediate Shell Forging 122X208VA1 Tensile Specimens P10 and P9 (Tangential Orientation)

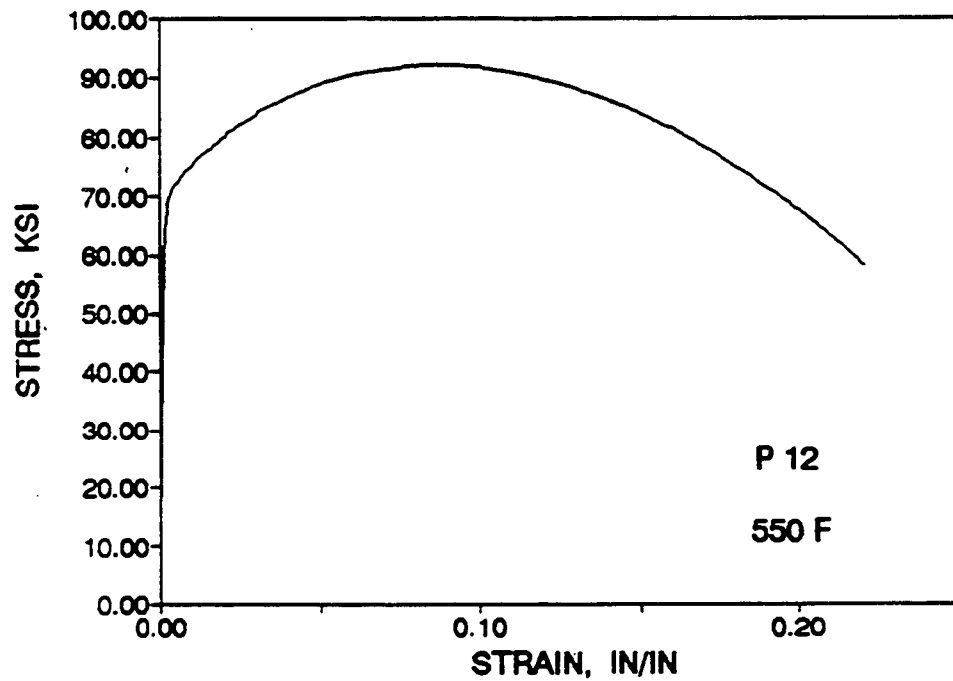
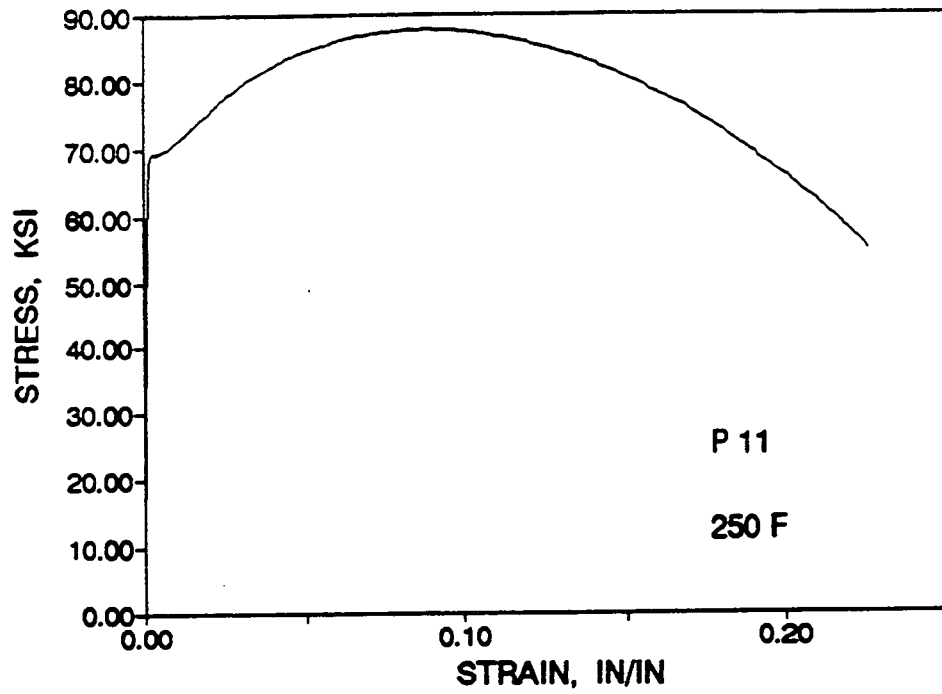


Figure 5-19 Engineering Stress-Strain Curves for Intermediate Shell Forging 122X208VA1 Tensile Specimens P11 and P12 (Tangential Orientation)

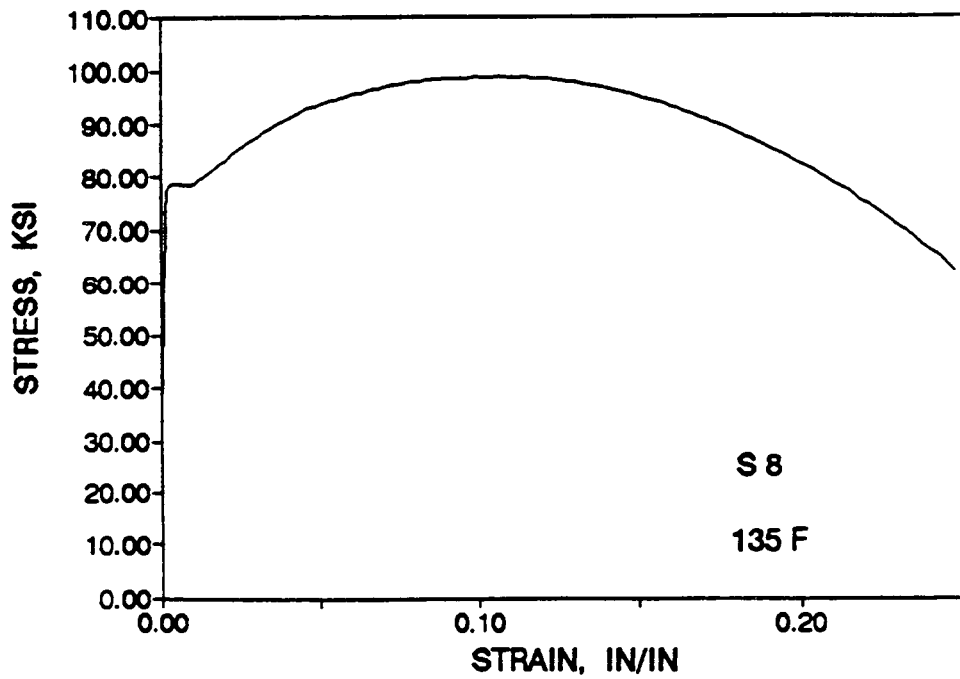
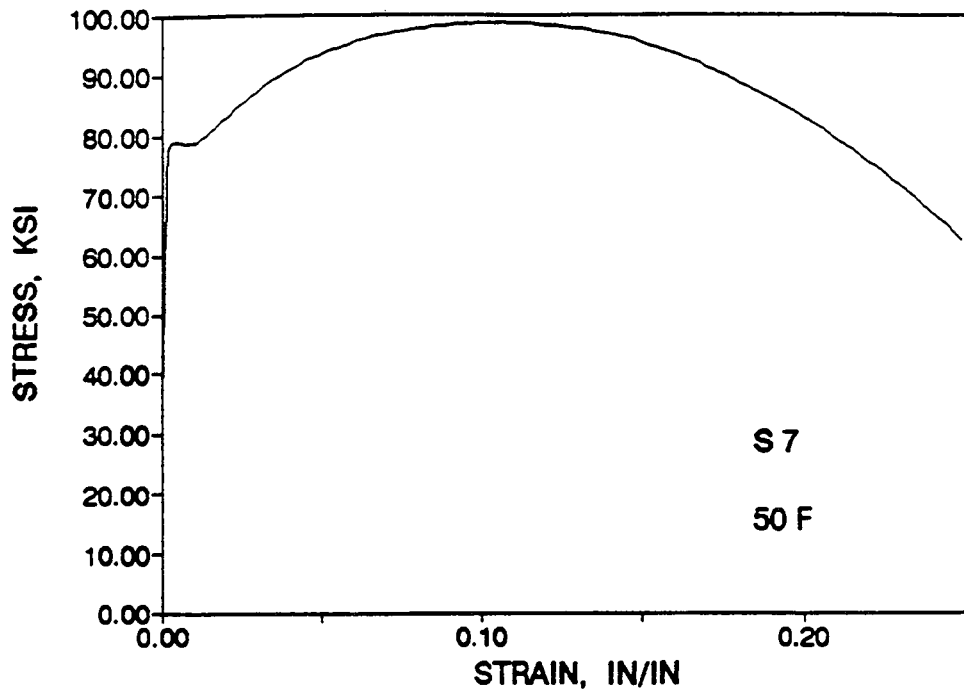


Figure 5-20 Engineering Stress-Strain Curves for Lower Shell Forging 123X167VA1 Tensile Specimens S7 and S8 (Tangential Orientation)



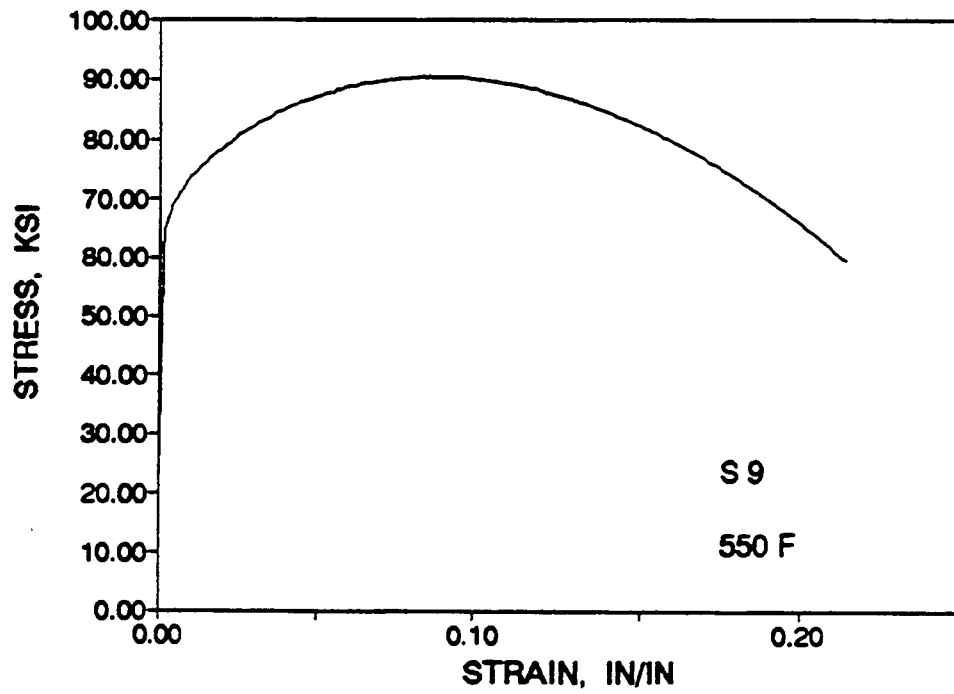


Figure 5-21 Engineering Stress-Strain Curve for Lower Shell Forging 123X167VA1 Tensile Specimen S9 (Tangential Orientation)

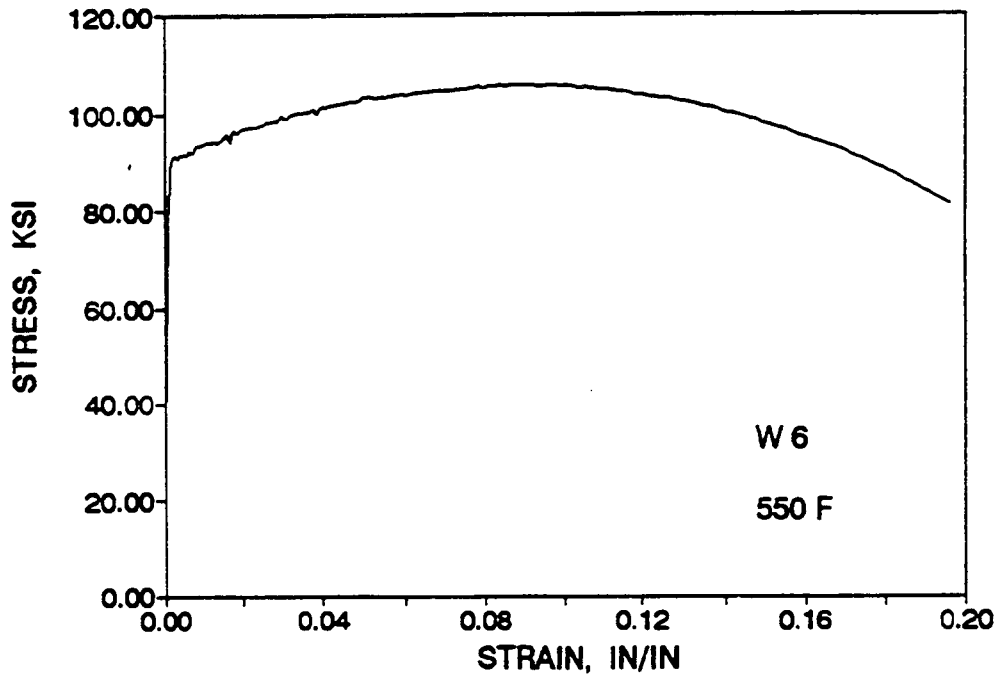
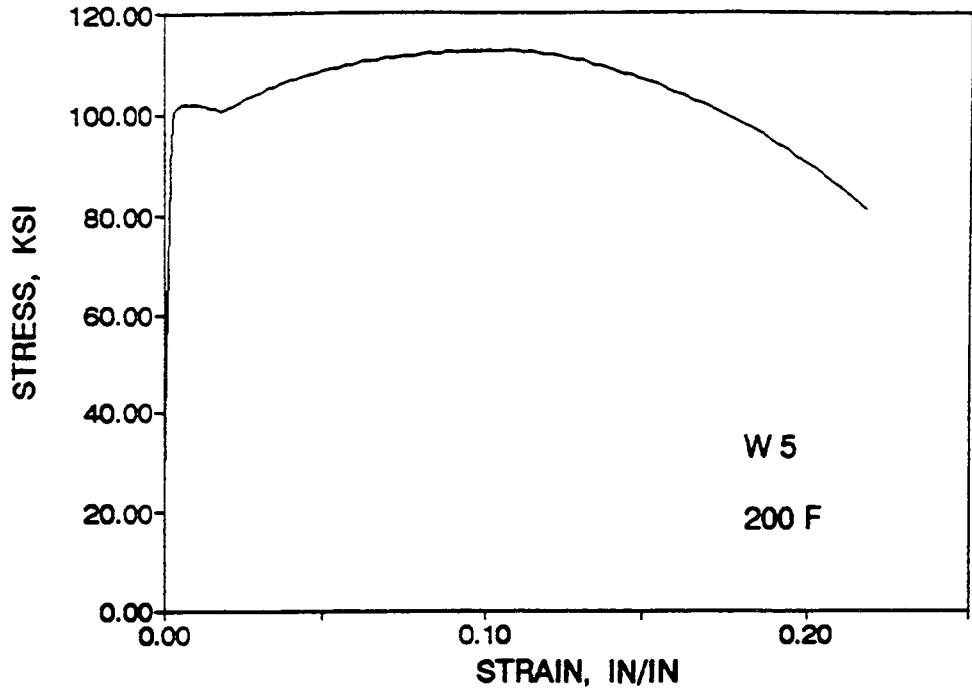


Figure 5-22 Engineering Stress-Strain Curves for Weld Metal Tensile Specimens W5 and W6

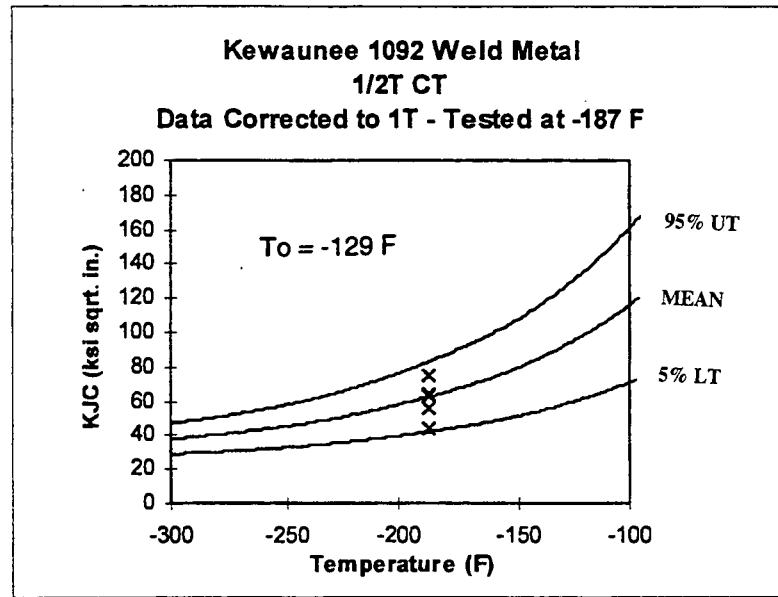


Figure 5-23 Unirradiated Kewaunee Surveillance Weld Master Curve Fit for 1/2T-CT Specimens

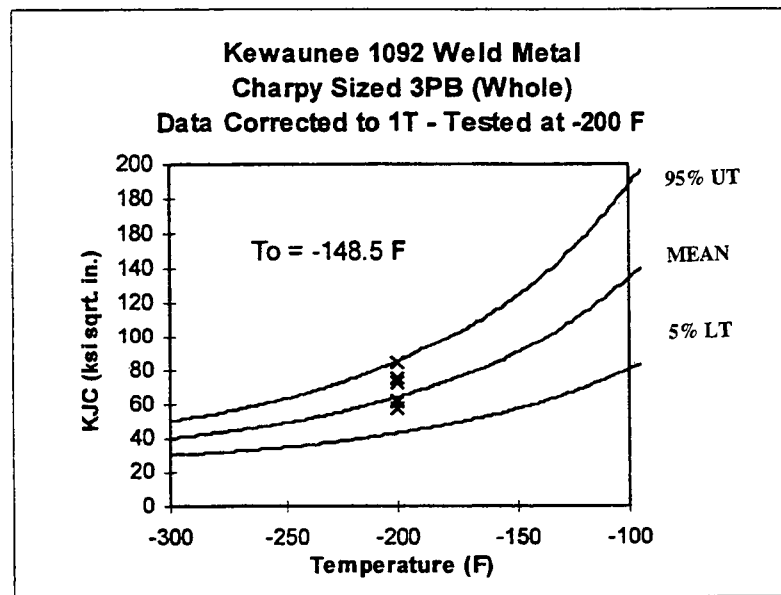


Figure 5-24 Unirradiated Kewaunee Surveillance Weld Master Curve Fit for Precracked Charpy Size 3PB Specimens

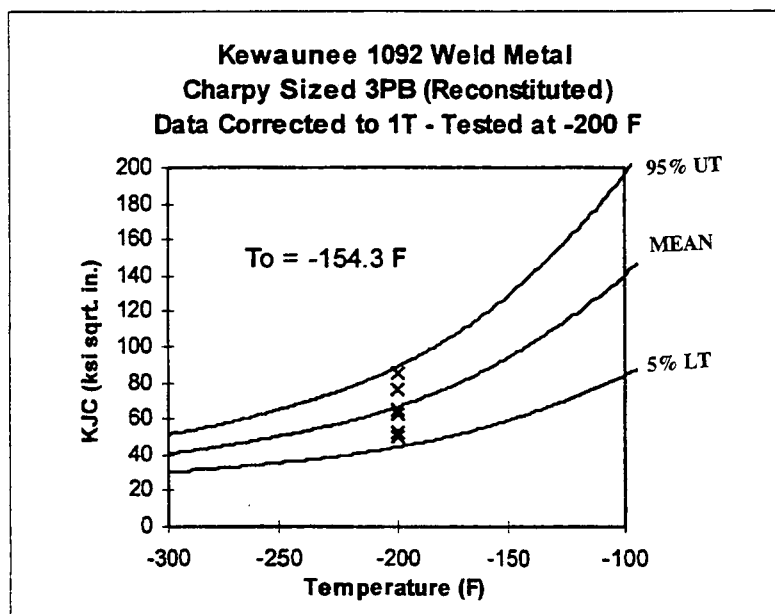


Figure 5-25 Unirradiated Kewaunee Surveillance Weld Master Curve Fit for Precracked and Reconstituted Charpy Size 3PB Specimens

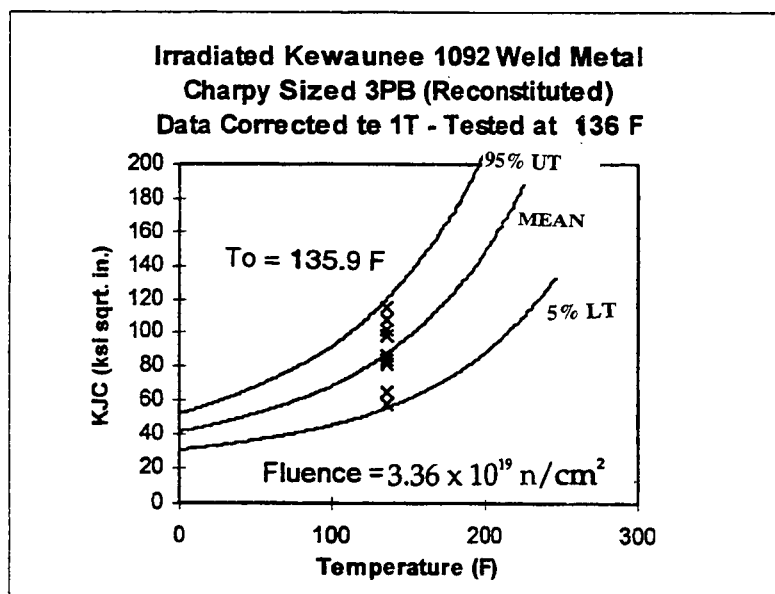


Figure 5-26 Irradiated Kewaunee Surveillance Weld Master Curve Fit for Precracked and Reconstituted Charpy Size 3PB Specimens

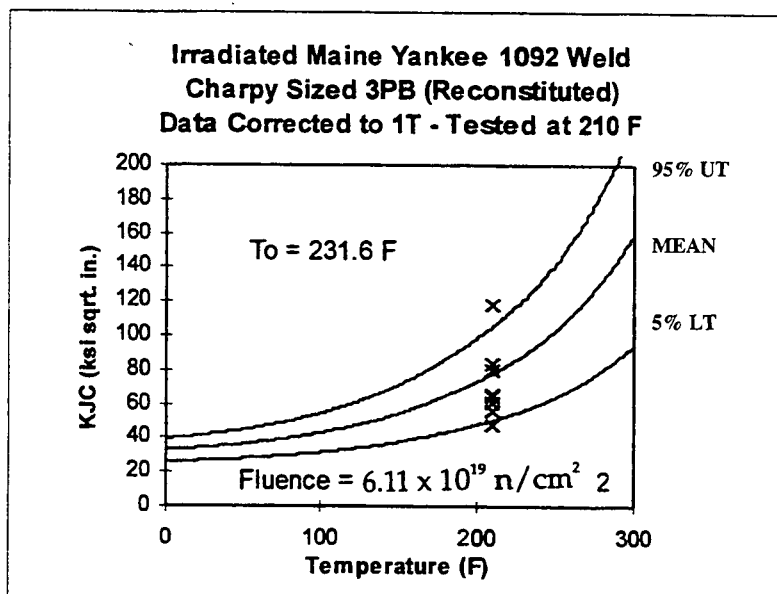


Figure 5-27 Irradiated Maine Yankee Surveillance Weld Master Curve Fit for Precracked and Reconstituted Charpy Size 3PB Specimens

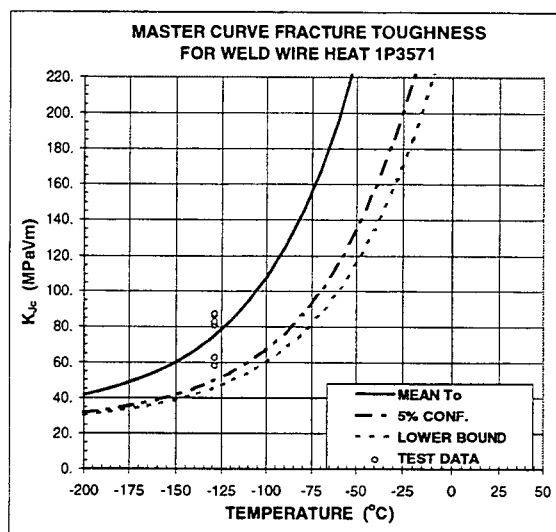


Figure 5-28 Unirradiated Maine Yankee Surveillance Weld Master Curve Fit for Precracked Charpy Size 3PB Specimens

## 6.0 RADIATION ANALYSIS AND NEUTRON DOSIMETRY

### 6.1 KEWAUNEE

#### 6.1.1 Introduction

This section is being revised in order to incorporate ENDF/B-VI based dosimetry reaction cross-sections that have been released in the SNLRML dosimetry cross-section compendium. The evaluations provided in Revision 0 of this report were based on the use of dosimetry cross-sections derived from the ENDF/B-V dosimetry files. The neutron transport calculations described in this revision are based on the ENDF/B-VI based BUGLE-93 library. This transport cross-section library was also used in Revision 0 to this report. In addition to the updated dosimetry cross-sections, changes in the projected future plant operation as reflected by fuel management changes and projected future operating times were also included in the updated fluence estimates for the future.

Knowledge of the neutron environment within the reactor pressure vessel and surveillance capsule geometry is required as an integral part of LWR pressure vessel surveillance programs for two reasons. First, in order to interpret the neutron radiation-induced material property changes observed in the test specimens, the neutron environment (energy spectrum, flux, fluence) to which the test specimens were exposed must be known. Second, in order to relate the changes observed in the test specimens to the present and future condition of the reactor vessel, a relationship must be established between the neutron environment at various positions within the reactor vessel and that experienced by the test specimens. The former requirement is normally met by employing a combination of rigorous analytical techniques and measurements obtained with passive neutron flux monitors contained in each of the surveillance capsules. The latter information is derived solely from analysis.

The use of fast neutron fluence ( $E > 1.0$  MeV) to correlate measured material property changes to the neutron exposure of the material for light water reactor applications has traditionally been accepted for development of damage trend curves as well as for the implementation of trend curve data to assess vessel condition. In recent years, however, it has been suggested that an exposure model that accounts for differences in neutron energy spectra between surveillance capsule locations and positions within the vessel wall could lead to an improvement in the uncertainties associated with damage trend curves as well as to a more accurate evaluation of damage gradients through the pressure vessel wall.

Because of this potential shift away from a threshold fluence toward an energy dependent damage function for data correlation, ASTM Standard Practice E853, "Analysis and Interpretation of Light Water Reactor Surveillance Results,"<sup>[21]</sup> recommends reporting displacements per iron atom (dpa) along with fluence ( $E > 1.0$  MeV) to provide a data base for future reference. The energy dependent dpa function to be used for this evaluation is specified in ASTM Standard Practice E693, "Characterizing Neutron Exposures in Ferritic Steels in Terms of Displacements per Atom."<sup>[22]</sup> The application of the dpa parameter to the assessment of embrittlement gradients through the thickness of the pressure vessel wall has already been

promulgated in Revision 2 to the Regulatory Guide 1.99, "Radiation Embrittlement of Reactor Vessel Materials."

This section provides the results of the neutron dosimetry evaluations performed in conjunction with the analysis of test specimens contained in surveillance Capsule S, withdrawn at the end of the nineteenth fuel cycle. Also included is an update of dosimetry contained in Capsules V, R, and P, withdrawn at the conclusion of Cycles 1, 5, and 13, respectively. This update is based on current methodology and nuclear data; and together with the Capsule S results provides a consistent up to date data base for use in evaluating material properties of the Kewaunee reactor vessel.

In all cases, fast neutron exposure parameters in terms of fast neutron fluence ( $E > 1.0$  MeV), fast neutron fluence ( $E > 0.1$  MeV), and iron atom displacements (dpa) are established for the capsule irradiation history. The analytical formalism relating the measured capsule exposure to the exposure of the vessel wall is described and used to project the integrated exposure of the vessel itself. Also uncertainties associated with the derived exposure parameters at the surveillance capsule and with the projected exposure of the pressure vessel are provided.

### 6.1.2 Discrete Ordinates Analysis

A plan view of the reactor geometry at the core midplane is shown in Figure 4-1. Six irradiation capsules attached to the thermal shield are included in the reactor design to constitute the reactor vessel surveillance program. The capsules are located at azimuthal angles of  $57^\circ$ ,  $67^\circ$ ,  $77^\circ$ ,  $237^\circ$ ,  $247^\circ$ , and  $257^\circ$  relative to the core cardinal axes as shown in Figure 4-1.

A plan view of a surveillance capsule holder attached to the thermal shield is shown in Figure 6-1. The stainless steel specimen containers are 1-inch square and approximately 64 inches in height. The containers are positioned axially such that the specimens are centered about the core midplane, thus spanning the central 5.33 feet of the 12-foot high reactor core.

From a neutron transport standpoint, the surveillance capsule structures are significant. They have a marked effect on both the distribution of neutron flux and the neutron energy spectrum in the water annulus between the thermal shield and the reactor vessel. In order to properly determine the neutron environment at the test specimen location, the capsules themselves must be included in the analytical model.

In performing the fast neutron exposure evaluations for the surveillance capsules and reactor vessel, two distinct sets of transport calculations were carried out. The first, a single computation in the conventional forward mode, was used primarily to obtain relative neutron energy distributions throughout the reactor geometry as well as to establish relative radial distributions of exposure parameters  $\{\phi(E > 1.0 \text{ MeV}), \phi(E > 0.1 \text{ MeV}), \text{ and dpa}\}$  through the vessel wall. The neutron spectral information was required for the interpretation of neutron dosimetry withdrawn from the surveillance capsule as well as for the determination of exposure parameter ratios; i.e.,  $\text{dpa} / \phi(E > 1.0 \text{ MeV})$ , within the pressure vessel geometry. The relative radial gradient information was required to permit the projection of measured exposure

parameters to locations interior to the pressure vessel wall; i.e., the 1/4T, 1/2T, and 3/4T locations.

The second set of calculations consisted of a series of adjoint analyses relating the fast neutron flux ( $E > 1.0$  MeV) at surveillance capsule positions, and several azimuthal locations on the pressure vessel inner radius to neutron source distributions within the reactor core. The importance functions generated from these adjoint analyses provided the basis for all absolute exposure projections and comparison with measurement. These importance functions, when combined with cycle specific neutron source distributions, yielded absolute predictions of neutron exposure at the locations of interest for each cycle of irradiation and established the means to perform similar predictions and dosimetry evaluations for all subsequent fuel cycles. It is important to note that the cycle specific neutron source distributions utilized in these analyses included not only spatial variations of fission rates within the reactor core but also accounted for the effects of varying neutron yield per fission and fission spectrum introduced by the build-up of plutonium as the burnup of individual fuel assemblies increased.

The absolute cycle specific data from the adjoint evaluations together with relative neutron energy spectra and radial distribution information from the forward calculation provided the means to:

1. Evaluate neutron dosimetry obtained from surveillance capsule locations.
2. Extrapolate dosimetry results to key locations at the inner radius and through the thickness of the pressure vessel wall.
3. Enable a direct comparison of analytical prediction with measurement.
4. Establish a mechanism for projection of pressure vessel exposure as the design of each new fuel cycle evolves.

The forward transport calculation for the reactor model summarized in Figures 4-1 and 6-1 was carried out in R,  $\theta$  geometry using the DORT two-dimensional discrete ordinates code<sup>[23]</sup> and the BUGLE-93 cross-section library<sup>[24]</sup>. The BUGLE-93 library is a 47 group ENDF/B-VI based data set produced specifically for light water reactor applications. In these analyses anisotropic scattering was treated with a  $P_3$  expansion of the cross-sections and the angular discretization was modeled with an  $S_3$  order of angular quadrature.

The reference core power distribution utilized in the forward analysis was derived from statistical studies of long-term operation of Westinghouse 2-loop plants. Inherent in the development of this reference core power distribution is the use of an out-in fuel management strategy; i.e., fresh fuel on the core periphery. Furthermore, for the peripheral fuel assemblies, a  $2\sigma$  uncertainty derived from the statistical evaluation of plant to plant and cycle to cycle variations in peripheral power was used. Since it is unlikely that a single reactor would have a power distribution at the nominal  $+2\sigma$  level for a large number of fuel cycles, the use of this reference distribution is expected to yield somewhat conservative results.



All adjoint analyses were also carried out using an  $S_8$  order of angular quadrature and the P3 cross-section approximation from the BUGLE-93 library. Adjoint source locations were chosen at several azimuthal locations along the pressure vessel inner radius as well as the geometric center of each surveillance capsule. Again, these calculations were run in  $R, \theta$  geometry to provide neutron source distribution importance functions for the exposure parameter of interest, in this case,  $\phi(E > 1.0 \text{ MeV})$ . Having the importance functions and appropriate core source distributions, the response of interest could be calculated as:

$$R(r, \theta) = \int_r \int_\theta \int_E I(r, \theta, E) S(r, \theta, E) r dr d\theta dE$$

where:

$R(r, \theta)$	=	$\phi(E > 1.0 \text{ MeV})$ at radius $r$ and azimuthal angle $\theta$
$I(r, \theta, E)$	=	Adjoint importance function at radius, $r$ , azimuthal angle $\theta$ , and neutron source energy $E$ .
$S(r, \theta, E)$	=	Neutron source strength at core location $r, \theta$ and energy $E$ .

Although the adjoint importance functions used in the analysis were based on a response function defined by the threshold neutron flux ( $E > 1.0 \text{ MeV}$ ), prior calculations have shown that, while the implementation of low leakage loading patterns significantly impact the magnitude and the spatial distribution of the neutron field, changes in the relative neutron energy spectrum are of second order. Thus, for a given location, the ratio of  $dpa/\phi(E > 1.0 \text{ MeV})$  is insensitive to changing core source distributions. In the application of these adjoint importance functions to the Kewaunee reactor the iron displacement rates ( $dpa$ ) and the neutron flux ( $E > 0.1 \text{ MeV}$ ) were computed on a cycle specific basis by using  $dpa/\phi(E > 1.0 \text{ MeV})$  and  $\phi(E > 0.1 \text{ MeV})/\phi(E > 1.0 \text{ MeV})$  ratios from the forward analysis in conjunction with the cycle specific  $\phi(E > 1.0 \text{ MeV})$  solutions from the individual adjoint evaluations.

The reactor core power distributions used in the plant specific reactor pressure vessel adjoint calculations were taken from the fuel cycle design reports for the first twenty-two operating cycles of Kewaunee.

Selected results from the neutron transport analyses are provided in Tables 6-1 through 6-7. The data listed in these tables establish the means for absolute comparisons of analysis and measurement for the capsule irradiation period and provide the means to correlate dosimetry results with the corresponding neutron exposure of the pressure vessel wall.

In Table 6-1, the calculated exposure parameters  $\phi(E > 1.0 \text{ MeV})$ ,  $\phi(E > 0.1 \text{ MeV})$ , and  $dpa$  are given at the specimen geometric center of the three surveillance capsule positions for both the design basis and the plant specific core power distributions. The plant specific data, based on the adjoint transport analysis, are meant to establish the absolute comparison of measurement with analysis. The design basis data derived from the forward calculation are provided as a point of reference against which plant specific fluence evaluations can be compared. Similar data is given in Table 6-2, 6-3 and 6-4 for the pressure vessel inner radius. Again, the pertinent exposure parameters are listed for both the design basis and the plant specific power

distributions. It is important to note that the data for the vessel inner radius were taken at the clad/base metal interface and, thus, represent the maximum exposure levels of the vessel wall itself.

Radial gradient information for neutron flux ( $E > 1.0$  MeV), neutron flux ( $E > 0.1$  MeV), and iron atom displacement rate is given in Tables 6-5, 6-6, and 6-7, respectively. The data, obtained from the forward neutron transport calculation, are presented on a relative basis for each exposure parameter at several azimuthal locations. Exposure parameter distributions within the wall may be obtained by normalizing the calculated or projected exposure at the vessel inner radius to the gradient data given in Tables 6-5 through 6-7.

For example, the neutron flux ( $E > 1.0$  MeV) at the 1/4T position on the  $0^\circ$  azimuth is given by:

$$\phi_{1/4T}(0^\circ) = \phi(168.04, 0^\circ) F(172.17, 0^\circ)$$

where:  $\phi_{1/4T}(0^\circ) =$  Projected neutron flux at the 1/4T position on the  $0^\circ$  azimuth

$\phi(168.04, 0^\circ) =$  Projected or calculated neutron flux at the vessel inner radius on the  $0^\circ$  azimuth.

$F(172.17, 0^\circ) =$  Relative radial distribution function from Table 6-5.

Similar expressions apply for exposure parameters in terms of  $\phi$  ( $E > 0.1$  MeV) and dpa/sec.

### 6.1.3 Neutron Dosimetry

The passive neutron sensors included in the Kewaunee surveillance program are listed in Table 6-8. Also given in Table 6-8 are the primary nuclear reactions and associated nuclear constants that were used in the evaluation of the neutron energy spectrum within the capsule and the subsequent determination of the various exposure parameters of interest;  $\phi$  ( $E > 1.0$  MeV),  $\phi$  ( $E > 0.1$  MeV), dpa.

The relative locations of the neutron sensors within the capsules are shown in Figure 4-2. The iron, nickel, copper, and cobalt-aluminum monitors, in wire form, were placed in holes drilled in spacers at several axial levels within the capsules. The cadmium-shielded neptunium and uranium fission monitors were accommodated within the dosimeter block located near the center of the capsule.

The use of passive monitors such as those listed in Table 6-8 does not yield a direct measure of the energy dependent flux level at the point of interest. Rather, the activation or fission process is a measure of the integrated effect that the time- and energy-dependent neutron flux has on the target material over the course of the irradiation period. An accurate assessment of the average neutron flux level incident on the various monitors may be derived from the activation

measurements only if the irradiation parameters are well known. In particular, the following variables are of interest:

- The specific activity of each monitor.
- The operating history of the reactor.
- The energy response of the monitor.
- The neutron energy spectrum at the monitor location.
- The physical characteristics of the monitor.

The specific activity of each of the neutron monitors was determined using established ASTM procedures<sup>[25-36]</sup>. Following sample preparation and weighing, the activity of each monitor was determined by means of a lithium-drifted germanium, Ge(Li), gamma spectrometer. The irradiation history of the Kewaunee reactor during Cycles 1 through 19 was obtained from NUREG-0020, "Licensed Operating Reactors Status Summary Report" for the applicable period.

The irradiation history applicable to Capsules V, R, P, and S are given in Table 6-9. Measured and derived saturated reaction product specific activities at surveillance capsule specimen geometric center, as well as, derived full power reaction rates at surveillance capsule specimen geometric center are listed in Tables 6-10, 6-11, 6-12 and 6-13 for Capsules V, R, P, and S, respectively. Saturated activity and reaction rate values were derived using the pertinent data from Tables 6-8 and 6-9.

Values of key fast neutron exposure parameters were derived from the measured reaction rates using the FERRET least squares adjustment code<sup>[37]</sup>. The FERRET approach used the reaction rate data and the calculated neutron energy spectrum at the geometric center of the specimens as input and proceeded to adjust a priori (calculated) group fluxes to produce a best fit (in a least squares sense) to the reaction rate data. The exposure parameters along with associated uncertainties were then obtained from the adjusted spectra.

In the FERRET evaluations, a log-normal least-squares algorithm weights both the a priori values and the measured data in accordance with the assigned uncertainties and correlations. In general, the measured values  $f$  are linearly related to the flux  $\phi$  by some response matrix  $A$ :

$$f^{(s,\alpha)} = \sum_g A_{ig}^{(s)} \phi_g^{(\alpha)}$$

where  $i$  indexes the measured values belonging to a single data set  $s$ ,  $g$  designates the energy group and  $\alpha$  delineates spectra that may be simultaneously adjusted. For example,

$$R_i = \sum_g \sigma_{ig} \phi_g$$

relates a set of measured reaction rates  $R_i$  to a single spectrum  $\phi_g$  by the multigroup cross section  $\sigma_{ig}$ . (In this case, FERRET also adjusts the cross-sections.) The log-normal approach

automatically accounts for the physical constraint of positive fluxes, even with the large assigned uncertainties.

In the FERRET analysis of the dosimetry data, the continuous quantities (i.e., fluxes and cross-sections) were approximated in 53 groups. The calculated fluxes from the discrete ordinates analysis were expanded into the FERRET group structure using the SAND-II code<sup>[38]</sup>. This procedure was carried out by first expanding the a priori spectrum into the SAND-II 620 group structure using a SPLINE interpolation procedure for interpolation in regions where group boundaries do not coincide. The 620-point spectrum was then easily collapsed to the group scheme used in FERRET.

The cross-sections were also collapsed into the 53 energy-group structure using SAND II with calculated spectra (as expanded to 620 groups) as weighting functions. The cross sections were taken from the SNLRML dosimetry file<sup>[39]</sup>. Uncertainty estimates and 53 x 53 covariance matrices were constructed for each cross section. Correlations between cross sections were neglected due to data and code limitations, but are expected to be unimportant.

For each set of data or a priori values, the inverse of the corresponding relative covariance matrix  $M$  is used as a statistical weight. In some cases, as for the cross sections, a multigroup covariance matrix is used. More often, a simple parameterized form is used:

$$M_{gg'} = R_N + (R_g)^2 * (R_{g'}) * (P_{gg'})$$

where  $R_N$  specifies an overall fractional normalization uncertainty (i.e., complete correlation) for the corresponding set of values. The fractional uncertainties  $R_g$  specify additional random uncertainties for group  $g$  that are correlated with a correlation matrix:

$$P_{gg'} = (1 - \theta) \delta_{gg'} + \theta \exp[-(g-g')^2 / 2\gamma^2]$$

The first term specifies purely random uncertainties while the second term describes short-range correlations over a range  $\gamma$  ( $\theta$  specifies the strength of the latter term).

For the a priori calculated fluxes, a short-range correlation of  $\gamma = 6$  groups was used. This choice implies that neighboring groups are strongly correlated when  $\theta$  is close to 1. Strong long-range correlations (or anticorrelations) were justified based on information presented by R.E. Maerker<sup>[40]</sup>. Maerker's results are closely duplicated when  $\gamma = 6$ . For the integral reaction rate covariances, simple normalization and random uncertainties were combined as deduced from experimental uncertainties.

Results of the FERRET evaluations of the Capsules V, R, P, and S dosimetry are given in Table 6-14, 6-15, 6-16 and 6-17. The data summarized in these tables include fast neutron exposure evaluations in terms of fluence ( $E > 1.0$  MeV), fluence ( $E > 0.1$  MeV) and iron atom displacements (dpa). Summaries of the fit of the best estimate spectrum for each of the capsules are provided in Tables 6-18, 6-19, 6-20 and 6-21. In general, excellent results were achieved in the fits of the best estimate spectra to the individual experimental reaction rates. The best

estimate spectra from the least squares evaluations are given in Tables 6-22, 6-23, 6-24 and 6-25 in the FERRET 53 energy group structure.

A summary of the best estimate and calculated neutron exposure of Capsules V, R, P, and S are presented in Table 6-26. The agreement between calculation and measurement falls within  $\pm 28\%$  for all fast neutron exposure parameters listed.

Neutron exposure projections at key locations on the pressure vessel inner radius are given in Table 6-27. Along with the current 16.2 EFPY exposure, projections are also provided for an exposure period of 25 EFPY, 33 EFPY (40 year plant design life), and 51 EFPY (20 year plant life extension).

In computing these vessel exposures, the calculated values from Table 6-2, 6-3, and 6-4 were scaled by the average best estimate/calculation ratios observed from evaluations of dosimetry from Capsules V, R, P, and S. The resultant best estimate exposure rates were then used to compute the integrated exposure of the vessel beltline. This procedure resulted in the following bias factors being applied to the analytical results:

$$\text{Flux (E > 1.0 MeV)} \quad \text{Bias} = 1.056$$

$$\text{Flux (E > 0.1 MeV)} \quad \text{Bias} = 1.146$$

$$\text{dpa/sec} \quad \text{Bias} = 1.096$$

Projections for future operation were based on the assumption that the time averaged exposure rates for cycles 21 and 22 would continue to be applicable throughout plant life. Table 6-28 is a forecast of the Kewaunee in-core fuel management (assumed for calculation purposes only) based on historical data.

In the calculation of exposure gradients for the Kewaunee reactor vessel, exposure projections to 25 EFPY, 33 EFPY, and 51 EFPY were also employed. Data based on both a fluence ( $E > 1.0$  MeV) slope and a plant specific dpa slope through the vessel wall are provided in Table 6-29. In order to access  $RT_{\text{NDT}}$  vs. fluence trend curves, dpa equivalent fast neutron fluence levels for the 1/4T and 3/4T positions were defined by the relations

$$\phi (1/4T) = \phi (\text{surface}) \left\{ \frac{\text{dpa} (1/4T)}{\text{dpa} (\text{surface})} \right\}$$

$$\phi (3/4T) = \phi (\text{surface}) \left\{ \frac{\text{dpa} (3/4T)}{\text{dpa} (\text{surface})} \right\}$$

Using this approach results in the dpa equivalent fluence values listed in Table 6-29.

In Table 6-30 updated lead factors are listed for each of the Kewaunee surveillance capsules. These data may be used as a guide in establishing future withdrawal schedules for the remaining capsules.

The incorporation of the SNLRML cross-section library, additional fuel cycle designs, and new estimates of future operating times resulted in small changes to both surveillance capsule and pressure vessel fluence estimates. The impact on capsule exposures can be seen in the following comparison.

CAPSULE	Current Evaluation Fluence [n/cm <sup>2</sup> ]	Prior Evaluation Fluence [n/cm <sup>2</sup> ]
V	5.97e+18 ± 7%	6.29e+18 ± 8%
R	1.81e+19 ± 9%	1.94E+19 ± 10%
P	2.74e+19 ± 7%	2.89e+19 ± 8%
S	3.36e+19 ± 7%	3.45e+19 ± 8%

The observed changes in best estimate fluence range from 3%-7% and fall within the 1 $\sigma$  uncertainties of 7%-10% that are associated with the various capsule dosimetry evaluations.

The impact of the revised analysis on projected maximum vessel exposures can be seen in the following comparison of the best estimate exposures at the 0.0 degree location at the vessel inner radius.

Operating Time [EFPY]	Current Evaluation Fluence [n/cm <sup>2</sup> ]	Prior Evaluation Fluence [n/cm <sup>2</sup> ]
16.2	1.73e+19	1.82e+19
25.0	2.57e+19	2.64e+19
33.0	3.34e+19	
34.0		3.49e+19
51.0	5.06e+19	5.09e+19

The observed changes in the best estimate pressure vessel exposure range from 1%-5% and fall well within the typical uncertainty of 12%-17% associated with vessel fluence projections.

## 6.2 MAINE YANKEE

In addition to the data obtained from the Kewaunee surveillance program, additional fracture toughness data were derived from an accelerated surveillance capsule (A-35) withdrawn from the Maine Yankee reactor. In order to provide a consistent data base for use in this evaluation, the dosimetry from the Maine Yankee accelerated capsule was re-evaluated using current technology and ENDF/B-VI based neutron transport and dosimetry reaction rate cross-sections.

This re-evaluation of the Maine Yankee capsule utilized the same procedures described earlier in this section for both the plant specific neutron transport calculation and the least squares adjustment used to determine the best estimate capsule exposure. The results of the re-evaluation of the second accelerated capsule indicated that the surveillance specimens had been irradiated for a period of 4.5 effective full power years and had experienced the following integrated fast neutron exposure:

$\Phi(E > 1.0 \text{ MeV})$	$6.11 \times 10^{19} \text{ n/cm}^2$	Uncertainty	8%
Iron Atom Displacements (dpa)	$8.96 \times 10^{-2} \text{ dpa}$	Uncertainty	10%

These exposure values can be used in conjunction with the Kewaunee capsule exposure data, also presented in this section, to provide a consistent set of data for use in developing embrittlement projections for the Kewaunee vessel material.

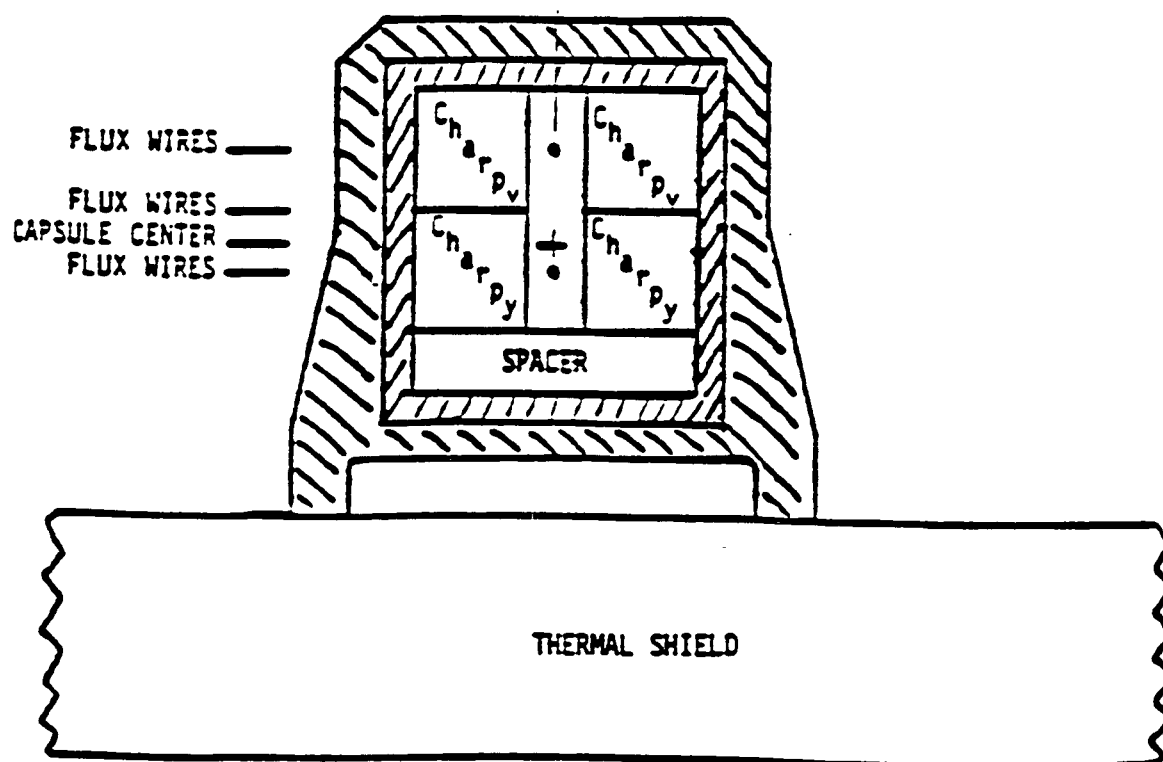


Figure 6-1 Plan View of Reactor Vessel Surveillance Capsule



TABLE 6-1

## CALCULATED NEUTRON EXPOSURE PARAMETERS AT SURVEILLANCE CAPSULE SPECIMEN GEOMETRIC CENTER

Iron Displacement Rate,	$\phi(E > 1.0\text{MeV}),$			$\phi(E > 0.1\text{MeV}),$			Iron Displacement Rate		
	n/cm <sup>2</sup> -sec			n/cm <sup>2</sup> -sec			dpa/sec		
	13.0°	23.0°	33.0°	13.0°	23.0°	33.0°	13.0°	23.0°	33.0°
DESIGN BASIS	$1.67 \times 10^{11}$	$9.86 \times 10^{10}$	$9.07 \times 10^{10}$	$6.07 \times 10^{11}$	$3.28 \times 10^{11}$	$3.05 \times 10^{11}$	$2.97 \times 10^{-10}$	$1.68 \times 10^{-10}$	$1.56 \times 10^{-10}$
CYCLE 1	$1.34 \times 10^{11}$	$7.60 \times 10^{10}$	$6.92 \times 10^{10}$	$4.85 \times 10^{11}$	$2.53 \times 10^{11}$	$2.33 \times 10^{11}$	$2.37 \times 10^{-10}$	$1.30 \times 10^{-10}$	$1.19 \times 10^{-10}$
CYCLE 2	$1.42 \times 10^{11}$	$8.68 \times 10^{10}$	$8.20 \times 10^{10}$	$5.16 \times 10^{11}$	$2.89 \times 10^{11}$	$2.76 \times 10^{11}$	$2.52 \times 10^{-10}$	$1.48 \times 10^{-10}$	$1.41 \times 10^{-10}$
CYCLE 3	$9.26 \times 10^{10}$	$7.58 \times 10^{10}$	$7.71 \times 10^{10}$	$3.37 \times 10^{11}$	$2.52 \times 10^{11}$	$2.59 \times 10^{11}$	$1.64 \times 10^{-10}$	$1.29 \times 10^{-10}$	$1.32 \times 10^{-10}$
CYCLE 4	$9.96 \times 10^{10}$	$6.22 \times 10^{10}$	$6.13 \times 10^{10}$	$3.62 \times 10^{11}$	$2.07 \times 10^{11}$	$2.06 \times 10^{11}$	$1.77 \times 10^{-10}$	$1.06 \times 10^{-10}$	$1.05 \times 10^{-10}$
CYCLE 5	$1.13 \times 10^{11}$	$7.34 \times 10^{10}$	$6.93 \times 10^{10}$	$4.09 \times 10^{11}$	$2.44 \times 10^{11}$	$2.33 \times 10^{11}$	$2.00 \times 10^{-10}$	$1.25 \times 10^{-10}$	$1.19 \times 10^{-10}$
CYCLE 6	$1.04 \times 10^{11}$	$7.33 \times 10^{10}$	$7.26 \times 10^{10}$	$3.77 \times 10^{11}$	$2.44 \times 10^{11}$	$2.44 \times 10^{11}$	$1.84 \times 10^{-10}$	$1.25 \times 10^{-10}$	$1.25 \times 10^{-10}$
CYCLE 7	$9.02 \times 10^{10}$	$6.11 \times 10^{10}$	$5.96 \times 10^{10}$	$3.28 \times 10^{11}$	$2.03 \times 10^{11}$	$2.00 \times 10^{11}$	$1.60 \times 10^{-10}$	$1.04 \times 10^{-10}$	$1.02 \times 10^{-10}$
CYCLE 8	$1.05 \times 10^{11}$	$7.30 \times 10^{10}$	$7.09 \times 10^{10}$	$3.80 \times 10^{11}$	$2.43 \times 10^{11}$	$2.38 \times 10^{11}$	$1.86 \times 10^{-10}$	$1.25 \times 10^{-10}$	$1.22 \times 10^{-10}$
CYCLE 9	$1.09 \times 10^{11}$	$7.24 \times 10^{10}$	$6.77 \times 10^{10}$	$3.96 \times 10^{11}$	$2.41 \times 10^{11}$	$2.28 \times 10^{11}$	$1.93 \times 10^{-10}$	$1.24 \times 10^{-10}$	$1.16 \times 10^{-10}$
CYCLE 10	$1.01 \times 10^{11}$	$6.99 \times 10^{10}$	$6.61 \times 10^{10}$	$3.67 \times 10^{11}$	$2.32 \times 10^{11}$	$2.22 \times 10^{11}$	$1.80 \times 10^{-10}$	$1.19 \times 10^{-10}$	$1.13 \times 10^{-10}$
CYCLE 11	$9.84 \times 10^{10}$	$6.78 \times 10^{10}$	$6.33 \times 10^{10}$	$3.58 \times 10^{11}$	$2.26 \times 10^{11}$	$2.13 \times 10^{11}$	$1.75 \times 10^{-10}$	$1.16 \times 10^{-10}$	$1.09 \times 10^{-10}$
CYCLE 12	$1.08 \times 10^{11}$	$6.81 \times 10^{10}$	$6.07 \times 10^{10}$	$3.92 \times 10^{11}$	$2.26 \times 10^{11}$	$2.04 \times 10^{11}$	$1.92 \times 10^{-10}$	$1.16 \times 10^{-10}$	$1.04 \times 10^{-10}$
CYCLE 13	$1.07 \times 10^{11}$	$7.38 \times 10^{10}$	$6.97 \times 10^{10}$	$3.88 \times 10^{11}$	$2.45 \times 10^{11}$	$2.34 \times 10^{11}$	$1.90 \times 10^{-10}$	$1.26 \times 10^{-10}$	$1.20 \times 10^{-10}$
CYCLE 14	$1.03 \times 10^{11}$	$7.19 \times 10^{10}$	$6.79 \times 10^{10}$	$3.74 \times 10^{11}$	$2.39 \times 10^{11}$	$2.28 \times 10^{11}$	$1.83 \times 10^{-10}$	$1.23 \times 10^{-10}$	$1.16 \times 10^{-10}$
CYCLE 15	$1.05 \times 10^{11}$	$7.25 \times 10^{10}$	$6.75 \times 10^{10}$	$3.81 \times 10^{11}$	$2.41 \times 10^{11}$	$2.27 \times 10^{11}$	$1.86 \times 10^{-10}$	$1.24 \times 10^{-10}$	$1.16 \times 10^{-10}$
CYCLE 16	$8.28 \times 10^{10}$	$6.91 \times 10^{10}$	$6.86 \times 10^{10}$	$3.01 \times 10^{11}$	$2.30 \times 10^{11}$	$2.30 \times 10^{11}$	$1.47 \times 10^{-10}$	$1.18 \times 10^{-10}$	$1.18 \times 10^{-10}$
CYCLE 17	$8.61 \times 10^{10}$	$6.91 \times 10^{10}$	$6.69 \times 10^{10}$	$3.13 \times 10^{11}$	$2.30 \times 10^{11}$	$2.25 \times 10^{11}$	$1.53 \times 10^{-10}$	$1.18 \times 10^{-10}$	$1.15 \times 10^{-10}$
CYCLE 18	$8.38 \times 10^{10}$	$6.99 \times 10^{10}$	$7.12 \times 10^{10}$	$3.04 \times 10^{11}$	$2.32 \times 10^{11}$	$2.39 \times 10^{11}$	$1.49 \times 10^{-10}$	$1.19 \times 10^{-10}$	$1.22 \times 10^{-10}$
CYCLE 19	$9.16 \times 10^{10}$	$7.04 \times 10^{10}$	$6.76 \times 10^{10}$	$3.33 \times 10^{11}$	$2.34 \times 10^{11}$	$2.27 \times 10^{11}$	$1.63 \times 10^{-10}$	$1.20 \times 10^{-10}$	$1.16 \times 10^{-10}$

TABLE 6-2

CALCULATED AZIMUTHAL VARIATION OF NEUTRON FLUX ( $E > 1.0 \text{ MeV}$ ) AT THE PRESSURE  
VESSEL CLAD/BASE METAL INTERFACE

	$\phi(E > 1.0 \text{ MeV}), \text{ n/cm}^2\text{-sec}$			
	$0.0^\circ$	$15.0^\circ$	$30.0^\circ$	$45.0^\circ$
DESIGN BASIS	$5.20 \times 10^{10}$	$3.18 \times 10^{10}$	$2.15 \times 10^{10}$	$1.80 \times 10^{10}$
CYCLE 1	$4.23 \times 10^{10}$	$2.54 \times 10^{10}$	$1.65 \times 10^{10}$	$1.41 \times 10^{10}$
CYCLE 2	$4.41 \times 10^{10}$	$2.73 \times 10^{10}$	$1.94 \times 10^{10}$	$1.67 \times 10^{10}$
CYCLE 3	$2.97 \times 10^{10}$	$1.92 \times 10^{10}$	$1.81 \times 10^{10}$	$1.57 \times 10^{10}$
CYCLE 4	$3.11 \times 10^{10}$	$1.95 \times 10^{10}$	$1.47 \times 10^{10}$	$1.25 \times 10^{10}$
CYCLE 5	$3.59 \times 10^{10}$	$2.22 \times 10^{10}$	$1.65 \times 10^{10}$	$1.44 \times 10^{10}$
CYCLE 6	$3.31 \times 10^{10}$	$2.08 \times 10^{10}$	$1.71 \times 10^{10}$	$1.51 \times 10^{10}$
CYCLE 7	$2.90 \times 10^{10}$	$1.79 \times 10^{10}$	$1.41 \times 10^{10}$	$1.24 \times 10^{10}$
CYCLE 8	$3.32 \times 10^{10}$	$2.09 \times 10^{10}$	$1.68 \times 10^{10}$	$1.47 \times 10^{10}$
CYCLE 9	$3.55 \times 10^{10}$	$2.16 \times 10^{10}$	$1.62 \times 10^{10}$	$1.34 \times 10^{10}$
CYCLE 10	$3.21 \times 10^{10}$	$2.02 \times 10^{10}$	$1.58 \times 10^{10}$	$1.32 \times 10^{10}$
CYCLE 11	$3.10 \times 10^{10}$	$1.97 \times 10^{10}$	$1.52 \times 10^{10}$	$1.29 \times 10^{10}$
CYCLE 12	$3.52 \times 10^{10}$	$2.13 \times 10^{10}$	$1.48 \times 10^{10}$	$1.23 \times 10^{10}$
CYCLE 13	$3.36 \times 10^{10}$	$2.13 \times 10^{10}$	$1.67 \times 10^{10}$	$1.38 \times 10^{10}$
CYCLE 14	$3.26 \times 10^{10}$	$2.06 \times 10^{10}$	$1.62 \times 10^{10}$	$1.34 \times 10^{10}$
CYCLE 15	$3.34 \times 10^{10}$	$2.10 \times 10^{10}$	$1.62 \times 10^{10}$	$1.32 \times 10^{10}$
CYCLE 16	$2.32 \times 10^{10}$	$1.73 \times 10^{10}$	$1.63 \times 10^{10}$	$1.36 \times 10^{10}$
CYCLE 17	$2.42 \times 10^{10}$	$1.78 \times 10^{10}$	$1.60 \times 10^{10}$	$1.33 \times 10^{10}$
CYCLE 18	$2.36 \times 10^{10}$	$1.74 \times 10^{10}$	$1.67 \times 10^{10}$	$1.44 \times 10^{10}$
CYCLE 19	$2.58 \times 10^{10}$	$1.87 \times 10^{10}$	$1.61 \times 10^{10}$	$1.35 \times 10^{10}$
CYCLE 20	$2.62 \times 10^{10}$	$1.87 \times 10^{10}$	$1.70 \times 10^{10}$	$1.49 \times 10^{10}$
CYCLE 21	$2.70 \times 10^{10}$	$1.86 \times 10^{10}$	$1.65 \times 10^{10}$	$1.46 \times 10^{10}$
CYCLE 22	$3.05 \times 10^{10}$	$2.02 \times 10^{10}$	$1.60 \times 10^{10}$	$1.29 \times 10^{10}$

TABLE 6-3

CALCULATED AZIMUTHAL VARIATION OF NEUTRON FLUX ( $E > 0.1$  MeV) AT  
THE PRESSURE VESSEL CLAD/BASE METAL INTERFACE

	$\phi(E > 0.1\text{MeV}), \text{ n/cm}^2\text{-sec}$			
	$0.0^\circ$	$15.0^\circ$	$30.0^\circ$	$45.0^\circ$
DESIGN BASIS	$1.41 \times 10^{11}$	$8.67 \times 10^{10}$	$5.65 \times 10^{10}$	$4.68 \times 10^{10}$
CYCLE 1	$1.14 \times 10^{11}$	$6.94 \times 10^{10}$	$4.34 \times 10^{10}$	$3.67 \times 10^{10}$
CYCLE 2	$1.19 \times 10^{11}$	$7.45 \times 10^{10}$	$5.09 \times 10^{10}$	$4.34 \times 10^{10}$
CYCLE 3	$8.04 \times 10^{10}$	$5.25 \times 10^{10}$	$4.75 \times 10^{10}$	$4.09 \times 10^{10}$
CYCLE 4	$8.40 \times 10^{10}$	$5.33 \times 10^{10}$	$3.86 \times 10^{10}$	$3.25 \times 10^{10}$
CYCLE 5	$9.70 \times 10^{10}$	$6.06 \times 10^{10}$	$4.34 \times 10^{10}$	$3.76 \times 10^{10}$
CYCLE 6	$8.95 \times 10^{10}$	$5.67 \times 10^{10}$	$4.49 \times 10^{10}$	$3.93 \times 10^{10}$
CYCLE 7	$7.85 \times 10^{10}$	$4.89 \times 10^{10}$	$3.70 \times 10^{10}$	$3.24 \times 10^{10}$
CYCLE 8	$8.98 \times 10^{10}$	$5.72 \times 10^{10}$	$4.41 \times 10^{10}$	$3.82 \times 10^{10}$
CYCLE 9	$9.58 \times 10^{10}$	$5.89 \times 10^{10}$	$4.27 \times 10^{10}$	$3.49 \times 10^{10}$
CYCLE 10	$8.66 \times 10^{10}$	$5.51 \times 10^{10}$	$4.16 \times 10^{10}$	$3.43 \times 10^{10}$
CYCLE 11	$8.39 \times 10^{10}$	$5.38 \times 10^{10}$	$4.00 \times 10^{10}$	$3.36 \times 10^{10}$
CYCLE 12	$9.51 \times 10^{10}$	$5.81 \times 10^{10}$	$3.89 \times 10^{10}$	$3.20 \times 10^{10}$
CYCLE 13	$9.09 \times 10^{10}$	$5.82 \times 10^{10}$	$4.38 \times 10^{10}$	$3.59 \times 10^{10}$
CYCLE 14	$8.81 \times 10^{10}$	$5.62 \times 10^{10}$	$4.27 \times 10^{10}$	$3.50 \times 10^{10}$
CYCLE 15	$9.03 \times 10^{10}$	$5.72 \times 10^{10}$	$4.27 \times 10^{10}$	$3.43 \times 10^{10}$
CYCLE 16	$6.28 \times 10^{10}$	$4.71 \times 10^{10}$	$4.27 \times 10^{10}$	$3.53 \times 10^{10}$
CYCLE 17	$6.54 \times 10^{10}$	$4.86 \times 10^{10}$	$4.20 \times 10^{10}$	$3.46 \times 10^{10}$
CYCLE 18	$6.37 \times 10^{10}$	$4.75 \times 10^{10}$	$4.39 \times 10^{10}$	$3.76 \times 10^{10}$
CYCLE 19	$6.97 \times 10^{10}$	$5.11 \times 10^{10}$	$4.24 \times 10^{10}$	$3.51 \times 10^{10}$
CYCLE 20	$7.09 \times 10^{10}$	$5.12 \times 10^{10}$	$4.46 \times 10^{10}$	$3.88 \times 10^{10}$
CYCLE 21	$7.30 \times 10^{10}$	$5.08 \times 10^{10}$	$4.35 \times 10^{10}$	$3.80 \times 10^{10}$
CYCLE 22	$8.25 \times 10^{10}$	$5.50 \times 10^{10}$	$4.20 \times 10^{10}$	$3.35 \times 10^{10}$

TABLE 6-4  
CALCULATED AZIMUTHAL VARIATION OF IRON DISPLACEMENT RATE (dpa) AT  
THE PRESSURE VESSEL CLAD/BASE METAL INTERFACE

	<u>Iron Atom Displacement Rate, dpa/sec</u>			
	<u>0.0°</u>	<u>15.0°</u>	<u>30.0°</u>	<u>45.0°</u>
DESIGN BASIS	$8.48 \times 10^{-11}$	$5.23 \times 10^{-11}$	$3.49 \times 10^{-11}$	$2.91 \times 10^{-11}$
CYCLE 1	$6.89 \times 10^{-11}$	$4.18 \times 10^{-11}$	$2.68 \times 10^{-11}$	$2.29 \times 10^{-11}$
CYCLE 2	$7.19 \times 10^{-11}$	$4.49 \times 10^{-11}$	$3.15 \times 10^{-11}$	$2.70 \times 10^{-11}$
CYCLE 3	$4.85 \times 10^{-11}$	$3.16 \times 10^{-11}$	$2.94 \times 10^{-11}$	$2.55 \times 10^{-11}$
CYCLE 4	$5.07 \times 10^{-11}$	$3.21 \times 10^{-11}$	$2.38 \times 10^{-11}$	$2.03 \times 10^{-11}$
CYCLE 5	$5.85 \times 10^{-11}$	$3.65 \times 10^{-11}$	$2.68 \times 10^{-11}$	$2.34 \times 10^{-11}$
CYCLE 6	$5.40 \times 10^{-11}$	$3.42 \times 10^{-11}$	$2.77 \times 10^{-11}$	$2.45 \times 10^{-11}$
CYCLE 7	$4.73 \times 10^{-11}$	$2.95 \times 10^{-11}$	$2.29 \times 10^{-11}$	$2.02 \times 10^{-11}$
CYCLE 8	$5.42 \times 10^{-11}$	$3.36 \times 10^{-11}$	$2.73 \times 10^{-11}$	$2.38 \times 10^{-11}$
CYCLE 9	$5.78 \times 10^{-11}$	$3.55 \times 10^{-11}$	$2.64 \times 10^{-11}$	$2.17 \times 10^{-11}$
CYCLE 10	$5.23 \times 10^{-11}$	$3.32 \times 10^{-11}$	$2.57 \times 10^{-11}$	$2.14 \times 10^{-11}$
CYCLE 11	$5.06 \times 10^{-11}$	$3.24 \times 10^{-11}$	$2.47 \times 10^{-11}$	$2.09 \times 10^{-11}$
CYCLE 12	$5.74 \times 10^{-11}$	$3.50 \times 10^{-11}$	$2.40 \times 10^{-11}$	$2.00 \times 10^{-11}$
CYCLE 13	$5.48 \times 10^{-11}$	$3.51 \times 10^{-11}$	$2.71 \times 10^{-11}$	$2.24 \times 10^{-11}$
CYCLE 14	$5.31 \times 10^{-11}$	$3.39 \times 10^{-11}$	$2.64 \times 10^{-11}$	$2.18 \times 10^{-11}$
CYCLE 15	$5.45 \times 10^{-11}$	$3.36 \times 10^{-11}$	$2.64 \times 10^{-11}$	$2.14 \times 10^{-11}$
CYCLE 16	$3.79 \times 10^{-11}$	$2.84 \times 10^{-11}$	$2.64 \times 10^{-11}$	$2.20 \times 10^{-11}$
CYCLE 17	$3.95 \times 10^{-11}$	$2.93 \times 10^{-11}$	$2.60 \times 10^{-11}$	$2.15 \times 10^{-11}$
CYCLE 18	$3.85 \times 10^{-11}$	$2.86 \times 10^{-11}$	$2.71 \times 10^{-11}$	$2.34 \times 10^{-11}$
CYCLE 19	$4.21 \times 10^{-11}$	$3.08 \times 10^{-11}$	$2.62 \times 10^{-11}$	$2.18 \times 10^{-11}$
CYCLE 20	$4.27 \times 10^{-11}$	$3.09 \times 10^{-11}$	$2.76 \times 10^{-11}$	$2.42 \times 10^{-11}$
CYCLE 21	$4.40 \times 10^{-11}$	$3.06 \times 10^{-11}$	$2.69 \times 10^{-11}$	$2.37 \times 10^{-11}$
CYCLE 22	$4.98 \times 10^{-11}$	$3.32 \times 10^{-11}$	$2.59 \times 10^{-11}$	$2.09 \times 10^{-11}$

**TABLE 6-5**  
**RELATIVE RADIAL DISTRIBUTIONS OF NEUTRON FLUX (E > 1.0 MeV)**  
**WITHIN THE PRESSURE VESSEL WALL**

Radius (cm)	0.0°	15.0°	30.0°	45.0°
168.04 <sup>(1)</sup>	1.000	1.000	1.000	1.000
168.27	0.986	0.988	0.988	0.988
168.88	0.938	0.944	0.943	0.944
169.75	0.860	0.868	0.867	0.869
170.89	0.755	0.764	0.764	0.767
172.17	0.644	0.653	0.653	0.657
173.49	0.542	0.553	0.552	0.555
174.90	0.448	0.459	0.457	0.461
176.30	0.369	0.379	0.378	0.381
177.50	0.311	0.321	0.320	0.323
178.91	0.253	0.264	0.263	0.266
180.42	0.202	0.212	0.211	0.213
181.51	0.170	0.181	0.180	0.181
182.60	0.142	0.153	0.153	0.153
183.90	0.112	0.124	0.125	0.125
184.55 <sup>(2)</sup>	0.104	0.117	0.118	0.118

NOTES: 1) Base Metal Inner Radius  
2) Base Metal Outer Radius

**TABLE 6-6**  
**RELATIVE RADIAL DISTRIBUTIONS OF NEUTRON FLUX ( $E > 0.1$  MeV)**  
**WITHIN THE PRESSURE VESSEL WALL**

Radius (cm)	0.0°	15.0°	30.0°	45.0°
168.04 <sup>(1)</sup>	1.000	1.000	1.000	1.000
168.27	1.005	1.008	1.007	1.008
168.88	1.001	1.008	1.007	1.008
169.75	0.978	0.991	0.991	0.993
170.89	0.932	0.953	0.953	0.956
172.17	0.873	0.899	0.899	0.902
173.49	0.807	0.838	0.839	0.842
174.90	0.735	0.771	0.772	0.775
176.30	0.665	0.704	0.706	0.707
177.50	0.604	0.647	0.650	0.650
178.91	0.535	0.581	0.585	0.583
180.42	0.464	0.511	0.517	0.513
181.51	0.411	0.462	0.470	0.463
182.60	0.359	0.412	0.423	0.413
183.90	0.295	0.350	0.366	0.356
184.55 <sup>(2)</sup>	0.278	0.335	0.351	0.342

NOTES: 1) Base Metal Inner Radius  
2) Base Metal Outer Radius

**TABLE 6-7**  
**RELATIVE RADIAL DISTRIBUTIONS OF IRON DISPLACEMENT RATE (dpa)**  
**WITHIN THE PRESSURE VESSEL WALL**

Radius (cm)	0.0°	15.0°	30.0°	45.0°
168.04 <sup>(1)</sup>	1.000	1.000	1.000	1.000
168.27	0.986	0.989	0.989	0.989
168.88	0.945	0.952	0.951	0.951
169.75	0.881	0.891	0.890	0.891
170.89	0.797	0.810	0.809	0.811
172.17	0.707	0.723	0.721	0.723
173.49	0.623	0.642	0.638	0.641
174.90	0.542	0.563	0.559	0.561
176.30	0.470	0.493	0.489	0.490
177.50	0.414	0.438	0.435	0.435
178.91	0.356	0.381	0.379	0.378
180.42	0.300	0.326	0.324	0.322
181.51	0.261	0.289	0.289	0.285
182.60	0.225	0.254	0.256	0.251
183.90	0.183	0.214	0.219	0.214
184.55 <sup>(2)</sup>	0.172	0.204	0.210	0.204

NOTES: 1) Base Metal Inner Radius  
2) Base Metal Outer Radius

TABLE 6-8  
NUCLEAR PARAMETERS FOR NEUTRON FLUX MONITORS

<u>Fission Monitor Material</u>	<u>Reaction of Interest</u>	<u>Target Weight Fraction</u>	<u>Response Range</u>	<u>Product Half-Life</u>	<u>Yield (%)</u>
Copper	$\text{Cu}^{63}(\text{n},\alpha)\text{Co}^{60}$	0.6917	$E > 4.7 \text{ MeV}$	5.271 yrs	
Iron	$\text{Fe}^{54}(\text{n},\text{p})\text{Mn}^{54}$	0.0580	$E > 1.0 \text{ MeV}$	312.5 days	
Nickel	$\text{Ni}^{58}(\text{n},\text{p})\text{Co}^{58}$	0.6827	$E > 1.0 \text{ MeV}$	70.78 days	
Uranium-238*	$\text{U}^{238}(\text{n},\text{f})\text{Cs}^{137}$	1.0	$E > 0.4 \text{ MeV}$	30.12 yrs	6.00
Neptunium-237*	$\text{Np}^{237}(\text{n},\text{f})\text{Cs}^{137}$	1.0	$E > 0.08 \text{ MeV}$	30.12 yrs	6.27
Cobalt-Aluminum	$\text{Co}^{59}(\text{n},\gamma)\text{Co}^{60}$	0.0015	$E > 0.015 \text{ MeV}$	5.272 yrs	
Cobalt-Aluminum*	$\text{Co}^{59}(\text{n},\gamma)\text{Co}^{60}$	0.0015	Epithermal	5.271 yrs	

\*Denotes that monitor is cadmium shielded.



**TABLE 6-9**  
**MONTHLY THERMAL GENERATION DURING THE FIRST NINETEEN FUEL CYCLES**  
**OF THE KEWAUNEE REACTOR**

<u>THERMAL GENERATION MONTH (MW-hr)</u>		<u>THERMAL GENERATION MONTH (MW-hr)</u>		<u>THERMAL GENERATION MONTH (MW-hr)</u>		<u>THERMAL GENERATION MONTH (MW-hr)</u>	
3/74	0	6/76	1,171,872	9/78	1,137,041	12/80	1,188,454
4/74	121,412	7/76	1,180,703	10/78	1,208,085	1/81	1,223,429
5/74	600,420	8/76	1,190,960	11/78	1,129,396	2/81	1,077,953
6/74	864,909	9/76	1,060,865	12/78	1,200,591	3/81	1,136,912
7/74	776,871	10/76	1,198,895	1/79	1,212,033	4/81	777,154
8/74	1,172,100	11/76	1,145,875	2/79	1,047,590	5/81	0
9/74	655,831	12/76	1,187,141	3/79	1,135,718	6/81	777,459
10/74	317,628	1/77	606,787	4/79	1,151,567	7/81	1,204,230
11/74	752,190	2/77	0	5/79	979,438	8/81	1,222,464
12/74	907,703	3/77	179,775	6/79	0	9/81	1,161,892
1/75	781,842	4/77	999,717	7/79	0	10/81	1,170,754
2/75	928,272	5/77	1,188,560	8/79	740,156	11/81	1,148,183
3/75	1,096,956	6/77	1,156,447	9/79	1,126,633	12/81	1,219,280
4/75	827,400	7/77	1,201,271	10/79	1,184,602	1/82	1,203,474
5/75	874,521	8/77	1,049,588	11/79	1,167,457	2/82	1,075,185
6/75	777,805	9/77	1,175,016	12/79	1,202,648	3/82	1,224,649
7/75	842,326	10/77	1,207,031	1/80	713,133	4/82	326,008
8/75	1,175,609	11/77	1,175,653	2/80	1,124,815	5/82	208,610
9/75	604,163	12/77	1,194,097	3/80	1,223,050	6/82	1,163,350
10/75	916,973	1/78	1,218,479	4/80	1,175,492	7/82	1,218,118
11/75	823,299	2/78	1,098,398	5/80	349,621	8/82	1,222,402
12/75	1,171,599	3/78	1,203,881	6/80	137,929	9/82	1,180,708
1/76	1,106,166	4/78	811,877	7/80	1,186,866	10/82	1,214,805
2/76	501,575	5/78	72,462	8/80	1,125,341	11/82	1,178,287
3/76	0	6/78	1,016,869	9/80	946,334	12/82	1,077,471
4/76	377,039	7/78	1,129,811	10/80	1,181,104	1/83	1,218,455
5/76	685,126	8/78	1,182,936	11/80	1,183,962	2/83	1,102,759

**TABLE 6-9 (Continued)**  
**MONTHLY THERMAL GENERATION DURING THE FIRST NINETEEN FUEL CYCLES**  
**OF THE KEWAUNEE REACTOR**

<u>THERMAL GENERATION MONTH (MW-hr)</u>		<u>THERMAL GENERATION MONTH (MW-hr)</u>		<u>THERMAL GENERATION MONTH (MW-hr)</u>		<u>THERMAL GENERATION MONTH (MW-hr)</u>	
3/83	649,484	6/85	1,179,472	9/87	1,168,054	12/89	1,182,173
4/83	0	7/85	1,218,713	10/87	1,219,759	1/90	1,217,978
5/83	526,179	8/85	1,148,512	11/87	1,176,994	2/90	1,104,275
6/83	1,174,626	9/85	1,178,061	12/87	1,215,302	3/90	69,012
7/83	1,159,011	10/85	1,222,974	1/88	1,217,528	4/90	347,514
8/83	1,223,940	11/85	1,121,094	2/88	1,134,763	5/90	1,211,562
9/83	1,184,200	12/85	1,181,301	3/88	57,885	6/90	1,172,482
10/83	1,224,069	1/86	1,217,881	4/88	478,699	7/90	1,224,388
11/83	1,183,857	2/86	1,067,018	5/88	1,195,654	8/90	1,224,227
12/83	1,224,505	3/86	0	6/88	1,180,894	9/90	1,182,733
1/84	1,225,897	4/86	267,903	7/88	1,196,631	10/90	1,224,609
2/84	1,139,329	5/86	1,191,848	8/88	1,067,560	11/90	1,182,652
3/84	532,963	6/86	1,176,926	9/88	1,088,933	12/90	1,208,996
4/84	0	7/86	1,218,187	10/88	1,221,808	1/91	1,220,109
5/84	837,414	8/86	1,179,835	11/88	1,169,480	2/91	1,100,105
6/84	1,144,593	9/86	1,180,207	12/88	1,219,313	3/91	285,385
7/84	1,199,335	10/86	1,202,091	1/89	1,204,791	4/91	0
8/84	1,222,297	11/86	1,179,133	2/89	755,230	5/91	694,766
9/84	1,183,431	12/86	1,215,853	3/89	0	6/91	1,180,240
10/84	1,205,018	1/87	1,215,680	4/89	537,116	7/91	1,210,778
11/84	1,183,532	2/87	924,655	5/89	1,221,793	8/91	1,211,741
12/84	1,222,229	3/87	0	6/89	902,394	9/91	1,171,047
1/85	1,224,279	4/87	959,357	7/89	1,221,968	10/91	1,147,457
2/85	271,048	5/87	1,185,857	8/89	1,221,653	11/91	1,182,454
3/85	0	6/87	1,146,829	9/89	1,182,431	12/91	1,211,606
4/85	682,721	7/87	1,183,725	10/89	1,222,999	1/92	1,222,525
5/85	1,212,434	8/87	1,219,047	11/89	1,181,532	2/92	1,143,608

TABLE 6-9 (Continued)  
MONTHLY THERMAL GENERATION DURING THE FIRST NINETEEN FUEL CYCLES  
OF THE KEWAUNEE REACTOR

THERMAL  
GENERATION  
MONTH (MW-hr)

3/92	225,433
4/92	351,235
5/92	1,226,398
6/92	1,185,833
7/92	1,227,301
8/92	1,228,782
9/92	1,063,233
10/92	1,229,699
11/92	1,113,009
12/92	1,227,368
1/93	1,136,925
2/93	1,085,208
3/93	156,579
4/93	381,383
5/93	1,227,217
6/93	754,286
7/93	1,226,890
8/93	1,226,800
9/93	1,184,271
10/93	1,227,961
11/93	1,186,431
12/93	1,223,457
1/94	929,429
2/94	1,105,268
3/94	1,200,731
4/94	22,616

TABLE 6-10  
MEASURED SENSOR ACTIVITIES AND REACTION RATES  
SURVEILLANCE CAPSULE V

<u>Monitor and Axial Location</u>	Measured Activity (dis/sec-gm)	Specimen Geometric Center Saturated Activity (dis/sec-gm)	Reaction Rate (RPS/NUCLEUS)
<u>Cu-63 (n,<math>\alpha</math>) Co-60</u>			
Top-Mid	$6.89 \times 10^4$	$4.43 \times 10^5$	
Bot-Mid	$7.83 \times 10^4$	$5.03 \times 10^5$	
Average	$7.36 \times 10^4$	$4.73 \times 10^5$	$7.22 \times 10^{-17}$
<u>Fe-54(n,p) Mn-54</u>			
Top	$1.93 \times 10^6$	$5.54 \times 10^6$	
Top-Mid	$1.76 \times 10^6$	$5.06 \times 10^6$	
Middle	$1.84 \times 10^6$	$5.29 \times 10^6$	
Bot-Mid	$1.82 \times 10^6$	$5.24 \times 10^6$	
Bottom	$1.98 \times 10^6$	$5.70 \times 10^6$	
Average	$1.87 \times 10^6$	$5.37 \times 10^6$	$8.58 \times 10^{-15}$
<u>Ni-58 (n,p) Co-58</u>			
Middle	$1.17 \times 10^7$	$7.50 \times 10^7$	$1.07 \times 10^{-14}$
<u>U-238 (n,f) Cs-137 (Cd)</u>			
Middle	$2.47 \times 10^5$	$9.11 \times 10^6$	$6.00 \times 10^{-14}$
<u>Np-237(n,f) Cs-137 (Cd)</u>			
Middle	$2.18 \times 10^6$	$8.00 \times 10^7$	$5.02 \times 10^{-13}$

TABLE 6-10 (Continued)  
 MEASURED SENSOR ACTIVITIES AND REACTION RATES  
 SURVEILLANCE CAPSULE V

<u>Monitor and Axial Location</u>	<u>Measured Activity (dis/sec-gm)</u>	<u>Specimen Geometric Center Saturated Activity (dis/sec-gm)</u>	<u>Reaction Rate (RPS/NUCLEUS)</u>
<u>Co-59 (n,g) Co-60</u>			
Top	$2.27 \times 10^7$	$1.58 \times 10^8$	$1.03 \times 10^{-11}$
<u>Co-59 (n,g) Co-60 (Cd)</u>			
Top	$1.01 \times 10^7$	$6.47 \times 10^7$	
Bottom	$1.02 \times 10^7$	$6.49 \times 10^7$	
Average	$1.01 \times 10^7$	$6.48 \times 10^7$	$4.23 \times 10^{-12}$

TABLE 6-11  
MEASURED SENSOR ACTIVITIES AND REACTION RATES  
SURVEILLANCE CAPSULE R

<u>Monitor and Axial Location</u>	Measured Activity (dis/sec-gm)	Specimen Geometric Center Saturated Activity (dis/sec-gm)	Reaction Rate (RPS/NUCLEUS)
<u>Cu-63 (n,<math>\alpha</math>) Co-60</u>			
Top-Mid	$1.65 \times 10^5$	$3.83 \times 10^5$	$5.84 \times 10^{-17}$
<u>Fe-54(n,p) Mn-54</u>			
Top	$2.25 \times 10^6$	$4.71 \times 10^6$	
Top-Mid	$2.09 \times 10^6$	$4.37 \times 10^6$	
Middle	$2.11 \times 10^6$	$4.42 \times 10^6$	
Bottom	$2.32 \times 10^6$	$4.85 \times 10^6$	
Average	$2.19 \times 10^6$	$4.59 \times 10^6$	$7.34 \times 10^{-15}$
<u>Ni-58 (n,p) Co-58</u>			
Middle	$1.31 \times 10^7$	$6.82 \times 10^7$	$9.74 \times 10^{-15}$
<u>U-238 (n,f) Cs-137 (Cd)</u>			
Middle	$7.99 \times 10^5$	$8.60 \times 10^6$	$5.67 \times 10^{-14}$
<u>Np-237(n,f) Cs-137 (Cd)</u>			
Middle	$2.31 \times 10^6$	$2.48 \times 10^7$	$1.56 \times 10^{-13}$
<u>Co-59 (n,g) Co-60</u>			
Top	$5.31 \times 10^7$	$1.34 \times 10^8$	
Bottom	$5.57 \times 10^7$	$1.40 \times 10^8$	
Average	$5.44 \times 10^7$	$1.37 \times 10^8$	$8.94 \times 10^{-12}$

TABLE 6-11 (Continued)  
 MEASURED SENSOR ACTIVITIES AND REACTION RATES  
 SURVEILLANCE CAPSULE R

<u>Monitor and Axial Location</u>	<u>Measured Activity (dis/sec-gm)</u>	<u>Specimen Geometric Center Saturated Activity (dis/sec-gm)</u>	<u>Reaction Rate (RPS/NUCLEUS)</u>
<u>Co-59 (n,g) Co-60 (Cd)</u>			
Top	$2.63 \times 10^7$	$6.07 \times 10^7$	
Bottom	$2.36 \times 10^6$	$5.45 \times 10^6$	
Average	$1.43 \times 10^7$	$3.31 \times 10^7$	$2.16 \times 10^{-12}$

TABLE 6-12  
MEASURED SENSOR ACTIVITIES AND REACTION RATES  
SURVEILLANCE CAPSULE P

<u>Monitor and Axial Location</u>	<u>Measured Activity (dis/sec-gm)</u>	<u>Specimen Geometric Center Saturated Activity (dis/sec-gm)</u>	<u>Reaction Rate (RPS/NUCLEUS)</u>
<u>Cu-63 (n,<math>\alpha</math>) Co-60</u>			
Top-Mid	$2.12 \times 10^5$	$2.89 \times 10^5$	
Bot-Mid	$2.44 \times 10^5$	$3.33 \times 10^5$	
Average	$2.28 \times 10^5$	$3.11 \times 10^5$	$4.74 \times 10^{-17}$
<u>Fe-54(n,p) Mn-54</u>			
Top	$2.74 \times 10^6$	$3.96 \times 10^6$	
Top-Mid	$1.95 \times 10^6$	$2.82 \times 10^6$	
Middle	$2.11 \times 10^6$	$3.05 \times 10^6$	
Bot-Mid	$2.19 \times 10^6$	$3.17 \times 10^6$	
Bottom	$2.33 \times 10^6$	$3.37 \times 10^6$	
Average	$2.26 \times 10^6$	$3.28 \times 10^6$	$5.24 \times 10^{-15}$
<u>Ni-58 (n,p) Co-58</u>			
Middle	$2.44 \times 10^7$	$4.47 \times 10^7$	$6.38 \times 10^{-15}$
<u>U-238 (n,f) Cs-137 (Cd)</u>			
Middle	$1.13 \times 10^6$	$5.45 \times 10^6$	$3.59 \times 10^{-14}$
<u>Np-237(n,f) Cs-137 (Cd)</u>			
Middle	$8.28 \times 10^6$	$3.98 \times 10^7$	$2.50 \times 10^{-13}$



TABLE 6-12 (Continued)  
 MEASURED SENSOR ACTIVITIES AND REACTION RATES  
 SURVEILLANCE CAPSULE P

<u>Monitor and Axial Location</u>	<u>Measured Activity (dis/sec-gm)</u>	<u>Specimen Geometric Center Saturated Activity (dis/sec-gm)</u>	<u>Reaction Rate (RPS/NUCLEUS)</u>
<u>Co-59 (n,g) Co-60</u>			
Top	$4.20 \times 10^7$	$6.28 \times 10^7$	
Bottom	$5.01 \times 10^7$	$7.49 \times 10^7$	
Average	$4.61 \times 10^7$	$6.89 \times 10^7$	$4.49 \times 10^{-12}$
<u>Co-59 (n,g) Co-60 (Cd)</u>			
Top	$1.79 \times 10^7$	$2.45 \times 10^7$	
Bottom	$2.04 \times 10^7$	$2.80 \times 10^7$	
Average	$1.92 \times 10^7$	$2.62 \times 10^7$	$1.71 \times 10^{-12}$

TABLE 6-13  
MEASURED SENSOR ACTIVITIES AND REACTION RATES  
SURVEILLANCE CAPSULE S

<u>Monitor and Axial Location</u>	<u>Measured Activity (dis/sec-gm)</u>	<u>Specimen Geometric Center Saturated Activity (dis/sec-gm)</u>	<u>Reaction Rate (RPS/NUCLEUS)</u>
<u>Cu-63 (n,<math>\alpha</math>) Co-60</u>			
Top-Mid	$2.15 \times 10^5$	$2.74 \times 10^5$	
Bot-Mid	$2.38 \times 10^5$	$3.03 \times 10^5$	
Average	$2.27 \times 10^5$	$2.88 \times 10^5$	$4.40 \times 10^{-17}$
<u>Fe-54(n,p) Mn-54</u>			
Top	$1.53 \times 10^6$	$2.97 \times 10^6$	
Top-Mid	$1.39 \times 10^6$	$2.70 \times 10^6$	
Middle	$1.52 \times 10^6$	$2.95 \times 10^6$	
Bot-Mid	$1.49 \times 10^6$	$2.90 \times 10^6$	
Average	$1.48 \times 10^6$	$2.88 \times 10^6$	$4.61 \times 10^{-15}$
<u>Ni-58 (n,p) Co-58</u>			
Middle	$6.92 \times 10^6$	$4.59 \times 10^7$	$6.55 \times 10^{-15}$
<u>U-238 (n,f) Cs-137 (Cd)</u>			
Middle	$1.31 \times 10^6$	$4.67 \times 10^6$	$3.08 \times 10^{-14}$
<u>Np-237(n,f) Cs-137 (Cd)</u>			
Middle	$7.90 \times 10^6$	$2.81 \times 10^7$	$1.76 \times 10^{-13}$

TABLE 6-13 (Continued)  
 MEASURED SENSOR ACTIVITIES AND REACTION RATES  
 SURVEILLANCE CAPSULE S

<u>Monitor and Axial Location</u>	<u>Measured Activity (dis/sec-gm)</u>	<u>Specimen Geometric Center Saturated Activity (dis/sec-gm)</u>	<u>Reaction Rate (RPS/NUCLEUS)</u>
<u>Co-59 (n,g) Co-60</u>			
Bottom	$4.38 \times 10^7$	$6.07 \times 10^7$	
Bottom	$4.48 \times 10^7$	$6.21 \times 10^7$	
Average	$4.43 \times 10^7$	$6.14 \times 10^7$	$4.01 \times 10^{-12}$
<u>Co-59 (n,g) Co-60 (Cd)</u>			
Top	$2.14 \times 10^7$	$2.72 \times 10^7$	
Bottom	$2.10 \times 10^7$	$2.67 \times 10^7$	
Average	$2.12 \times 10^7$	$2.69 \times 10^7$	$1.76 \times 10^{-12}$

**TABLE 6-14**  
**SUMMARY OF NEUTRON DOSIMETRY RESULTS AT**  
**SURVEILLANCE CAPSULE V SPECIMEN GEOMETRIC CENTER**

<u>EXPOSURE RATES</u>	<u>TIME AVERAGED</u>
$\phi$ (E > 1.0 MeV), n/cm <sup>2</sup> -sec	$1.47 \times 10^{11} \pm 7\%$
$\phi$ (E > 0.1 MeV), n/cm <sup>2</sup> -sec	$6.23 \times 10^{11} \pm 15\%$
dpa/sec	$2.77 \times 10^{-10} \pm 10\%$
$\phi$ (E < 0.414 eV), n/cm <sup>2</sup> -sec	$2.54 \times 10^{11} \pm 26\%$
<u>INTEGRATED</u>	<u>CAPSULE EXPOSURE</u>
$\Phi$ (E > 1.0 MeV), n/cm <sup>2</sup>	$5.97 \times 10^{18} \pm 7\%$
$\Phi$ (E > 0.1 MeV), n/cm <sup>2</sup>	$2.53 \times 10^{19} \pm 15\%$
dpa	$1.13 \times 10^{-2} \pm 10\%$
$\Phi$ (E < 0.414 eV), n/cm <sup>2</sup>	$1.03 \times 10^{19} \pm 26\%$

NOTE: Total Irradiation Time = 1.29 EFPY

**TABLE 6-15**  
**SUMMARY OF NEUTRON DOSIMETRY RESULTS AT**  
**SURVEILLANCE CAPSULE R SPECIMEN GEOMETRIC CENTER**

<u>TIME AVERAGED</u>	<u>EXPOSURE RATES</u>
$\phi$ (E > 1.0 MeV), n/cm <sup>2</sup> -sec	$1.24 \times 10^{11} \pm 9\%$
$\phi$ (E > 0.1 MeV), n/cm <sup>2</sup> -sec	$4.63 \times 10^{11} \pm 20\%$
dpa/sec	$2.18 \times 10^{10} \pm 14\%$
$\phi$ (E < 0.414 eV), n/cm <sup>2</sup> -sec	$2.70 \times 10^{11} \pm 26\%$
 <u>INTEGRATED</u>	 <u>CAPSULE EXPOSURE</u>
$\Phi$ (E > 1.0 MeV), n/cm <sup>2</sup>	$1.81 \times 10^{19} \pm 9\%$
$\Phi$ (E > 0.1 MeV), n/cm <sup>2</sup>	$6.75 \times 10^{19} \pm 20\%$
dpa	$3.18 \times 10^{12} \pm 14\%$
$\Phi$ (E < 0.414 eV), n/cm <sup>2</sup>	$3.94 \times 10^{19} \pm 26\%$

NOTE: Total Irradiation Time = 4.62 EFPY

TABLE 6-16  
SUMMARY OF NEUTRON DOSIMETRY RESULTS AT  
SURVEILLANCE CAPSULE P SPECIMEN GEOMETRIC CENTER

<u>EXPOSURE RATES</u>	<u>TIME AVERAGED</u>
$\phi$ (E > 1.0 MeV), n/cm <sup>2</sup> -sec	$7.81 \times 10^{10} \pm 7\%$
$\phi$ (E > 0.1 MeV), n/cm <sup>2</sup> -sec	$2.96 \times 10^{11} \pm 15\%$
dpa/sec	$1.39 \times 10^{-10} \pm 10\%$
$\phi$ (E < 0.414 eV), n/cm <sup>2</sup> -sec	$1.23 \times 10^{11} \pm 25\%$
 <u>EXPOSURE</u>	 <u>INTEGRATED CAPSULE</u>
$\Phi$ (E > 1.0 MeV), n/cm <sup>2</sup>	$2.74 \times 10^{19} \pm 7\%$
$\Phi$ (E > 0.1 MeV), n/cm <sup>2</sup>	$1.04 \times 10^{20} \pm 15\%$
dpa	$4.88 \times 10^{-2} \pm 10\%$
$\Phi$ (E < 0.414 eV), n/cm <sup>2</sup>	$4.33 \times 10^{19} \pm 25\%$

NOTE: Total Irradiation Time = 11.13 EFPY

**TABLE 6-17**  
**SUMMARY OF NEUTRON DOSIMETRY RESULTS AT**  
**SURVEILLANCE CAPSULE S SPECIMEN GEOMETRIC CENTER**

<u>EXPOSURE RATES</u>	<u>TIME AVERAGED</u>
$\phi$ (E > 1.0 MeV), n/cm <sup>2</sup> -sec	$6.57 \times 10^{10} \pm 7\%$
$\phi$ (E > 0.1 MeV), n/cm <sup>2</sup> -sec	$2.24 \times 10^{11} \pm 15\%$
dpa/sec	$1.11 \times 10^{-10} \pm 10\%$
$\phi$ (E < 0.414 eV), n/cm <sup>2</sup> -sec	$9.43 \times 10^{10} \pm 26\%$
<u>EXPOSURE</u>	<u>INTEGRATED CAPSULE</u>
$\Phi$ (E > 1.0 MeV), n/cm <sup>2</sup>	$3.36 \times 10^{19} \pm 7\%$
$\Phi$ (E > 0.1 MeV), n/cm <sup>2</sup>	$1.14 \times 10^{20} \pm 15\%$
dpa	$5.69 \times 10^{-2} \pm 10\%$
$\Phi$ (E < 0.414 eV), n/cm <sup>2</sup>	$4.82 \times 10^{19} \pm 26\%$

NOTE: Total Irradiation Time = 16.2 EFPY

TABLE 6-18

COMPARISON OF MEASURED AND FERRET CALCULATED REACTION RATES AT  
SURVEILLANCE CAPSULE V SPECIMEN GEOMETRIC CENTER

<u>Reaction</u>	<u>Measured</u>	<u>Best Estimate</u>	<u>C/M</u>
Cu-63 (n, $\alpha$ ) Co-60	$7.21 \times 10^{-17}$	$7.06 \times 10^{-17}$	0.98
Fe-54 (n,p) Mn-54	$8.58 \times 10^{-15}$	$8.36 \times 10^{-15}$	0.97
Ni-58 (n,p) Co-58	$1.07 \times 10^{-14}$	$1.18 \times 10^{-14}$	1.10
U-238 (n,f) Cs-137 (Cd)	$5.18 \times 10^{-14}$	$4.69 \times 10^{-14}$	0.90
Np-237 (n,f) Cs-137 (Cd)	$5.02 \times 10^{-13}$	$4.68 \times 10^{-13}$	0.93
Co-59 (n, $\delta$ ) Co-60	$1.03 \times 10^{-11}$	$1.03 \times 10^{-11}$	1.00
Co-59 (n, $\delta$ ) Co-60 (Cd)	$4.23 \times 10^{-12}$	$4.22 \times 10^{-12}$	1.00



TABLE 6-19  
COMPARISON OF MEASURED AND FERRET CALCULATED REACTION RATES AT  
SURVEILLANCE CAPSULE R SPECIMEN GEOMETRIC CENTER

<u>Reaction</u>	<u>Measured</u>	<u>Best Estimate</u>	<u>BE/M</u>
Cu-63 (n, $\alpha$ ) Co-60	$5.84 \times 10^{-17}$	$5.79 \times 10^{-17}$	0.99
Fe-54 (n,p) Mn-54	$7.34 \times 10^{-15}$	$7.29 \times 10^{-15}$	0.99
Ni-58 (n,p) Co-58	$9.74 \times 10^{-15}$	$1.02 \times 10^{-14}$	1.05
U-238 (n,f) Cs-137 (Cd)	$4.64 \times 10^{-14}$	$4.06 \times 10^{-14}$	0.87
Co-59 (n, $\delta$ ) Co-60	$8.94 \times 10^{-12}$	$8.93 \times 10^{-12}$	1.00
Co-59 (n, $\delta$ ) Co-60 (Cd)	$2.16 \times 10^{-12}$	$2.17 \times 10^{-12}$	1.00

TABLE 6-20  
COMPARISON OF MEASURED AND FERRET CALCULATED REACTION RATES AT  
SURVEILLANCE CAPSULE P SPECIMEN GEOMETRIC CENTER

<u>Reaction</u>	<u>Measured</u>	<u>Best Estimate</u>	<u>BE/M</u>
Cu-63 (n, $\alpha$ ) Co-60	$4.74 \times 10^{-17}$	$4.66 \times 10^{-17}$	0.98
Fe-54 (n,p) Mn-54	$5.24 \times 10^{-15}$	$5.05 \times 10^{-15}$	0.96
Ni-58 (n,p) Co-58	$6.38 \times 10^{-15}$	$7.00 \times 10^{-15}$	1.10
U-238 (n,f) Cs-137 (Cd)	$2.83 \times 10^{-14}$	$2.60 \times 10^{-14}$	0.92
Np-237 (n,f) Cs-137 (Cd)	$2.50 \times 10^{-13}$	$2.34 \times 10^{-13}$	0.94
Co-59 (n, $\delta$ ) Co-60	$4.49 \times 10^{-12}$	$4.50 \times 10^{-12}$	1.00
Co-59 (n, $\delta$ ) Co-60 (Cd)	$1.71 \times 10^{-12}$	$1.71 \times 10^{-12}$	1.00

**TABLE 6-21**  
**COMPARISON OF MEASURED AND FERRET CALCULATED REACTION RATES AT**  
**SURVEILLANCE CAPSULE S SPECIMEN GEOMETRIC CENTER**

<u>Reaction</u>	<u>Measured</u>	<u>Best Estimate</u>	<u>BE/M</u>
Cu-63 (n, $\alpha$ ) Co-60	$4.40 \times 10^{-17}$	$4.37 \times 10^{-17}$	0.99
Fe-54 (n,p) Mn-54	$4.61 \times 10^{-15}$	$4.71 \times 10^{-15}$	1.02
Ni-58 (n,p) Co-58	$6.55 \times 10^{-15}$	$6.48 \times 10^{-15}$	0.99
U-238 (n,f) Cs-137 (Cd)	$2.34 \times 10^{-14}$	$2.29 \times 10^{-14}$	0.98
Np-237 (n,f) Cs-137 (Cd)	$1.76 \times 10^{-13}$	$1.78 \times 10^{-13}$	1.01
Co-59 (n, $\delta$ ) Co-60	$4.01 \times 10^{-12}$	$4.01 \times 10^{-12}$	1.00
Co-59 (n, $\delta$ ) Co-60 (Cd)	$1.76 \times 10^{-12}$	$1.75 \times 10^{-12}$	1.00

**TABLE 6-22**  
**BEST ESTIMATE NEUTRON ENERGY SPECTRUM AT**  
**SURVEILLANCE CAPSULE V SPECIMEN GEOMETRIC CENTER**

<u>Group</u>	<u>Energy</u> <u>(MeV)</u>	<u>Best Est. Flux</u> <u>(n/cm<sup>2</sup>-sec)</u>	<u>Group</u>	<u>Energy</u> <u>(MeV)</u>	<u>Best Est. Flux</u> <u>(n/cm<sup>2</sup>-sec)</u>
1	1.73x10 <sup>1</sup>	9.01x10 <sup>6</sup>	28	9.12x10 <sup>-3</sup>	2.94x10 <sup>10</sup>
2	1.49x10 <sup>1</sup>	1.92x10 <sup>7</sup>	29	5.53x10 <sup>-3</sup>	3.16x10 <sup>10</sup>
3	1.35x10 <sup>1</sup>	7.16x10 <sup>7</sup>	30	3.36x10 <sup>-3</sup>	9.99x10 <sup>9</sup>
4	1.16x10 <sup>1</sup>	1.97x10 <sup>8</sup>	31	2.84x10 <sup>-3</sup>	9.61x10 <sup>9</sup>
5	1.00x10 <sup>1</sup>	4.47x10 <sup>8</sup>	32	2.40x10 <sup>-3</sup>	9.45x10 <sup>9</sup>
6	8.61x10 <sup>0</sup>	7.95x10 <sup>8</sup>	33	2.04x10 <sup>-3</sup>	2.85x10 <sup>10</sup>
7	7.41x10 <sup>0</sup>	1.96x10 <sup>9</sup>	34	1.23x10 <sup>-3</sup>	2.88x10 <sup>10</sup>
8	6.07x10 <sup>0</sup>	3.06x10 <sup>9</sup>	35	7.49x10 <sup>-4</sup>	2.76x10 <sup>10</sup>
9	4.97x10 <sup>0</sup>	6.62x10 <sup>9</sup>	36	4.54x10 <sup>-4</sup>	2.57x10 <sup>10</sup>
10	3.68x10 <sup>0</sup>	8.42x10 <sup>9</sup>	37	2.75x10 <sup>-4</sup>	2.82x10 <sup>10</sup>
11	2.87x10 <sup>0</sup>	1.65x10 <sup>10</sup>	38	1.67x10 <sup>-4</sup>	3.00x10 <sup>10</sup>
12	2.23x10 <sup>0</sup>	2.26x10 <sup>10</sup>	39	1.01x10 <sup>-4</sup>	2.91x10 <sup>10</sup>
13	1.74x10 <sup>0</sup>	3.14x10 <sup>10</sup>	40	6.14x10 <sup>-5</sup>	2.89x10 <sup>10</sup>
14	1.35x10 <sup>0</sup>	3.46x10 <sup>10</sup>	41	3.73x10 <sup>-5</sup>	2.84x10 <sup>10</sup>
15	1.11x10 <sup>0</sup>	6.04x10 <sup>10</sup>	42	2.26x10 <sup>-5</sup>	2.74x10 <sup>10</sup>
16	8.21x10 <sup>-1</sup>	6.84x10 <sup>10</sup>	43	1.37x10 <sup>-5</sup>	2.63x10 <sup>10</sup>
17	6.39x10 <sup>-1</sup>	7.45x10 <sup>10</sup>	44	8.32x10 <sup>-6</sup>	2.56x10 <sup>10</sup>
18	4.98x10 <sup>-1</sup>	5.01x10 <sup>10</sup>	45	5.04x10 <sup>-6</sup>	2.53x10 <sup>10</sup>
19	3.88x10 <sup>-1</sup>	7.11x10 <sup>10</sup>	46	3.06x10 <sup>-6</sup>	2.50x10 <sup>10</sup>
20	3.02x10 <sup>-1</sup>	8.23x10 <sup>10</sup>	47	1.86x10 <sup>-6</sup>	2.47x10 <sup>10</sup>
21	1.83x10 <sup>-1</sup>	7.79x10 <sup>10</sup>	48	1.13x10 <sup>-6</sup>	2.20x10 <sup>10</sup>
22	1.11x10 <sup>-1</sup>	5.78x10 <sup>10</sup>	49	6.83x10 <sup>-7</sup>	1.86x10 <sup>10</sup>
23	6.74x10 <sup>-2</sup>	4.66x10 <sup>10</sup>	50	4.14x10 <sup>-7</sup>	3.21x10 <sup>10</sup>
24	4.09x10 <sup>-2</sup>	2.77x10 <sup>10</sup>	51	2.51x10 <sup>-7</sup>	3.75x10 <sup>10</sup>
25	2.55x10 <sup>-2</sup>	2.63x10 <sup>10</sup>	52	1.52x10 <sup>-7</sup>	4.42x10 <sup>10</sup>
26	1.99x10 <sup>-2</sup>	1.67x10 <sup>10</sup>	53	9.24x10 <sup>-8</sup>	1.40x10 <sup>11</sup>
27	1.50x10 <sup>-2</sup>	2.74x10 <sup>10</sup>			

NOTE: Tabulated energy levels represent the upper energy of each group.

**TABLE 6-23**  
**BEST ESTIMATE NEUTRON ENERGY SPECTRUM AT**  
**SURVEILLANCE CAPSULE R SPECIMEN GEOMETRIC CENTER**

<u>Group</u>	<u>Energy (MeV)</u>	<u>Best Est. Flux (n/cm<sup>2</sup>-sec)</u>	<u>Group</u>	<u>Energy (MeV)</u>	<u>Best Est. Flux (n/cm<sup>2</sup>-sec)</u>
1	1.73x10 <sup>1</sup>	6.53x10 <sup>6</sup>	28	9.12x10 <sup>-3</sup>	2.07x10 <sup>10</sup>
2	1.49x10 <sup>1</sup>	1.41x10 <sup>7</sup>	29	5.53x10 <sup>-3</sup>	2.22x10 <sup>10</sup>
3	1.35x10 <sup>1</sup>	5.37x10 <sup>7</sup>	30	3.36x10 <sup>-3</sup>	6.98x10 <sup>9</sup>
4	1.16x10 <sup>1</sup>	1.51x10 <sup>8</sup>	31	2.84x10 <sup>-3</sup>	6.64x10 <sup>9</sup>
5	1.00x10 <sup>1</sup>	3.53x10 <sup>8</sup>	32	2.40x10 <sup>-3</sup>	6.40x10 <sup>9</sup>
6	8.61x10 <sup>0</sup>	6.48x10 <sup>8</sup>	33	2.04x10 <sup>-3</sup>	1.87x10 <sup>10</sup>
7	7.41x10 <sup>0</sup>	1.65x10 <sup>9</sup>	34	1.23x10 <sup>-3</sup>	1.83x10 <sup>10</sup>
8	6.07x10 <sup>0</sup>	2.65x10 <sup>9</sup>	35	7.49x10 <sup>-4</sup>	1.68x10 <sup>10</sup>
9	4.97x10 <sup>0</sup>	5.89x10 <sup>9</sup>	36	4.54x10 <sup>-4</sup>	1.50x10 <sup>10</sup>
10	3.68x10 <sup>0</sup>	7.53x10 <sup>9</sup>	37	2.75x10 <sup>-4</sup>	1.59x10 <sup>10</sup>
11	2.87x10 <sup>0</sup>	1.47x10 <sup>10</sup>	38	1.67x10 <sup>-4</sup>	1.42x10 <sup>10</sup>
12	2.23x10 <sup>0</sup>	1.98x10 <sup>10</sup>	39	1.01x10 <sup>-4</sup>	1.62x10 <sup>10</sup>
13	1.74x10 <sup>0</sup>	2.66x10 <sup>10</sup>	40	6.14x10 <sup>-5</sup>	1.64x10 <sup>10</sup>
14	1.35x10 <sup>0</sup>	2.81x10 <sup>10</sup>	41	3.73x10 <sup>-5</sup>	1.67x10 <sup>10</sup>
15	1.11x10 <sup>0</sup>	4.69x10 <sup>10</sup>	42	2.26x10 <sup>-5</sup>	1.68x10 <sup>10</sup>
16	8.21x10 <sup>-1</sup>	5.13x10 <sup>10</sup>	43	1.37x10 <sup>-5</sup>	1.67x10 <sup>10</sup>
17	6.39x10 <sup>-1</sup>	5.41x10 <sup>10</sup>	44	8.32x10 <sup>-6</sup>	1.67x10 <sup>10</sup>
18	4.98x10 <sup>-1</sup>	3.55x10 <sup>10</sup>	45	5.04x10 <sup>-6</sup>	1.69x10 <sup>10</sup>
19	3.88x10 <sup>-1</sup>	4.94x10 <sup>10</sup>	46	3.06x10 <sup>-6</sup>	1.71x10 <sup>10</sup>
20	3.02x10 <sup>-1</sup>	5.64x10 <sup>10</sup>	47	1.86x10 <sup>-6</sup>	1.72x10 <sup>10</sup>
21	1.83x10 <sup>-1</sup>	5.30x10 <sup>10</sup>	48	1.13x10 <sup>-6</sup>	1.56x10 <sup>10</sup>
22	1.11x10 <sup>-1</sup>	3.93x10 <sup>10</sup>	49	6.83x10 <sup>-7</sup>	1.40x10 <sup>10</sup>
23	6.74x10 <sup>-2</sup>	3.18x10 <sup>10</sup>	50	4.14x10 <sup>-7</sup>	2.66x10 <sup>10</sup>
24	4.09x10 <sup>-2</sup>	1.91x10 <sup>10</sup>	51	2.51x10 <sup>-7</sup>	3.41x10 <sup>10</sup>
25	2.55x10 <sup>-2</sup>	1.82x10 <sup>10</sup>	52	1.52x10 <sup>-7</sup>	4.35x10 <sup>10</sup>
26	1.99x10 <sup>-2</sup>	1.17x10 <sup>10</sup>	53	9.24x10 <sup>-8</sup>	1.66x10 <sup>11</sup>
27	1.50x10 <sup>-2</sup>	1.93x10 <sup>10</sup>			

NOTE: Tabulated energy levels represent the upper energy of each group.

TABLE 6-24  
BEST ESTIMATE NEUTRON ENERGY SPECTRUM AT  
SURVEILLANCE CAPSULE P SPECIMEN GEOMETRIC CENTER

Group	Energy (MeV)	Best Est. Flux (n/cm <sup>2</sup> -sec)	Group	Energy (MeV)	Best Est. Flux (n/cm <sup>2</sup> -sec)
1	1.73x10 <sup>1</sup>	6.38x10 <sup>6</sup>	28	9.12x10 <sup>-3</sup>	1.30x10 <sup>10</sup>
2	1.49x10 <sup>1</sup>	1.35x10 <sup>7</sup>	29	5.53x10 <sup>-3</sup>	1.39 x10 <sup>10</sup>
3	1.35x10 <sup>1</sup>	4.94x10 <sup>7</sup>	30	3.36x10 <sup>-3</sup>	4.38x10 <sup>9</sup>
4	1.16x10 <sup>1</sup>	1.34x10 <sup>8</sup>	31	2.84x10 <sup>-3</sup>	4.20x10 <sup>9</sup>
5	1.00x10 <sup>1</sup>	3.01x10 <sup>8</sup>	32	2.40x10 <sup>-3</sup>	4.11x10 <sup>9</sup>
6	8.61x10 <sup>0</sup>	5.25x10 <sup>8</sup>	33	2.04x10 <sup>-3</sup>	1.23x10 <sup>10</sup>
7	7.41x10 <sup>0</sup>	1.29x10 <sup>9</sup>	34	1.23x10 <sup>-3</sup>	1.23x10 <sup>10</sup>
8	6.07x10 <sup>0</sup>	1.96x10 <sup>9</sup>	35	7.49x10 <sup>-4</sup>	1.17x10 <sup>10</sup>
9	4.97x10 <sup>0</sup>	4.01x10 <sup>9</sup>	36	4.54x10 <sup>-4</sup>	1.08x10 <sup>10</sup>
10	3.68x10 <sup>0</sup>	4.80x10 <sup>9</sup>	37	2.75x10 <sup>-4</sup>	1.16x10 <sup>10</sup>
11	2.87x10 <sup>0</sup>	9.21x10 <sup>9</sup>	38	1.67x10 <sup>-4</sup>	1.20x10 <sup>10</sup>
12	2.23x10 <sup>0</sup>	1.22x10 <sup>10</sup>	39	1.01x10 <sup>-4</sup>	1.20x10 <sup>10</sup>
13	1.74x10 <sup>0</sup>	1.62x10 <sup>10</sup>	40	6.14x10 <sup>-5</sup>	1.19x10 <sup>10</sup>
14	1.35x10 <sup>0</sup>	1.74x10 <sup>10</sup>	41	3.73x10 <sup>-5</sup>	1.18x10 <sup>10</sup>
15	1.11x10 <sup>0</sup>	2.94x10 <sup>10</sup>	42	2.26x10 <sup>-5</sup>	1.15x10 <sup>10</sup>
16	8.21x10 <sup>-1</sup>	3.23x10 <sup>10</sup>	43	1.37x10 <sup>-5</sup>	1.11x10 <sup>10</sup>
17	6.39x10 <sup>-1</sup>	3.43x10 <sup>10</sup>	44	8.32x10 <sup>-6</sup>	1.09x10 <sup>10</sup>
18	4.98x10 <sup>-1</sup>	2.29x10 <sup>10</sup>	45	5.04x10 <sup>-6</sup>	1.08x10 <sup>10</sup>
19	3.88x10 <sup>-1</sup>	3.19x10 <sup>10</sup>	46	3.06x10 <sup>-6</sup>	1.07x10 <sup>10</sup>
20	3.02x10 <sup>-1</sup>	3.70x10 <sup>10</sup>	47	1.86x10 <sup>-6</sup>	1.07x10 <sup>10</sup>
21	1.83x10 <sup>-1</sup>	3.36x10 <sup>10</sup>	48	1.13x10 <sup>-6</sup>	9.57x10 <sup>9</sup>
22	1.11x10 <sup>-1</sup>	2.55x10 <sup>10</sup>	49	6.83x10 <sup>-7</sup>	8.15x10 <sup>9</sup>
23	6.74x10 <sup>-2</sup>	2.05x10 <sup>10</sup>	50	4.14x10 <sup>-7</sup>	1.35x10 <sup>10</sup>
24	4.09x10 <sup>-2</sup>	1.22x10 <sup>10</sup>	51	2.51x10 <sup>-7</sup>	1.89x10 <sup>10</sup>
25	2.55x10 <sup>-2</sup>	1.15x10 <sup>10</sup>	52	1.52x10 <sup>-7</sup>	2.99x10 <sup>10</sup>
26	1.99x10 <sup>-2</sup>	7.40x10 <sup>9</sup>	53	9.24x10 <sup>-8</sup>	6.10x10 <sup>10</sup>
27	1.50x10 <sup>-2</sup>	1.22x10 <sup>10</sup>			

NOTE: Tabulated energy levels represent the upper energy of each group.

**TABLE 6-25**  
**BEST ESTIMATE NEUTRON ENERGY SPECTRUM AT**  
**SURVEILLANCE CAPSULE S SPECIMEN GEOMETRIC CENTER**

<u>Group</u>	<u>Energy (MeV)</u>	<u>Best Est. Flux (n/cm<sup>2</sup>-sec)</u>	<u>Group</u>	<u>Energy (MeV)</u>	<u>Best Est. Flux (n/cm<sup>2</sup>-sec)</u>
1	1.73x10 <sup>1</sup>	5.56x10 <sup>6</sup>	28	9.12x10 <sup>-3</sup>	1.11x10 <sup>10</sup>
2	1.49x10 <sup>1</sup>	1.20x10 <sup>7</sup>	29	5.53x10 <sup>-3</sup>	1.21x10 <sup>10</sup>
3	1.35x10 <sup>1</sup>	4.45x10 <sup>7</sup>	30	3.36x10 <sup>-3</sup>	3.86x10 <sup>9</sup>
4	1.16x10 <sup>1</sup>	1.22x10 <sup>8</sup>	31	2.84x10 <sup>-3</sup>	3.75x10 <sup>9</sup>
5	1.00x10 <sup>1</sup>	2.80x10 <sup>8</sup>	32	2.40x10 <sup>-3</sup>	3.71x10 <sup>9</sup>
6	8.61x10 <sup>0</sup>	4.94x10 <sup>8</sup>	33	2.04x10 <sup>-3</sup>	1.13x10 <sup>10</sup>
7	7.41x10 <sup>0</sup>	1.22x10 <sup>9</sup>	34	1.23x10 <sup>-3</sup>	1.14x10 <sup>10</sup>
8	6.07x10 <sup>0</sup>	1.86x10 <sup>9</sup>	35	7.49x10 <sup>-4</sup>	1.11x10 <sup>10</sup>
9	4.97x10 <sup>0</sup>	3.83x10 <sup>9</sup>	36	4.54x10 <sup>-4</sup>	1.04x10 <sup>10</sup>
10	3.68x10 <sup>0</sup>	4.49x10 <sup>9</sup>	37	2.75x10 <sup>-4</sup>	1.14x10 <sup>10</sup>
11	2.87x10 <sup>0</sup>	8.32x10 <sup>9</sup>	38	1.67x10 <sup>-4</sup>	1.26x10 <sup>10</sup>
12	2.23x10 <sup>0</sup>	1.04x10 <sup>10</sup>	39	1.01x10 <sup>-4</sup>	1.18x10 <sup>10</sup>
13	1.74x10 <sup>0</sup>	1.33x10 <sup>10</sup>	40	6.14x10 <sup>-5</sup>	1.15x10 <sup>10</sup>
14	1.35x10 <sup>0</sup>	1.37x10 <sup>10</sup>	41	3.73x10 <sup>-5</sup>	1.13x10 <sup>10</sup>
15	1.11x10 <sup>0</sup>	2.22x10 <sup>10</sup>	42	2.26x10 <sup>-5</sup>	1.09x10 <sup>10</sup>
16	8.21x10 <sup>-1</sup>	2.37x10 <sup>10</sup>	43	1.37x10 <sup>-5</sup>	1.04x10 <sup>10</sup>
17	6.39x10 <sup>-1</sup>	2.46x10 <sup>10</sup>	44	8.32x10 <sup>-6</sup>	1.01x10 <sup>10</sup>
18	4.98x10 <sup>-1</sup>	1.64x10 <sup>10</sup>	45	5.04x10 <sup>-6</sup>	9.95x10 <sup>9</sup>
19	3.88x10 <sup>-1</sup>	2.28x10 <sup>10</sup>	46	3.06x10 <sup>-6</sup>	9.82x10 <sup>9</sup>
20	3.02x10 <sup>-1</sup>	2.66x10 <sup>10</sup>	47	1.86x10 <sup>-6</sup>	9.69x10 <sup>9</sup>
21	1.83x10 <sup>-1</sup>	2.53x10 <sup>10</sup>	48	1.13x10 <sup>-6</sup>	8.63x10 <sup>9</sup>
22	1.11x10 <sup>-1</sup>	1.91x10 <sup>10</sup>	49	6.83x10 <sup>-7</sup>	7.17x10 <sup>9</sup>
23	6.74x10 <sup>-2</sup>	1.57x10 <sup>10</sup>	50	4.14x10 <sup>-7</sup>	1.22x10 <sup>10</sup>
24	4.09x10 <sup>-2</sup>	9.61x10 <sup>9</sup>	51	2.51x10 <sup>-7</sup>	1.41x10 <sup>10</sup>
25	2.55x10 <sup>-2</sup>	9.28x10 <sup>9</sup>	52	1.52x10 <sup>-7</sup>	1.65x10 <sup>10</sup>
26	1.99x10 <sup>-2</sup>	6.08x10 <sup>9</sup>	53	9.24x10 <sup>-8</sup>	5.16x10 <sup>10</sup>
27	1.50x10 <sup>-2</sup>	1.02x10 <sup>10</sup>			

NOTE: Tabulated energy levels represent the upper energy of each group.

TABLE 6-26

COMPARISON OF CALCULATED AND BEST ESTIMATE EXPOSURE LEVELS FOR  
KEWAUNEE SURVEILLANCE CAPSULES AT SPECIMEN GEOMETRIC CENTER

CAPSULE V

	<u>Calculated</u>	<u>Best Estimate</u>	<u>BE/C</u>
$\Phi(E > 1.0 \text{ MeV}) \{n/cm^2\}$	$5.42 \times 10^{18}$	$5.97 \times 10^{18}$	1.10
$\Phi(E > 0.1 \text{ MeV}) \{n/cm^2\}$	$1.98 \times 10^{19}$	$2.53 \times 10^{19}$	1.28
dpa	$9.47 \times 10^{-3}$	$1.13 \times 10^{-2}$	1.19

CAPSULE R

	<u>Calculated</u>	<u>Best Estimate</u>	<u>BE/C</u>
$\Phi(E > 1.0 \text{ MeV}) \{n/cm^2\}$	$1.69 \times 10^{19}$	$1.81 \times 10^{19}$	1.07
$\Phi(E > 0.1 \text{ MeV}) \{n/cm^2\}$	$6.15 \times 10^{19}$	$6.75 \times 10^{19}$	1.10
dpa	$2.95 \times 10^{-2}$	$3.18 \times 10^{-2}$	1.08

CAPSULE P

	<u>Calculated</u>	<u>Best Estimate</u>	<u>BE/C</u>
$\Phi(E > 1.0 \text{ MeV}) \{n/cm^2\}$	$2.52 \times 10^{19}$	$2.74 \times 10^{19}$	1.09
$\Phi(E > 0.1 \text{ MeV}) \{n/cm^2\}$	$8.42 \times 10^{19}$	$1.04 \times 10^{20}$	1.23
dpa	$4.24 \times 10^{-2}$	$4.88 \times 10^{-2}$	1.15

CAPSULE S

	<u>Calculated</u>	<u>Best Estimate</u>	<u>BE/C</u>
$\Phi(E > 1.0 \text{ MeV}) \{n/cm^2\}$	$3.49 \times 10^{19}$	$3.36 \times 10^{19}$	0.96
$\Phi(E > 0.1 \text{ MeV}) \{n/cm^2\}$	$1.18 \times 10^{20}$	$1.14 \times 10^{20}$	0.97
dpa	$5.90 \times 10^{-2}$	$5.69 \times 10^{-2}$	0.97



**TABLE 6-27**  
**NEUTRON EXPOSURE PROJECTIONS AT KEY LOCATIONS**  
**ON THE PRESSURE VESSEL CLAD/BASE METAL INTERFACE**

**16.2 EFPY**

	<u>0°</u>	<u>15°</u>	<u>30°</u>	<u>45°</u>
$\Phi t$ ( $E > 1.0$ MeV), n/cm <sup>2</sup>	$1.73 \times 10^{19}$	$1.11 \times 10^{19}$	$8.78 \times 10^{18}$	$7.45 \times 10^{18}$
$\Phi t$ ( $E > 0.1$ MeV), n/cm <sup>2</sup>	$5.08 \times 10^{19}$	$3.29 \times 10^{19}$	$2.51 \times 10^{19}$	$2.10 \times 10^{19}$
Iron Atom Displacements, dpa	$2.93 \times 10^{-2}$	$1.90 \times 10^{-2}$	$1.48 \times 10^{-2}$	$1.25 \times 10^{-2}$

**25 EFPY**

	<u>0°</u>	<u>15°</u>	<u>30°</u>	<u>45°</u>
$\Phi t$ ( $E > 1.0$ MeV), n/cm <sup>2</sup>	$2.57 \times 10^{19}$	$1.68 \times 10^{19}$	$1.36 \times 10^{19}$	$1.15 \times 10^{19}$
$\Phi t$ ( $E > 0.1$ MeV), n/cm <sup>2</sup>	$7.53 \times 10^{19}$	$4.96 \times 10^{19}$	$3.87 \times 10^{19}$	$3.25 \times 10^{19}$
Iron Atom Displacements, dpa	$4.34 \times 10^{-2}$	$2.86 \times 10^{-2}$	$2.29 \times 10^{-2}$	$1.94 \times 10^{-2}$

**33 EFPY**

	<u>0°</u>	<u>15°</u>	<u>30°</u>	<u>45°</u>
$\Phi t$ ( $E > 1.0$ MeV), n/cm <sup>2</sup>	$3.34 \times 10^{19}$	$2.19 \times 10^{19}$	$1.79 \times 10^{19}$	$1.52 \times 10^{19}$
$\Phi t$ ( $E > 0.1$ MeV), n/cm <sup>2</sup>	$9.77 \times 10^{19}$	$6.49 \times 10^{19}$	$5.11 \times 10^{19}$	$4.29 \times 10^{19}$
Iron Atom Displacements, dpa	$5.64 \times 10^{-2}$	$3.74 \times 10^{-2}$	$3.02 \times 10^{-2}$	$2.56 \times 10^{-2}$

**51 EFPY**

	<u>0°</u>	<u>15°</u>	<u>30°</u>	<u>45°</u>
$\Phi t$ ( $E > 1.0$ MeV), n/cm <sup>2</sup>	$5.06 \times 10^{19}$	$3.35 \times 10^{19}$	$2.77 \times 10^{19}$	$2.34 \times 10^{19}$
$\Phi t$ ( $E > 0.1$ MeV), n/cm <sup>2</sup>	$1.48 \times 10^{20}$	$9.93 \times 10^{19}$	$7.89 \times 10^{19}$	$6.62 \times 10^{19}$
Iron Atom Displacements, dpa	$8.55 \times 10^{-2}$	$5.72 \times 10^{-2}$	$4.66 \times 10^{-2}$	$3.94 \times 10^{-2}$

**TABLE 6-28**  
**KEWAUNEE IN-CORE FUEL MANAGEMENT FORECAST**  
**(ASSUMED FOR CALCULATIONAL PURPOSES ONLY)**

Cycle	Startup Date	License Date	Shutdown Date	Cycle Length	Equivalent Full Power Days	Thermal Capacity Factor (%)	EFPY
20					319		17.07
21					469		18.36
22*	06-10-97		09-26-98	473	446	94.3	19.58
23	12-13-98		03-11-00	454	430	94.6	20.76
24	05-28-00		09-15-01	475	450	94.6	21.99
25	12-02-01		04-05-03	489	463	94.7	23.26
26	05-18-03		10-02-04	503	476	94.7	24.56
27	11-21-04		04-08-06	510	476	94.7	25.86
28	05-21-06		10-06-07	503	476	94.7	27.17
29	11-18-07		04-04-09	503	476	94.7	28.47
30	05-17-09		10-02-10	503	476	94.7	29.77
31	11-14-10		03-31-12	503	476	94.7	31.07
32	05-13-12		12-21-13	587	524	89.3	32.51
40 Yr Lic			12-31-13				
33		-	10-04-14	503	487	96.8	33.84
34	11-30-14		04-16-16	503	487	96.8	35.18
35	05-29-16		10-14-17	503	487	96.8	36.51
36	11-26-17		04-13-19	503	487	96.8	37.84
37	05-26-19		10-10-20	503	487	96.8	39.18
38	11-22-20		04-09-22	503	487	96.8	40.51
39	05-22-22		10-07-23	503	487	96.8	41.84
40	11-19-23		04-05-25	503	487	96.8	43.18
41	05-18-25		10-03-26	503	487	96.8	44.51
42	11-15-26		04-01-28	503	487	96.8	45.84
43	06-14-28		10-30-29	503	487	96.8	47.18
44	12-12-29		04-29-31	503	487	96.8	48.51
45	06-11-31		10-26-32	503	487	96.8	49.84
46	12-08-32		-	-	-	-	-
60 Yr Lic		-	12-31-33	389	376	96.8	51.18

\*Current Operating Cycle

TABLE 6-29  
NEUTRON EXPOSURE VALUES FOR THE KEWAUNEE REACTOR VESSEL

25 EFPY

	<u>NEUTRON FLUENCE (E &gt; 1.0 MeV) SLOPE</u> (n/cm <sup>2</sup> )			<u>dpa SLOPE</u> (equivalent n/cm <sup>2</sup> )		
	<u>Surface</u>	<u>1/4 T</u>	<u>3/4 T</u>	<u>Surface</u>	<u>1/4 T</u>	<u>3/4 T</u>
0°(a)	2.57 X 10 <sup>19</sup>	1.65 X 10 <sup>19</sup>	5.19 X 10 <sup>18</sup>	2.57 X 10 <sup>19</sup>	1.82 X 10 <sup>19</sup>	7.71 X 10 <sup>18</sup>
15°	1.68 X 10 <sup>19</sup>	1.10 X 10 <sup>19</sup>	3.56 X 10 <sup>18</sup>	1.68 X 10 <sup>19</sup>	1.21 X 10 <sup>19</sup>	5.48 X 10 <sup>18</sup>
30°	1.36 X 10 <sup>19</sup>	8.88 X 10 <sup>18</sup>	2.87 X 10 <sup>18</sup>	1.36 X 10 <sup>19</sup>	9.77 X 10 <sup>18</sup>	4.41 X 10 <sup>18</sup>
45°	1.15 X 10 <sup>19</sup>	7.55 X 10 <sup>18</sup>	2.45 X 10 <sup>18</sup>	1.15 X 10 <sup>19</sup>	8.31 X 10 <sup>18</sup>	3.70 X 10 <sup>18</sup>

33 EFPY

	<u>NEUTRON FLUENCE (E &gt; 1.0 MeV) SLOPE</u> (n/cm <sup>2</sup> )			<u>dpa SLOPE</u> (equivalent n/cm <sup>2</sup> )		
	<u>Surface</u>	<u>1/4 T</u>	<u>3/4 T</u>	<u>Surface</u>	<u>1/4 T</u>	<u>3/4 T</u>
0°(a)	3.34 X 10 <sup>19</sup>	2.15 X 10 <sup>19</sup>	6.74 X 10 <sup>18</sup>	3.34 X 10 <sup>19</sup>	2.37 X 10 <sup>19</sup>	1.00 X 10 <sup>19</sup>
15°	2.19 X 10 <sup>19</sup>	1.43 X 10 <sup>19</sup>	4.65 X 10 <sup>18</sup>	2.19 X 10 <sup>19</sup>	1.58 X 10 <sup>19</sup>	7.14 X 10 <sup>18</sup>
30°	1.79 X 10 <sup>19</sup>	1.17 X 10 <sup>19</sup>	3.78 X 10 <sup>18</sup>	1.79 X 10 <sup>19</sup>	1.29 X 10 <sup>19</sup>	5.80 X 10 <sup>18</sup>
45°	1.52 X 10 <sup>19</sup>	9.99 X 10 <sup>18</sup>	3.24 X 10 <sup>18</sup>	1.52 X 10 <sup>19</sup>	1.10 X 10 <sup>19</sup>	4.89 X 10 <sup>18</sup>

51 EFPY

	<u>NEUTRON FLUENCE (E &gt; 1.0 MeV) SLOPE</u> (n/cm <sup>2</sup> )			<u>dpa SLOPE</u> (equivalent n/cm <sup>2</sup> )		
	<u>Surface</u>	<u>1/4 T</u>	<u>3/4 T</u>	<u>Surface</u>	<u>1/4 T</u>	<u>3/4 T</u>
0°(a)	5.06 X 10 <sup>19</sup>	3.26 X 10 <sup>19</sup>	1.02 X 10 <sup>19</sup>	5.06 X 10 <sup>19</sup>	3.58 X 10 <sup>19</sup>	1.52 X 10 <sup>19</sup>
15°	3.35 X 10 <sup>19</sup>	2.19 X 10 <sup>19</sup>	7.11 X 10 <sup>18</sup>	3.35 X 10 <sup>19</sup>	2.42 X 10 <sup>19</sup>	1.09 X 10 <sup>19</sup>
30°	2.76 X 10 <sup>19</sup>	1.80 X 10 <sup>19</sup>	5.83 X 10 <sup>18</sup>	2.76 X 10 <sup>19</sup>	1.98 X 10 <sup>19</sup>	8.94 X 10 <sup>18</sup>
45°	2.34 X 10 <sup>19</sup>	1.54 X 10 <sup>19</sup>	4.98 X 10 <sup>18</sup>	2.34 X 10 <sup>19</sup>	1.69 X 10 <sup>19</sup>	7.53 X 10 <sup>18</sup>

(a) Maximum point on the pressure vessel

TABLE 6-30  
UPDATED LEAD FACTORS FOR KEWAUNEE SURVEILLANCE CAPSULES

<u>Capsule</u>	<u>Lead Factor</u>
V	3.17 <sup>(a)</sup>
R	3.18 <sup>(b)</sup>
P	2.10 <sup>(c)</sup>
S	2.13 <sup>(d)</sup>
T	2.23 <sup>(d)</sup>
N	2.13 <sup>(d)</sup>

- (a) Plant specific evaluation based on end of Cycle 1 calculated fluence.  
(b) Plant specific evaluation based on end of Cycle 5 calculated fluence.  
(c) Plant specific evaluation based on end of Cycle 13 calculated fluence.  
(d) Plant specific evaluation based on end of Cycle 19 calculated fluence

## 7.0 SURVEILLANCE CAPSULE REMOVAL SCHEDULE

The following surveillance capsule removal schedule meets the requirements of ASTM E185-82 and is recommended for future capsules to be removed from the Kewaunee reactor vessel:

Capsule	Location	Lead Factor	Removal Time (EFPY) <sup>(a)</sup>	Fluence (n/cm <sup>2</sup> , E > 1.0 MeV)
V	77°	3.17	1.29	5.97 x 10 <sup>18</sup>
R	257°	3.18	4.57	1.81 x 10 <sup>19</sup>
P	247°	2.10	11.08	2.74 x 10 <sup>19</sup>
S	57°	2.13	16.2	3.36 x 10 <sup>19</sup>
N	237°	2.13	EOL	See note b
T	67°	2.23	Standby	---

- (a) Effective Full Power Years (EFPY) from plant startup.
- (b) Capsule N should be removed before it receives a fluence of  $6.72 \times 10^{19}$  n/cm<sup>2</sup> (E > 1.0 MeV) (i.e., twice the peak vessel EOL surface fluence of  $3.36 \times 10^{19}$  n/cm<sup>2</sup> (E > 1.0 MeV)). This capsule may be held without testing following withdrawal. Capsule N will reach a fluence of approximately  $5.099 \times 10^{19}$  n/cm<sup>2</sup> (E > 1.0 MeV) at 22.26 EFPY. This is approximately equal to the reactor vessel peak surface fluence of  $5.06 \times 10^{19}$  n/cm<sup>2</sup> (E > 1.0 MeV) at 51 EFPY (60 calendar year life).

## 8.0 CONCLUSIONS

The evaluation of the reactor vessel materials contained in surveillance capsule S removed from the Kewaunee surveillance program and capsule A-35 removed from the Maine Yankee surveillance program led to the following conclusions:

### 8.1 FLUENCE EVALUATION

#### 8.1.1 Kewaunee Capsule S

- The capsule received an average fast neutron fluence ( $E > 1.0$  MeV) of  $3.36 \times 10^{19}$  n/cm<sup>2</sup> after 16.2 effective full power years (EFPY) of plant operation calculated using the latest ENDF-VI dosimetry cross-sections. The prior evaluation of this fluence was  $3.45 \times 10^{19}$  n/cm<sup>2</sup> for the EFPY calculated using the ENDF-V dosimetry cross-sections.
- The incorporation of the SNLRML cross-section library, a change in fuel cycle design, and new estimates of future operating times resulted in small changes to both surveillance capsule and pressure vessel fluence estimates.
- The calculated end-of-life (33 EFPY) and extended life (51 EFPY) maximum neutron fluence ( $E > 1.0$  MeV) using the latest ENDF-VI dosimetry cross sections for the Kewaunee reactor vessel is as follows:

	33 EFPY	51 EFPY
Vessel inner radius*	$3.34 \times 10^{19}$ n/cm <sup>2</sup>	$5.06 \times 10^{19}$ n/cm <sup>2</sup>
Vessel 1/4 thickness	$2.15 \times 10^{19}$ n/cm <sup>2</sup>	$3.26 \times 10^{19}$ n/cm <sup>2</sup>
Vessel 3/4 thickness	$6.74 \times 10^{18}$ n/cm <sup>2</sup>	$1.02 \times 10^{19}$ n/cm <sup>2</sup>

\* Clad/base metal interface

- The observed changes in best estimate fluence range from 3%-7% and fall within the 1 $\sigma$  uncertainties of 7%-10% that are associated with the various capsule dosimetry evaluations.
- The impact of the revised analysis on projected maximum vessel exposures can be seen in the following comparison of the best estimate exposures at the peak (0.0 degree) location at the vessel inner radius.

Operating Time [EFPY]	Current Evaluation Fluence [n/cm <sup>2</sup> ]	Prior Evaluation Fluence [n/cm <sup>2</sup> ]
16.2	$1.73 \times 10^{19}$	$1.82 \times 10^{19}$
25.0	$2.57 \times 10^{19}$	$2.64 \times 10^{19}$
33.0 (EOL)	$3.34 \times 10^{19}$	
34.0 (EOL)		$3.49 \times 10^{19}$
51.0	$5.06 \times 10^{19}$	$5.09 \times 10^{19}$

- The projected changes in the best estimate pressure vessel exposure range from 1%-5% and fall well within the typical uncertainty of 12%-17% associated with vessel fluence projections.

### 8.1.2 Maine Yankee Capsule A-35

- The capsule received an average fast neutron fluence ( $E > 1.0$  MeV) of  $6.11 \times 10^{19}$  n/cm<sup>2</sup> determined using the latest ENDF-VI dosimetry cross sections after 4.5 effective full power years (EFPY) of plant operation.

## 8.2 CHARPY V-NOTCH IMPACT TESTS

### 8.2.1 Kewaunee Capsule S

#### 8.2.1.1 Forging Material

- Irradiation of the reactor vessel intermediate shell forging 122X208VA1 Charpy specimens, oriented with the longitudinal axis of the specimen parallel to the working direction of the forging (tangential orientation), to  $3.36 \times 10^{19}$  n/cm<sup>2</sup> ( $E > 1.0$  MeV) resulted in a 30 ft-lb transition temperature increase of 60°F and a 50 ft-lb transition temperature increase of 35°F. This results in an irradiated 30 ft-lb transition temperature of 35°F and an irradiated 50 ft-lb transition temperature of 50°F for the tangentially oriented specimens.
- Irradiation of the reactor vessel lower shell forging 123X167VA1 Charpy specimens, oriented with the longitudinal axis of the specimen parallel to the working direction of the forging (tangential orientation), to  $3.36 \times 10^{19}$  n/cm<sup>2</sup> ( $E > 1.0$  MeV) resulted in a 30 ft-lb transition temperature increase of 50°F and a 50 ft-lb transition temperature increase of 48°F. This results in an irradiated 30 ft-lb transition temperature of 0°F and an irradiated 50 ft-lb transition temperature of 23°F for tangentially oriented specimens.
- The average upper shelf energy of the intermediate shell forging 122X208VA1 (tangential orientation) resulted in an average energy decrease of 12 ft-lbs after irradiation to  $3.36 \times 10^{19}$  n/cm<sup>2</sup> ( $E > 1.0$  MeV). This results in an irradiated average upper shelf energy of 148 ft-lb for the tangentially oriented specimens.
- The average upper shelf energy of the lower shell forging 123X167VA1 (tangential orientation) resulted in an average energy decrease of 5 ft-lb after irradiation to  $3.36 \times 10^{19}$  n/cm<sup>2</sup> ( $E > 1.0$  MeV). This results in an irradiated average upper shelf energy of 152 ft-lb for the tangentially oriented specimens.

#### 8.2.1.2 WeId Metal (1P3571)

- Irradiation of the weld metal Charpy specimens to  $3.36 \times 10^{19}$  n/cm<sup>2</sup> ( $E > 1.0$  MeV) resulted in a 30 ft-lb transition temperature increase of 250°F and a 50 ft-lb transition

temperature increase of 268°F. This results in an irradiated 30 ft-lb transition temperature of 200°F and an irradiated 50 ft-lb transition temperature of 258°F.

- The average upper shelf energy of the weld metal Charpy specimens resulted in an average energy decrease of 62 ft-lb after irradiation to  $3.36 \times 10^{19}$  n/cm<sup>2</sup> (E > 1.0 MeV). This results in an irradiated average upper shelf energy of 64 ft-lb for the weld metal specimens.

#### 8.2.1.3 HAZ

- The average upper shelf energy of the weld HAZ metal decreased 41 ft-lb after irradiation to  $3.36 \times 10^{19}$  n/cm<sup>2</sup> (E > 1.0 MeV). This results in an irradiated average upper shelf energy of 139 ft-lb for the weld HAZ metal.
- Irradiation of the weld Heat-Affected-Zone (HAZ) metal Charpy specimens to  $3.36 \times 10^{19}$  n/cm<sup>2</sup> (E > 1.0 MeV) resulted in a 30 ft-lb transition temperature increase of 200°F and a 50 ft-lb transition temperature increase of 225°F. This results in an irradiated 30 ft-lb transition temperature of 85°F and an irradiated 50 ft-lb transition temperature of 155°F.

#### 8.2.1.4 Correlation Monitor Material

- Irradiation of the ASTM correlation monitor material (HSST Plate 02) Charpy specimens, oriented with the longitudinal axis of the specimen parallel to the major rolling direction of the plate (longitudinal orientation), to  $3.36 \times 10^{19}$  n/cm<sup>2</sup> (E > 1.0 MeV) resulted in a 30 ft-lb transition temperature increase of 158°F and a 50 ft-lb transition temperature increase of 160°F. This results in an irradiated 30 ft-lb transition temperature of 203°F and an irradiated 50 ft-lb transition temperature of 240°F for longitudinally oriented specimens.
- The average upper shelf energy of the ASTM correlation monitor material (HSST Plate 02) (longitudinal orientation) resulted in an average energy decrease of 25 ft-lb after irradiation to  $3.36 \times 10^{19}$  n/cm<sup>2</sup> (E > 1.0 MeV). This results in an irradiated average upper shelf energy of 98 ft-lb for the longitudinally oriented specimens.

#### 8.2.2 Maine Yankee Capsule A-35

- Charpy V-notch test results were not used in this report. The results, however, were reported in WCAP-9875 issued in March 1981. The results were also used with the other Maine Yankee surveillance results in WCAP-15074.

### 8.3 "MASTER CURVE" FRACTURE TOUGHNESS TESTS

- 1/2T-CT specimens of the Kewaunee weld material in the unirradiation condition resulted in an initial Master Curve T<sub>0</sub> transition temperature of -129°F.



- Whole and reconstituted Charpy size precracked three point bend specimens of the Kewaunee weld material in the unirradiated condition resulted in initial Master Curve  $T_0$  transition temperatures of  $-148^{\circ}\text{F}$  and  $-154^{\circ}\text{F}$ , respectively. These values, as compared to the 1/2T-CT results, are within the typical data scatter for these tests.
- Whole Charpy size precracked three point bend specimens of the Maine Yankee weld material in the unirradiated condition resulted in an initial Master Curve  $T_0$  transition temperature of  $-158^{\circ}\text{F}$ .
- Irradiation of the Kewaunee weld metal precracked three point bend reconstituted Charpy specimens to  $3.36 \times 10^{19} \text{ n/cm}^2$  ( $E > 1.0 \text{ MeV}$ ) resulted in a Master Curve  $T_0$  transition temperature increase of  $284^{\circ}\text{F}$ . This results in an irradiated Master Curve  $T_0$  transition temperature of  $136^{\circ}\text{F}$ , based upon an initial unirradiated to value of  $-148^{\circ}\text{F}$  as determined from precracked Charpy specimens.
- Irradiation of the Maine Yankee weld metal precracked three point bend reconstituted Charpy specimens to  $6.11 \times 10^{19} \text{ n/cm}^2$  ( $E > 1.0 \text{ MeV}$ ) resulted in a Master Curve  $T_0$  transition temperature increase of  $390^{\circ}\text{F}$ . This results in an irradiated  $T_0$  transition temperature of  $232^{\circ}\text{F}$ , based upon an initial  $T_0$  value of  $-158^{\circ}\text{F}$  as determined from precracked Charpy specimens.

## 8.4 ANALYSIS

### 8.4.1 Charpy V-notch Toughness

- A comparison of the Kewaunee reactor vessel beltline material test results with the Regulatory Guide 1.99, Revision 2, predictions led to the following conclusions:
  - For Capsule S the intermediate shell forging 122X208VA1 and the lower shell forging 123X167VA1 surveillance material measured 30 ft-lb transition temperature increases are slightly greater than the Regulatory Guide 1.99, Revision 2, predictions. However, Regulatory Guide 1.99, Revision 2, requires a 2 sigma allowance of  $34^{\circ}\text{F}$  for base metal be added to the predicted reference transition temperature to obtain a conservative upper bound value. The measured reference transition temperatures of these materials are bounded by the 2 sigma allowance for shift prediction (for all capsule results for the forgings).
  - The measured 30 ft-lb transition temperature increase for the weld metal is less than the Regulatory Guide 1.99, Revision 2, prediction for fluences greater than  $2.74 \times 10^{19} \text{ n/cm}^2$ , but less than the Regulatory Guide prediction for lower fluences. On average, the data for the weld metal are close to the Regulatory Guide predictions.
  - The surveillance capsule S test results for all materials (weld, forgings, and correlation monitor plate) indicate that the surveillance material average upper

shelf energy decreases are less than the Regulatory Guide 1.99, Revision 2, predictions.

- The Regulatory Guide 1.99, Revision 2, credibility evaluation of the Kewaunee surveillance program weld metal presented in Appendix B of this report indicates that the Kewaunee reactor vessel surveillance results are credible.
- The initial  $RT_{NDT}$  evaluation for the Kewaunee surveillance weld metal presented in Appendix C of this report indicates that the initial  $RT_{NDT}$  of  $-50^{\circ}\text{F}$ . Note that the vessel girth weld was made from the same weld wire heat 1P3571.
- The capsule S surveillance results (if assumed to be adequate surrogates of the reactor vessel) indicate that the beltline region materials should have adequate toughness throughout the life of the vessel (33 EFPY) since the measured capsule S fluence is approximately equal to the peak vessel inner surface fluence at 33 EFPY.
- All beltline surveillance materials exhibit a more than adequate upper shelf energy level for continued safe plant operation and are expected to maintain an upper shelf energy of no less than 50 ft-lb throughout the life of the vessel (33 EFPY) as required by 10CFR50, Appendix G.

#### 8.4.2 Master Curve Fracture Toughness

- Master Curve fracture toughness based transition temperature increase ( $\Delta T_o$ ) due to the irradiation of  $3.36 \times 10^{19} \text{ n/cm}^2$  ( $E > 1.0 \text{ MeV}$ ) is higher than the 30 ft-lb Charpy V-notch toughness based transition temperature increase ( $\Delta T_{30}$ ) using the Charpy-size specimens ( $284^{\circ}\text{F}$  vs.  $250^{\circ}\text{F}$ ).
- Based on all of the test data combined used the multi-temperature maximum likelihood evaluation method, an increase of  $292^{\circ}\text{F}$  in the Master Curve  $T_o$  transition temperature for the Kewaunee surveillance weld is obtained. That was based on a maximum likelihood initial  $T_o$  of  $-144^{\circ}\text{F}$  (from the combined results of 1/2T compact specimens, precracked Charpy specimens, and reconstituted precracked Charpy specimens) and an irradiated condition  $T_o$  of  $148^{\circ}\text{F}$  (from the results of irradiated reconstituted precracked Charpy specimens and 1XWOL specimens).
- Master Curve transition temperature data for the Maine Yankee surveillance weld, when analyzed using the multi-temperature, maximum likelihood method, yields the same results as those generated following ASTM E1921-97. As for the Kewaunee surveillance weld, the Master Curve transition temperature increase ( $\Delta T_o$ ) is higher than the 30 ft-lb Charpy V-notch transition temperature ( $390^{\circ}\text{F}$  vs.  $345^{\circ}\text{F}$ ) for the Maine Yankee surveillance weld.

## 9.0 REFERENCES

1. E. Terek, G.N. Wrights and J.F. Williams, WCAP-14279, Rev. 0, "Analysis of Capsule S from the Wisconsin Public Service Corporation Kewaunee Nuclear Reactor Vessel Radiation Surveillance Program", March 1995.
2. ORNL RSCI Data Library Collection DLC-175, *BUGLE-93 Production and Testing of the VITAMIN-B6 Fine-Group and the BUGLE-93 Broad Group Neutron/Photon Cross-Section Libraries Derived from ENDF/B-VI Nuclear Data*.
3. ASTM E1253, "Guide for Reconstitution of Irradiated Charpy Specimens" in ASTM Standards, Section 00. American Society for Testing and Materials.
4. WCAP 9875, "Analysis of the Maine Yankee Reactor Vessel Second Accelerated Surveillance Capsule", S.E. Yanichko, S.L. Anderson, et. al., March 1981.
5. Yanichko, S. E., Lege, D. J., Zula, G. C., *Wisconsin Public Service Corp. Kewaunee Nuclear Power Plant Reactor Vessel Radiation Surveillance Program*, WCAP-8107, April 1973.
6. ASTM E185-82, *Standard Practice for Conducting Surveillance Tests for Light-Water Cooled Nuclear Power Reactor Vessels, E706 (IF)*, in ASTM Standards, Section 3, American Society for Testing and Materials, Philadelphia, PA, 1993.
7. Section III of the ASME Boiler and Pressure Vessel Code, Appendix G, *Protection Against Nonductile Failure*.
8. ASTM E208, *Standard Test Method for Conducting Drop-Weight Test to Determine Nil-Ductility Transition Temperature of Ferritic Steels*, in ASTM Standards, Section 3, American Society for Testing and Materials, Philadelphia, PA.
9. Code of Federal Regulations, 10CFR50, "Fracture Toughness Requirements for Light Water Reactor Pressure Vessels," U.S. Nuclear Regulatory Commission, Washington, D.C. December 19, 1995
10. Code of Federal Regulations, 10CFR50, Appendix G, *Fracture Toughness Requirements*, and Appendix H, *Reactor Vessel Material Surveillance Program Requirements*, U.S. Nuclear Regulatory Commission, Washington, D.C.
11. ASTM E1921-97, "Standard Test Method for Determination of Reference Temperature, To, for Ferritic Steels in the Transition Range" in ASTM Standards, Section 3, American Society for Testing and Materials.
12. WCAP 15075, "Master Curve Strategies for RPV Assessment", R.G. Lott, M.T. Kirk, and C.C. Kim, September 1988.

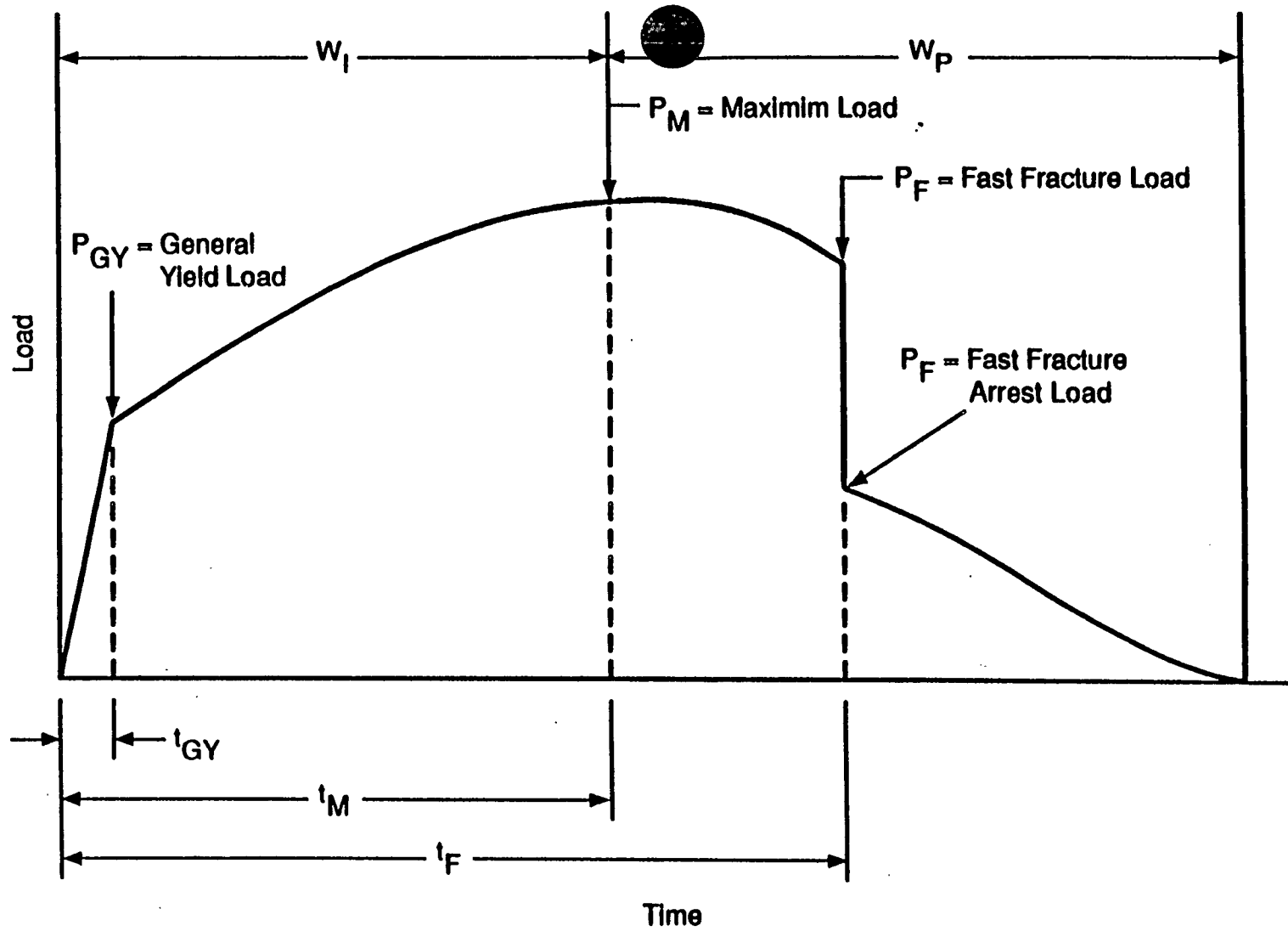
13. Server, W. L., Tomes, C., Kim, C., *Evaluation of the 1P3571 Weld Metal from the Surveillance Programs for Kewaunee and Maine Yankee*, WCAP-15074, June 1998.
14. ASTM E23-93a, *Standard Test Methods for Notched Bar Impact Testing of Metallic Materials*, in ASTM Standards, Section 3, American Society for Testing and Materials, Philadelphia, PA, 1993.
15. ASTM A370-92, *Standard Test Methods and Definitions for Mechanical Testing of Steel Products*, in ASTM Standards, Section 3, American Society for Testing and Materials, Philadelphia, PA, 1993.
16. ASTM E8-93, *Standard Test Methods for Tension Testing of Metallic Materials*, in ASTM Standards, Section 3, American Society for Testing and Materials, Philadelphia, PA, 1993.
17. ASTM E21-92, *Standard Test Methods for Elevated Temperature Tension Tests of Metallic Materials*, in ASTM Standards, Section 3, American Society for Testing and Materials, Philadelphia, PA, 1993.
18. ASTM E83-93, *Standard Practice for Verification and Classification of Extensometers*, in ASTM Standards, Section 3, American Society for Testing and Materials, Philadelphia, PA, 1993.
19. NRC-92-081, *Reactor Vessel Structural Integrity*, Letter from the Wisconsin Public Service Corporation to the U. S. Nuclear Regulatory Commission, Dated July 2, 1992.
20. CE-NPSD-1118, Rev. 0, "Fracture Toughness Characterization of CERP Materials".
21. ASTM Designation E853-87, *Standard Practice for Analysis and Interpretation of Light-Water Reactor Surveillance Results*, in ASTM Standards, Section 12, American Society for Testing and Materials, Philadelphia, PA, 1991.
22. ASTM Designation E693-79, *Standard Practice for Characterizing Neutron Exposures in Ferritic Steels in Terms of Displacements per Atom (dpa)*, in ASTM Standards, Section 12, American Society for Testing and Materials, Philadelphia, PA, 1991.
23. ORNL RSIC Code Package CCC-543, *TORT-DORT Two- and Three-Dimensional Discrete Ordinates Transport Version 2.7.3*, May 1993.
24. ORNL RSCI Data Library Collection DLC-175, *BUGLE-93 Production and Testing of the VITAMIN-B6 Fine-Group and the BUGLE-93 Broad Group Neutron/Photon Cross-Section Libraries Derived from ENDF/B-VI Nuclear Data*.
25. ASTM Designation E482-89, *Standard Guide for Application of Neutron Transport Methods for Reactor Vessel Surveillance*, in ASTM Standards, Section 12, American Society for Testing and Materials, Philadelphia, PA, 1991.

26. ASTM Designation E560-84, *Standard Recommended Practice for Extrapolating Reactor Vessel Surveillance Dosimetry Results*, in ASTM Standards, Section 12, American Society for Testing and Materials, Philadelphia, PA, 1991.
27. ASTM Designation E706-87, *Standard Master Matrix for Light-Water Reactor Pressure Vessel Surveillance Standard*, in ASTM Standards, Section 12, American Society for Testing and Materials, Philadelphia, PA, 1991.
28. ASTM Designation E261-90, *Standard Practice for Determining Neutron Fluence Rate, Fluence, and Spectra by Radioactivation Techniques*, in ASTM Standards, Section 12, American Society for Testing and Materials, Philadelphia, PA, 1991.
29. ASTM Designation E262-86, *Standard Method for Determining Thermal Neutron Reaction and Fluence Rates by Radioactivation Techniques*, in ASTM Standards, Section 12, American Society for Testing and Materials, Philadelphia, PA, 1991.
30. ASTM Designation E263-88, *Standard Method for Measuring Fast-Neutron Reaction Rates by Radioactivation of Iron*, in ASTM Standards, Section 12, American Society for Testing and Materials, Philadelphia, PA, 1991.
31. ASTM Designation E264-87, *Standard Method for Measuring Fast-Neutron Reaction Rates by Radioactivation of Nickel*, in ASTM Standards, Section 12, American Society for Testing and Materials, Philadelphia, PA, 1991.
32. ASTM Designation E481-86, *Standard Method for Measuring Neutron Fluence Rate by Radioactivation of Cobalt and Silver*, in ASTM Standards, Section 12, American Society for Testing and Materials, Philadelphia, PA, 1991.
33. ASTM Designation E523-92, *Standard Test Method for Measuring Fast-Neutron Reaction Rate by Radioactivation of Copper*, in ASTM Standards, Section 12, American Society for Testing and Materials, Philadelphia, PA, 1993.
34. ASTM Designation E704-90, *Standard Test Method for Measuring Reaction Rates by Radioactivation of Uranium-238*, in ASTM Standards, Section 12, American Society for Testing and Materials, Philadelphia, PA, 1991.
35. ASTM Designation E705-90, *Standard Test Method for Measuring Reaction Rates by Radioactivation of Neptunium-237*, in ASTM Standards, Section 12, American Society for Testing and Materials, Philadelphia, PA, 1991.
36. ASTM Designation E1005-84, *Standard Test Method for Application and Analysis of Radiometric Monitors for Reactor Vessel Surveillance*, in ASTM Standards, Section 12, American Society for Testing and Materials, Philadelphia, PA, 1991.

37. F. A. Schmittroth, *FERRET Data Analysis Code*, HEDL-TME 79-40, Hanford Engineering Development Laboratory, Richland, WA, September 1979.
38. W. N. McElroy, S. Berg and T. Crocket, *A Computer-Automated Iterative Method of Neutron Flux Spectra Determined by Foil Activation*, AFWL-TR-7-41, Vol. I-IV, Air Force Weapons Laboratory, Kirkland AFB, NM, July 1967.
39. ORNL RSIC Data Library Collection DLC-178, "SNLRML Recommended Dosimetry Cross-Section Compendium," July 1994.
40. EPRI-NP-2188, *Development and Demonstration of an Advanced Methodology for LWR Dosimetry Applications*, R. E. Maerker, et al., 1981

**APPENDIX A**  
**LOAD-TIME RECORDS FOR CHARPY SPECIMEN TESTS**

A-1

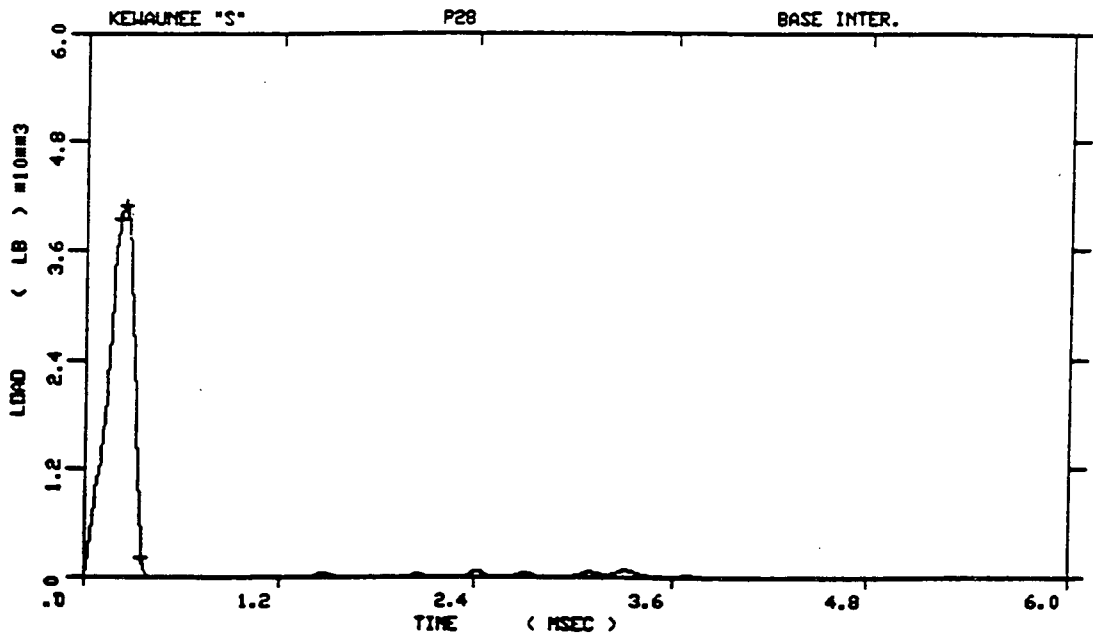


$W_I$  = Fracture Initiation Region  
 $W_P$  = Fracture Propagation Region

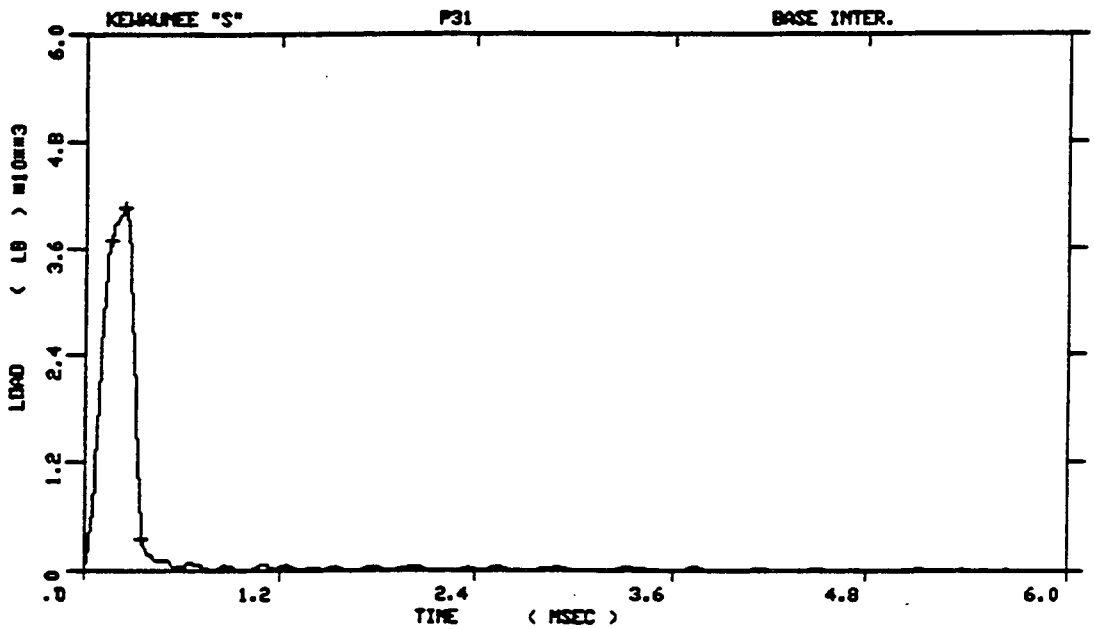
$t_{GY}$  = Time to General Yielding  
 $t_M$  = Time to Maximum Load  
 $t_F$  = Time to Fast (Brittle) Fracture Start

Fig. A-1-Idealized load-time record



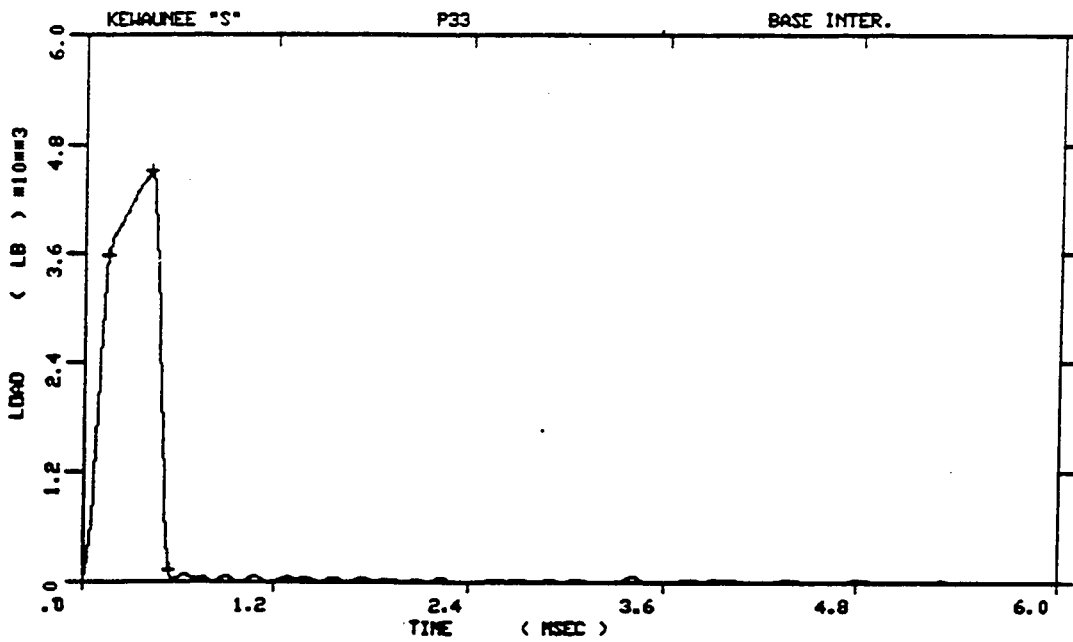


KEWAUNEE "S"  
 SPECIMEN NUMBER : P28  
 MATERIAL : BASE INTER.  
 CAPSULE : KEWAUNEE "S"

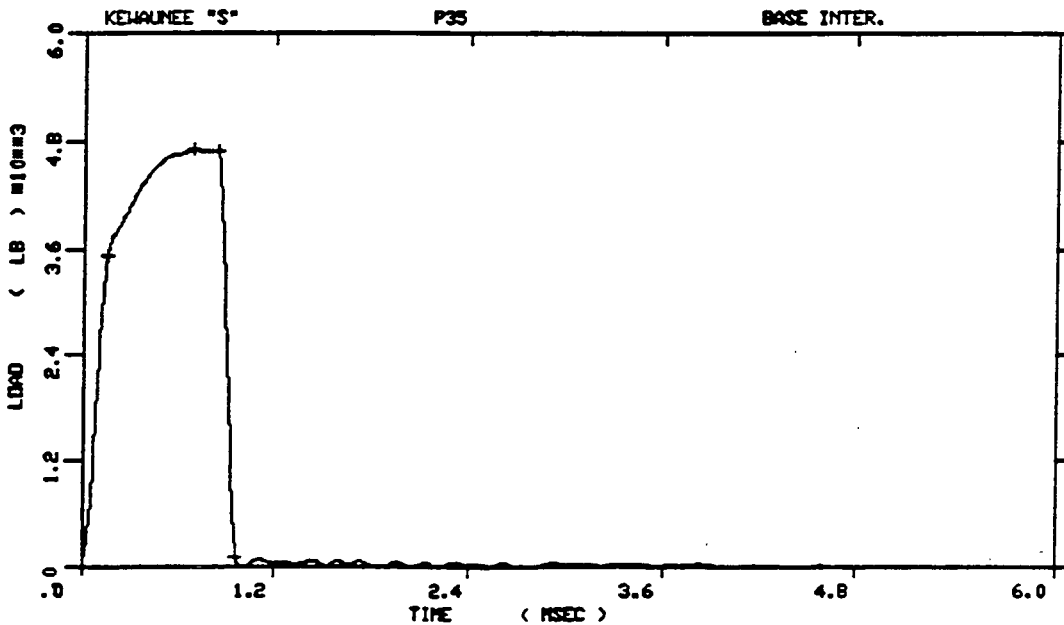


KEWAUNEE "S"  
 SPECIMEN NUMBER : P31  
 MATERIAL : BASE INTER.  
 CAPSULE : KEWAUNEE "S"

Figure A-2. Load-time records for Specimens P28 and P31.

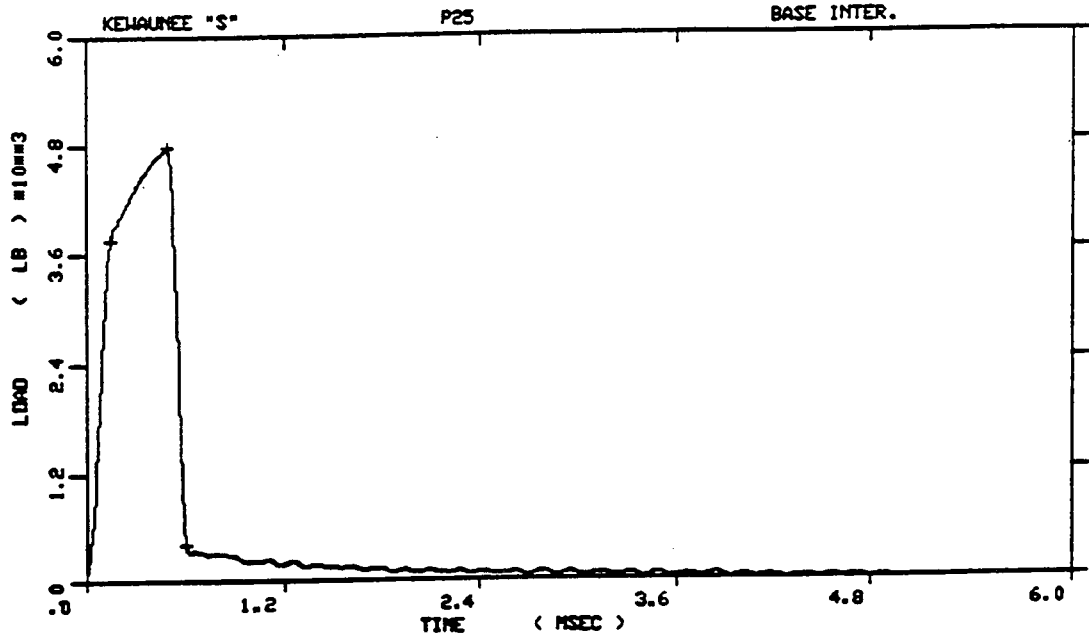


KEWAUNEE "S"  
 SPECIMEN NUMBER : P33  
 MATERIAL : BASE INTER.  
 CAPSULE : KEWAUNEE "S"

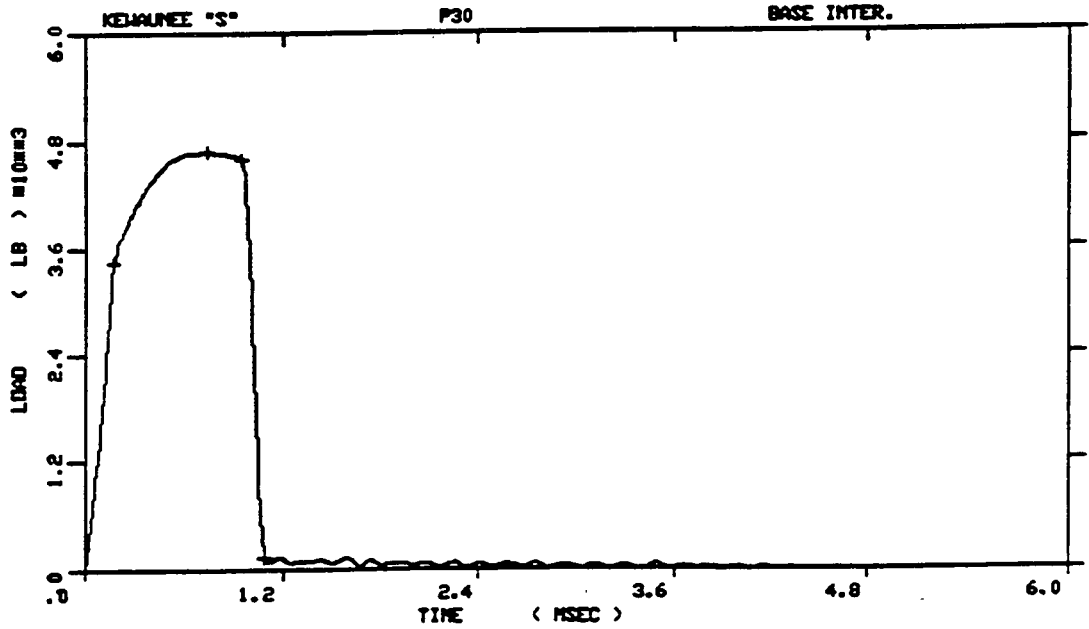


KEWAUNEE "S"  
 SPECIMEN NUMBER : P35  
 MATERIAL : BASE INTER.  
 CAPSULE : KEWAUNEE "S"

Figure A-3. Load-time records for Specimens P33 and P35.

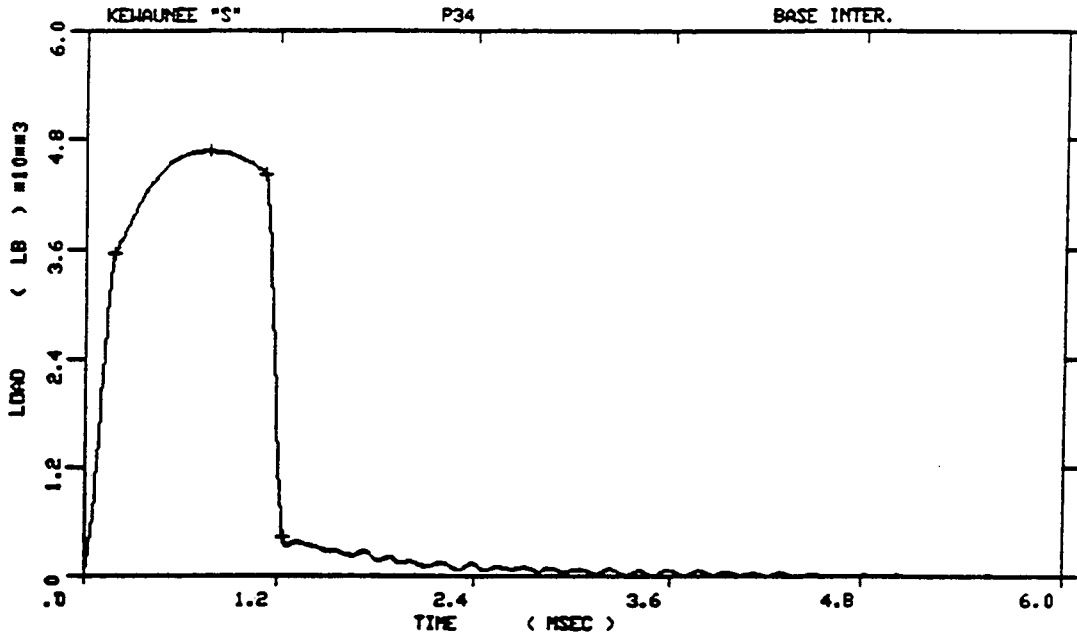


KEWAUNEE "S"  
 SPECIMEN NUMBER : P25  
 MATERIAL : BASE INTER.  
 CAPSULE : KEWAUNEE "S"

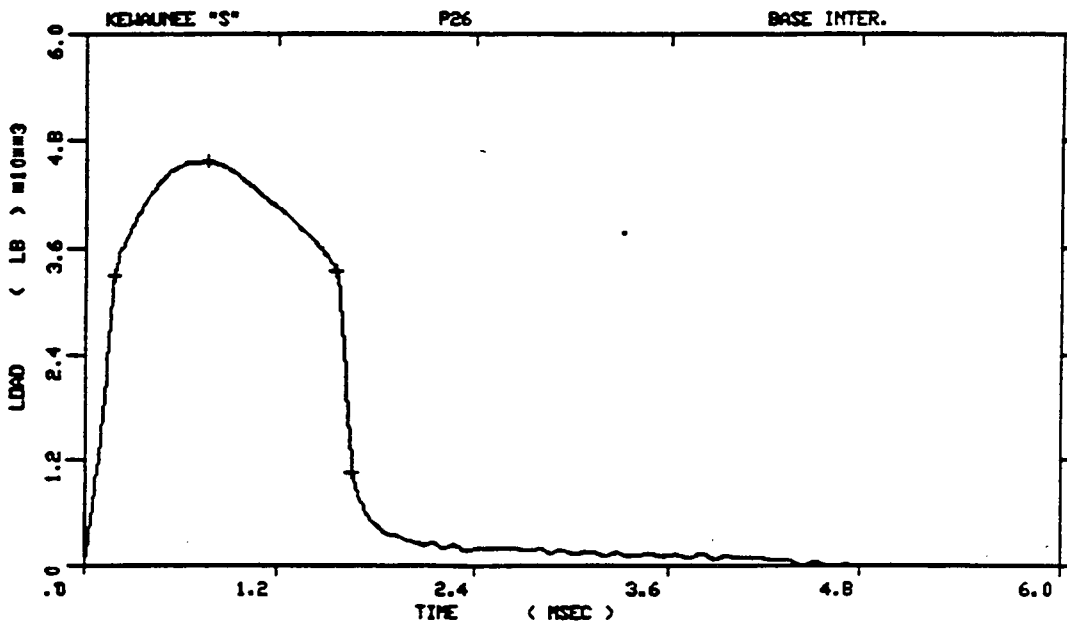


KEWAUNEE "S"  
 SPECIMEN NUMBER : P30  
 MATERIAL : BASE INTER.  
 CAPSULE : KEWAUNEE "S"

Figure A-4. Load-time records for Specimens P25 and P30.

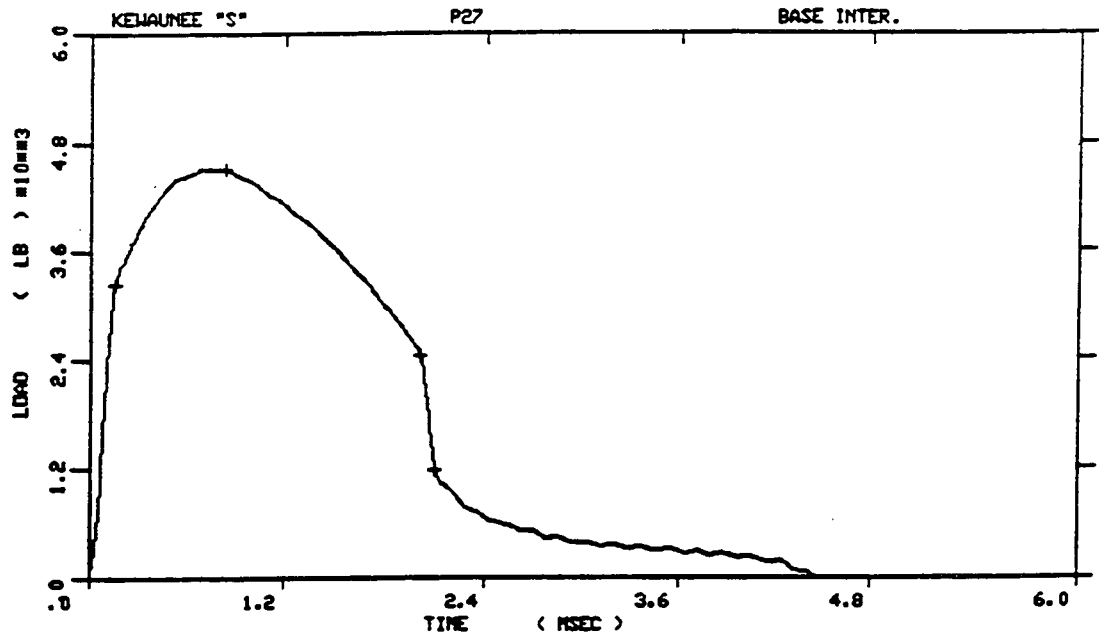


KEWAUNEE "S"  
 SPECIMEN NUMBER : P34  
 MATERIAL : BASE INTER.  
 CAPSULE : KEWAUNEE "S"

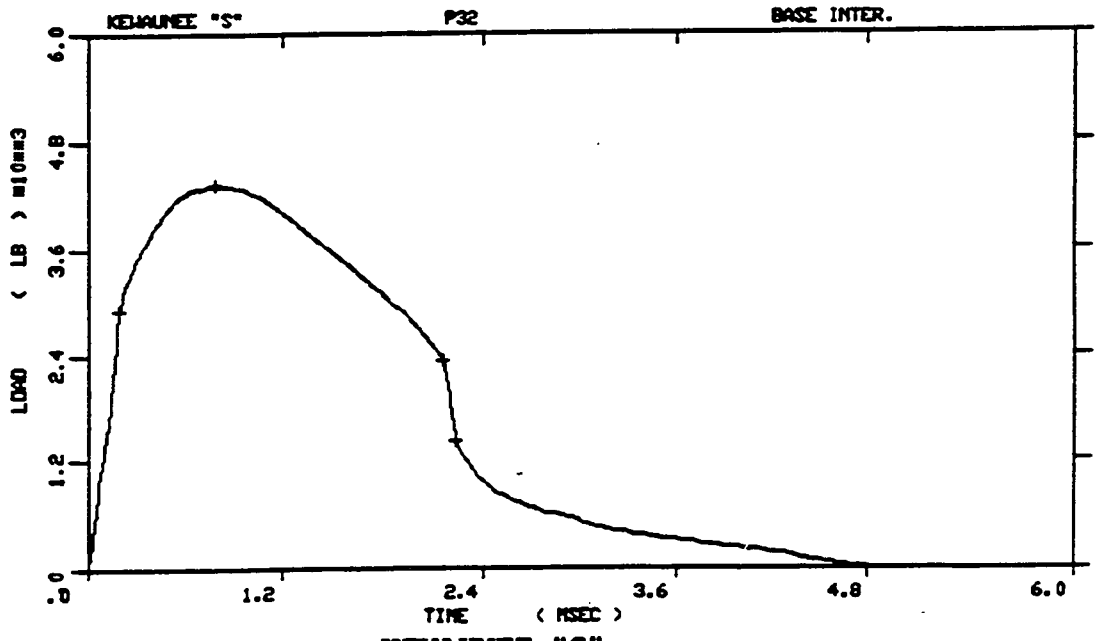


KEWAUNEE "S"  
 SPECIMEN NUMBER : P26  
 MATERIAL : BASE INTER.  
 CAPSULE : KEWAUNEE "S"

Figure A-5. Load-time records for Specimens P34 and P26.

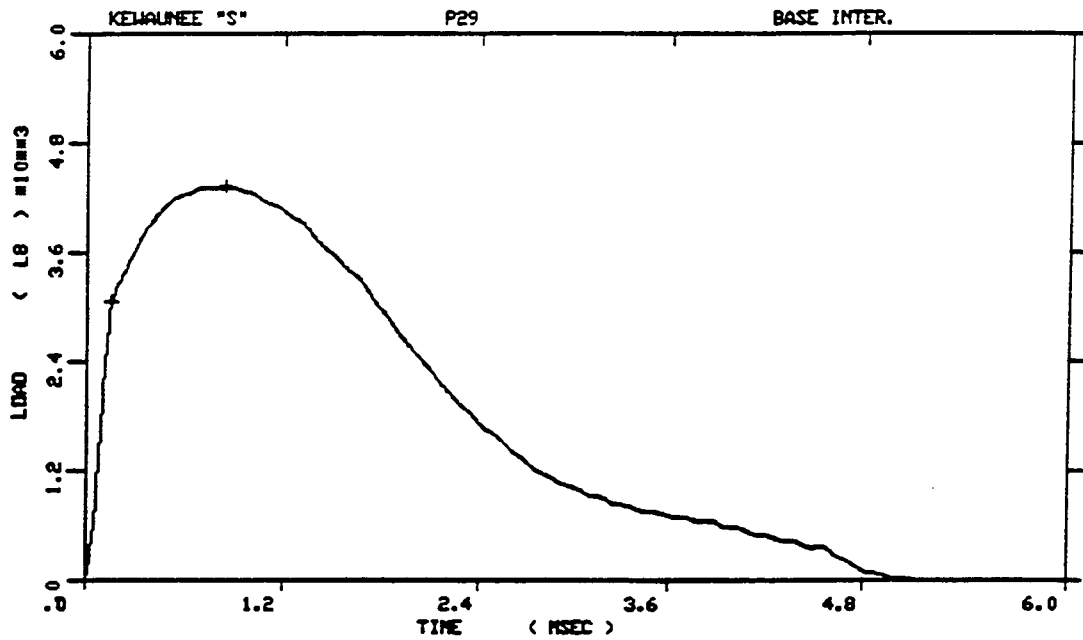


KEWAUNEE "S"  
 SPECIMEN NUMBER : P27  
 MATERIAL : BASE INTER.  
 CAPSULE : KEWAUNEE "S"

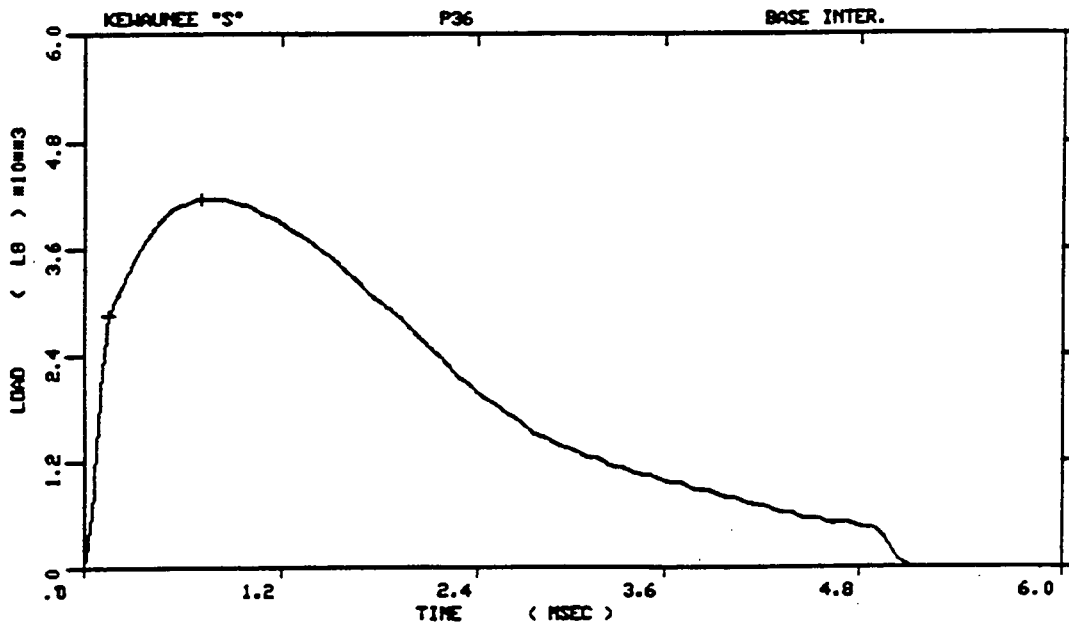


KEWAUNEE "S"  
 SPECIMEN NUMBER : P32  
 MATERIAL : BASE INTER.  
 CAPSULE : KEWAUNEE "S"

Figure A-6. Load-time records for Specimens P27 and P32.

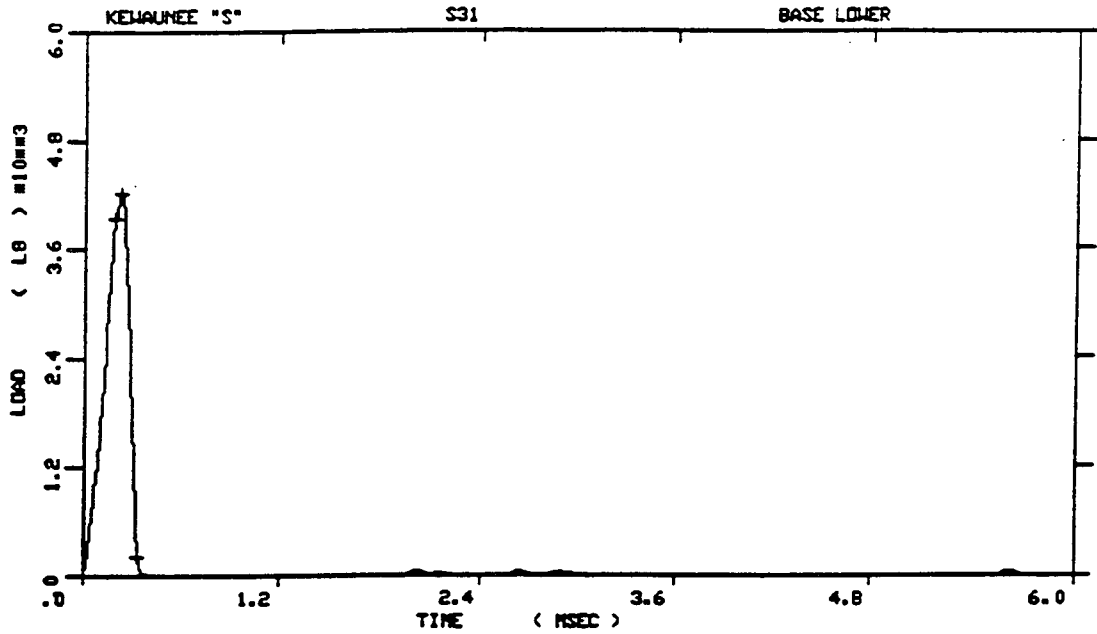


KEWAUNEE "S"  
 SPECIMEN NUMBER : P29  
 MATERIAL : BASE INTER.  
 CAPSULE : KEWAUNEE "S"

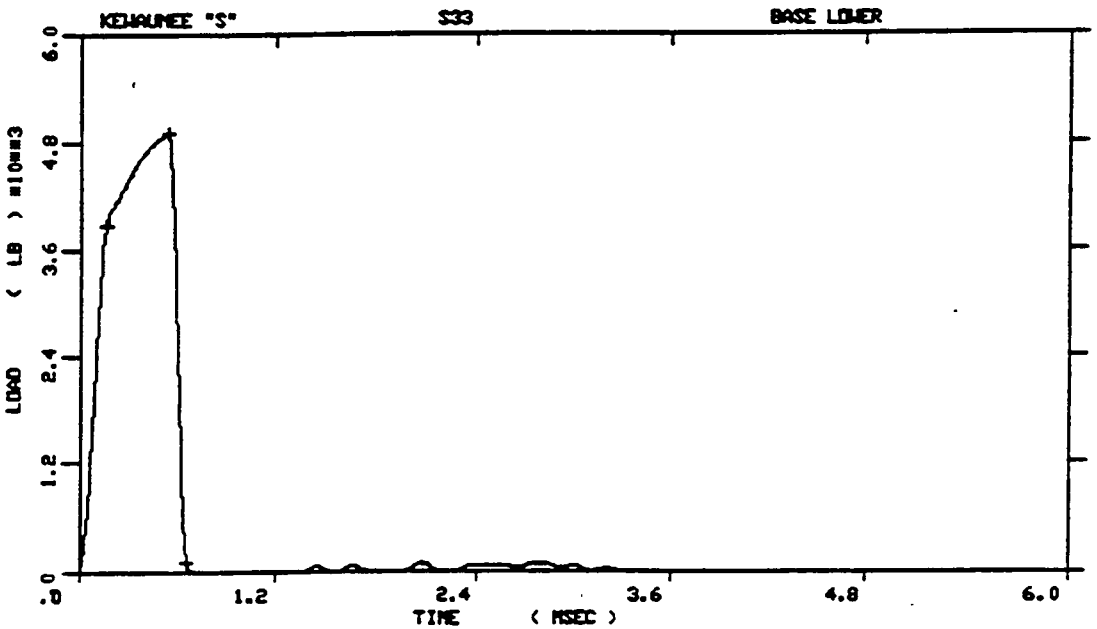


KEWAUNEE "S"  
 SPECIMEN NUMBER : P36  
 MATERIAL : BASE INTER.  
 CAPSULE : KEWAUNEE "S"

Figure A-7. Load-time records for Specimens P29 and P36.

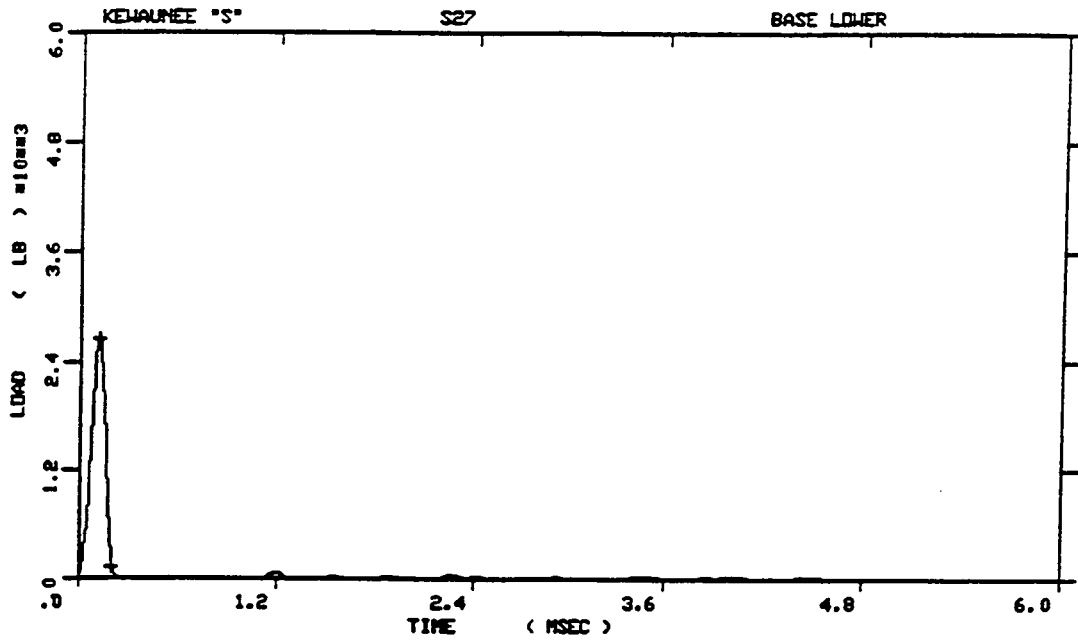


KEWAUNEE "S"  
 SPECIMEN NUMBER : S31  
 MATERIAL : BASE LOWER  
 CAPSULE : KEWAUNEE "S"

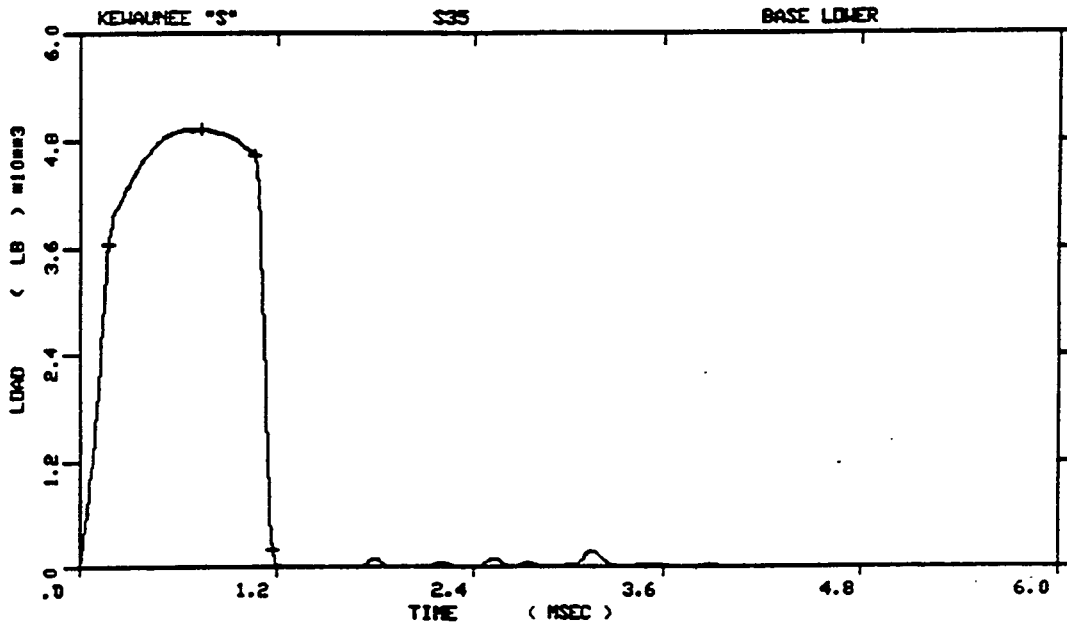


KEWAUNEE "S"  
 SPECIMEN NUMBER : S33  
 MATERIAL : BASE LOWER  
 CAPSULE : KEWAUNEE "S"

Figure A-8. Load-time records for Specimens S31 and S33.



KEWAUNEE "S"  
 SPECIMEN NUMBER : S27  
 MATERIAL : BASE LOWER  
 CAPSULE : KEWAUNEE "S"

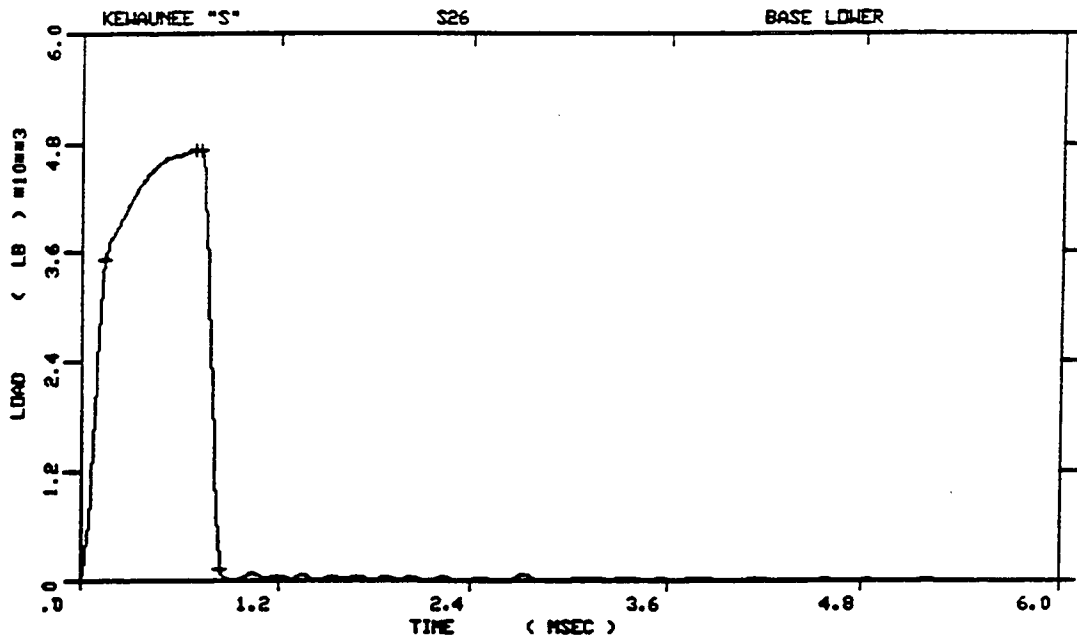


KEWAUNEE "S"  
 SPECIMEN NUMBER : S35  
 MATERIAL : BASE LOWER  
 CAPSULE : KEWAUNEE "S"

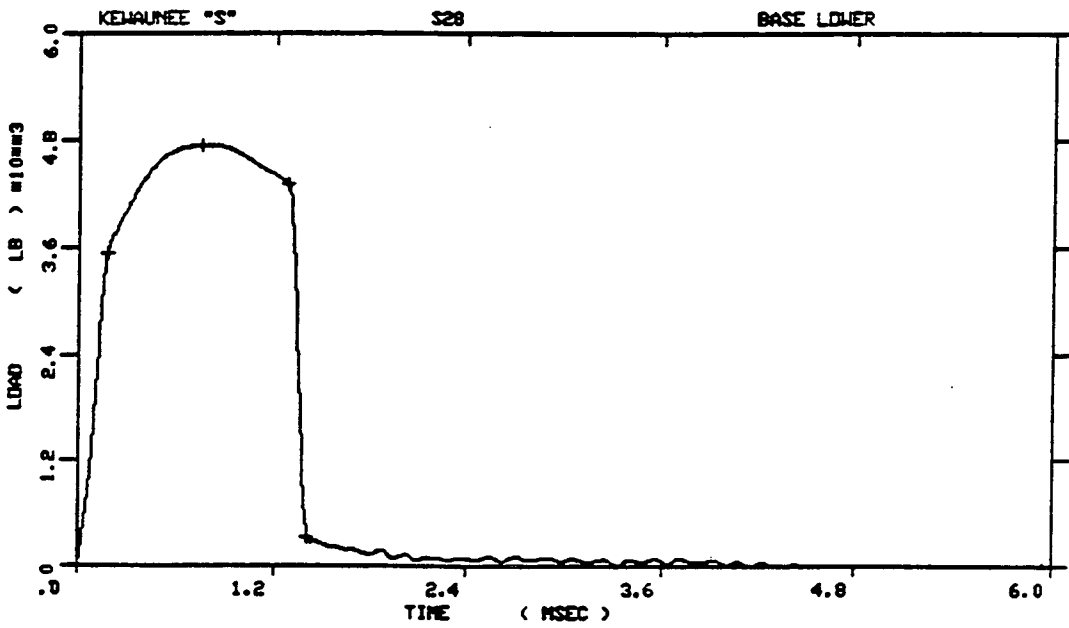
Figure A-9. Load-time records for Specimens S27 and S35.





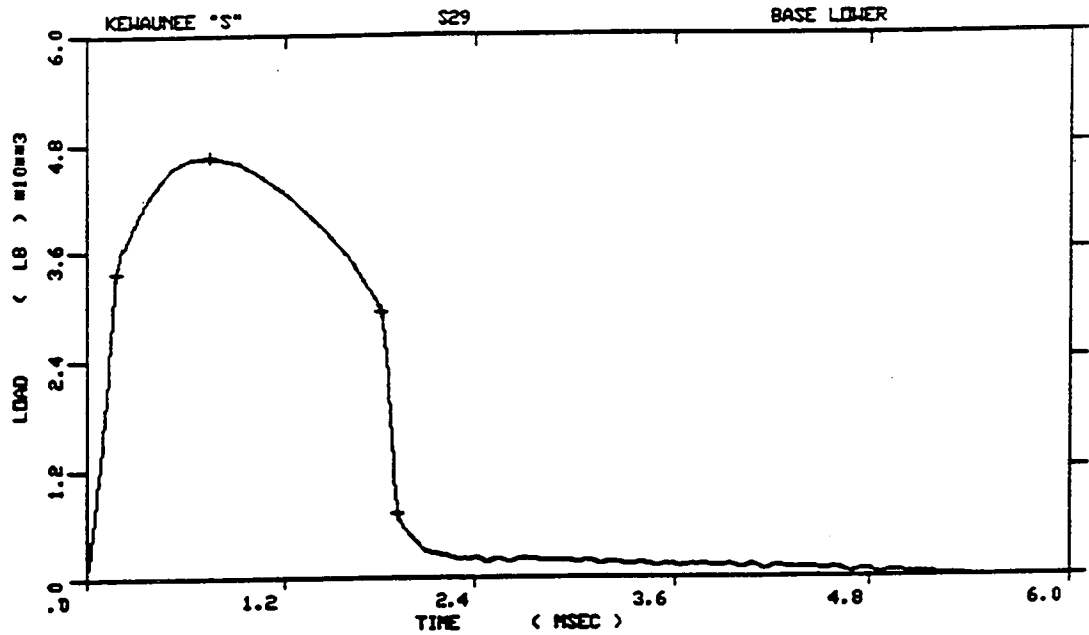


SPECIMEN NUMBER : S26  
 MATERIAL : BASE LOWER  
 CAPSULE : KEWAUNEE "S"

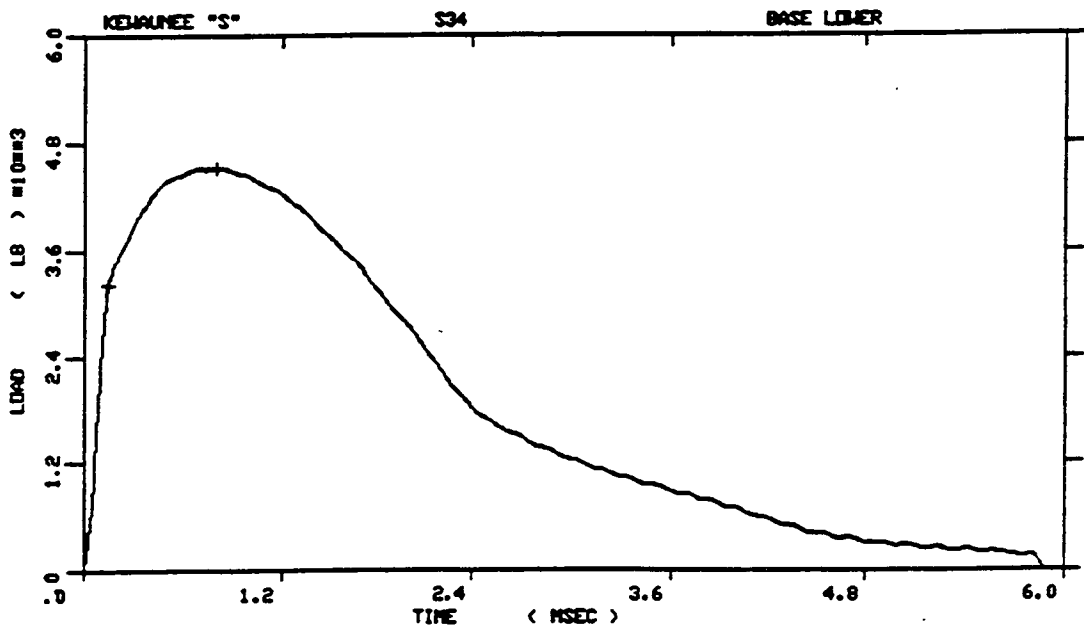


SPECIMEN NUMBER : S28  
 MATERIAL : BASE LOWER  
 CAPSULE : KEWAUNEE "S"

Figure A-11. Load-time records for Specimens S26 and S28.

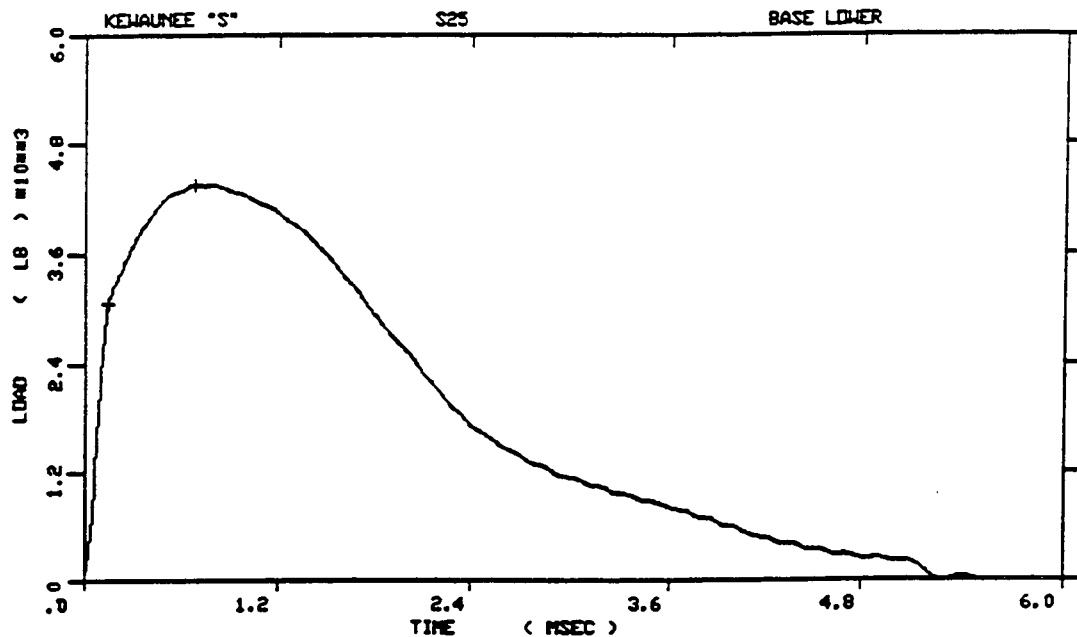


KEWAUNEE "S"  
 SPECIMEN NUMBER :S29  
 MATERIAL :BASE LOWER  
 CAPSULE :KEWAUNEE "S"

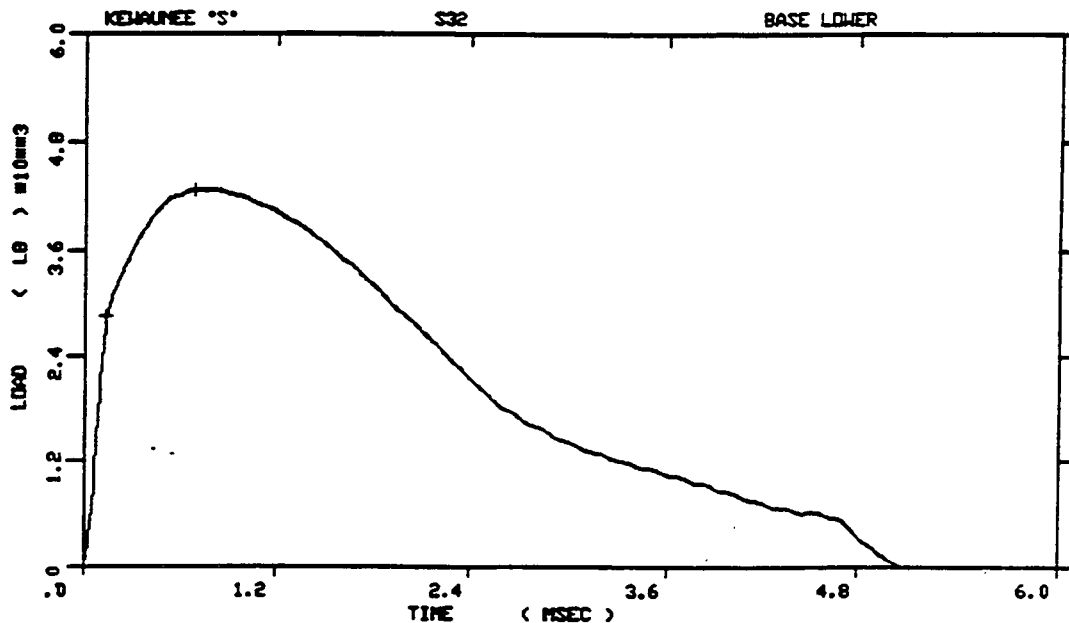


KEWAUNEE "S"  
 SPECIMEN NUMBER :S34  
 MATERIAL :BASE LOWER  
 CAPSULE :KEWAUNEE "S"

Figure A-12. Load-time records for Specimens S29 and S34.

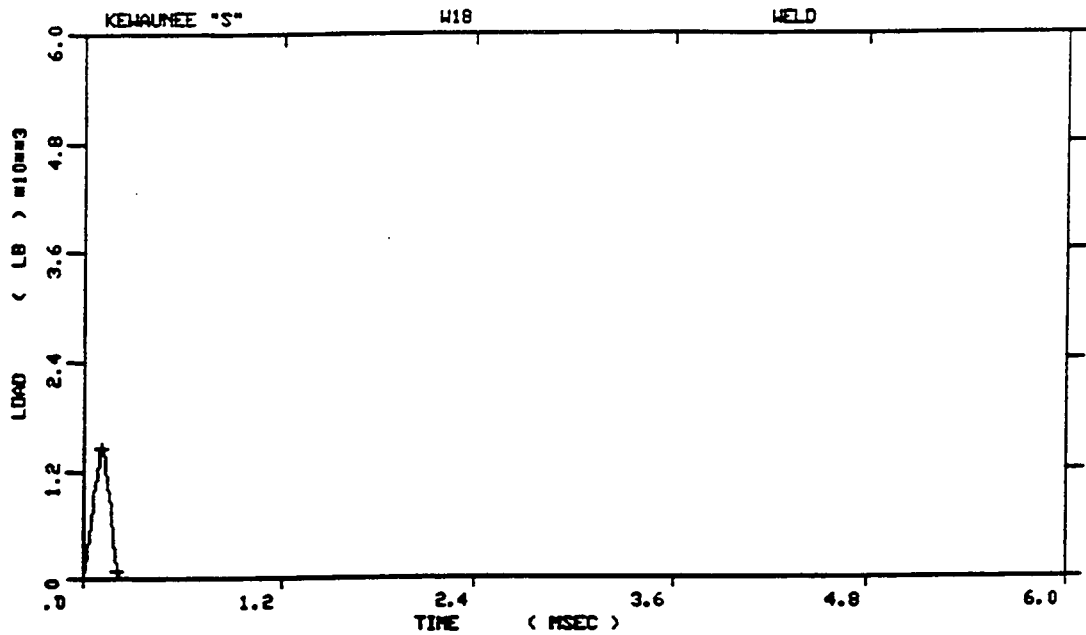


KEWAUNEE "S"  
 SPECIMEN NUMBER : S25  
 MATERIAL : BASE LOWER  
 CAPSULE : KEWAUNEE "S"

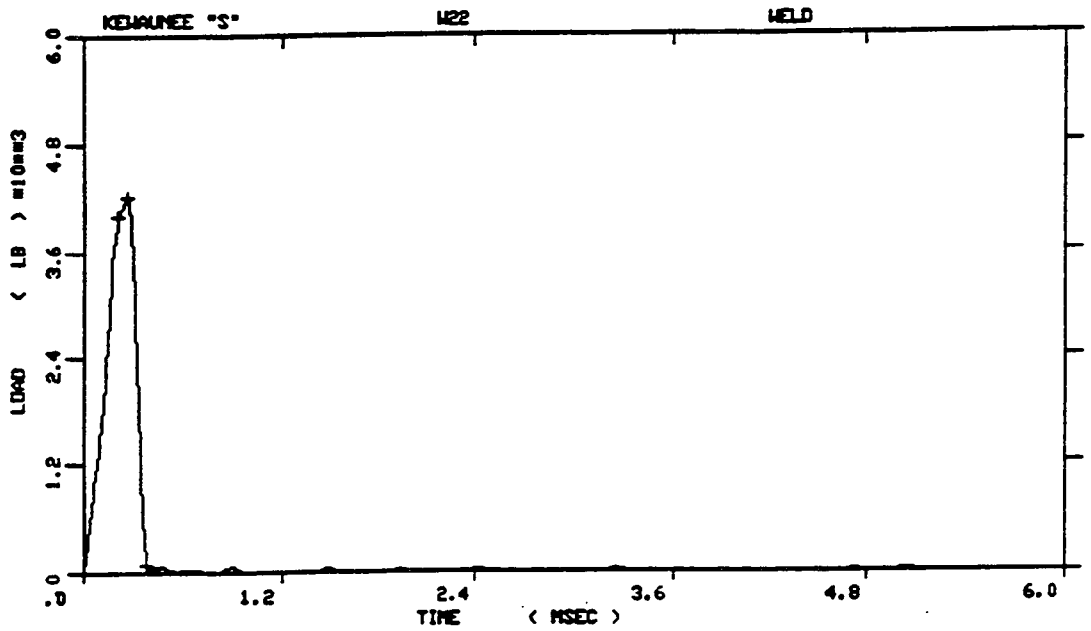


KEWAUNEE "S"  
 SPECIMEN NUMBER : S32  
 MATERIAL : BASE LOWER  
 CAPSULE : KEWAUNEE "S"

Figure A-13. Load-time records for Specimens S25 and S32.

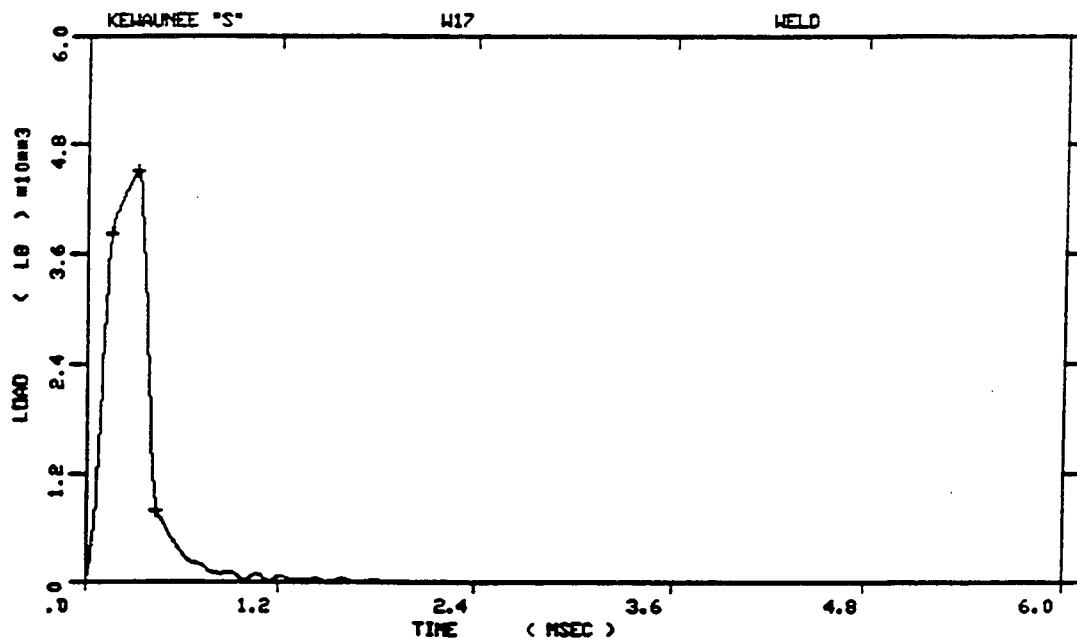


KEWAUNEE "S"  
 SPECIMEN NUMBER : W18  
 MATERIAL : WELD  
 CAPSULE : KEWAUNEE "S"

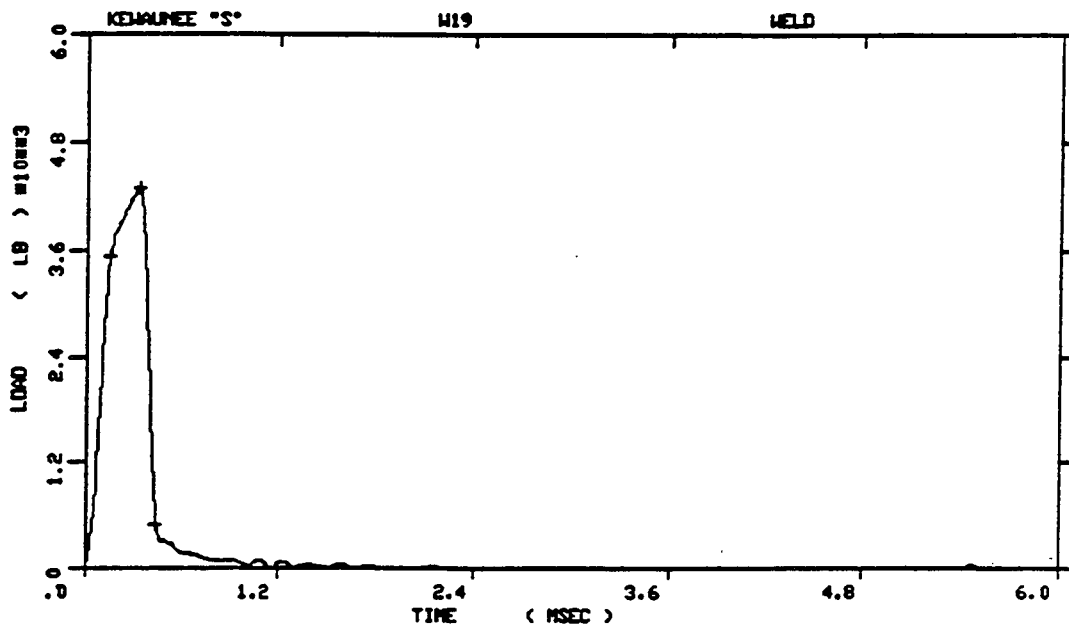


KEWAUNEE "S"  
 SPECIMEN NUMBER : W22  
 MATERIAL : WELD  
 CAPSULE : KEWAUNEE "S"

Figure A-14. Load-time records for Specimens W18 and W22.

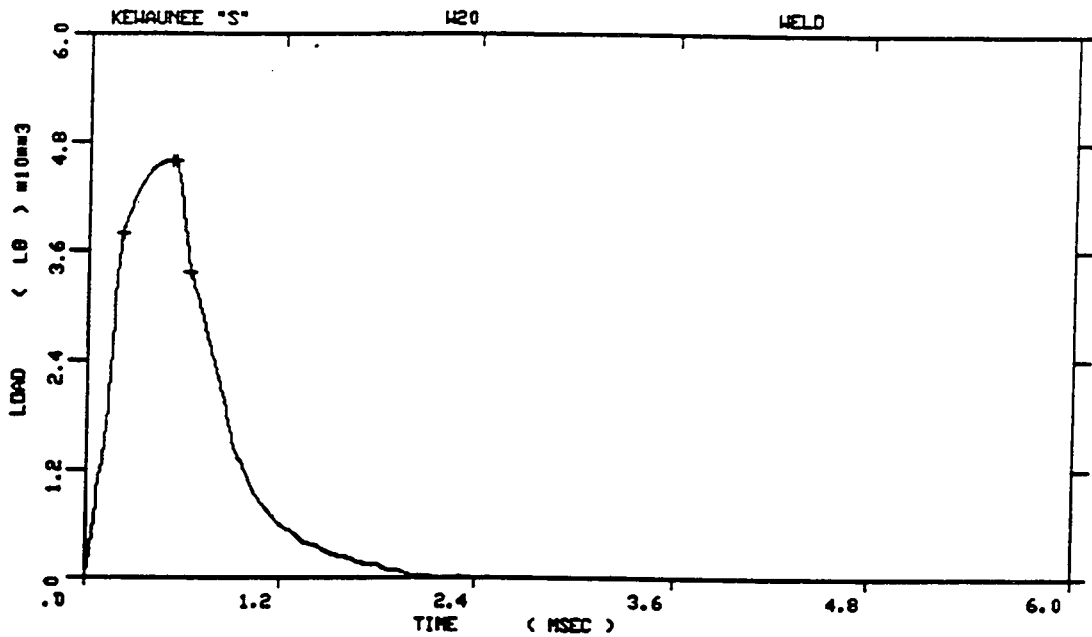


KEWAUNEE "S"  
 SPECIMEN NUMBER : W17  
 MATERIAL : WELD  
 CAPSULE : KEWAUNEE "S"

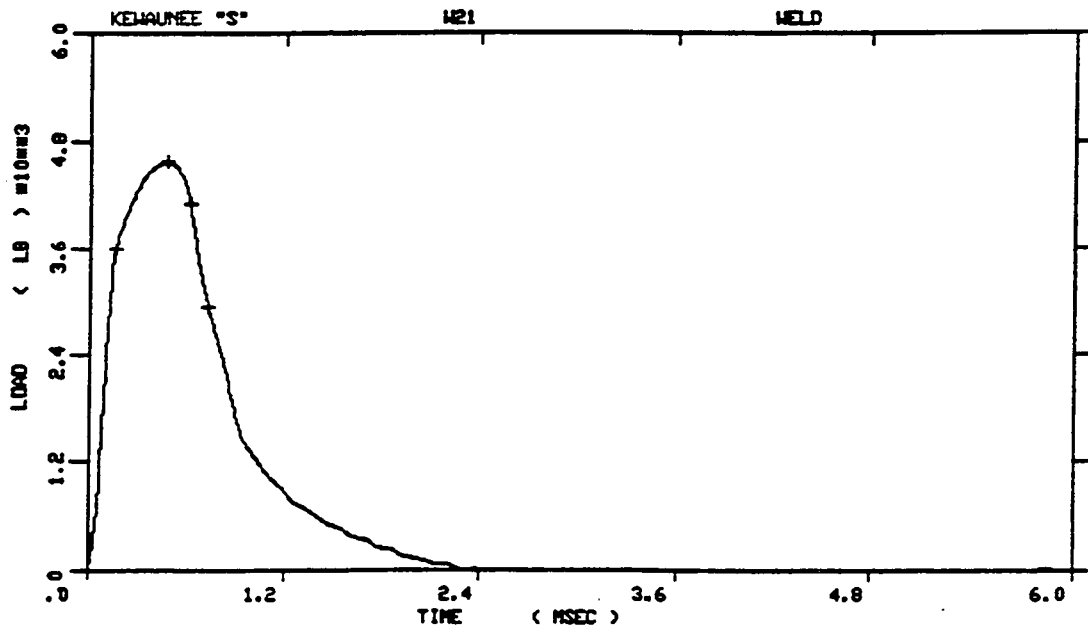


KEWAUNEE "S"  
 SPECIMEN NUMBER : W19  
 MATERIAL : WELD  
 CAPSULE : KEWAUNEE "S"

Figure A-15. Load-time records for Specimens W17 and W19.

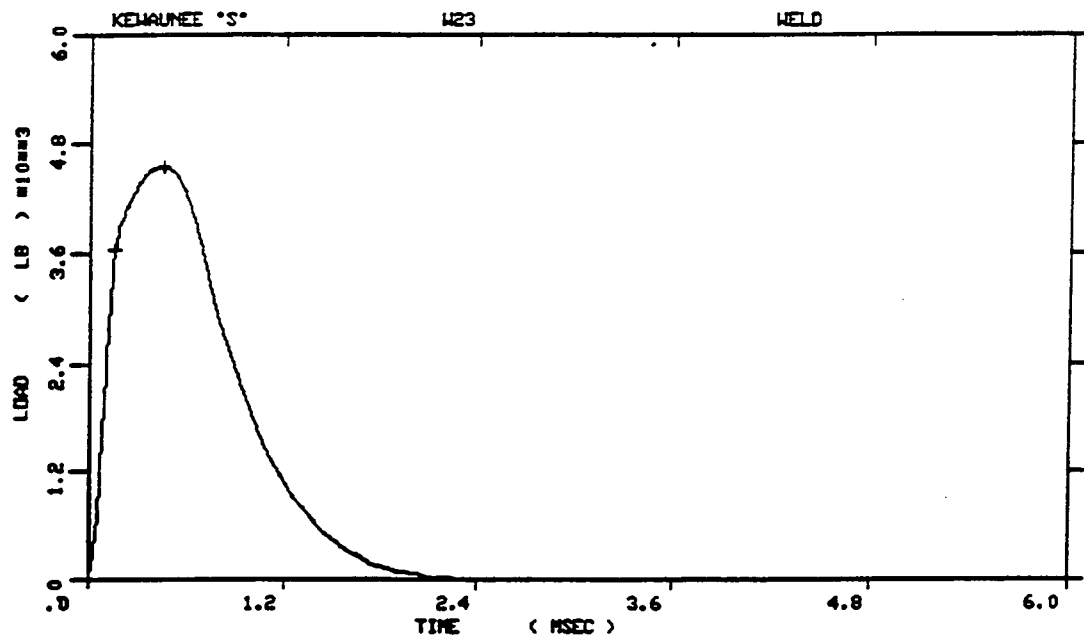


KEWAUNEE "S"  
 SPECIMEN NUMBER : W20  
 MATERIAL : WELD  
 CAPSULE : KEWAUNEE "S"

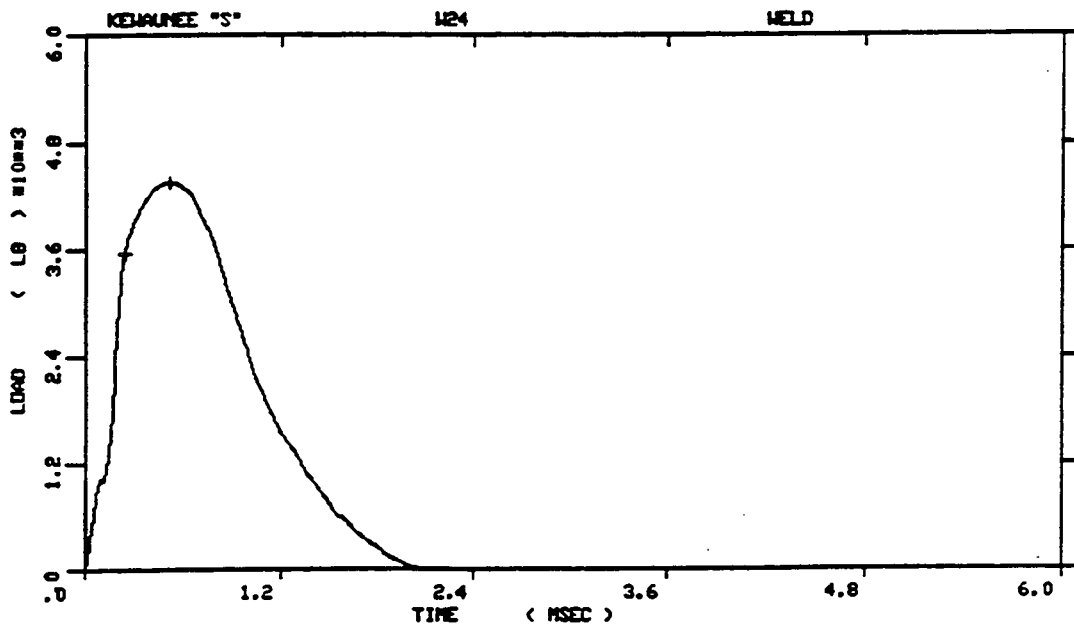


KEWAUNEE "S"  
 SPECIMEN NUMBER : W21  
 MATERIAL : WELD  
 CAPSULE : KEWAUNEE "S"

Figure A-16. Load-time records for Specimens W20 and W21.



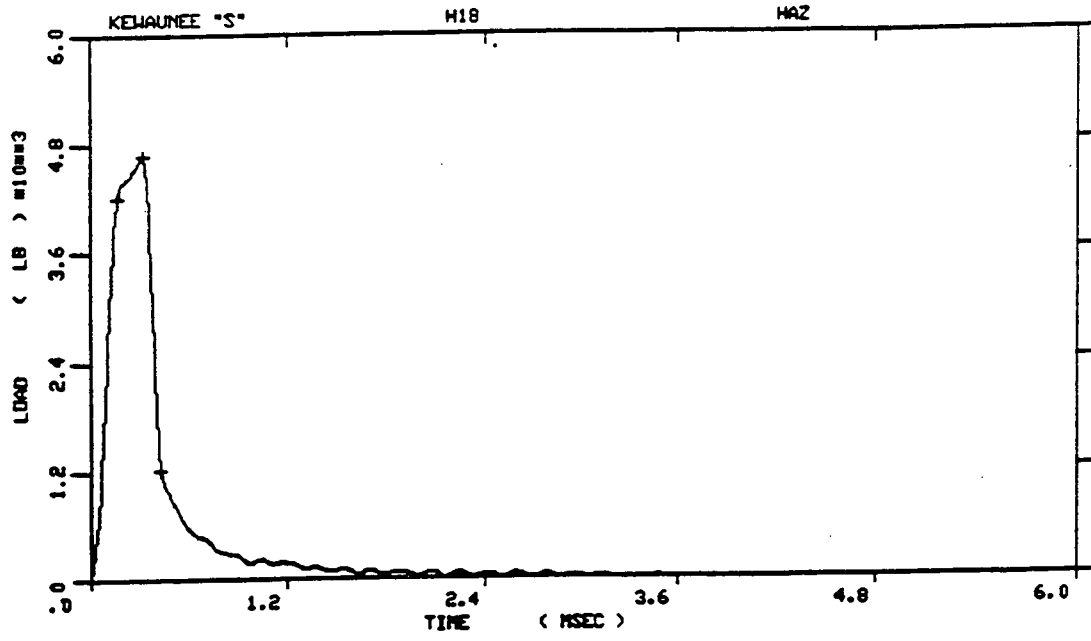
KEWAUNEE "S"  
 SPECIMEN NUMBER :W23  
 MATERIAL :WELD  
 CAPSULE :KEWAUNEE "S"



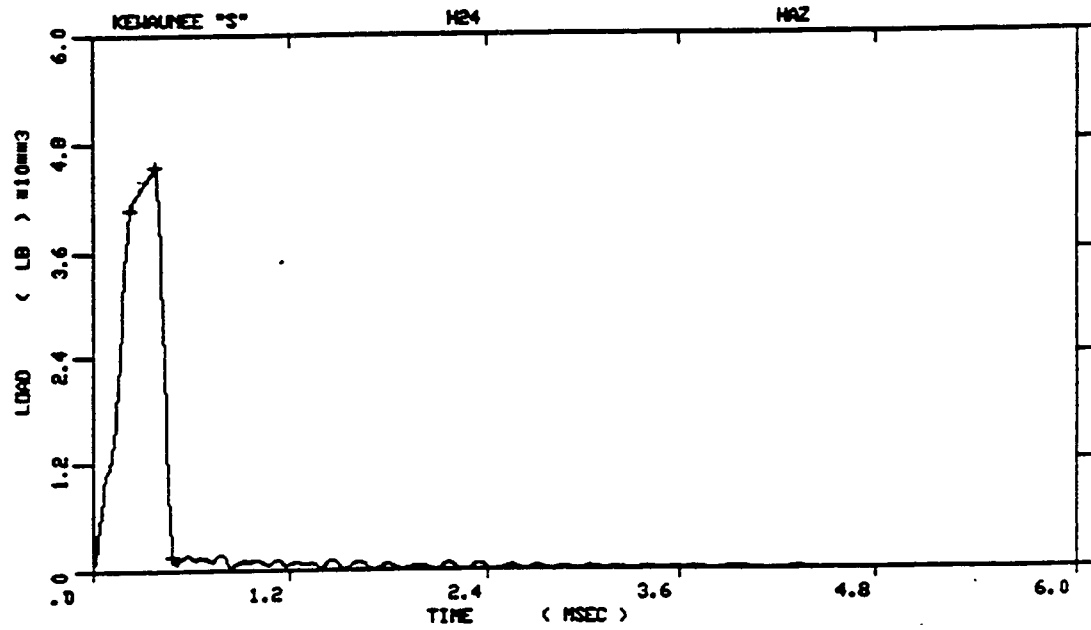
KEWAUNEE "S"  
 SPECIMEN NUMBER :W24  
 MATERIAL :WELD  
 CAPSULE :KEWAUNEE "S"

Figure A-17. Load-time records for Specimens W23 and W24.



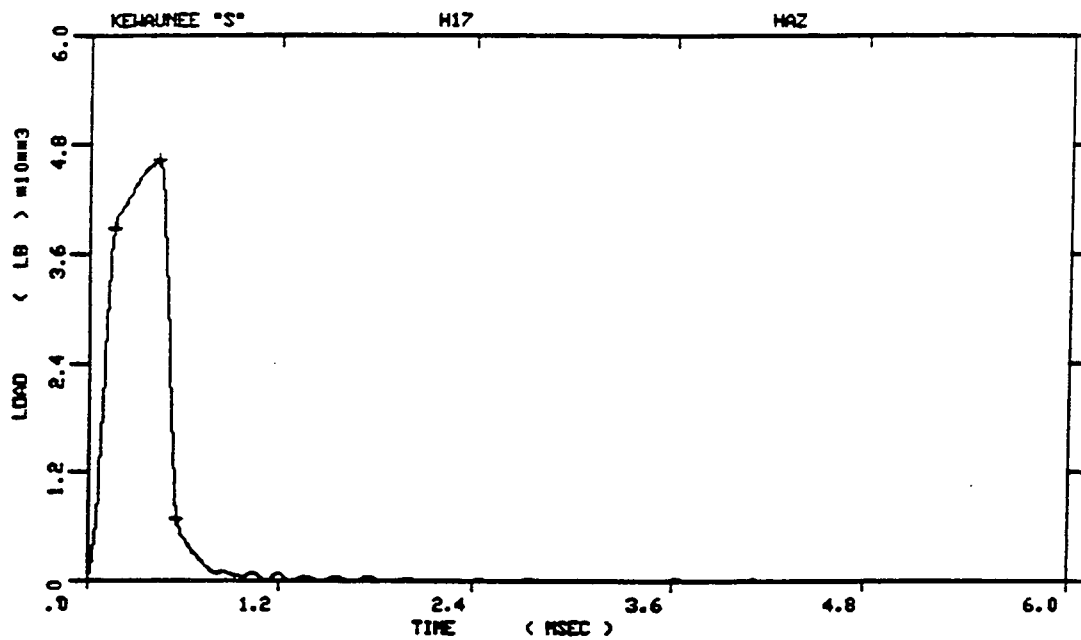


KEWAUNEE "S"  
 SPECIMEN NUMBER :H18  
 MATERIAL :HAZ  
 CAPSULE :KEWAUNEE "S"

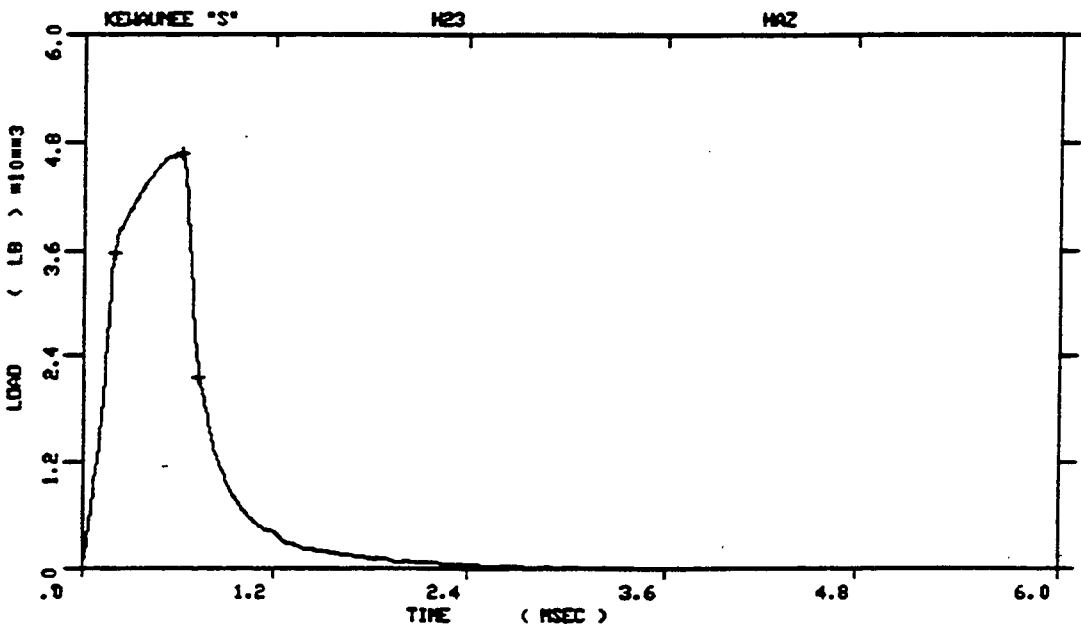


KEWAUNEE "S"  
 SPECIMEN NUMBER :H24  
 MATERIAL :HAZ  
 CAPSULE :KEWAUNEE "S"

Figure A-18. Load-time records for Specimens H18 and H24.

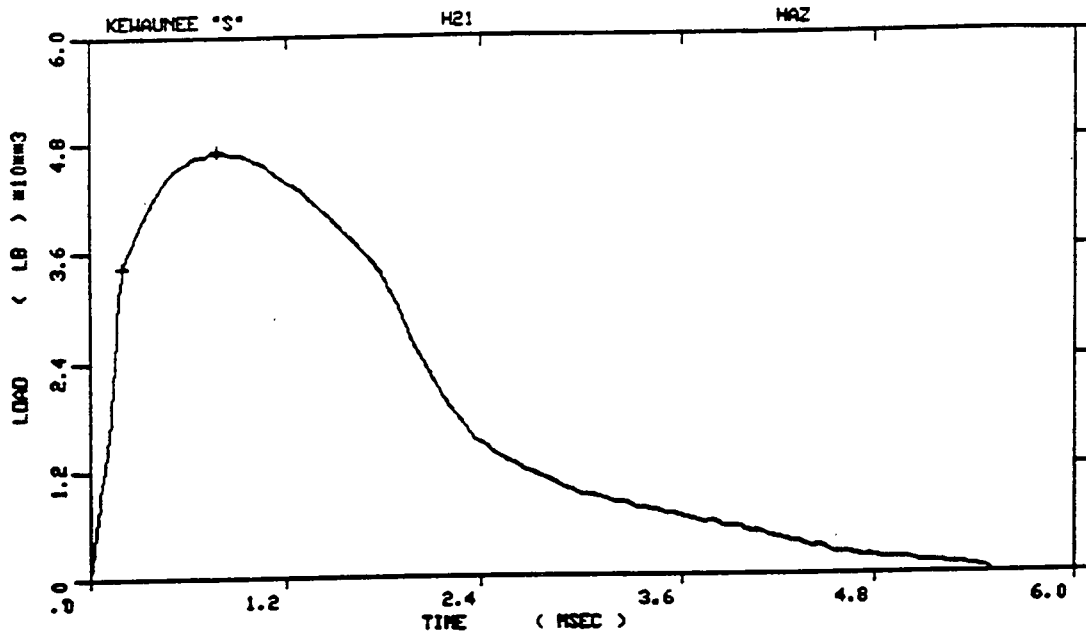


KEWAUNEE "S"  
 SPECIMEN NUMBER : H17  
 MATERIAL : HAZ  
 CAPSULE : KEWAUNEE "S"

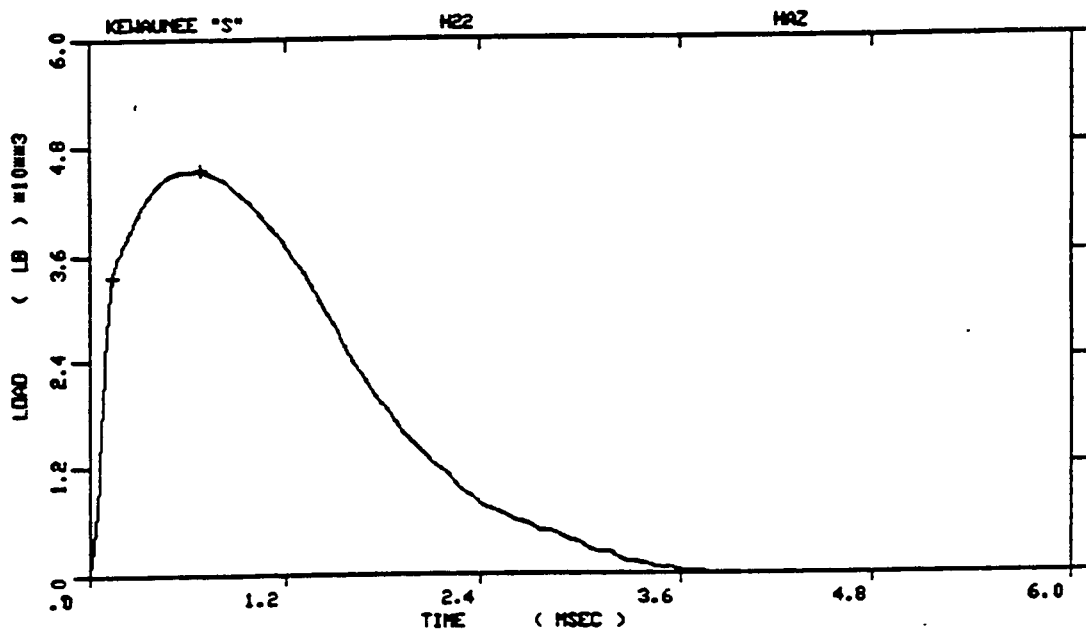


KEWAUNEE "S"  
 SPECIMEN NUMBER : H23  
 MATERIAL : HAZ  
 CAPSULE : KEWAUNEE "S"

Figure A-19. Load-time records for Specimens H17 and H23.

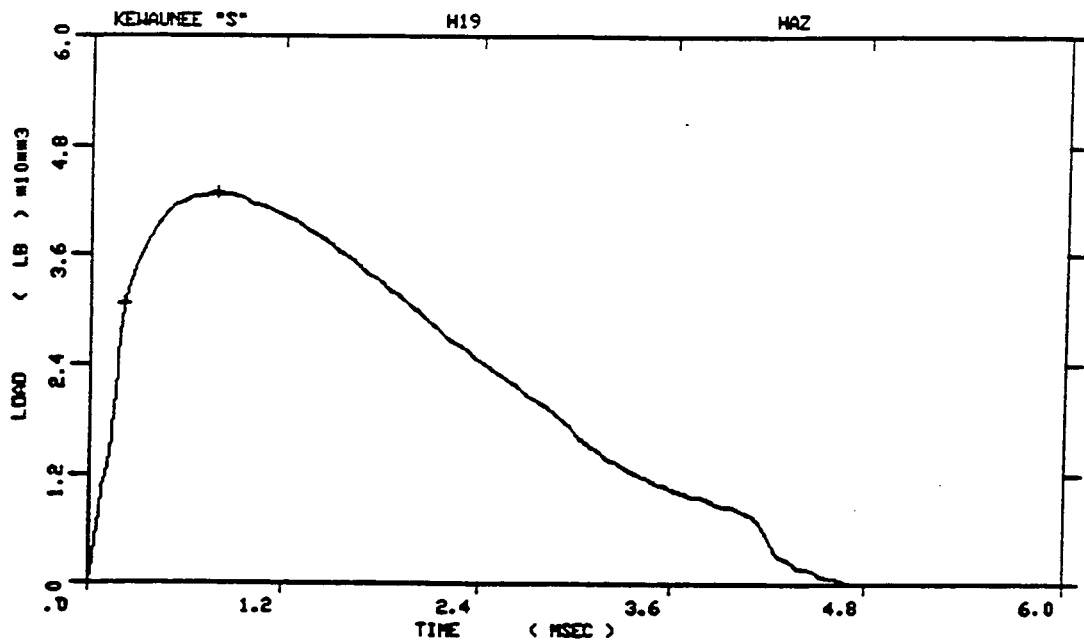


KEWAUNEE "S"  
 SPECIMEN NUMBER : H21  
 MATERIAL : HAZ  
 CAPSULE : KEWAUNEE "S"

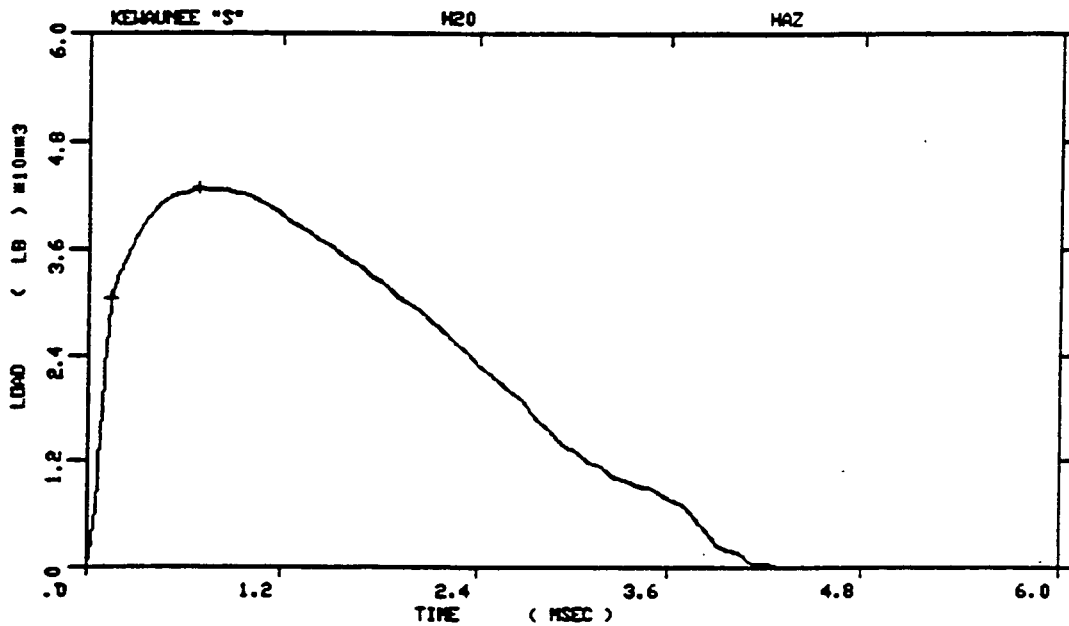


KEWAUNEE "S"  
 SPECIMEN NUMBER : H22  
 MATERIAL : HAZ  
 CAPSULE : KEWAUNEE "S"

Figure A-20. Load-time records for Specimens H21 and H22.

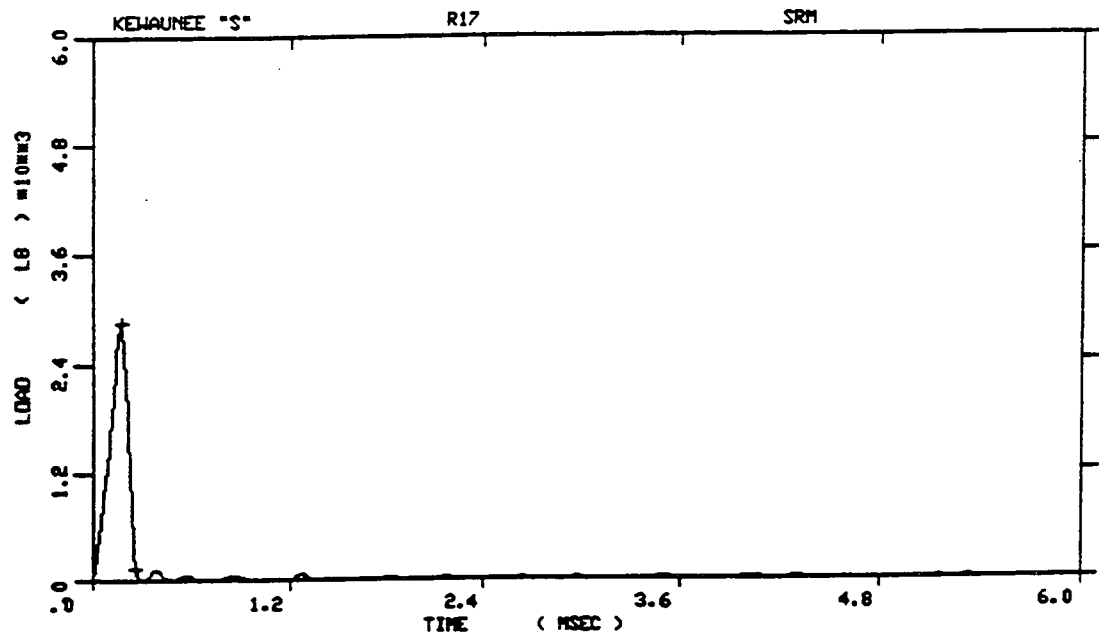


KEWAUNEE "S"  
 SPECIMEN NUMBER : H19  
 MATERIAL : HAZ  
 CAPSULE : KEWAUNEE "S"

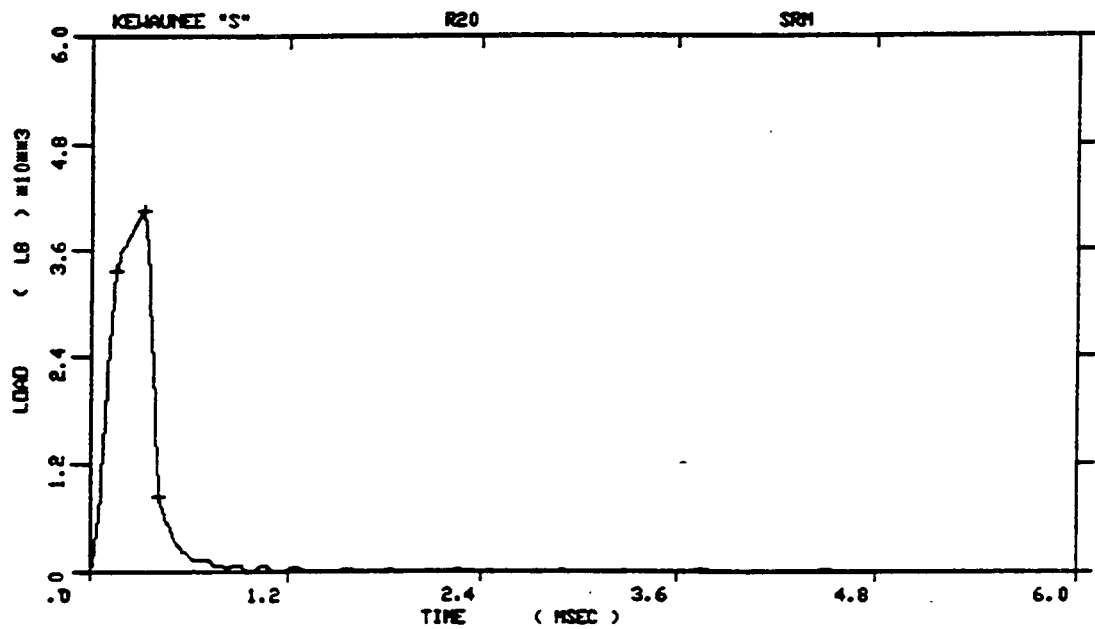


KEWAUNEE "S"  
 SPECIMEN NUMBER : H20  
 MATERIAL : HAZ  
 CAPSULE : KEWAUNEE "S"

Figure A-21. Load-time records for Specimens H19 and H20.

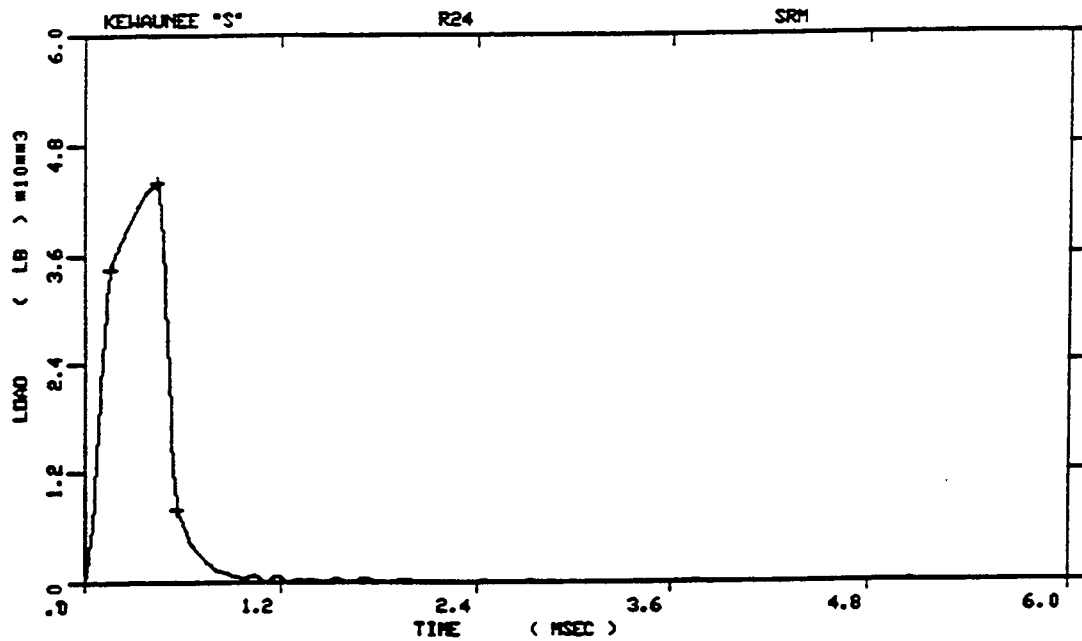


KEWAUNEE "S"  
 SPECIMEN NUMBER :R17  
 MATERIAL :SRM  
 CAPSULE :KEWAUNEE "S"

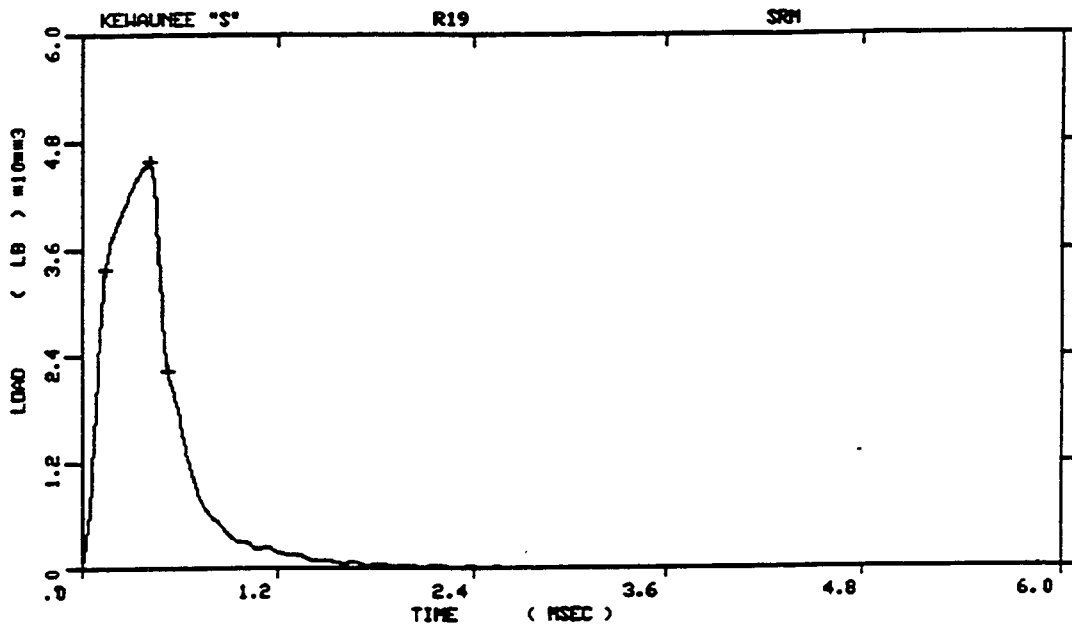


KEWAUNEE "S"  
 SPECIMEN NUMBER :R20  
 MATERIAL :SRM  
 CAPSULE :KEWAUNEE "S"

Figure A-22. Load-time records for Specimens R17 and R20.

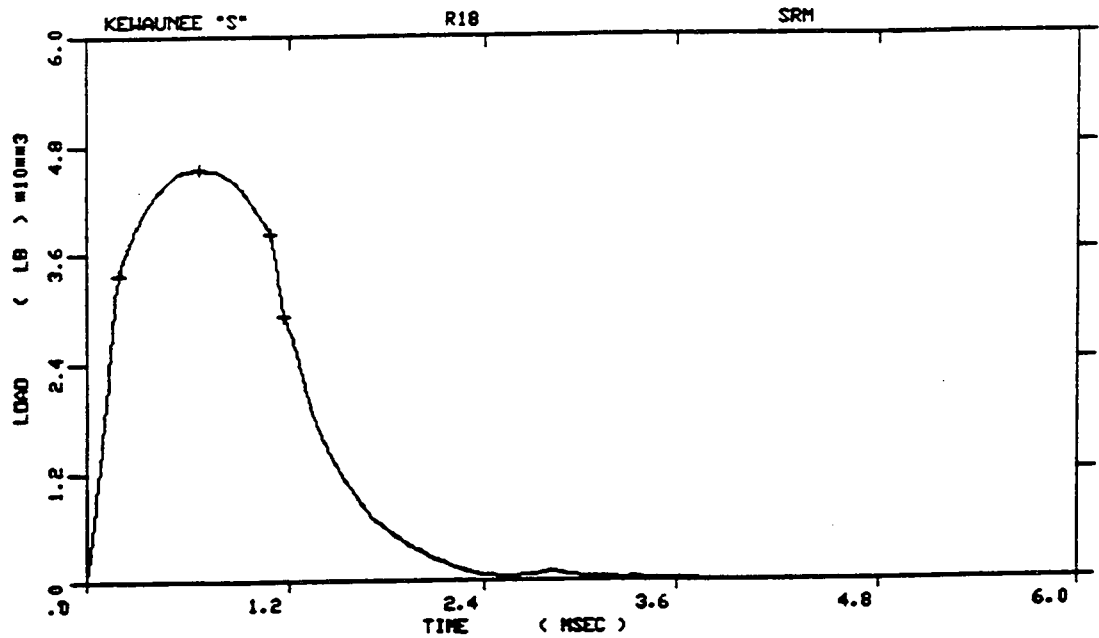


KEWAUNEE "S"  
 SPECIMEN NUMBER :R24  
 MATERIAL :SRM  
 CAPSULE :KEWAUNEE "S"

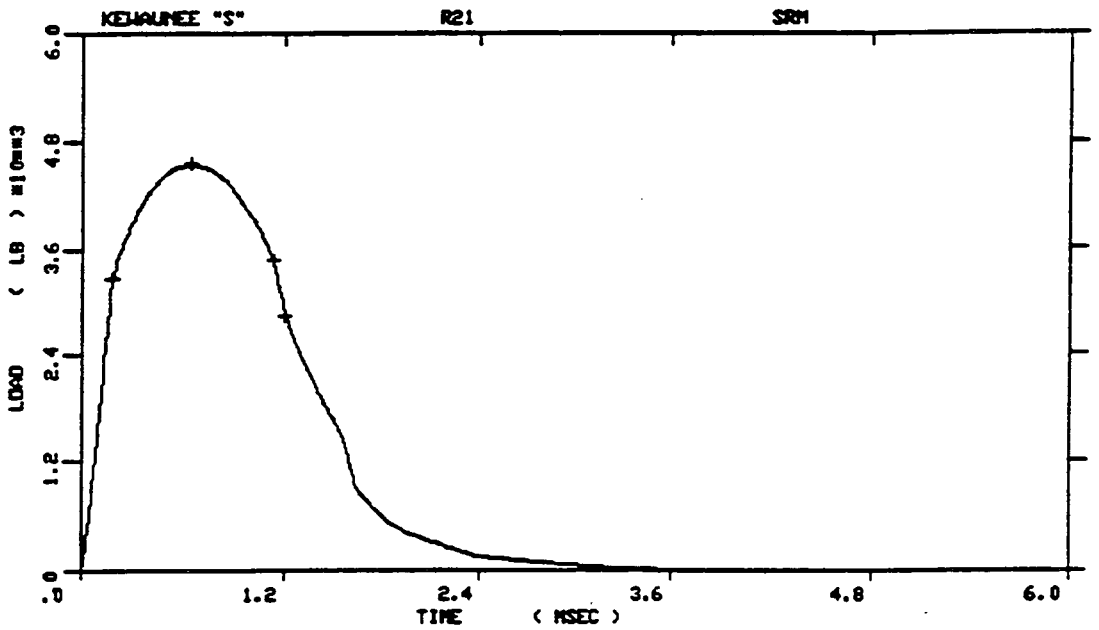


KEWAUNEE "S"  
 SPECIMEN NUMBER :R19  
 MATERIAL :SRM  
 CAPSULE :KEWAUNEE "S"

Figure A-23. Load-time records for Specimens R24 and R19.

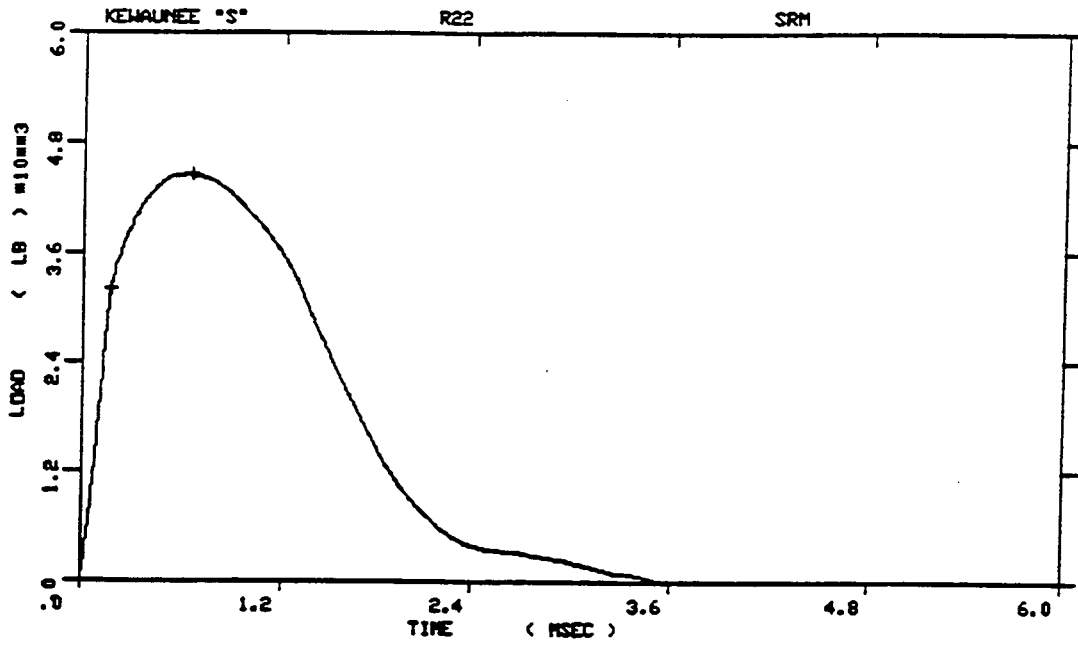


KEWAUNEE "S"  
 SPECIMEN NUMBER :R18  
 MATERIAL :SRM  
 CAPSULE :KEWAUNEE "S"

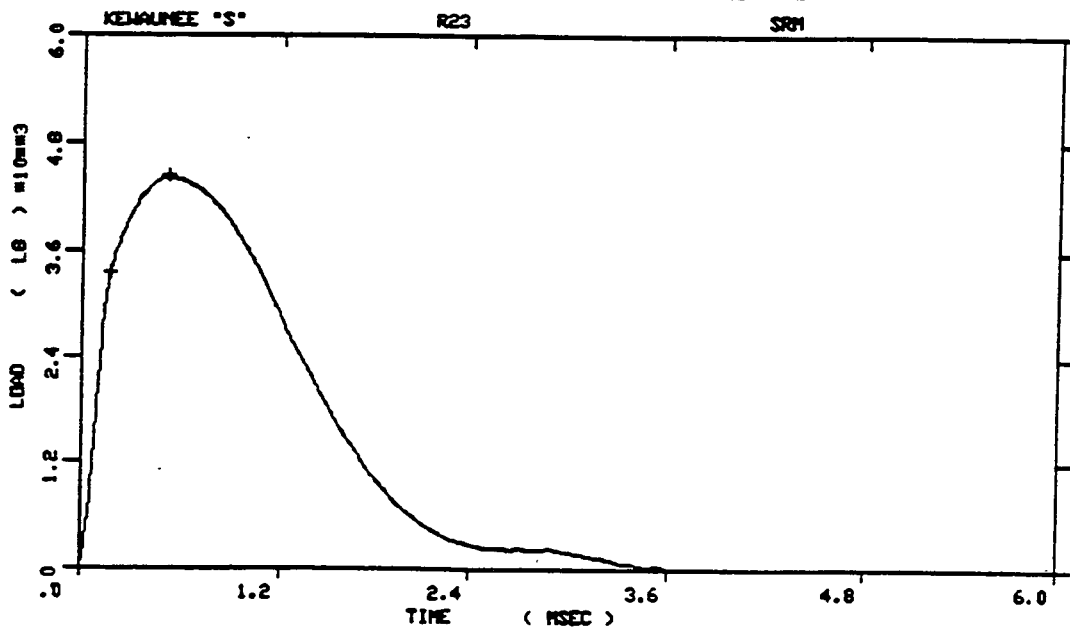


KEWAUNEE "S"  
 SPECIMEN NUMBER :R21  
 MATERIAL :SRM  
 CAPSULE :KEWAUNEE "S"

Figure A-24. Load-time records for Specimens R18 and R21.



KEWAUNEE "S"  
 SPECIMEN NUMBER :R22  
 MATERIAL :SRM  
 CAPSULE :KEWAUNEE "S"



KEWAUNEE "S"  
 SPECIMEN NUMBER :R23  
 MATERIAL :SRM  
 CAPSULE :KEWAUNEE "S"

Figure A-25. Load-time records for Specimens R22 and R23.



## APPENDIX B

# DOCUMENTATION OF THE CREDIBILITY OF THE KEWAUNEE WELD METAL SURVEILLANCE PROGRAM TEST RESULTS

### INTRODUCTION:

Regulatory Guide 1.99, Revision 2, describes general procedures acceptable to the NRC staff for calculating the effects of neutron radiation embrittlement of the low-alloy steels currently used for light-water-cooled reactor vessels. Position C.2 of Regulatory Guide 1.99, Revision 2, describes the method for calculating the adjusted reference temperature and Charpy upper-shelf energy of reactor vessel beltline materials using surveillance capsule data. The methods of Position C.2 can only be applied when two or more credible surveillance data sets become available from the reactor in question.

To date there have been four surveillance capsules removed from the Kewaunee reactor vessel. To use these surveillance data sets, they must be shown to be credible. In accordance with the discussion of Regulatory Guide 1.99, Revision 2, there are five requirements that must be met for the surveillance data to be judged credible.

The purpose of this evaluation is to apply the credibility requirements of Regulatory Guide 1.99, Revision 2, to the Kewaunee reactor vessel surveillance weld data and determine if the Kewaunee surveillance weld data are credible.

### EVALUATION:

Criterion 1: Materials in the capsules should be those judged most like to be controlling with regard to radiation embrittlements.

The beltline region of the reactor vessel is defined in Appendix G to 10CFR Part 50, "Fracture Toughness Requirements", as follows:

- "the reactor vessel (shell material including welds, heat affected zones, and plated or forgings) that directly surrounds the effective height of the active core and adjacent regions of the reactor vessel that are predicted to experience sufficient neutron radiation damage to be considered in the selection of the most limiting material with regard to radiation damage."

The Kewaunee reactor vessel consists of the following beltline region materials:

- Intermediate Shell Forging 122×208VA1
- Lower Shell Forging 123×167VA1
- Girth Weld 1P3571

The Kewaunee surveillance program utilizes longitudinal and transverse test specimens from the lower and intermediate shell forgings. The surveillance weld metal was fabricated with weld wire heat number 1P3571 (Linde 1092 Flux, flux lot 3958), which represents the girth weld in the beltline region. The Kewaunee vessel girth weld was also fabricated using weld wire heat 1P3571 with Linde 1092 flux lot 3958.

Based on the above discussion, the Kewaunee surveillance materials match the vessel beltline materials and, therefore, meet this criterion. The weld metal is the most limiting with regard to radiation embrittlement.

Criterion 2: Scatter in the plots of Charpy energy versus temperature for the irradiated and unirradiated conditions should be small enough to permit the determination of the 30 ft-lb temperature and upper shelf energy unambiguously.

Plots of the Charpy energy versus temperature for the unirradiated and irradiated condition are presented in Section 5 and Appendix C of this report.

Based on engineering judgment, the scatter in the data presented in these plots is small enough to permit the determination of the 30 ft-lb temperature and the upper shelf energy of the Kewaunee surveillance weld metal unambiguously. Therefore, the Kewaunee surveillance weld program meets the intent of this criterion.

Criterion 3: When there are two or more sets of surveillance data from one reactor, the scatter of  $\Delta RT_{NDT}$  values about a best-fit line drawn as described in Regulatory Position 2.1 normally should be less than 28°F for welds and 17°F for base metal. Even if the fluence range is large (two or more orders of magnitude), the scatter should not exceed twice those values. Even if the data fails this criterion for use in shift calculations, they may be credible for determining decrease in upper shelf energy if the upper shelf can be clearly determined, following the definition given in ASTM E185-82.

The functional form of the least squares method as described in Regulatory Position 2.1 is utilized to determine a best-fit line for this data and to determine if the scatter of these  $\Delta RT_{NDT}$  values about this line is less than 28°F for the Kewaunee weld metal.

Following is the calculation of the best-fit for the circumferential 1P3571 weld as described in Regulatory Position 2.1 of the Regulatory Guide 1.99, Revision 2. Note that the adjusted shift is equal to the measured shift in this evaluation.

	Cu (wt%)	Ni (wt%)	CF, deg. F
1P3571 Kewaunee Only	0.219	0.724	187.16
Kewaunee Surveillance	0.219	0.724	187.16

Capsule	Measured Shift, Deg. F	Adjusted Shift, Deg. F	Fluence $10^{19}$ n/cm <sup>2</sup> (E>1meV)	Fluence Function (ff)	Adjusted Shift X ff	ff <sup>2</sup>	Predicted Shift, Deg. F	Adj. Shift - Predicted Shift, Deg. F
V	175	175	0.597	0.855567	149.72424	0.732	164.5	10.5
R	235	235	1.81	1.162814	273.26124	1.35214	223.6	11.4
P	230	230	2.74	1.268842	291.8337	1.60996	244.0	-14.0
S	250	250	3.36	1.317261	329.31514	1.73518	253.3	-3.3
$\Sigma =$					1044.1343	5.42927		

CF = 192.32 deg. F
--------------------

The scatter of  $\Delta RT_{NDT}$  values about a best-fit line drawn as described in Regulatory Position 2.1 is less than 28°F as shown above in the last column. Therefore, this criterion is met.

**Criterion 4** The irradiation temperature of the Charpy specimens in the capsule should match the vessel wall temperature at the cladding/base metal interface within +/- 25°F.

The capsule specimens are located in the reactor between the thermal shield and the vessel wall and are positioned opposite the center of the core. The test capsules are in baskets attached to the thermal shield. The location of the specimens with respect to the beltline weld provides assurance that the reactor vessel wall and the specimens experience equivalent operating conditions and will not differ by more than 25°F.

**Criterion 5** The surveillance data for the correlation monitor material in the capsule should fall within the scatter band of the data base for that material.

The surveillance data for the correlation monitor material are given in WCAP-8107, WCAP-8908, WCAP-9878, WCAP-12020 and Section 5 of this report. The surveillance data for the correlation monitor material is typical for that material.

---

## CONCLUSIONS:

Regulatory Guide 1.99, Revision 2, allows the use of either procedure C.1 or C.2 as explained below:

If utilization of Regulatory Guide 1.99, Revision 2, Position C.2.1 gives a higher value of adjusted reference temperature than that given by using the procedures of Regulatory Guide 1.99, Revision 2, Position C.1.1, the surveillance data should be used; and if utilization of Regulatory Guide 1.99, Revision 2, Position C.2.1 gives a lower value, either position may be used.

For Kewaunee, Regulatory Guide 1.99, Revision 2, Position C.2.1 gives a lower value of adjusted reference temperature as documented in this report. Thus, the use of Regulatory Guide 1.99, Revision 2, Position C.2.1 is acceptable.

Based on the above criteria responses and the application of engineering judgment, the surveillance data for the circumferential weld have been determined credible.

## APPENDIX C

### DETERMINATION OF SURVEILLANCE WELD INITIAL $RT_{NDT}$

#### INTRODUCTION

The initial  $RT_{NDT}$  of the Kewaunee surveillance weld will be determined per the methodology presented in the ASME Code, Section III, Division 1, NB-2330 Standard.

Per NB-2331, pressure retaining material for vessels, other than bolting, shall be tested as follows.

- Establish a reference temperature  $RT_{NDT}$ ; this shall be done as follows:
  - a) Determine a temperature  $T_{NDT}$  that is at or above the nil-ductility transition temperature by drop weight tests.
  - b) At a temperature not greater than  $T_{NDT} + 60^{\circ}\text{F}$ , each specimen of the CV test (NB-2321.2) shall exhibit at least 35 mils lateral expansion and not less than 50 ft-lb absorbed energy. Retesting in accordance with NB-2350 is permitted. When these requirements are met,  $T_{NDT}$  is the reference temperature  $RT_{NDT}$ .
  - c) In the event that the requirements of (b) above are not met, conduct additional CV tests in groups of three specimens (NB-2321.2) to determine the temperature  $T_{cv}$  at which they are met. In this case the reference temperature  $RT_{NDT} = T_{cv} - 60^{\circ}\text{F}$ . Thus, the reference temperature  $RT_{NDT}$  is the higher of  $T_{NDT}$  and  $(T_{cv} - 60^{\circ}\text{F})$ .
  - d) When a CV test has not been performed at  $T_{NDT} + 60^{\circ}\text{F}$ , or when the CV test at  $T_{NDT} + 60^{\circ}\text{F}$  does not exhibit a minimum of 50 ft-lb and 35 mils lateral expansion, a temperature representing a minimum of 50 ft-lb and 35 mils lateral expansion may be obtained from a full CV impact curve developed from the minimum data points of all the CV tests performed.

#### EVALUATION

In WCAP-14042, "Kewaunee Weld Drop Weight Test Program Results", the nil-ductility transition temperature of the surveillance program weldment was determined to be  $-50^{\circ}\text{F}$ . The surveillance weldment is essentially identical to the Kewaunee beltline girth weld with the exception of the stress relieving.

Both weldments were made with 3/16 inch diameter B-4 wire, heat number 1P3571, and Linde 1092 flux, lot number 3958, by a submerged arc process. The surveillance program weldment was stress relieved at  $1150 \pm 25^{\circ}\text{F}$  for 19-1/4 hours, and the Kewaunee reactor vessel girth weld was stress relieved at  $1150 \pm 25^{\circ}\text{F}$  for 16-1/2 hours.

Figure C-1 is a plot of the Charpy energy versus temperature and the Charpy lateral expansion versus temperature for the unirradiated surveillance weld metal (this data was obtained from the surveillance program WCAP-8107). In this figure the curves are drawn as a lower bound curve.

Criterion a Determine a temperature  $T_{NDT}$  that is at or above the nil-ductility transition temperature by drop weight tests.

The drop weight NDTT is  $-50^{\circ}\text{F}$ ; therefore  $T_{NDT} = -50^{\circ}\text{F}$

Criterion b At a temperature not greater than  $T_{NDT} + 60^{\circ}\text{F}$ , each specimen of the CV test (NB-2321.2) shall exhibit at least 35 mils lateral expansion and not less than 50 ft-lb absorbed energy. Retesting in accordance with NB-2350 is permitted. When these requirements are met,  $T_{NDT}$  is the reference temperature  $RT_{NDT}$ .

As can be seen in Figure C-1, the Charpy tests performed at a temperature of  $T_{NDT} + 60^{\circ}\text{F} = 10^{\circ}\text{F}$  resulted in a Charpy energy greater than 50 ft-lb and a lateral expansion greater than 35 mils. Hence, this criterion is met.

Criterion c In the event that the requirements of (b) above are not met, conduct additional CV tests in groups of three specimens (NB-2321.2) to determine the temperature  $T_{cv}$  at which they are met. In this case the reference temperature  $RT_{NDT} = T_{cv} - 60^{\circ}\text{F}$ . Thus, the reference temperature  $RT_{NDT}$  is the higher of  $T_{NDT}$  and  $(T_{cv} - 60^{\circ}\text{F})$ .

A group of three CV tests were performed at  $10^{\circ}\text{F}$  ( $T_{NDT} + 60^{\circ}\text{F}$ ) and resulted in greater than 50 ft-lbs of energy and greater than 35 mils lateral expansion. Based on this criterion the Initial  $RT_{NDT}$  is the higher of  $T_{NDT}$  and  $(T_{cv} - 60^{\circ}\text{F})$ , however, for this case they are equal. Hence, the initial  $RT_{NDT}$  of the weld metal is  $-50^{\circ}\text{F}$ .

Criterion d When a CV test has not been performed at  $T_{NDT} + 60^{\circ}\text{F}$ , or when the CV test at  $T_{NDT} + 60^{\circ}\text{F}$  does not exhibit a minimum of 50 ft-lb and 35 mils lateral expansion, a temperature representing a minimum of 50 ft-lb and 35 mils lateral expansion may be obtained from a full CV impact curve developed from the minimum data points of all the CV tests performed.

In Figure C-1, one data point at  $40^{\circ}\text{F}$  is less than 50 ft-lbs. This data point does not follow the trend of the other 23 data points. Thus, based on engineering judgment this point was not used in the development of the bounding Charpy curve.

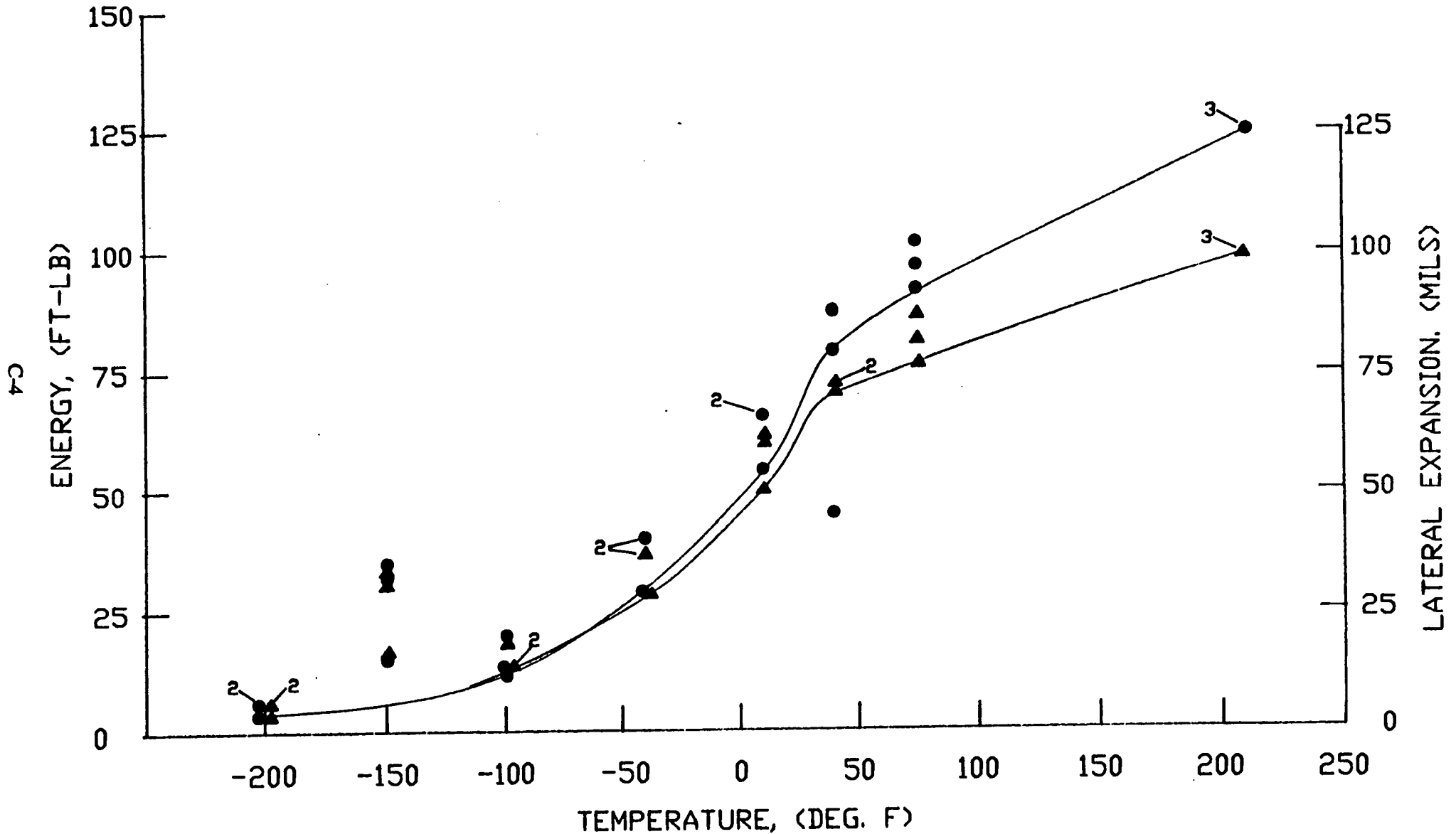
Criterion d was reviewed for completeness. A review of Figure C-1 reveals that by using a lower bound curve the material exhibits 50 ft-lbs of energy and 35 mils lateral expansion at  $0^{\circ}\text{F}$ . From criterion c the initial  $RT_{NDT}$  is the higher of  $T_{NDT}$  ( $= -50^{\circ}\text{F}$ ) and  $(T_{cv} - 60^{\circ}\text{F})$  ( $= -60^{\circ}\text{F}$ ). Hence, the initial  $RT_{NDT}$  is  $-50^{\circ}\text{F}$ .

## CONCLUSION

Based on ASME Code, Section III, Division 1, NB-2330 criterion b, the initial  $RT_{NDT}$  of the surveillance weld metal is  $-50^{\circ}\text{F}$ . Evaluation using the other criterion (c and b) also result in an initial  $RT_{NDT}$  of  $-50^{\circ}\text{F}$ . It is felt that the surveillance weld is the proper surrogate for the Kewaunee girth weld in terms of initial  $RT_{NDT}$ . More details are presented in WCAP-15074.

FIGURE C-1

DETERMINATION OF KEWAUNEE GIRTH WELD IRT<sub>NDT</sub>  
 (B-4 WELD WIRE, HT# 1P3571 & LINDE 1092 FLUX LOT# 3958)



● ENERGY, (FT-LB)  
 ▲ LATERAL EXPANSION, (MILS)